Isolation and characterization of DARPins against human EphB4

Dissertation zur Erlangung des akademischen Grades des

Doktors der Naturwissenschaften (Dr. rer. nat.)

eingereicht im Fachbereich Biologie, Chemie, Pharmazie

der Freien Universität Berlin

vorgelegt von

Weronika Trun

aus Miastko - Polen

Februar 2011

Die Arbeit wurde im Zeitraum von September 2006 bis Januar 2010 unter der Leitung von Dr. Dieter Zopf in der TRG Oncology, Bayer Schering Pharma AG, Berlin, angefertigt.

1. Gutachter	Adjunct Prof. Dr. Sanna- Maria Käkönen Institute of Biomedicine University of Turku, Turku, Finland
2. Gutachter	Prof. Dr. Rupert Mutzel, Institut für Biologie Freie Universität Berlin, Berlin, Germany

Disputation am 10 Juni 2011

ABSTRACT

The receptor tyrosine kinase EphB4 has recently become an attractive target for oncology due to its overexpression in a wide variety of human cancers and its potential involvement in tumor angiogenesis. Thus, diverse therapeutic approaches directed towards inhibition of EphB4 signaling are being developed including small molecule inhibitors of the intracellular kinase domain and biologics like immunoglobulins or peptides, which prevent extracellular ligand binding and receptor signaling. An alternative novel approach to conventional biologics is the generation of Designed Ankyrin Repeat Proteins (DARPins). DARPins are molecules with antibody-like recognition properties characterized by binding to target molecules with high affinity and specificity.

This thesis presents the *in vitro* selection of DARPins against EphB4 from a combinatorial library using phage display technology. Two unique DARPins were isolated, which specifically bind to the intracellular domain of EphB4. Moreover eight DARPins were selected, which specifically bind to the extracellular domain of human EphB4 with affinities in the low nanomolar range. Using surface plasmon resonance (SPR) analysis two classes of DARPins were identified. One class competes with the EphB4 ligand ephrin-B2 for binding to a common site (DARPin AB1) and the other targets different epitopes (BD2, BG9). DARPins from both classes prevent ligand induced EphB4 phosphorylation in a cell-based assay and impair tube formation by endothelial cells *in vitro*. Additionally AB1, which cross reacts with mouse EphB4, was shown to inhibit VEGF / FGF-2 induced angiogenesis *in vivo*.

In summary, DARPins have been isolated which can exert antiangiogenic effects *in vitro* and *in vivo* by specifically binding to EphB4 and therefore may have the potential as therapeutics for the treatment of cancer. Finally highly selective DARPins can be used as vehicles for the delivery of toxic or diagnostic agents for therapy and also imaging. Results of this dissertation could contribute to development of an effective drug for the therapy of tumors or angiogenesis-related diseases and also to examine the underlying mechanisms.

ZUSAMMENFASSUNG

Die Rezeptor-Tyrosinkinase EphB4 wurde aufgrund ihrer Überexpression in einer Vielzahl von humanen Tumoren und ihrer potenziellen Funktion in der Tumorangiogenese als ein attraktives Target für die Krebstherapie identifiziert. Demzufolge werden diverse therapeutische Ansätze entwickelt, bei denen die EphB4 Signaltransduktion inhibiert wird, einschließlich kleinmolekularer Wirkstoffe (small molecules) als Inhibitoren der intrazellulären Kinase-Domäne und „biologics“, wie Immunglobuline oder Peptide, die die extrazelluläre Ligandenbindung und die Signaltransduktion verhindern. Eine neuartige Alternative zu herkömmlichen Biologics stellen DARPins (Designed Ankyrin Repeat Proteins) dar. Sie gehören zu den Antikörpermimetika und sind durch eine hohe Bindungsspezifität und Bindungsaffinität gekennzeichnet.

Im Rahmen dieser Arbeit wurde die *In vitro*-Selektion von DARPins gegen EphB4 aus einer kombinatorischen Bibliothek mittels Phage Display Technologie erfolgreich durchgeführt. Dabei wurden 10 charakteristisch unterschiedliche DARPins isoliert, die hochspezifisch und mit Affinitäten im nanomolaren Bereich an die extrazelluläre Domäne und an die intrazelluläre Domäne von humanem EphB4 Rezeptor binden. Mittels Surface Plasmon Resonance (SPR)-Analyse konnte für die extracellulär bindenden DARPins gezeigt werden, dass sie sich in zwei Klassen unterteilen. Eine Klasse bindet kompetitiv mit dem EphB4-Liganden ephrin-B2 an eine gemeinsame Region des Rezeptors (DARPin AB1), während die anderen Binder unterschiedliche Epitope erkennen (BD2, BG9). Interessanterweise verhindern DARPins aus beiden Klassen die ligandinduzierte EphB4-Phosphorylierung in einem zellbasierten Assay und beeinträchtigen die Ausbildung neuer Gefäßstrukturen durch Endothelzellen *in vitro*. Darüber hinaus wurde in einem Maussurrogatmodell gezeigt, dass AB1, der mit Maus-EphB4 kreuzreagiert, VEGF / FGF-2 induzierte Angiogenese *in vivo* hemmen kann.

Diese Resultate zeigen klar auf, dass die isolierten EphB4 DARPins affin und spezifisch an EphB4 binden und eine antiangiogene Wirkung in vitro und in vivo entfalten und daher das Potenzial für ein Therapeutikum zur Behandlung von

Krebs besitzen. Schließlich können hochspezifische DARPins auch als Träger für therapeutisch wirksame Effektoren dienen, wie beispielsweise Toxine, Zytostatika oder Radioisotope zur Bildgebung von Tumoren. Die vorliegenden Daten könnten zu der Entwicklung eines wirksamen Medikaments für die Therapie von Tumoren und anderen angiogeneseabhängigen Erkrankungen beitragen und stellen Werkzeuge zur Verfügung, die die Untersuchung der zugrunde liegenden Mechanismen ermöglichen.

TABLE OF CONTENTS

ABSTRACT 3

ZUSAMMENFASSUNG 4

TABLE OF CONTENTS 6

ABBREVIATIONS 10

1 INTRODUCTION 12

1.1 Angiogenesis 12

1.1.1 Angiogenesis as a therapeutic target 12

1.1.2 Mechanisms of blood vessel formation 13

1.1.3 Pathological angiogenesis in tumor 15

1.2 The Receptor Tyrosine Kinase Family 17

1.2.1 Eph and ephrins structure 18

1.2.2 Receptor dimerization and larger membrane complexes 21

1.2.3 Cellular functions mediated by Eph receptor 23

1.2.4 Eph molecules are involved in angiogenesis 25

1.2.5 EphB4 in tumor progression 26

1.2.6 Therapeutic significance of EphB4 28

1.3 New generation of biologics 30

1.3.1 From natural to the designed ankyrin repeat protein 31

1.3.2 *In vitro* display technology 33

1.3.3 DARPins properties 34

1.3.4 Potential application of DARPins 35

1.4 Aims of the PhD thesis 38

1.5 Thesis structure 40

2 MATERIALS AND METHODS 41

2.1 Materials 41

2.1.1 Phage display and bacterial work reagents 41

2.1.2 Enzymes and reagents for cloning 42

2.1.3 Reagents and buffers for protein purification 43

2.1.4 Reagents and buffers for SDS-PAGE and Western blot 43
2.1.5 Buffers and reagents for binding assays (ELISA, FACS, IP, SPR) 44
2.1.6 Recombinant proteins 44
2.1.7 Primary and secondary antibodies 45
2.1.8 Animals and cell lines 46
2.1.9 Cell culture media and supplements 46
2.1.10 Kits and reagents for cellular assays 47
2.1.11 Kit and reagents for *in vivo* assay 47
2.1.12 Disposables 48
2.1.13 Devices 49
2.1.14 Software 50
2.2 Display methodology 51
2.2.1 Phage display 51
2.2.2 Bacterial culture 53
2.2.3 Pool phage amplification 53
2.2.4 Isolation and amplification of a single phage clone 54
2.2.5 Phage precipitation and purification 54
2.3 Molecular biological methods 55
2.3.1 DNA purification 55
2.3.2 Restriction enzyme digestion 56
2.3.3 Agarose gel electrophoresis 56
2.3.4 DNA ligation 57
2.3.5 Transformation of *E. coli* 58
2.4 Protein chemistry methods 59
2.4.1 Large scale DARPin expression 59
2.4.2 DARPin purification 59
2.4.3 Determination of protein concentration 62
2.4.4 SDS-PAGE 63
2.4.5 Western blot 64
2.5 Binding analysis 65
2.5.1 Immobilization of target proteins 65
2.5.2 Enzyme-linked Immunosorbent Assay (ELISA) 66
2.5.3 Flow cytometry analysis 67

2.5.4 Surface plasmon resonance analysis of protein interaction 68
2.5.5 Immunoprecipitation 71
2.6 Cellular assays 72
2.6.1 Cell lines and culture 72
2.6.2 Kinase phosphorylation assay 72
2.6.3 Tube formation assay 73
2.6.4 Apoptosis assay 74
2.6.5 Internalization 74
2.6.6 EphB4 inhibition by cell transfection of ICD-EphB4 DARPins 75
2.7 Directed *in vivo* angiogenesis assay 76
2.8 Statistical analysis 78

3 RESULTS 79

3.1 EphB4 DARPin isolation and characterization workflow 79
3.2 Selection of DARPins against the extracellular domain of human EphB4 .. 80
3.2.1 Phage display of DARPin library 80
3.2.2 Isolation of EphB4 specific phage binders from DARPin library 81
3.2.3 Expression and purification of DARPin 84
3.2.4 Characterization of DARPins by size exclusion chromatography 87
3.3 Analysis of the binding characteristics of EphB4 DARPins 90
3.3.1 DARPin binding to the recombinant hEphB4 ECD 90
3.3.2 Binding of EphB4 DARPins to other EphB receptors 92
3.3.3 Analysis of EphB4 DARPins binding to EphB4 expressing cells 94
3.3.4 Binding kinetics of EphB4 DARPins to EphB4 96
3.4 Functional characterization of EphB4 DARPins 107
3.4.1 Competitive binding analysis of EphB4 DARPins and ephrin-B2 107
3.4.2 Inhibition of ligand induced EphB4 receptor phosphorylation using EphB4 DARPins 112
3.4.3 Effect of EphB4 DARPins on tube formation of endothelial cells *in vitro* 114
3.4.4 Effects of EphB4 DARPins on angiogenesis *in vivo* 116
3.4.5 Effects of EphB4 DARPins on apoptosis in tumor cells *in vitro* 116
3.4.6 Analysis of DARPin-induced internalization of EphB4 116

4 DISCUSSION 116

4.1 Isolation of EphB4 binders from a DARPin phage library 116
4.2 Selected DARPins bind EphB4 with high specificity 116
4.3 DARPins bind EphB4 with nanomolar affinities as determined by SPR ... 116
4.4 DARPins interact with EphB4 in monovalent or bivalent binding model ... 116
4.5 EphB4 DARPin binds competitively to EphB4 116
4.6 EphB4 DARPins bind to different sites of EphB4 116
4.7 EphB4 DARPins prevent ligandinduced EphB4 phosphorylation 116
4.8 EphB4 DARPin AB1 exert antiangiogenic effects *in vitro* and *in vivo* 116
4.9 DARPins induce EphB4 internalization in tumor cells 116
4.10 EphB4 DARPins present different characteristics 116
4.11 Conclusions and potential applications of DARPins 116

5 APPENDIX 116

5.1 Supplementary results 116
5.2 EphB4 ICD DARPins 116
5.2.1 Isolation and characterization of DARPins against the intracellular domain of EphB4 116
5.2.2 Isolation of EphB4 ICD specific phage DARPin binders 116
5.2.3 Functional characterization of EphB4 ICD DARPins 116
5.3 Vector maps 116
5.3.1 Vector pMPAG3 116
5.3.2 Vector pMPAG6 116
5.4 Structure of EphB4 DARPin 116

LIST OF FIGURES 116

LIST OF TABLES 116

REFERENCES 116

ACKNOWLEDGEMENTS 116

EHRENWÖRTLICHE ERKLÄRUNG 116

ABBREVIATIONS

aa	amino acid
Amp	ampicillin
Ang	angiopoietin family
AR	ankyrin repeat
ATP	adenosine triphosphate
BSA	bovine serum albumin
Cam	chloramphenicol
cfu	colony forming units
DARPin	Designed Ankyrin Repeat Proteins
DARPin-pIII	DARPin fused to the surface of filamentous phage
ddH_2O	double distilled water
EC	endothelial cell
ECD	extracellular domain
EGFRs	epidermal growth factor receptors
ELISA	enzyme-linked immunosorbent assay
Eph	erythropoietin-producing human hepatocellular carcinoma
EphB4	Eph receptor B4 (also known as HTK, MYK1, TYRO11)
ephrin-B2	Eph family receptor interacting protein B2 (Lerk-5, Eplg5, Htk-L, EFNB2)
FACS	fluorescence activated cell sorting
FGF-2	fibroblast growth factor-2
FITC	fluorescein isothiocyanate
FN	fibronectin type III repeat
GE3S	GST-mEphB3-SAM
GE4S	GST-mEphB4-SAM
HER2	human epidermal growth factor receptor (ErbB2)
HRP	horse radish peroxidase
HUVEC	human umbilical vein endothelial cell

ICD	intracellular domain
IEC	ion exchange chromatography
IMAC	immobilized metal ion affinity chromatography
IPTG	isopropyl-β-D-thiogalactopyranosid
LBD	ligand binding domain
MAPK	mitogen activated protein kinase
MMP	matrix metalloproteinase
n.s.	not significant
N3C, N4C	DARPins with 3 or 4 repeats between N- and C- cap
PDZ	PSD-95 postsynaptic density protein, Disc large, Zona occludens tight junction protein
pEphB4	phosphorylated EphB4
RBD	receptor binding domain
R_{eq}	response at the equilibrium
RLU	relative light units
rpm	rounds per minutes
RT	room temperature
RTK	receptor tyrosine kinases
RU	resonance units
SAM	sterile alpha motif
SDS-PAGE	sodium dodecyl sulfate polyacrylamide gel electrophoresis
SEC	size exclusion chromatography
SPR	surface plasmon resonance
SRP	signal recognition particle
VEGF	vascular endothelial growth factor
ZAP	saporin

1 INTRODUCTION

1.1 Angiogenesis

Despite considerable advances in surgery, imaging techniques and therapy methods in the past decades, the prognosis of cancer remains poor. The current standard treatment, beside the surgical removal of a cancerous growth, relies mainly on radiation, hormone and chemotherapy. These therapies are often associated with adverse side effects, resulting from the damage of healthy proliferating cells, and the major limitation, which is tumor drug resistance. To improve the conventional treatment methods, alternative approaches have been identified directed toward the processes in the stromal microenvironment. The growth of solid tumors requires efficient recruitment of blood vessels. Thus, targeting of angiogenesis and vasculogenesis represents a progressive strategy for cancer treatment. In contrast to the tumor tissue consisting of heterogeneous, malignant cells with high mutation rate, endothelial cells are readily accessible from the circulation and genetically stable (Kerbel 1997). Therefore, the vascular endothelium provides a therapeutic window with lower risk of resistance compared with conventional cytostatics.

1.1.1 Angiogenesis as a therapeutic target

Since the publication of Folkman's hypothesis in 1970s that solid tumors are angiogenesis-dependent (Folkman 1972), great progress has been achieved in the identification of key molecules and cellular pathways involved in this process. Therapies aimed at the tumor vasculature have been designed either to prevent the formation of new vessels (antiangiogenic approach) or to damage already formed tumor vessels (vascular targeting). However, the second strategy requires specific targets to damage tumor vasculature without harming normal tissues. In the past few years, many angiogenesis inhibitors were

identified and several were developed for anticancer treatment. The first breakthrough was bevacizumab (Avastin; Genentech), a humanized monoclonal antibody directed against vascular endothelial growth factor (VEGF) approved by the Food and Drug Administration for the therapy of metastatic colorectal cancer (Ferrara et al. 2004). Thereafter other antiangiogenic drugs, sunitinib (Sutent; Pfizer) and sorafenib (Nexavar; Bayer), small molecular inhibitors of several receptor tyrosine kinases were approved for the treatment of renal cell carcinoma (Motzer et al. 2006; Escudier et al. 2007). Additional indication of sorafenib is the hepatocellular carcinoma (Llovet et al. 2008).

Beside tumor growth, abnormal angiogenesis is also associated with other pathological processes including metastasis, diabetic retinopathy, psoriasis and arthritis, where the inhibitors could be beneficial. Moreover, promoting new vessel growth is of particular importance in ischemic cardiovascular disorders, such as coronary artery disease and peripheral arterial disease, which are a significant health problem worldwide (Ferrara and Kerbel 2005). Pro- and antiangiogenic strategies hold a great promise, as the angiogenesis is a multi-stage process that can be affected by agents in one or more crucial steps. Especially the field of cancer therapy requires identification and characterization of target molecules and pathways that are specific for tumor-associated blood vessels or are involved in the angiogenesis.

1.1.2 Mechanisms of blood vessel formation

Blood vessel formation is an essential process for organ growth during embryonic development. The formation of the cardiovascular system begins with differentiation of the common precursor cell, the hemangioblasts into endothelial and hematopoietic cells (Carmeliet 2005). In the process named vasculogenesis, endothelial cells (EC) give rise to a primitive vascular plexus (Figure 1). During subsequent remodeling, a mechanism termed as angiogenesis, blood vessels undergo sprouting, branching and differential growth. The first stage involves endothelial cells proliferation, chemotactic migration and tubule formation. Further functional maturation requires

recruitment of supporting cells, pericytes and smooth muscle cells that cover nascent endothelial channels. The vascular network expands into highly organized vascular system of arteries and veins accompanied by lymph vessels.

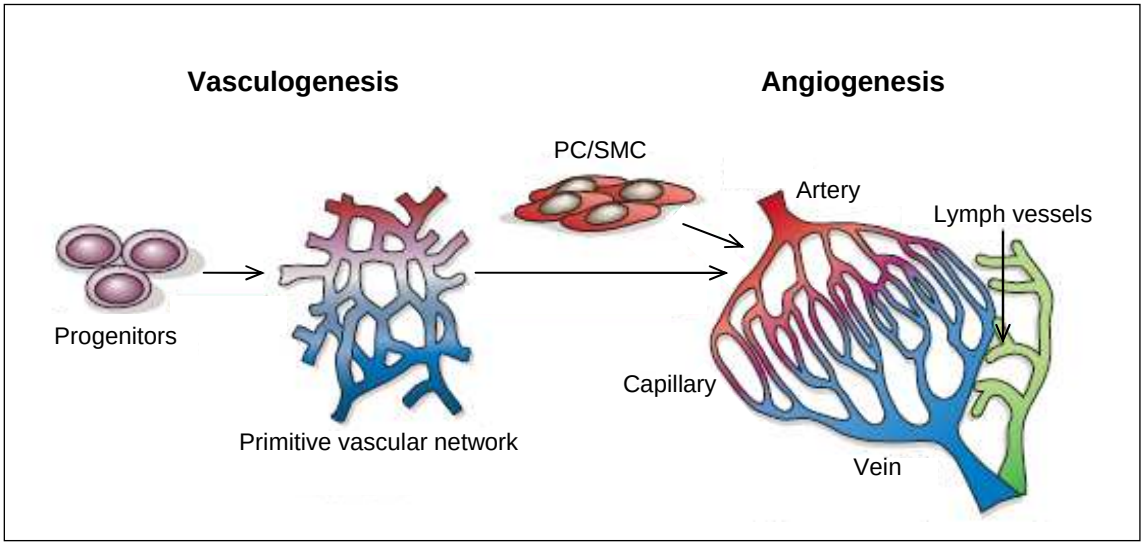

Figure 1. Vasculogenesis and angiogenesis process. Primary vasculature arises from endothelial progenitors during vasculogenesis. In the following angiogenesis process primitive vascular labyrinth is remodeled into a hierarchical network of arteries (red) and veins (blue) with the adhesion of pericytes (PCs) and smooth muscle cells (SMC). Lymph vessels development is based on transdifferentiation from the embryonic veins (Carmeliet 2005).

In the adult, the angiogenic process normally remains quiescent with the exception of wound healing following tissue damage and female reproductive organs. The postnatal vessel growth is dependent on the balance between pro- and antiangiogenic regulators. Various growth factors and cytokines are involved in the activation of the angiogenesis process. Vascular endothelial growth factor (VEGF) family belongs to one of the first identified pathways (Jussila and Alitalo 2002; Ferrara et al. 2003). Receptor tyrosine kinases, mainly VEGFR-1 and VEGFR-2 mediate the biological responses of VEGF, which are stimulation of vascular endothelial cell growth, survival and proliferation. Although VEGF is the key angiogenic regulator, it works in combination with other factors. The most important partners are angiopoietins

(Ang1-4), ligands of Tie-2 receptor, involved in sprouting, maintenance and regression of blood vessels (Yancopoulos et al. 2000). Another major angiogenic stimulator is fibroblast growth factor-2 (FGF-2), which is a member of the family of heparin-binding growth factors. FGF-2 by binding to several FGF receptors leads to proliferation, migration and differentiation of endothelial cells (Bikfalvi et al. 1997).

More recently, members of the Eph family, the largest group of receptor tyrosine kinases (RTKs), were identified. The Eph receptors and their corresponding ephrin ligands are both cell membrane proteins and play an important role in organizing of vascular cells into stable network. In particular, they determine arterial versus venous identity of endothelial cells in the primary vascular plexus (Adams et al. 1999).

Under physiological conditions the activity of growth factors is compensated by vascular inhibitors. Various endogenous antiangiogenic factors have been characterized such as angiostatin, fragment of plasminogen and several matrix derived proteins: endostatin, thrombospondin-1 and tumstatin (Nyberg et al. 2005). Angiogenesis is coordinated by a very sensitive interplay of regulatory factors and any disproportion between stimulators and inhibitors contributes to disease. When the stimulus becomes excessive, the balance is tilted resulting in the angiogenic switch and abnormal activation of vascular growth.

1.1.3 Pathological angiogenesis in tumor

A typical solid tumor cannot exceed 2 mm in diameter without access to oxygen and nutrients (Folkman 1971). In response to hypoxia and other environmental and cellular stimuli, a malignant tumor turns on the angiogenic switch and begins to secret growth factors including VEGF, which promote new blood vessel formation. Up-regulation of VEGF initiates vasodilatation and increased vascular permeability of the neighboring blood vessels. Ang2 initiates vascular regression by loosing cell contacts between endothelial and smooth muscle cells and cell-matrix interactions (Yancopoulos et al. 2000). This allows

extravasation of plasma into the interstitial space. Leaking plasma contains proteolytic enzymes, such as matrix metalloproteinases (MMPs), which mediate degradation of the vascular basement membrane and extracellular matrix (Kalluri 2003). Once the surrounding matrix was disintegrated, endothelial cells migrate into the perivascular space toward the tumor. Behind the migrating column, endothelial cells assemble three-dimensionally in capillary-like tubes and proliferate creating a central lumen of a new vessel. Eph and ephrin molecules are involved in establishing of endothelial cell-cell interactions. Furthermore, the circulating bone marrow-derived endothelial progenitors are incorporated into the growing vascular wall, where they differentiate into mature endothelial cells (Carmeliet 2000; Bergers and Benjamin 2003; Plank and Sleeman 2003).

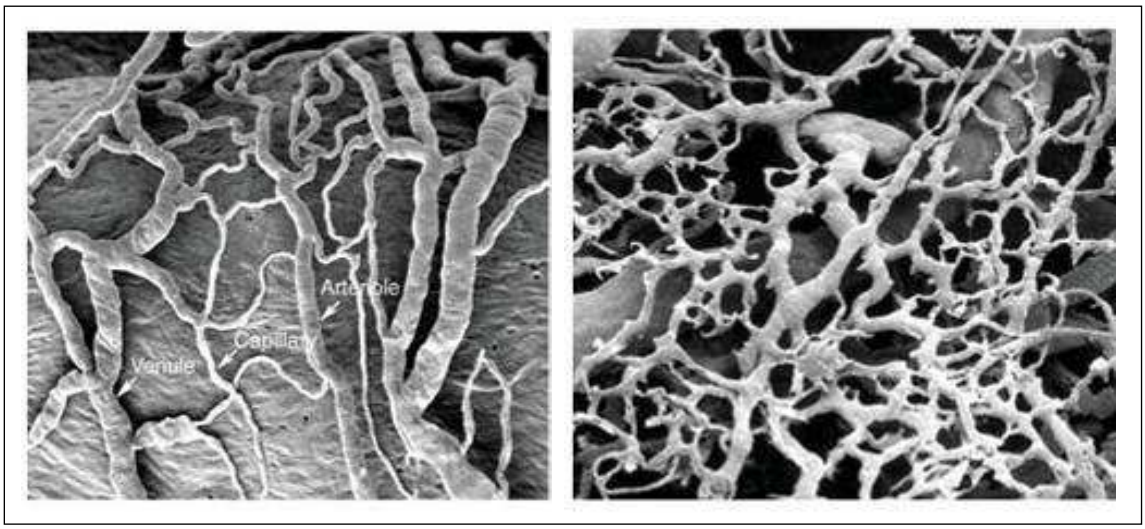

Figure 2. Microscopic imaging of normal and tumor vasculature. Healthy vasculature has orderly architecture and mature blood vessels (left). In a tumor (right) vasculature is abnormal, fragile and characterized by disordered architecture (McDonald and Choyke 2003).

In normal vasculature, this is accompanied by production of the basement membrane and attraction of pericytes. In the tumor, the angiogenic switch remains turned on and the continuous production of angiogenic factors prevents the maturation process of the vessels (Hashizume et al. 2000; Morikawa et al. 2002; Bergers and Benjamin 2003). Therefore, the tumor vasculature is

irregularly shaped, tortuous, and leaky and can have dead ends (Figure 2). The formation and permanent expansion of the vascular network facilitates rapid growth of the tumor and increases metastatic potential. A promising therapeutic strategy is disruption of the expansion of vascular network in one or more of its stages, which would lead to the tumor starvation and interrupt its development. The approaches concentrate on pharmacological inhibition of numerous proangiogenic molecules (Ferrara and Kerbel 2005). There is growing evidence showing that interaction between the receptor tyrosine kinase Eph and its ligand ephrin is of great importance during the angiogenesis and progression of malignant tumor, and will be discussed in greater detail in the following chapter.

1.2 The Receptor Tyrosine Kinase Family

In the crucial biological processes, communication between individual cells is essential for their development and survival. Information from the extracellular environment must be transmitted to intracellular signaling pathways. This is achieved through activation of specific membrane proteins. The significant cell surface mediators of physiological responses are receptor tyrosine kinases. RTKs comprise a large family of single-pass transmembrane receptors with an extracellular ligand recognition region and a cytoplasmic domain with kinase activity. They are activated by many polypeptide growth factors, cytokines and hormones, which are either membrane-bound or secreted, soluble proteins binding in paracrine or autocrine manner. The activated catalytic kinase domain initiates signal transduction cascades by phosphorylation of specific substrates (Cadena and Gill 1992). RTK-mediated signals regulate a range of cellular events, such as cell growth, differentiation, migration, adhesion and apoptosis.

There are approximately 100 protein tyrosine kinases known in the human genome, thereof 58 encode receptor tyrosine kinases (Robinson et al. 2000). RTKs can be classified into 20 subfamilies based on their structure. The catalytic domains are well conserved and share 32 to 95% sequence homology. The ligand binding domain is the most distinctive region. The extracellular domain is composed of several structural motifs, such as IgG-like domains,

cysteine-rich regions and fibronectin type III repeats. These subdomains are diversely assembled within the receptor, individually for the members of each family (van der Geer et al. 1994). The structurally related RTK subfamilies include for example epidermal growth factor receptors, insulin and insulin-like growth factor receptors, platelet-derived growth factor receptors, vascular endothelial growth factor receptors, fibroblast growth factor receptors and the most recently identified group of Eph receptors (Yarden and Ullrich 1988).

1.2.1 Eph and ephrins structure

The Eph receptors represent the largest subfamily of RTKs consisting of at least 14 structurally related members that are known in mammals. The first Eph receptor was isolated during the screening for tyrosine kinases involved in cancer from an Erythropoietin-producing human hepatocellular carcinoma cell line (Hirai et al. 1987). Initially described as orphan receptors without known ligands and function, Ephs were later found to be involved in a number of physiological and pathological processes. Moreover, they bind to at least eight ephrin ligands (Eph family receptor interacting proteins), which are unique in that they are membrane-attached cell surface molecules. Depending on the method of cellular attachment, ephrins were naturally divided into class A and B. Whereas the classification of Ephs into two subfamilies EphA (EphA1-8, EphA10) and EphB (EphB1-4, EphB6) is based on the sequence homology of their extracellular domains (Eph Nomenclature Committee 1997). This grouping also corresponds to their binding affinities to the ephrin-A or ephrin-B ligands. EphA receptors preferentially bind to ephrin-A ligands and EphB to ephrin-B ligands, however EphA4 recognizes ephrins of both classes (Gale et al. 1996), and ephrin-A5 interacts also with EphB2 beside EphA receptors (Himanen et al. 2004). Interestingly, EphB4 binds distinctive to a single ligand, ephrin-B2, and only weakly to ephrin-B1 and ephrin-B3.

The structure of Eph receptors, based on sequence comparisons, demonstrates strong similarity to other RTKs, especially within the intracellular domain. The glycosylated extracellular region contains an N-terminal immunoglobulin-like

ligand binding domain (LBD) followed by a cysteine-rich region and two fibronectin type III repeats (Figure 3). A transmembrane region separates the ectodomain from the catalytic domain. Eph intracellular side is comprised of a juxtamembrane region, a tyrosine kinase domain and a sterile alpha motif (SAM). The kinase domain contains an ATP-binding site in the cleft between the two lobes. SAM domain is 60-70 aa long and is implicated in the receptor oligomerization and binding of adaptor proteins, although it is not necessary for the kinase activity (Thanos et al. 1999; Boyd and Lackmann 2001). PSD-95 postsynaptic density protein, Disc large, Zona occludens tight junction protein (PDZ)-binding motif closes the receptor structure at its cytoplasmic C-terminal end. PDZ binding domain by interactions with adaptor proteins plays an important role in downstream signaling.

Eph receptors have at the N-terminal a globular domain of approximately 180 aa, which is exclusively involved in interaction with the ligand (Labrador et al. 1997). The cysteine-rich region does not participate in ligand binding, however it may stabilize the receptor-ligand complex. Likewise, both FN domains are redundant for the ligand interaction and signaling, and play only a structural function to maintain a distance between cells. The first structure of LBD was obtained for mouse EphB2 in X-ray crystallographic studies (Himanen et al. 1998). The domain folds into a compact jellyroll ß-sandwich composed of two antiparallel ß-sheets, the concave ß-sheet assembled of ß-strands C, F, F', L, H, I and the convex ß-sheet assembled of ß-strands D, E, A, M, G, K, J. ß-strands are connected by loops of different length and conformation, which are essential for ligand binding. Among these, loops D-E, E-F, G-H and J-K are responsible for the receptor / ligand dimerization (Chrencik et al. 2006b). Tetramerization is driven by the H-I loop, which was reported to be responsible for the subclass specificity, because of its conserved size and sequence within the same class, but different between the Eph classes (17 aa in B-class, 13 aa in the A-class).

Analysis of amino acid sequences of ephrin ligands revealed at the N-terminus the receptor binding domain (RBD) and a spacer region. At the C-terminus, the class A has a hydrophobic region, presenting the glycosylphosphatidylinositol

(GPI)-attachment site. In contrast, class B ligands possess a transmembrane region and a highly conserved cytoplasmic domain of 80 aa containing PDZ-binding motif. The structural information delivered for ephrin-B2 shows that the RBD is arranged in a globular ß-barrel with a Greek key folding topology, comprised of eight parallel and antiparallel strands arranged around a hydrophobic core in two sheets (Toth et al. 2001). The domain contains sites for receptor / ligand interaction and can form low-affinity cis-homodimers.

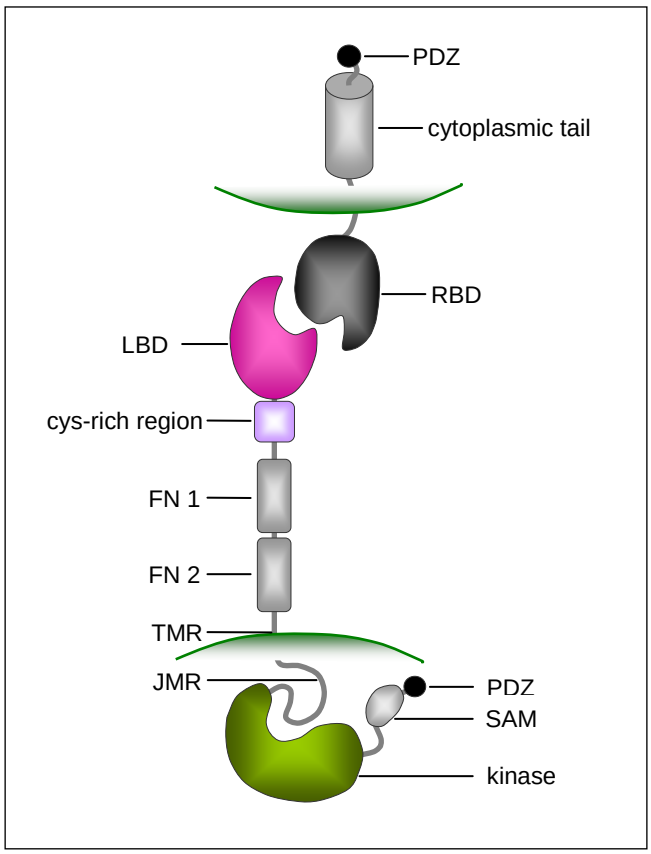

Figure 3. The domain structure of the Eph receptor and its ligand. The N-terminal domain includes a ligand binding site (LBD), a cysteine-rich region and two fibronectin type III repeats (FN). A single transmembrane domain (TMR) is followed by the intracellular domain comprised of a juxtamembrane region (JMR), a tyrosine kinase domain, sterile alpha (SAM) and PDZ-binding motifs. Ephrin-B consists of the receptor binding domain (RBD) and the cytoplasmic domain with a PDZ-binding motif at the C terminus (adapted from Himanen and Nikolov 2003a).

1.2.2 Receptor dimerization and larger membrane complexes

Eph receptors and their ephrin ligands are both membrane-bound molecules and require contact of neighboring cells. As a result of cell–cell contact, Eph receptors recognize ephrins in the opposite membrane and bind with 1:1 stoichiometry forming trans-heterotetramers and trigger signaling pathways in both directions (Himanen and Nikolov 2003a). The binding of ephrin to the Eph receptors occurs via interaction between their ectodomains (Figure 4). Biophysical and structural studies of the ephrin-B2 complex with EphB2 or EphB4 identified the character of binding and determinants for receptor specificity (Himanen et al. 2001; Chrencik et al. 2006a). Prior to the cellular contact, ephrins and Ephs are pre-clustered in sphingolipid / cholesterol enriched raft microdomains (Bruckner et al. 1999). A low-affine homodimer of ephrin-B2 initiates the interaction with the opposite standing receptor.

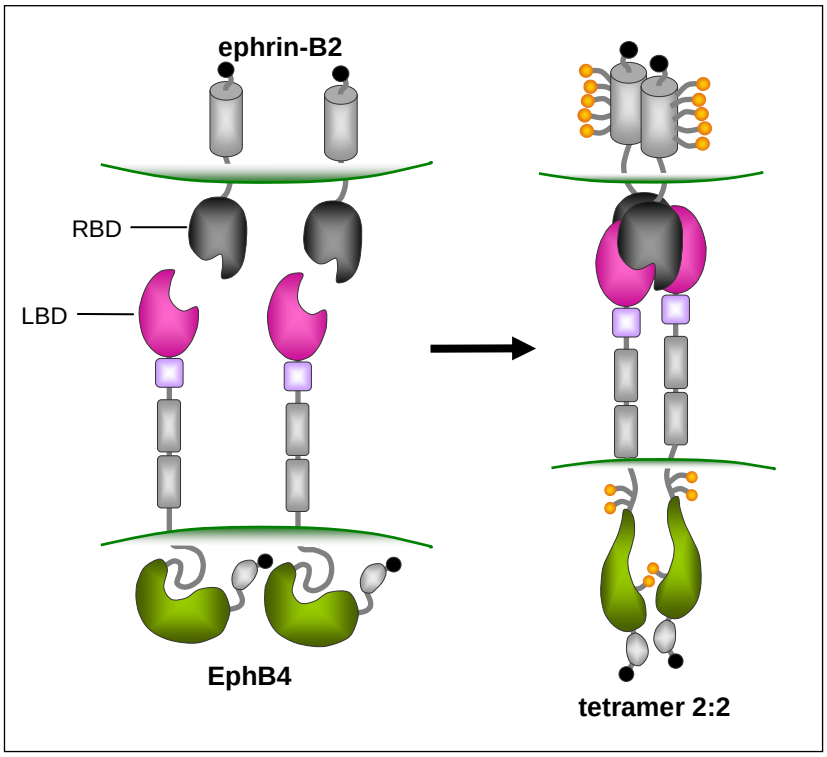

Figure 4. Formation of Eph / ephrin complex and activation of the bidirectional signaling. Eph receptor upon binding to the ephrin ligand undergoes dimerization, followed by creation of the heterotetramer composed of 2 Eph and 2 ephrin molecules and subsequent phosphorylation (yellow points) of cytoplasmic residues of receptors and ligands (Himanen and Nikolov 2003a).

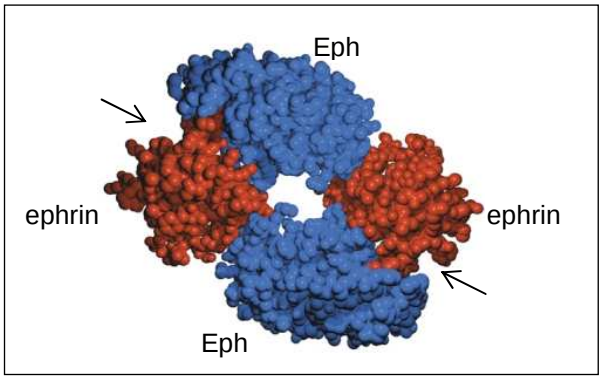

Figure 5. Crystal structure of LBD of EphB2 / ephrin-B2 complex. The tetramer is generated by two ligand (red) and receptor (blue) molecules. The high-affinity dimerization interfaces are pointed by arrows (Himanen and Nikolov 2003a).

The first step is formation of high-affine heterodimer by insertion of the extended ligand G-H loop into the hydrophobic binding cleft of Eph receptor, positioned above E and M strands. During dimerization, complementary interaction surfaces are exposed on the opposite side of the LBD domain (H-I loop) and the corresponding sites are created by the C-D loop of the ligand. Although this interface displays lower affinity, it conducts two Eph / ephrin dimers together and generates a heterotetramer (Figure 5). The complexes may contribute to further arrangement into higher-order clusters, depending on the density of surface molecules expression. The sites of the ephrin binding were identified in the cysteine-rich region of the receptor (Smith et al. 2004). SAM domain comprising 60–70 aa is also implicated in the receptor oligomerization (Thanos et al. 1999).

The arrangement of the Eph / ephrin complexes is essential for the initiation of bidirectional signaling (Himanen and Nikolov 2003a). The unbound Eph preserves its tyrosine kinase domain in an inactive conformation stabilized by inhibitory interactions with the juxtamembrane region. In the heterotetramer, molecules are precisely positioned, what causes fix orientation of their cytoplasmic domains and brings two intracellular kinase domains together. Eph receptors and also ephrin-B have multiple phosphorylation sites in their endodomains. Upon ligand binding Eph receptor undergoes phosphorylation at juxtamembrane tyrosine residues, what disrupts the association between this

segment and the kinase domain favoring ATP to be properly aligned in the substrate binding site. This leads to the activation of the catalytic domain and phosphorylation of other neighboring molecules.

Hence the receptor and the ligand are both membrane tethered, the signal is propagated into the receptor-expressing cell (forward signaling) and the ligand-expressing cell (reverse signaling). Once activated, Eph receptor interacts with adapter molecules such as small GTPases of the Rho and Ras family, Ras family of GTPase activating protein (RasGAP), Src-homology-2 (SH2) and SH3 domains, and Abl family (Bruckner and Klein 1998). In the ligand-expressing cell formation of tetrameric complexes also results in a repositioning of ephrin-B transmembrane and cytoplasmic domains. Further, the tyrosine residues of the C-terminal PDZ-binding domain are trans-phosphorylated by associated Src-family kinases and mediate reverse signaling (Holen et al. 2008).

1.2.3 Cellular functions mediated by Eph receptor

Cell–cell interaction through the Eph **/** ephrin axis triggers cellular responses via binding to a variety of cytoplasmic proteins and activation of signal transduction pathways. By contrast to most RTKs, Ephs and ephrins appear to affect the cytoskeleton rather than to control gene expression. They play an important role in organization of the actin cytoskeleton, cell shape, adhesion, repulsion and migration. Moreover, effects on the cell proliferation and differentiation have been reported. A distinctive feature of Eph **/** ephrin interaction is not only generation of bidirectional signaling, but also that the triggered signal may induce opposite results in affected cells. Although formation of Eph **/** ephrin heterotetramer is sufficient for receptor and ligand phosphorylation, the size of clusters defines the character of generated signals and induced biological effects. In contrast to other RTKs, which are engaged in growth regulation, Ephs do not directly promote cellular proliferation or transformation. However, activation of EphA receptors was reported to modulate cell proliferation of prostatic cancer cells by inhibition of Ras **/** MAPK (mitogen activated protein kinase) pathway (Miao et al. 2001). In general, Eph negatively regulate H-Ras

and its downstream MAP kinase pathway. MAPK cascade plays a role in the induction of proliferation and cell growth.

The result of cell-cell contact in Eph / ephrin axis is common and well-characterized cell motility (Pasquale 2005). The interaction can result either in an increased attraction or an opposite repulsion effect, depending on the cell type, particular pair of Eph and ephrin and their surface density. Moreover, the state of ephrin multimerization determines biological responses (Stein et al. 1998). A multimeric form of ephrin-B1 was reported to promote cellular attachment, but not the dimeric ligand, although both constructs of ephrin activated equally endogenous EphB1 receptor phosphorylation. Eph receptors regulate cellular adhesion by positive or negative affecting integrins, cell surface receptors, which attach to proteins in the extracellular matrix. For instance, EphA2 activation in PC3 prostate carcinoma cells leads to the recruitment of SH2 and further dephosphorylation of focal adhesion kinase (FAK), subsequently resulting in inactive conformation of integrins and decreased integrin-mediated adhesion (Miao et al. 2000).

Repulsion is one of the major tasks that are controlled by Eph / ephrin (Fuller et al. 2003). In general, after the initial attraction, cell attachment to each other and to the extracellular matrix can be reduced, causing a retraction between Eph- and ephrin-expressing cells. One of the mechanisms that convert initial cell adhesion into cell detachment is endocytosis (Figure 6). Eph / ephrin complexes together with fragments of the surrounding membrane derived from both cells are internalized in form of vesicles containing supposedly also associated proteins, which initiate signaling pathways (Egea and Klein 2007). The second known strategy is proteolytic cleavage of the ephrin. Several types of proteolytic enzymes cut the ephrin extracellular domain such as ADAM10 (a disintegrin and metalloprotease 10) activated by EphA3 / ephrin-A2 complex or serine proteases of the rhomboid family that cut ephrin-B (Hattori et al. 2000; Pascall and Brown 2004).

The outstanding mode of action between Eph receptors and their ligands leads to diverse biological effects. Repulsion was reported to navigate the growth cone of extending axons and outgrowth of collateral branches (Henkemeyer et

al. 1996). The axon pathfinding modulated by Eph molecules is *i.a.* significant for the establishment of proper connections in the developing retinotectal projection. Furthermore, the mosaic expression of Eph molecules contributes to cell sorting by decreased attraction of the cells. Eph molecules support the segmentation by pattering distinct regions and preventing Eph cells from crossing into ligand-expressing cells areas. During embryogenesis, the process of cell sorting is a critical event to create rhombomere boundaries in the developing hindbrain (Gale et al. 1996).

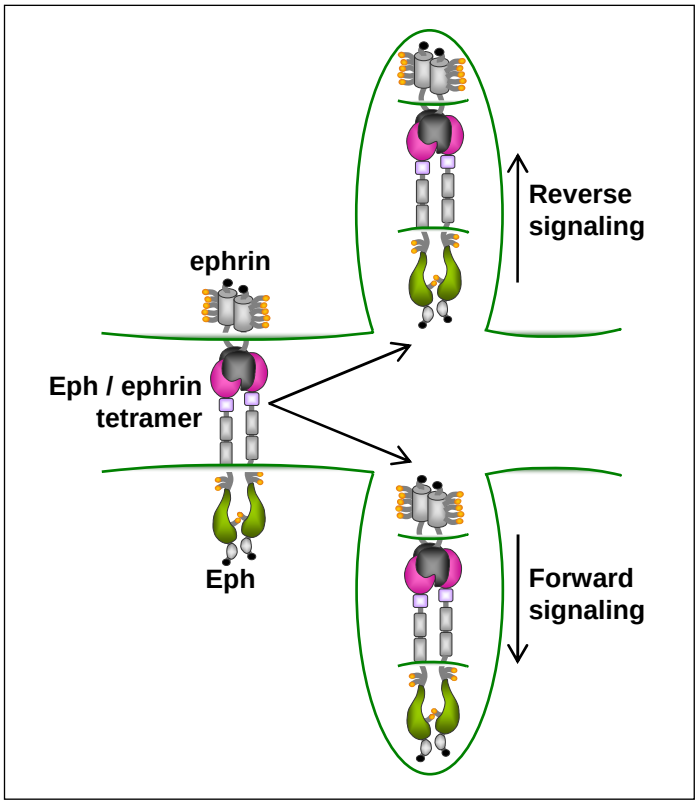

Figure 6. Internalization of the Eph / ephrin complex together with the surrounding plasma occurs via endocytosis. Vesicles can be internalized in both directions by the receptor- and ligand-expressing cell (Pasquale 2005).

1.2.4 Eph molecules are involved in angiogenesis

Eph were originally described as neuronal pathfinding molecules, but their functions are not restricted to the nervous system. Eph receptors and ephrins

were later found to be also involved in the directed growth, maturation and remodeling of the blood vessel system. The prominent function has EphB4 **/** ephrin-B2 interaction partners, which more than other Ephs control the cardiovascular development. EphB4 receptor is expressed only in venous endothelial cells, while the ligand ephrin-B2 is restricted to arterial endothelial cells and mesenchymal supporting cells (Wang et al. 1998). Repulsive and propulsive mechanisms segregate ligand and receptor expressing cells and prevent cell intermingling. It has been shown *in vitro* that EphB4 can mediate anti-adhesive and repulsive activities, while ephrin-B2 promotes opposite effects on adhesion and migration (Fuller et al. 2003; Hamada et al. 2003). Activation of EphB4 increases EC migration and proliferation via stimulation of phosphatidylinositol 3-kinase (PI3K) and phosphorylation of serine **/** threonine-specific kinase Akt **/** PKB (Steinle et al. 2002).

The EphB **/** ephrin-B system is a crucial and rate-limiting regulator of arterio-venous differentiation during the embryonic vascular development. These findings correspond to genetic loss of function experiments in mice. Targeted disruption of the EphB4 receptor gene results in lethality at day E9.5–10 of the embryonic development due to various cardiovascular defects (Gerety et al. 1999). The primitive vessels are present, but they fail to remodel into a mature network, because of the disrupted arterial-venous boundaries. Additionally, the knockout of ephrin-B2 with a similar phenotype as EphB4 mutation was reported (Wang et al. 1998; Adams et al. 1999). The expression of ephrin-B2 in pericytes and smooth muscle cells suggested that they may also play a role in vessel maturation and stabilization. The genetic disruption of other EphB receptors did not reveal vascular defects. Hence, EphB4 was brought into focus of developmental and pathological angiogenesis research.

1.2.5 EphB4 in tumor progression

The receptor tyrosine kinase EphB4 (also known as HTK, MYK1, TYRO11) and its ligand ephrin-B2 (Lerk-5, Eplg5, Htk-L, EFNB2) are important regulators of vascular development during embryogenesis as already described, but also

during vascularization of malignant tumors. Human tumor tissue examinations demonstrated EphB4 overexpression in various tumor types. Its up-regulation can promote, but in some cases reduce the tumorigenicity. In particular, an increased level of EphB4 was found in several human breast cancer specimens and most of the cell lines. The up-regulation is elicited by EphB4 gene amplification located in a region 7q22 that is known to be frequently amplified in mammary tumors (Kumar et al. 2006). Few signaling pathways additionally raise the level of EphB4, such as EGFR family via PI3K-Akt and Janus kinase - signal transducers and activator of transcription (JAK-STAT).

Overexpression of EphB4 is also present in the prostate, bladder, ovarian cancer, where the enhanced level of EphB4 expression correlates with tumor malignancy and metastasis occurrence (Xia et al. 2005b; Xia et al. 2006; Kumar et al. 2007). Moreover, EphB4 is up-regulated in endometrial hyperplasia and carcinomas, mesothelioma and melanoma (Berclaz et al. 2003; Xia et al. 2005a; Huang et al. 2007). Targeted knockdown of EphB4 using small interfering RNA and antisense oligodeoxynucleotide in ovarian, prostate, mammary and bladder cancer demonstrated reduced cell proliferation, migration and invasion as well as increased apoptosis via activation of caspase-8 pathway. Down-regulation of EphB4 significantly decreased growth of tumor xenografts and the microvascular density.

The mechanisms of tumorigenic activity of EphB4 are under investigation. EphB4 expressed on the cancer cells surface, stronger in the border regions of the tumor mass interacts with ephrin-B2 on the EC, pericytes and smooth muscle cells, enhancing angiogenesis and thereby tumor growth. This is regulated by the ligand reverse signaling and is independent on the receptor kinase activity (Noren et al. 2004). Furthermore, EphB4 can directly promote cancer malignancy and facilitate migration of tumor cells by inducing degradation of surrounding matrix proteins via regulation of matrix metalloproteases, MMP2 and MMP9 (Kumar et al. 2006). Apparently, EphB4 can also inhibit cell migration in particular cancer cell types in ligand-independent matter, by down-regulation of β1-integrin, which is important for the survival and invasiveness of many tumors (Noren et al. 2009).

1.2.6 Therapeutic significance of EphB4

Accumulating evidence suggests that EphB4 is significantly involved in pathological angiogenesis, tumor growth and metastasis, and therefore presents a potential target for selective therapeutic applications. To support this hypothesis soluble fusion proteins containing the extracellular domain of EphB4 (sEphB4) were designed to antagonize EphB4 **/** ephrin-B2 interaction. Generated sEphB4–expressing A375 melanoma cell line demonstrated defective cell–cell contacts, reduced proliferation and higher apoptosis level *in vitro*, and also reduced vascularization and growth of tumors in murine xenograft model (Martiny-Baron et al. 2004). Further experiments demonstrated that sEphB4 blocks EphB4 **/** ephrin-B2 bidirectional signaling, thereby inhibiting angiogenic effect of VEGF and FGF-2 and tumor growth *in vivo* (Kertesz et al. 2006). These data evaluate receptor EphB4 as a target for vascular proliferative diseases and cancer.

To date, several strategies are being developed for EphB4 targeting, mainly for cancer treatment, summarized in the Figure 7. Numerous small molecular weight inhibitors have been identified, which target the ATP binding site in the intracellular kinase domain. Since the ATP binding site is a highly conserved region within RTKs, the most important challenge is to develop selective inhibitors. In this regard, a series of 2,4-bis-anilinopyrimidine derivatives have been reported as and potent EphB4 inhibitor (Bardelle et al. 2008). EXEL-7647, a spectrum-selective kinase inhibitor against EGFR, VEGFR2, HER2 and EphB4 showed strong, dose-dependent inhibition of tumor growth (Gendreau et al. 2007). Recently EXEL-7647 has entered the phase II clinical trials for Non-Small-Cell Lung Cancer. Another small compound JI-101 that inhibits VEGFR2, PDGFRb and EphB4 (Sharma et al. 2010) is currently under evaluation in phase I / II in patients with advanced solid tumors[1].

[1] Information on clinical trials was obtained from the National Institutes of Health Clinical Trials web site (www.clinicaltrials.gov).

Other strategy is competition for the EphB4 / ephrin-B2 interaction using molecules binding to the extracellular domain of the receptor. Phage display studies have identified a 12 aa long peptide TNYL-RAW that binds EphB4 with the nanomolar affinity (Koolpe et al., 2005). TNYL-RAW has sequence similarities to the G-H loop of ephrin-B2, the region responsible for binding to the receptor, so the peptide compete with the ligand and occupies the same hydrophobic cleft of EphB4 LBD. As the result of blocked ephrin-B2 / EphB4 bidirectional signaling, TNYL-RAW inhibits capillary-like tube formation in ECs, suggesting antiangiogenic potential of this peptide (Salvucci et al., 2006). Recently, ^{64}Cu-labeled TNYL-RAW peptide was analyzed as a radiotracer for detection of EphB4 in CT26 and PC3M tumor xenografts (Xiong et al. 2010).

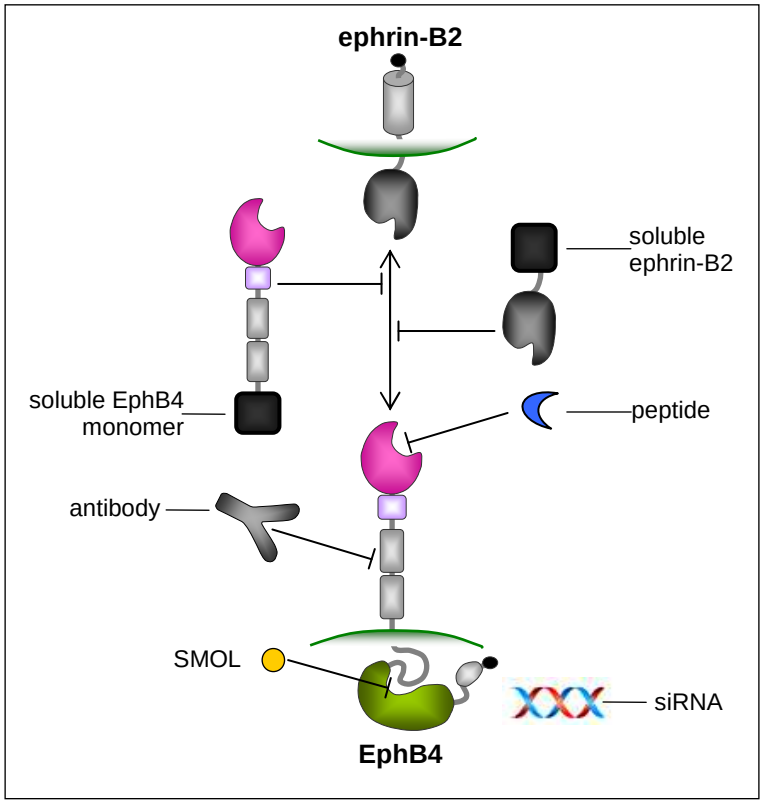

Figure 7. Potential anti-EphB4 strategies. Following agents were reported to inhibit forward and / or reverse signaling: multi-targeted tyrosine kinase inhibitors (SMOL), small interfering RNA (siRNA), antisense oligodeoxynucleotide (AS-ODN), soluble EphB4 or ephrin-B2, peptides and antibodies.

Two monoclonal EphB4-specific antibodies, with distinct mode of actions, were newly reported to have a significant antitumor activity in mouse xenografts models (Krasnoperov et al. 2010). One of these IgGs binds to the fibronectin type III repeat 2 of human and mouse EphB4, and thereby inhibits angiogenesis *in vitro* and *in vivo*, and tumor growth *in vivo*. Moreover, in combination with bevacizumab this antibody induces tumor regression. The second presented IgG induces receptor degradation and reduces proliferation of tumor cells by binding to the FN 1 domain of exclusively human EphB4.

EphB4 as a target has already attracted much attention, as shown by the variety of requested patent applications. A number of antibodies, peptides, polypeptides for the soluble extracellular domain, small compounds and polynucleotides have been claimed. Moreover, their therapeutic indications have been claimed mainly for treatment of cancer and angiogenesis-associated diseases. Selected molecules targeting EphB4 exhibit significant activity against both tumor and vasculature growth. However small molecules exhibit low specificity to the target and binders such as peptides presents low stability, since they undergo fast metabolic degradation. Therefore invention of new binders specifically recognizing the receptor EphB4 with antiangiogenic and antitumorigenic features poses a great challenge.

1.3 New generation of biologics

In the highly competitive pharmaceutical environment new drugs are expected to exhibit superiority over the existing treatment. An ideal drug aspires to have the following properties: high efficacy, safety, specificity and affinity for its target, and the appropriate pharmacokinetic profile would be an advantage. Moreover, the substance should be stable, low-cost in manufacture, easy to formulate and deliver. Due to the progress in protein engineering, diverse new formats of biologics with desired properties are being introduced. Several established *in vitro* display technologies substituted the immunization. During the past years numerous new molecules derived from non-immunoglobulin scaffolds have been discovered such as affibodies, avimers, adnectins,

anticalins and DARPins (Skerra 2007). They are collected in libraries, and thereby the specific binders can be extracted and evolved to drug candidates for therapy, diagnostics or research purposes. These antibody mimetics with various structure and characteristics stand in different phases of pre-clinical or clinical development. This chapter focuses on DARPins, a new generation of non-immunoglobulin biologics with a broad range of applications. The first molecule of this class is already under clinical investigation.

1.3.1 From natural to the designed ankyrin repeat protein

Designed Ankyrin Repeat Proteins (DARPins) are derived from natural ankyrin repeat (AR) proteins, which were found in all three kingdoms. In nature the main function of repeat domains is mediating protein-protein interactions (Bork 1993). AR are involved in diverse biologic tasks from cell–cell signaling, cytoskeleton organization, transcription and cell cycle regulation to development and inflammatory response reflecting their intracellular, membrane bound or extracellular localization (Li et al. 2006). Interestingly, no enzymatic activity has been reported for any ankyrin repeat proteins. AR have been found in the members of the INK4 family of tumor suppressors (p15, p16, p18, p19); transcriptional regulator IκBα, inhibitor of NF-κB and cytoskeleton regulator Ankyrin, present in human erythrocytes (reviewed in Mosavi et al. 2004).

A single AR domain has a relatively conserved L-shaped architecture. The 33 amino acid long motif is comprised of a ß-turn and two antiparallel α helices followed by a loop connected to the ß-turn of the next repeat (Figure 8 B). Consecutive repeats stack together forming an elongated and slightly curved domain with a hydrophobic core (Mosavi et al. 2004). Natural proteins contain usually between one and six repeats, but up to 30 AR motifs were observed. The crystal structure of several natural ankyrin domains has been solved.

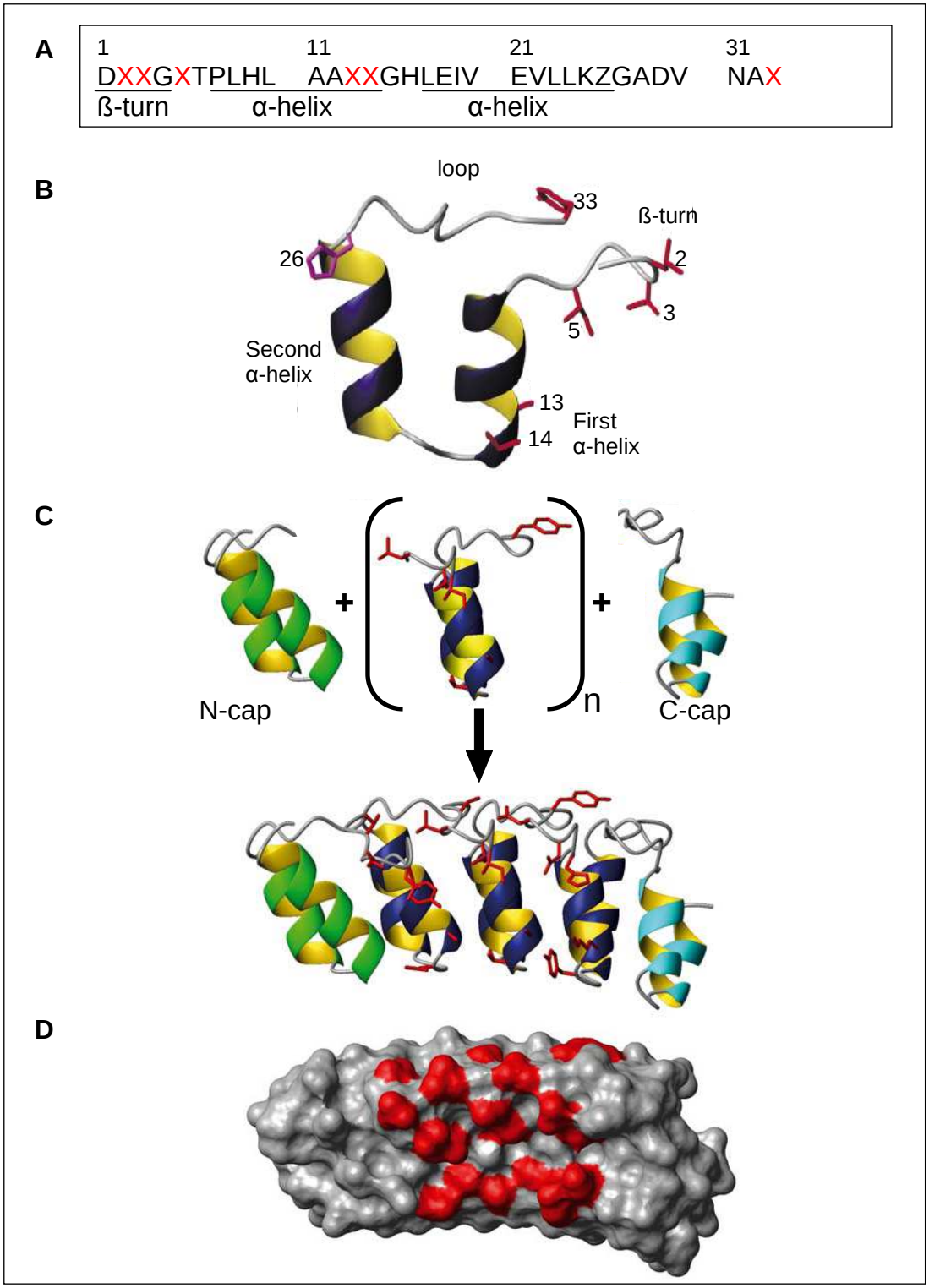

Figure 8. Modular architecture of DARPin. (A) The consensus sequence of a 33 aa long single repeat ankyrin module. X represents the potential interaction residues, which could be any amino acid except for G, C, and P. Z is a partly randomized position of the framework; it can be either N, H or Y. (B) The crystal structure of the ankyrin repeat with randomized positions highlighted in red and partly randomized position 26 in purple. (C) DARPin is composed of two caps (N- and C-) and several AR modules in between (n= 2-4). (D) The three

dimensional DARPin N3C with hydrophobic core and soluble amino acids on the surface. The randomized residues (highlighted in red) are arranged on the surface for the potential interaction with the target. (Forrer et al. 2003)

Based on the sequence alignment and structural analyses, the research group of Plückthun generated an artificial ankyrin repeat module (Kohl et al. 2003). Via consensus design they created a scaffold (Figure 8 A-B) with 6 variable residues integrated into the conserved framework, which is built of 27 amino acids (thereof 26 fixed and one can be either histidine, asparagine or tyrosine). The randomized regions can contain any amino acid except for proline and glycine, which are structurally unfavorable or cysteine, because it forms the disulfide bonds (Binz et al. 2003). The role of the framework is preserving the correct folding of the protein and exposing the variable residues on the surface for the interaction with a target. In the DARPin molecule, the defined number of internal repeats sealed by capping repeats forms a continuous hydrophobic core and a large solvent accessible surface. The sequence consists typically of two or three randomized modules flanked by N-terminal and C-terminal caps, designated N2C or N3C, respectively (Figure 8 C-D). In this manner, combinatorial DARPin libraries were generated with theoretical diversity for differing sequences of 10^{14} for N2C constructs or 10^{21} for N3C.

1.3.2 *In vitro* display technology

The rapid isolation of specific binders requires application of functional libraries with high diversities and a compatible selection technique. The *in vitro* display technology is a powerful tool for the generation of biologics with desired affinities and properties (Sergeeva et al. 2006). In phage display, the protein is displayed on the surface of a filamentous phage particle as a fusion protein with the minor coat protein III (pIII), whereby the respective DNA fragments are fused to the protein III gene of the phage virion (Paschke 2006). The power of the phage display lies in the stable linkage between genotype and phenotype and the robustness of the phage particle. This allows selection of binders in the

complex environment, particularly in the presence of detergents. The limiting factor of this technology is the bacterial transformation, which restricts the diversity of the initial library to 10^{10} members (Steiner et al. 2008).

The combinatorial libraries of ankyrin repeat proteins are either ribosome or phage displayed. The phage DARPin library is based on the phagemid vector that provides display of the protein of interest (POI) on the surface of a filamentous bacteriophage, which infects *Escherichia coli*. Using the co-translational signal recognition particle (SRP) pathway, the POI is translocated as a pIII fusion protein across the cytoplasmic membrane of *E. coli*. This allows an efficient display of fast-folding and stable proteins (Steiner et al. 2006).

1.3.3 DARPins properties

The process of rapid selection and production of DARPins have been developed. The selected library members were reported to have very favorable biophysical properties required for biotechnological applications (Binz et al. 2003; Binz et al. 2004). Expression of soluble DARPins can be performed in the cytoplasm of *Escherichia coli* in the low expressor strain XL1-blue at high levels reaching 200 mg/liter purified protein in simple shake flask cultures. Proteins were obtained using an immobilized metal ion affinity chromatography in a single purification step. Very characteristic for DARPins is the lack of disulfide bonds enabling their functionality in the intracellular reducing environment (Amstutz et al. 2005). The single domain and cysteine-free structure remains stable and monomeric in solution. DARPins reveal high thermodynamic stability with midpoints of denaturation above 66 ℃, which allows increased sample concentration and advanced formulation or lyophilization (Wetzel et al. 2008). Essentially for the clinical applications, DARPins are stable over weeks in serum at 37 ℃ (Za hnd et al. 2010). Due to the robust biophysical properties, DARPins can be fused to diverse action moieties. Conjugates with a toxin, cytokine, enzyme or radioactive isotopes offer further imaging or therapy possibilities.

The molecular weight of DARPin ranges from 14 to 21 kDa, depending on the number of composed modules, what has a great impact on the renal clearance, diffusion and capillary extravasation. Ten times smaller than a full IgG, DARPins are expected to have an improved tissue penetration compared to the antibody. On the other hand, DARPins are cleared through the kidney, resulting in a rather short serum half-life. However, attaching a polyethylene glycol (PEGylation) prolongs the circulation of DARPins (Zahnd et al. 2010). The modulation of molecule toward its adjusted pharmacokinetic allows achieving desired biological effect, such as maximal tumor accumulation.

1.3.4 Potential application of DARPins

Specific binders were isolated from the combinatorial libraries against a variety of proteins using the phage or ribosome display technology. Selected DARPins exhibit high specificity and affinity in the nanomolar to picomolar range, equal to that of antibodies. Moreover, upon binding they stabilize the protein conformation and facilitate crystallization. The first reported crystal structure of DARPin in complex with the target *E. coli* maltose binding protein determined by the X-ray crystallography revealed the character of binding (Figure 9). The randomized surface mediates the interaction with the target as designed (Binz et al. 2004).

The high specificity of DARPins along with their cytoplasmatic activity initiated selection of several binders against the intracellular MAP-kinase or caspase-2, which can be useful for the study on their signaling pathways in the natural environment (Amstutz et al. 2006; Schweizer et al. 2007). Interestingly, the caspase-2 binder showed very specific binding and an allosteric mechanism of inhibition. This finding can be exploited for the design of inhibitory compounds to interfere the apoptosis and inflammation processes, regulated by caspase-2.

Several DARPins are evaluated for potential medical applications. The most advanced is a DARPin-based VEGFA antagonist, which is under clinical investigation for the treatment of diabetic macula edema and wet age related

macular degeneration[2]. In the first instance the studies assess the efficacy, safety and tolerability after intravitreal injection. The common objective for monoclonal antibodies and biologics is targeting of tumor markers. DARPins have been selected against human epidermal growth factor receptor (HER2 **/** ErbB2), which is a breast cancer therapeutic target (Zahnd et al. 2006). HER2 overexpression in breast and ovarian cancer correlates with an aggressive tumor phenotype and poor prognosis for the patient. Specific HER2 DARPins with affinities in low nanomolar to picomolar range, have been evaluated as a diagnostic tool in both *in vitro* and *in vivo* tumor-targeting experiments (Zahnd et al. 2010). The affinity of binders correlated strongly with the tumor accumulation. DARPins demonstrated good penetration throughout the tumor mass and efficient pharmacokinetic, and therefore they could serve for delivering high levels of drug to the site of tumor.

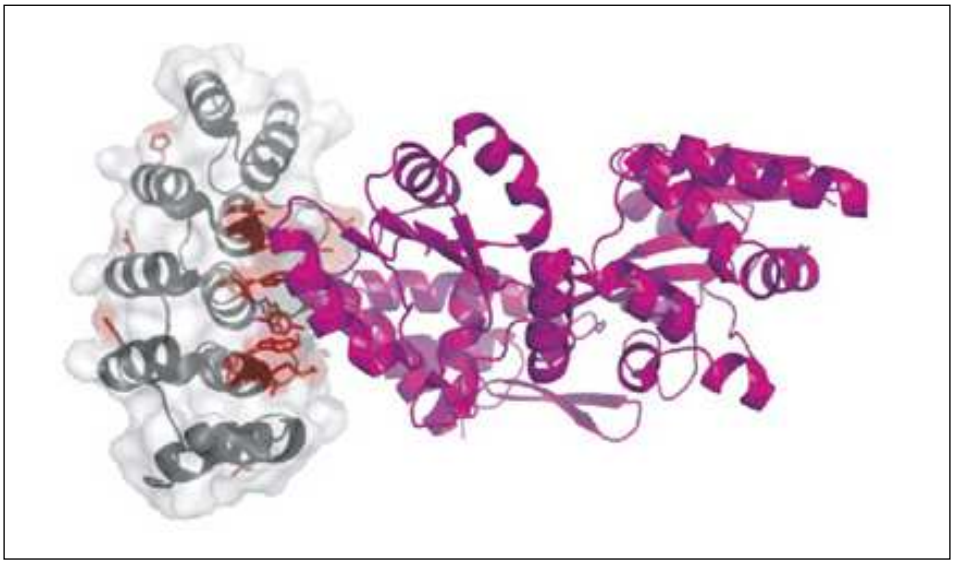

Figure 9. Crystal structure of DARPin off7 in complex with maltose binding protein. Target protein is colored in purple and DARPin protein in grey. The binding interface of DARPin is depicted in red (Binz et al. 2004).

[2] Information on clinical trials was obtained from the National Institutes of Health Clinical Trials web site (www.clinicaltrials.gov).

The number of DARPins isolated against a broad range of targets is growing. The published binders exhibit favorable properties such as specificity, affinity and stability. The described advantages, such as rapid selection, facilitated production and formulation possibilities propose DARPins for the pharmaceutical usage. DARPins are already successfully implemented in biomedical research. Alternatively to antibodies, DARPins are used in variuos immunoassays such as ELISA, flow cytometry, western blot and immunochemistry. In the field of therapeutic application, further studies addressing pharmacokinetic, efficacy, biodistribution and immunogenicity of DARPins are necessary to confirm their *in vivo* potential.

1.4 Aims of the PhD thesis

The future of cancer treatment is personalized medication and combination therapy. This requires well validated targets, specific biomarkers and selective drugs. Biologic agents have been already successfully implemented for the targeted cancer therapy and diagnostics. Beside antibodies, most current approaches aim to select alternative binding molecules. EphB4 receptor was shown to be involved in the process of angiogenesis and cancer progress. Several EphB4 inhibitors such as antibodies, peptides and small molecules have been identified, and the last is under evaluation in clinical trials. Small molecules exhibit rather low specificity to EphB4, and binders such as peptides undergo fast metabolic degradation. Therefore, this thesis addresses the implementation of Designed Ankyrin Repeat Proteins (DARPins) as novel binding molecules against EphB4 receptor.

The aim of this research was to generate EphB4 receptor binding proteins from a DARPin phage library and further characterize them. Initially, the focus of the studies was on the isolation of binders and investigation of their specificity and affinity. After selection of high quality binding molecules, the first purpose was to find a receptor inhibitor and investigate its mechanism of action. Therefore, several functional assays (flow cytometry, competitive binding analysis, kinase phosphorylation) were performed to analyze the cellular consequences of DARPins on the EphB4 expressing cells. It was of particular interest to identify a candidate exerting direct effects on angiogenesis, which was analyzed *in vitro* and *in vivo*. Selected DARPins could be of advantage in patients with highly vascularized tumors and possibly also in other diseases with increased angiogenesis such as diabetic retinopathy or psoriasis.

Additionally, the second strategy was followed, focused on the selection of EphB4 binders for conjugation to a toxin as antibody drug-conjugates. Specific EphB4 DARPins complexed with a toxin could be used as direct inhibitor of tumor cells proliferation (internalization analysis). Consequently, these DARPins present therapeutic candidates targeting EphB4 with a broad spectrum of potential applications, such as agents for the delivery of cytotoxic

drugs to the tumor site. Moreover, EphB4 binders could be further evolved as diagnostic agents for prognosis or monitoring of tumor growth and treatment.

The third aim of this study was the design of EphB4 DARPins for research on the receptor. Although EphB4 is a well established tumor target, there are still several unrevealed questions about EphB4 function and signaling. Therefore, specific binders will allow a better insight into the biology and role of EphB4 in cancer. Here, the goal was to isolate and characterize binders against the intracellular domain of EphB4. The study was designed to evaluate DARPins for immunoprecipitation of the receptor and phosphorylation analysis. As a consequence, DARPins could help to better understand the molecular mechanism of EphB4 activation and identification of potential interaction partners of the signaling pathway. This might lead to further identification of new targets for tumor therapy or biomarkers.

This thesis evaluates EphB4 DARPins as a potential drug and research tool. Moreover, these studies should support the analysis of EphB4 as antiangiogenic target and the underlying mechanisms. Thus, the results of the dissertation will contribute to preclinical development of targeted therapeutics to halt angiogenesis and tumor growth.

1.5 Thesis structure

The first part describes the initial work in selecting of binding molecules from the DARPin library. The extracellular domain of EphB4 was chosen as a target protein. Using phage display method specific binders were enriched, followed by their isolation and characterization. Identified DARPins were analyzed in binding assays to determine their affinities and binding sites.

In the second part the cellular activity of the DARPin was demonstrated. Various *in vitro* assays were performed: flow cytometry, tube formation assay, kinase activation assay. The effects of selected binders on EphB4 phosphorylation in the absence and presence of ephrin-B2, on the tube formation of endothelial cells and on the formation of blood vessels *in vivo* was studied. In parallel, selected DARPins were evaluated as a toxin conjugate by the internalization analysis.

The third part focused on the binders against the intracellular domain of EphB4 and establishing of functional assays for the research on the receptor. Finally, the potential application of EphB4 binding DARPins was discussed as an antiangiogenic factor and cancer therapeutic or for diagnostic applications.

I. Selection of DARPins against extracellular domain of EphB4 (presented in chapter 3.2 – 3.3)

II. Functional characterization of isolated EphB4 binders as antiangiogenic agent and direct antitumor strategy (chapter 3.4.6)

III. Selection of DARPins against intracellular domain of EphB4 and their characterization (presented in the Appendix 5.2)

2 MATERIALS AND METHODS

2.1 Materials

2.1.1 Phage display and bacterial work reagents

– 2 M TrisBase (neutralization buffer): Tris (242.2 mg/ml) sterile filtered (where indicated sterile filtration was performed through a 0.22 µm filter), stored at RT; Merck (Darmstadt; Germany)

– 200 mM Glycine-HCl pH 2.0 (elution buffer): glycine (15 mg/ml) adjusted with HCl to pH 2, sterile filtered, stored at RT; Calbiochem (San Diego, CA; USA)

– 2YT medium (2× Yeast-Tryptone): 31 g/l solved in double distilled water (ddH_2O), autoclaved, stored at RT; Invitrogen (Carlsbad, CA; USA)

– 2YT/Cam agar plates: 31 g/l 2YT medium, 1.5% (w/v) agar solved in ddH_2O, autoclaved, cooled to 60 °C, supplemented with 34 µg/ml Cam, poured to 10 cm ø petri dishes, stored at 4 °C

– 2YT/Cam: 2YT medium supplemented with 34 µg/ml Cam (prepared on the day of usage)

– 5× PEG / NaCl solution: 20% (w/v) polyethylene glycol (PEG) 6000 dissolved in warm 2.5 M NaCl, stored at 4 °C; Merck (Darmstadt; Germany)

– Agar Select powder; Invitrogen (Carlsbad, CA; USA)

– Ampicillin (Amp) sodium salt; stock solution: 50 mg/ml dissolved in ddH_2O, sterile filtered, stored at -20 °C; Sigma-Aldrich (Saint Louis, MO; U SA)

– Chloramphenicol (Cam) stock solution: 34 mg/ml dissolved in ethanol 70%, sterile filtered, stored at -20 °C; Calbiochem (San Diego, CA; USA)

– Glucose (Glu) 40% (w/v) stock solution: 400 mg/ml glucose dissolved in ddH_2O, sterile filtered, stored at RT; Sigma-Aldrich (Saint Louis, MO; USA)

– Glycerol 87%; Merck (Darmstadt; Germany)

– IPTG (Isopropyl-β-D-thiogalactopyranosid) stock solution: 1 M dissolved in ddH_2O, sterile filtered, stored at -20 °C; Calbiochem (San Diego, CA; USA)

– LB medium (Lysogeny Broth): 20 g/l solved in ddH_2O, autoclaved, stored at RT; Invitrogen (Carlsbad, CA; USA)

– LB/Glu/Amp agar plates: 20 g/l LB medium, 1.5% (w/v) agar, 1% (w/v) glucose solved in ddH_2O, autoclaved, cooled to 60 °C, supplemented with 5 0 µg/ml Amp, poured into ø 10 cm petri dishes, stored at 4 °C

– LB/Glu/Amp medium: LB medium supplemented with 1% glucose and 50 µg/ml Amp (prepared on the day of usage)

– TG-1; Stratagene (La Jolla, CA; USA)

– VCSM13 helper phage; Stratagene (La Jolla, CA; USA)

– XL-1 Blue, electroporation competent cells; Stratagene (La Jolla, CA; USA)

2.1.2 Enzymes and reagents for cloning

– 3 M sodium acetate pH 5.2; Merck (Darmstadt; Germany)

– 5-fold Orange G Loading Buffer; Trevigen (Gaithersburg, MD; USA)

– Agarose electrophoresis grade; Invitrogen (Carlsbad, CA; USA)

– DNA Typing Grade TAE Buffer (50×); Invitrogen (Carlsbad, CA; USA)

– Ethanol; Merck (Darmstadt; Germany)

– Ethidium bromide (10 mg/ml); Roth (Karlsruhe, Germany)

– Isopropanol; Merck (Darmstadt; Germany)

– Molecular weight markers: 1 Kb DNA Ladder, Low DNA Mass Ladder; Invitrogen (Carlsbad, CA; USA)

– N-butanol; Sigma-Aldrich (Saint Louis, MO; USA)

– NEB T4 DNA Ligase Reaction Buffer (10×); New England Biolabs (Ipswich, MA; USA)

– NEBuffer 2 (10×); New England Biolabs (Ipswich, MA; USA)

– NEBuffer for BamHI (10×); New England Biolabs (Ipswich, MA; USA)

– Nuclease-free water; Invitrogen (Carlsbad, CA; USA)

– Phagemid vector pMPAG3 (see Appendix 5.3.1); Molecular Partners (Zurich; Switzerland)

– Phagemid vector pMPAG6 (see Appendix 5.3.2); Molecular Partners (Zurich; Switzerland)

– Purified BSA for BamHI (100×); New England Biolabs (Ipswich, MA; USA)

– QIAprep Miniprep Kit with Vacuum Manifold system; Qiagen (Venlo; Netherlands)

– QIAQuick Gel Extraction Kit; Qiagen (Venlo; Netherlands)

– Restriction enzyme BamHI (20 U/µl); New England Biolabs (Ipswich, MA; USA)

– Restriction enzyme HindIII (20 U/µl); New England Biolabs (Ipswich, MA; USA)

– T4 DNA Ligase (20 U/µl); New England Biolabs (Ipswich, MA; USA)

2.1.3 Reagents and buffers for protein purification

– 10% Triton X-114 solution; Sigma-Aldrich (Saint Louis, MO; USA)

– Acetic acid, 25% glacial acetic acid in water; Merck (Darmstadt; Germany)

– BisTris buffer 25 nM; pH 6.7; Sigma-Aldrich (Saint Louis, MO; USA)

– B-PER Bacterial Protein Extraction Reagent; Pierce (Rockford, IL; USA)

– Bradford's protein assay dye reagent; Bio-Rad (Hercules, CA; USA)

– BSA protein standard (2 mg/ml) for serial dilution; Sigma-Aldrich (Saint Louis, MO; USA)

– Gel filtration molecular weight markers; Sigma-Aldrich (Saint Louis, MO; USA)

– Imidazole, stock solution 5 M (292.2 g/l) freshly prepared; Merck (Darmstadt; Germany)

– Nickel / NTA Sepharose 6 Fast Flow; GE Healthcare (Little Chalfont; UK)

– PBS with 0.005% Tween 20, sterile filtered (gel filtration running buffer)

– QCL-1000 Chromogenic Limulus Amebocyte Lysate (LAL) Endpoint Assay; Cambrex (East Rutherford, NJ; USA)

– TBSN buffer 50 mM TrisHCl, 0.4 M NaCl; adjusted with HCl to pH 7.4

2.1.4 Reagents and buffers for SDS-PAGE and Western blot

– 10% SDS; Invitrogen (Carlsbad, CA; USA)

– ATX Ponceau S red staining solution; Sigma-Aldrich (Saint Louis, MO; USA)

– Imperial Protein Stain; Pierce (Rockford, IL; USA)

– MagicMark XP Western Protein Standard; Invitrogen (Carlsbad, CA; USA)

– NuPage LDS Sample Buffer (4×); Invitrogen (Carlsbad, CA; USA)

– NuPage MES SDS Running Buffer (20×); Invitrogen (Carlsbad, CA; USA)

– NuPage MOPS SDS Running Buffer (20×); Invitrogen (Carlsbad, CA; USA)

– NuPage Novex 4–12% Bis-Tris Gel 1.0 mm, 10-15 well; Invitrogen (Carlsbad, CA; USA)

– NuPage Sample Reducing Agent (10×); Invitrogen (Carlsbad, CA; USA)

– SeeBlue Pre-Stained Standard; Invitrogen (Carlsbad, CA; USA)

– SuperSignal West Dura Extended Duration Substrate; Pierce (Rockford, IL; USA)

– Transfer buffer (10×): 144 g Glycine, 29 g Tris in 1 l ddH_2O
  Transfer solution: 100 ml 10× Transfer buffer, 0.1% SDS, 200 ml methanol, 690 ml ddH_2O

2.1.5 Buffers and reagents for binding assays (ELISA, FACS, IP, SPR)

– 0.1 M N-hydroxysuccinimide (NHS); GE Healthcare (Little Chalfont; UK)

– 0.4 M 1-ethyl-3-(3-dimethylaminopropyl)-carbodiimide (EDC); GE Healthcare (Little Chalfont; UK)

– 1 M ethanolamine-HCl, pH 8.5; GE Healthcare (Little Chalfont; UK)

– 10 mM sodium acetate pH 4.5; pH 5.0 and pH 5.5; GE Healthcare (Little Chalfont; UK)

– 25 mM Hepes pH 7.0; pH 7.5 and pH 8.0; GE Healthcare (Little Chalfont; UK)

– 25 mM MES pH 5.5; pH 6.0 and pH 6.5; GE Healthcare (Little Chalfont; UK)

– Albumin from bovine serum (BSA); Sigma-Aldrich (Saint Louis, MO; USA)

– BM Chemiluminescence ELISA substrate 3-aminophthalhydrazide Roche (Basel; Switzerland)

– DARPin off7 (control DARPin); Molecular Partners (Zurich, Switzerland)

– DARPin AB11 against lysozyme (control DARPin); Molecular Partners (Zurich, Switzerland)

– Dulbecco's Phosphate Buffered Saline solution with Ca2+, Mg2+ (PBS^{++}); Invitrogen (Carlsbad, CA; USA)

– Dulbecco's Phosphate Buffered Saline solution without Ca2+, Mg2+ (PBS); Biochrom (Berlin; Germany)

– FACS buffer: PBS supplemented with 0.5% BSA

– HBS-EP BIAcore running buffer; GE Healthcare (Little Chalfont; UK)

– Lysozyme from chicken egg white; Sigma-Aldrich (Saint Louis, MO; USA)

– PBS^{++} supplemented with 1% (w/v) BSA and 2% (w/v) milk (cell ELISA blocking buffer)

– PBST: PBS supplemented with 0.05% (v/v) Tween20

– PBSTB: PBST supplemented with 0.02% (w/v) BSA (ELISA blocking buffer)

– Protein G Sepharose 4 Fast Flow; GE Healthcare (Little Chalfont; UK)

– Sucofin non-fat dry milk powder; (Zevin; Germany)

– Tween20 (Polyoxyethylenesorbitan monolaurate); Sigma-Aldrich (Saint Louis, MO; USA)

2.1.6 Recombinant proteins

– ephrin-B2-Fc chimera (recombinant mouse ephrin-B2 with human Fc fusion, amino acids 1-227; R&D Systems (Minneapolis, MN; USA)

Extracellular domain (ECD) of EphB receptors:

– rEphB1-Fc ECD (rat EphB1 ECD with Fc fusion); R&D Systems (Minneapolis, MN; USA)

– mEphB2-Fc ECD (murine EphB2 ECD with Fc fusion); R&D Systems (Minneapolis, MN; USA)

– mEphB3-Fc ECD (murine EphB3 ECD with Fc fusion); R&D Systems (Minneapolis, MN; USA)

– hEphB4 ECD (human EphB4 ECD monomeric); R&D Systems (Minneapolis, MN; USA)

– hEphB4-Fc ECD (human EphB4 ECD with Fc fusion); Bayer (Leverkusen; Germany)

– mEphB4-Fc ECD (murine EphB4 ECD with Fc fusion); R&D Systems (Minneapolis, MN; USA)

– hEphB6-Fc ECD (human EphB6 ECD with Fc fusion); R&D Systems (Minneapolis, MN; USA)

– mEphB6-Fc ECD (murine EphB6 ECD with Fc fusion); R&D Systems (Minneapolis, MN; USA)

Intracellular domains (ICD) of EphB receptors:

– GE4S: GST-mEphB4-SAM protein (1.25 mg/ml); InVivo BioTech (Hennigsdorf, Germany)

– GE3S: GST-EphB3-SAM protein, (1.25 mg/ml); Bayer (Leverkusen; Germany)

– EphB1 ICD N-terminal His_6-tagged recombinant human EphB1; Millipore (Billerica, MA; USA)

– EphB2 ICD N-terminal His_6-tagged recombinant human EphB2; Millipore (Billerica, MA; USA)

– EphB3 ICD N-terminal His_6-tagged recombinant human EphB3; Carna Biosciences (Natick, MA; USA)

– EphB4 ICD N-terminal His_6-tagged recombinant human EphB4; Invitrogen (Carlsbad, CA; USA)

2.1.7 Primary and secondary antibodies

– ECL anti-mouse IgG HRP-linked antibody (Western blot); GE Healthcare (Little Chalfont; UK)

– Fluorescein isothiocyanate (FITC)-conjugated affinipure goat anti-human IgG+IgM (H+L) antibody; Jackson ImmunoResearch (West Grove, PA; USA)

– Fluorescein isothiocyanate (FITC)-conjugated affinipure goat anti-mouse IgG (H+L); Jackson ImmunoResearch (West Grove, PA; USA)

– Goat polyclonal anti-EphB4 N19; Santa Cruz Biotechnology (Santa Cruz, CA; USA)

– Goat-ZAP rabbit anti-goat IgG saporin-conjugated antibody,
Mab-ZAP goat anti-mouse IgG saporin-conjugated antibody,
Rab-ZAP goat anti-rabbit IgG saporin-conjugated antibody; Advanced Targeting Systems (San Diego, CA; USA)

– HRP-conjugated mouse anti-M13 monoclonal antibody; GE Healthcare (Little Chalfont; UK)

– Human anti-EphB4 HP63 Fab fragment (against EphB4 ECD); Bayer (Leverkusen; Germany)

– Mouse anti-c-myc monoclonal antibody (clone 9E10, 5 mg/ml); Roche (Basel; Switzerland)

– Mouse anti-EphB4 M01 monoclonal IgG2a; Abnova (Taipei; Taiwan)

– Mouse anti-EphB4 Receptor monoclonal $IgG_{1-\kappa}$ antibody; Zymed (San Francisco, CA; USA)

– Mouse anti-M13 monoclonal antibody; GE Healthcare (Little Chalfont; UK)

– Mouse anti-phosphotyrosine HRP-conjugated (clone 4G10TM); Millipore (Billerica, MA; USA)

– Mouse anti-phosphotyrosine HRP-conjugated monoclonal IgG2b antibody (clone PY20) applied for Western blotting; Sigma-Aldrich (Saint Louis, MO; USA)

– Mouse anti-RGS-His_4 monoclonal IgG_1 antibody (0.1 mg/ml); Qiagen (Venlo; Netherlands)

– Peroxidase-conjugated AffiniPure Goat Anti-Mouse IgG + IgM (H+L); Jackson ImmunoResearch (West Grove, PA; USA)

– Rabbit polyclonal anti-EphB4 (H-200); Santa Cruz Biotechnology (Santa Cruz, CA; USA)

– R-Phycoerythrin affinipure $F(ab')_2$ fragment goat anti-human IgG+IgM (H+L) antibody; Jackson ImmunoResearch (West Grove, PA; USA)

2.1.8 Animals and cell lines

– BALB/C Strain 028, 6–8 weeks old; Charles River Laboratories (Wilmington, MA; USA)

– HUVECs; American Type Cell Collection (ATCC; Manassas, VA; USA)

– MCF7; ATCC (Manassas, VA; USA)

– U-2 OS-hEphB4 (U-2 OS-713 clone #3 stably transfected with human EphB4 and C-terminally tagged with a myc and Streptavidin binding peptide); NMI (Reutlingen; Germany)

– U-2 OS; ATCC (Manassas, VA; USA)

2.1.9 Cell culture media and supplements

– Bovine insulin; Sigma-Aldrich (Saint Louis, MO; USA)

– Detach Kit for HUVECs: HEPES Buffered Saline, Trypsin / EDTA, Trypsin Neutralizing Solution; Promocell (Heidelberg; Germany)

– DMEM without phenol red, containing high glucose; Lonza (Basel; Switzerland)

– Endothelial Cell Growth Medium-2, SingleQuots kit (growth factors, cytokines and supplements); Lonza (Basel; Switzerland)

– Estradiol; Bayer (Leverkusen; Germany)

– FBS (Fetal bovine serum) heat inactivated for 30 min at 56 ℃; Biochrom (Berlin; Germany)

– L-glutamine; Biochrom (Berlin; Germany)

– RPMI-1640 without phenol red; Biochrom (Berlin; Germany)

2.1.10 Kits and reagents for cellular assays

– Alamar Blue assay; Invitrogen (Carlsbad, CA; USA)

– Angiokit Tubule Staining (mouse anti-human CD31, goat anti-mouse IgG alkaline phosphatase conjugate, BCIP / NBT substrate); TCS CellWorks (Buckingham; UK)

– Caspase-Glo 3/7 assay; Promega (Fitchburg, WI; USA)

– Cell lysis buffer: 50 mM Hepes pH 7.2; Sigma-Aldrich (Saint Louis, MO; USA);
150 mM NaCl; Merck (Darmstadt; Germany);
1 mM $MgCl_2$; Merck (Darmstadt; Germany);
1.5% Triton X-100; Sigma-Aldrich (Saint Louis, MO; USA);
10 mM $Na_4P_2O_7$; Sigma-Aldrich (Saint Louis, MO; USA);
100 mM NaF; Sigma-Aldrich (Saint Louis, MO; USA);
10% glycerol; Merck (Darmstadt; Germany);
and freshly added before the experiment per 25 ml:
500 µl phosphatase inhibitor cocktail II; Sigma-Aldrich (Saint Louis, MO; USA)
1 tablet complete proteinase inhibitor cocktail; Roche (Basel; Switzerland)

– FIX&PERM Cell Permeabilisation Solution; An der Grub (Kaumberg; Austria)

– Matrigel; Becton, Dickinson and Company (Franklin Lakes, NJ; USA)

– Paraformaldehyde 16% diluted with water 1:4; Alfa Aesar (Karlsruhe; Germany

– Prionex Reagent; Calbiochem (San Diego, CA; USA)

– PULSin; PolyPlus Transfection (New York, NY; USA)

– Staurosporine; Sigma-Aldrich (Saint Louis, MO; USA)

2.1.11 Kit and reagents for *in vivo* assay

– Brij 35 solution 30% (w/v); Sigma-Aldrich (Saint Louis, MO; USA)

– Collagenase / dispase enzymes (1 mg/ml); Roche (Basel; Switzerland)

– Directed In Vivo Angiogenesis Assay Kit; Trevigen (Gaithersburg, MD; USA)

– Drabkin's reagent; one vial was reconstituted with 1 l of ddH_2O and supplemented with 0.5 ml of the 30% Brij 35 Solution; Sigma-Aldrich (Saint Louis, MO; USA)

– Hemoglobin from bovine blood, 200 mg/ml; Sigma-Aldrich (Saint Louis, MO; USA)

– Ketavet 100 mg/ml diluted 1:2; Pfizer (New York, NY; USA)

– Xylazine (Rompun Vet I.M.) 2% diluted 1:10; Bayer (Leverkusen; Germany)

2.1.12 Disposables

– 48 well Costar, clear, tissue culture treated plate;
96-well Cellstar cell culture treated microplate, polystyrene, U-bottom, steril;
96-well flat clear bottom, black, polystyrene tissue culture treated plate;
96-well flat clear bottom, white, polystyrene tissue culture treated plate; Corning (Amsterdam; The Netherlands)

– 96-deep well U-bottom polystyrene plate; Thermo Fisher Scientific (Waltham, MA; USA)

– 96-well flat- bottom, clear, tissue culture treated microplates; TPP (Trasadingen; Switzerland)

– 96-well white plate Lumitrac 600, polystyrene, flat-bottom, Chimney plate;
96-well polystyrene, V-bottom, clear microplate; Greiner (Kremsmuenster, Austria)

– 96-well white polystyrene MaxiSorp plate; Nunc (Roskilde; Denmark)

– Blotting Filter Paper Whatman, 3 mm; GE Healthcare (Little Chalfont; UK)

– Blotting Filter Paper, 2.5 mm thick, 8.6 × 13.5 cm; Invitrogen (Carlsbad, CA; USA)

– Cell culture flask 300 cm^2, filter; TPP (Trasadingen; Switzerland)

– Cell culture flask 75 cm^2, 162 cm^2 filter; Corning (Amsterdam; The Netherlands)

– Centrifugal filter device Amicon Ultra 15 ml 5K; 4 ml 10K NMWL; Millipore (Billerica, MA; USA)

– Centrifugal filter device Microcon Ultracel YM-3 3000 NMWL; Millipore (Billerica, MA; USA)

– FACS tube 5 ml, round-bottom; Becton, Dickinson and Company (Franklin Lakes, NJ; USA)

– Gene Pulser Cuvette, sterile, 0.2 cm; Bio-Rad (Hercules, CA; USA)

– Handee Spin Cup Columns (Paper Membrane); Pierce (Rockford, IL; USA)

– Hyperfilm ECL (18 × 24 cm); GE Healthcare (Little Chalfont; UK)

– IMAC column 1 cm ø; Bio-Rad (Hercules, CA; USA)

– Invitrolon PVDF, filter paper 0.45 µm pore size 8.5 × 13.5 cm; Invitrogen (Carlsbad, CA; USA)

– Millex-GV 0.22 µm Syringe Driven Filter Unit; Millipore (Billerica, MA; USA)

– Millex-GV, syringe driven filter unit 0.22 µm, 4 mm; Millipore (Billerica, MA; USA)

– PD-10 prepacked desalting column; GE Healthcare (Little Chalfont; UK)

– Petrischale quadratisch with Nocken, 120 × 120 × 17 mm; Greiner (Kremsmuenster, Austria)

– QIAvac 6S Manifold- vacuum; Qiagen (Venlo; Netherlands)

– Sensor Chip CM5; GE Healthcare (Little Chalfont; UK)

– Slide-A-Lyzer Dialysis Cassette 3500 MWCO, 3-12 ml; Pierce (Rockford, IL; USA)

– Superdex 200 PC 3.2/30, 2.4 ml column; Pharmacia – GE Healthcare (Little Chalfont; UK)

2.1.13 Devices

– Cell counter: CASY Model TTC; Schärfe System (Reutlingen; Germany)

– Centrifuge: Jouan CR 4 22; Thermo Fisher Scientific (Waltham, MA; USA)

– Centrifuge: Megafuge 1.0R; Heraeus – Thermo Fisher Scientific (Waltham, MA; USA)

– Centrifuge: Sorvall RC 6, rotor SS-34; Thermo Fisher Scientific (Waltham, MA; USA)

– Chemi-imager: Image Station 440CF, Kodak 1D Image Analysis Software; Kodak digital science (Rochester, NY; USA)

– Chromatography facility: Biologic LP System; Bio-Rad (Hercules, CA; USA)

– Developer: Film Processor Curix 60; Agfa (Mortsel; Belgium)

– Digital photo camera; Nikon (Tokyo; Japan)

– Electroporation System: Gene Pulser II; Bio-Rad (Hercules, CA; USA)

– Flow cytometer: FACS Calibur, CellQuest Pro; Becton, Dickinson and Company (Franklin Lakes, NJ; USA)

– Incubation shaker for bacteria culture: Multitron; Infors HT (Bottmingen; Switzerland)

– Incubator for bacteria Heraeus 6000; Thermo Fisher Scientific (Waltham, MA; USA)

– Incubator for mammalian cells Heraeus BBD 6220; Thermo Fisher Scientific (Waltham, MA; USA)

– Inverse phase-contrast microscope; Zeiss (Oberkochen; Germany)

– Laboratory pH meter: Calimatic 761, Knick (Berlin; Germany)

– Laminar flow hood: Hera Safe; Thermo Fisher Scientific (Waltham, MA; USA)

– Luminescence and fluorescence microplate reader: Wallac Victor2; PerkinElmer (Waltham, MA; USA)

– Luminescence microplate reader: Victor light / Wallac 1420 Manager; Perkin Elmer (Waltham, MA; USA)

– Matrix multi channel pipette: 12.5, 250, 1250 µl; Thermo Fisher Scientific (Waltham, MA; USA)

– Power supply for electrophoresis: EPS 3501 XL; GE Healthcare (Little Chalfont; UK)

– SDS-PAGE electrophoresis and Western blotting equipment: XCell II SureLock Mini-Cell chamber with XCell II Blot Module and Sponge Pads; Invitrogen (Carlsbad, CA; USA)

– Shaker for microplates: Titramax 100; Heidolf (Kelheim; Germany)

– SMART-- Gel filtration system; Pharmacia – GE Healthcare (Little Chalfont; UK)

– Spectrophotometer: SmartSpec 300; Bio-Rad (Hercules, CA; USA)

– Spectrophotometer: NanoDropR ND-1000; Peqlab Biotechnologie (Erlangen; Germany)

– Spectrophotometer: Spectra Rainbow microplate reader; Tecan (Maennedorf; Switzerland)

– Surface plasmon resonance instrument: BIAcore 2000; GE Healthcare (Little Chalfont; UK)

– Table centrifuge 5415R; Eppendorf (Hamburg; Germany)

– Thermo cycler: Thermomixer compact; Eppendorf (Hamburg; Germany)

– Water bath: RM-6; MGW Lauda (Lauda-Koenigshofen; Germany)

2.1.14 Software

– BIA evaluation software 4.1; GE Healthcare (Little Chalfont; UK)

– CellQuest Pro; Becton, Dickinson and Company (Franklin Lakes, NJ; USA)

– EndNote 9.0; Thomson Reuters (New York, NY; USA)

– Graphpad Prism 3.0; GraphPad Software (La Jolla, CA; USA)

– Office 2003; Microsoft Corporation (Redmond, WA; USA)

– Particle analysis Software; Olympus (Tokyo; Japan)

– SigmaPlot Version 8.0; Systat (Chicago, IL; USA)

– SigmaStat Version 3.5; Systat (Chicago, IL; USA)

– Vector NTI Advance 10; Invitrogen (Carlsbad, CA; USA)

2.2 Display methodology

2.2.1 Phage display

Phage display is an *in vitro* method that allows selection of molecules with specific binding properties. EphB4 DARPins were isolated from a filamentous phage library (kindly provided by Molecular Partners; Zurich, Switzerland; Lot #1), with a diversity between 10^{10} and 10^{11} individual phage. The library constructs are based on the phagemid vector pMPAG3 (see Appendix 5.3.1 for the vector card). DARPin sequence is fused to the gene coding for the minor coat protein III (here named DARPin-pIII) and thereby displayed on the surface of filamentous phage particles after expression. Selection of DARPins was performed according to the scheme depicted in Figure 10. All reactions were carried out at room temperature (RT) unless indicated otherwise. Phage solution prior panning was incubated with BSA to a final concentration 0.2% in PBST for 0.5 h. The target protein hEphB4 ECD was immobilized in a 96-well MaxiSorp plate (50 µg/ml; 100 µl/well) and subsequently blocked with BSA (as described in 2.5.1). In the first selection cycle about 1.6×10^{13} phage particles of the library (1 ml) were exposed to the target coated in 10 wells. The later cycles were performed in 2 coated wells. The incubation was performed for 2 h to allow binding of phage to the target.

Then the phage supernatants were removed and the wells were washed three times with 300 µl PBST to remove the residual unbound phage particles. In the initial cycles washing was repeated three times. In the third cycle five washing steps increased the stringency of the selection. Bound phage were eluted with 100 µl/well of 200 mM glycine buffer pH 2 for 15 min. Eluates were pooled and neutralized with 90 µl 2 M TrisBase per ml of eluate. Selected phage were directly used for amplification in the *E. coli* culture as described in 2.2.3. Precipitated phage pool (2.2.5) was resuspended in 0.5 ml PBS, supplemented with 0.2% BSA and immediately applied to the next panning cycle. A total of three panning cycles was performed. After each panning cycle phage titers were determined for monitoring the enrichment (as described in 2.2.3).

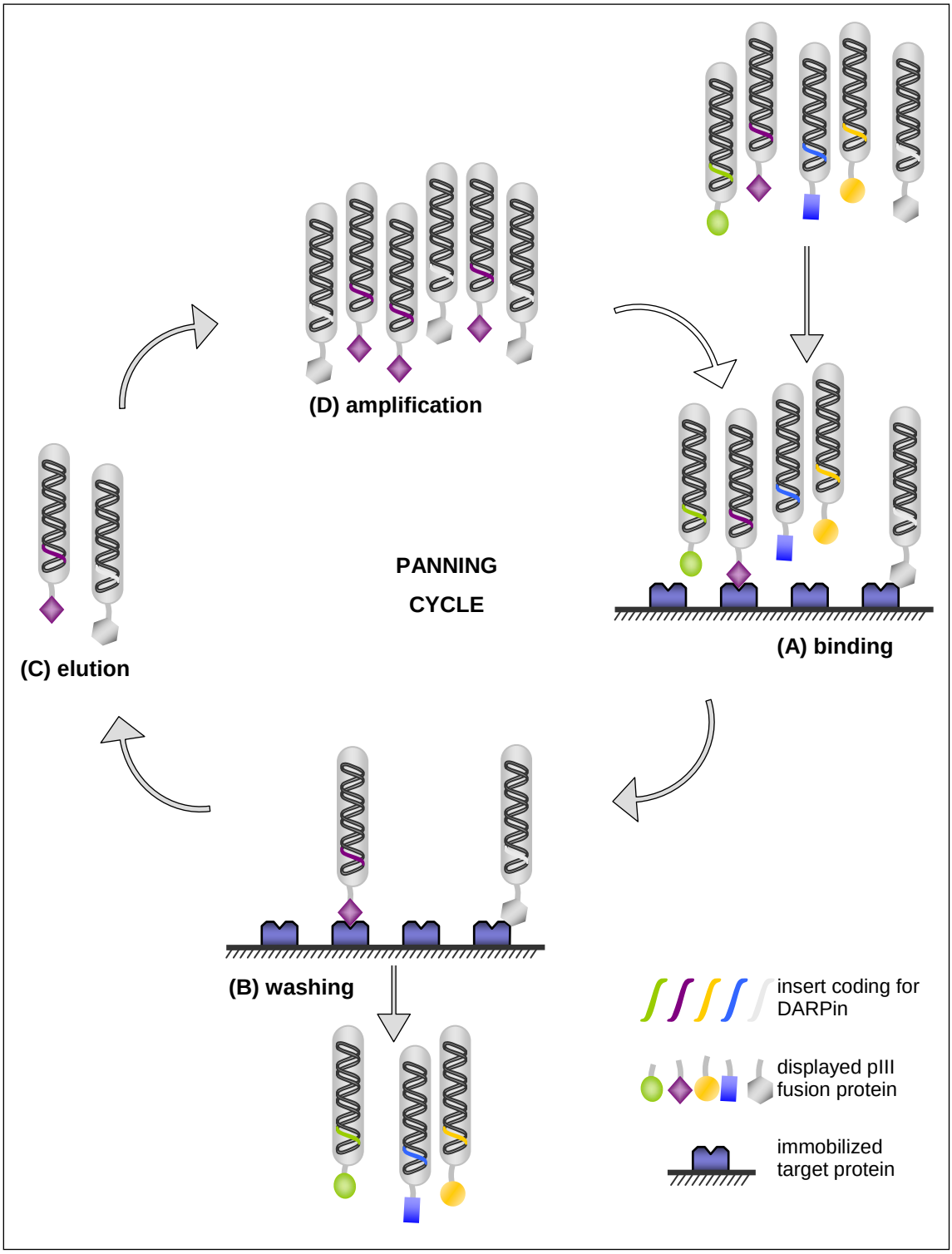

Figure 10. Schematic diagram of a DARPin phage display selection cycle. (A) A phage library displaying various DARPin proteins on the surface dependent on the cloned DARPin sequence is exposed to the immobilized target. (B) After a certain incubation time unbound phage particles are removed. (C) Bound phage are eluted at a low pH. (D) The isolated pool of phage is amplified and can be used for further panning cycles.

2.2.2 Bacterial culture

Escherichia coli TG1 laboratory strain was used for the propagation of phage carring pMPAG3. Bacteria, inoculated from the agar plates cultures were grown in 2YT medium in orbital shaker at 180 rpm and 37 °C. The bacterial growth was determined by measuring the optical density at 600 nm (OD_{600}). The selection of plasmid cultures was performed using 34 µg/ml Cam. Bacteria grown on the agar plates were incubated inverted at 37 ℃ for 24 h. Permanent preservation of clones was done by inoculation with single colonies from agar plates, growing overnight and storing at -80 ℃ in 2YT/Cam supplemented with 15% (v/v) glycerol. The *E. coli* XL1-blue strain was used for the propagation of pMPAG6. For DARPin expression bacteria were grown using a LB medium with 1% glucose addition (LB/Glu). The selection of a plasmid cultures was performed in medium supplemented with 50 µg/ml ampicillin (LB/Glu/Amp).

2.2.3 Pool phage amplification

Selected phage were amplified by inoculation of 10 ml TG-1 bacteria grown to an OD_{600} of 0.4–0.6 with the collected phage eluate and incubation for 1 h at 37 ℃. Phage output titers were determined by incu bating 100 µl of serial dilutions of the infected culture above (1:10 to 1:10000) on 2YT/Cam agar plates for 24 h and calculation from the colonies grown (cfu/ml). New phage particles were generated by dilution of 1 ml of the infected culture above with 2YT/Cam selection medium to an initial OD_{600}=0.1 and incubating the culture until an OD_{600} of 0.5 was reached. Then IPTG was added to 0.2 mM and VCSM13 helper phage to 10^{10} pfu/ml final concentrations and incubation was continued overnight at 30 ℃ with shaking. Amplifi ed phage from the overnight culture were precipitated (as described in 2.2.5). The reminder of the infected culture was incubated overnight in the presence of Cam at 34 µg/ml, subsequently supplemented with 15% (v/v) glycerol and stored as stock at -80 ℃. For the phage pool ELISA culture was inocu lated from the glycerol stock in 5 ml 2YT/Cam medium and grown as described above to analyze the enrichment of selection cycles.

2.2.4 Isolation and amplification of a single phage clone

For the isolation and amplification of a single phage clone 10 µl of a culture infected with the enriched phage eluate at the end of the third panning cycle was spread on 2YT/Cam agar plates and grown overnight at 37 ℃. For screening purpose, individual colonies were randomly picked and inoculated into 160 µl/well of 2YT/Cam medium in a 96-well plate. The culture plate covered with a gas permeable adhesive seal was incubated for 4 h in an orbital shaker at 37 ℃. 10 µl of the culture was transferred into new 96-well culture plate (master plate) containing 140 µl/well of fresh 2YT/Cam medium. The master plate was incubated overnight in a moist chamber at 30 ℃ with shaking, supplemented with 15% (v/v) glycerol and stored as stock at -80 ℃. The residual culture plate was induced with 50 µl/well of the 2YT/Cam supplemented with IPTG and VCSM13 helper phage to reach end concentrations of 0.2 mM and 10^{10} pfu/ml respectively. The plate was incubated overnight in a moist chamber at 30 ℃ with shaking and centrifuged for 1 0 min at 3000 × *g*. 150 µl phage supernatants supplemented with 0.2% BSA in PBST were analyzed by phage ELISA (as described in 2.5.2). Selected as positive clones, single phage clones were inoculated from the master plate in 10 ml 2YT/Cam to prepare glycerol stocks (as described in 2.2.3).

2.2.5 Phage precipitation and purification

Overnight cultures were pelleted by centrifugation for 10 min at 16000 × *g* and 4 ℃. Phage were precipitated from the supernatant by addition of one-fifth volume cold PEG / NaCl solution (2.1.1). After incubation on ice for 1 h precipitated phage were collected by centrifugation for 10 min at 6000 × *g* and 4 ℃. Pellets were resuspended in 0.5 ml PBS and t he insoluble material was removed by centrifugation for 10 min at 20000 × *g* and 4 ℃ in table top centrifuge. The absorbance of a phage suspension was measured at OD_{268} and the phage concentrations were calculated based on 1 OD_{268} equals 5×10^{12} phage/ml. Purified phage pool was immediately applied in the next panning cycle or phage ELISA analysis.

2.3 Molecular biological methods

2.3.1 DNA purification

DNA isolation: Plasmid DNA was isolated using a QIAprep Miniprep Kit and a Vacuum Manifold system according to the manufacturer's protocol. Briefly, a single colony generated from a bacterial stock solution was inoculated in 5 ml 2YT/Cam medium and grown overnight at 37 °C. Bacteria were harvested by centrifugation for 10 min at 2000 × *g* and 4 °C and resuspended in 250 µl buffer P1 containing RNase A. Bacteria were lysed under alkaline conditions in 250 µl buffer P2 (NaOH / SDS). By addition of 350 µl of the high-salt concentration buffer N3 denatured proteins, chromosomal DNA, cellular debris and SDS were precipitated and then removed by centrifugation (10 min, 17900 × *g*, 4 °C). The supernatant was applied to a QIAprep spin column and the DNA was adsorbed onto a silica membrane using a vacuum source. Contaminating endonucleases and salts were removed by sequential washing with 500 µl buffer PB and 750 µl Buffer PE. DNA was eluted with 50 µl nuclease-free water.

Quantification of DNA: The DNA concentration was determined by measuring the absorbance at 260 (A_{260}) and 280 (A_{280}) using a NanoDrop spectrophotometer. To assess purity of the isolated DNA, the ratio A_{260} / A_{280} was determined. Pure DNA exhibits A_{260} / A_{280} of 1.8. Samples with value lower than 1.8 indicating protein contamination were discarded and the DNA isolation was repeated. DNA up to 20 ng was analyzed by agarose gel electrophoresis and ethidium bromide fluorescent staining (2.3.3). The quantity of DNA was estimated by comparing the fluorescent yield of the samples with a series of low mass ladder standards at varying known concentrations.

Sequencing: The inserts of all isolated clones were sequenced by using the oligonucleotide odst03 (5'-CATAATCAAAATCACCGGAACCAG-3') as primer. 2 µg DNA in 20 µl nuclease-free water and 10 pmol of primer were send to Eurofins MWG (Ebersberg, Germany) for sequencing. The sequences were analyzed with Vector NTI software.

2.3.2 Restriction enzyme digestion

Selected DARPin sequences are subcloned into BamHI and HindIII restriction sites of the expression vector pMPAG6 (see Appendix 5.3.2 for the vector card). 10 µg phagemid and 5 µg pMPAG6 vector DNA were sequentially digested with the restriction enzymes BamHI and HindIII for 4 h at 37 ℃ each in a total volume of 80 µl (Table 1) using the buffers and conditions recommended by the manufacturer. Linearized DNAs after the first digestion were precipitated by adding 8.8 µl 3 M sodium acetate pH 5.2 and 200 µl cold 100% ethanol and incubation for 1 h at -80 ℃. The precipitated DNA was pelleted by centrifugation for 15 min at 16000 × *g* and 4 ℃ in table top centrifuge. DNA was dissolved in 20 µl nuclease-free water and subsequently subjected to the second digestion. Aliquots of each digestion reaction were analyzed by agarose gel electrophoresis along with undigested controls and DNA size markers.

Table 1. Digestion reaction mixture. All components were added and mixed prior to the enzyme addition.

First digestion:	
Component	**Amount**
DNA	5-10 µg
10× NEBuffer for BamHI	8 µl
BamHI (20 U/µl)	6 µl
100× BSA	0,8 µl
Water	q.s.
total volume	80 µl

Second digestion:	
Component	**Amount**
DNA	20 µl
10× NEBuffer 2	8 µl
HindIII (20 U/µl)	6 µl
Water	q.s.
total volume	80 µl

2.3.3 Agarose gel electrophoresis

For analytical gel electrophoresis, 1 g agarose powder was boiled in the 100 ml of 1-fold DNA Typing Grade TAE Buffer, light cooled and supplemented with

ethidium bromide at a final concentration of 0.2 µg/ml and cast to 5 mm height. Samples and molecular weight markers (1 Kb DNA Ladder or Low DNA Mass Ladder) were mixed with 5-fold Orange G Loading. Electrophoresis was performed in a horizontal electrophoresis chamber filled with 1-fold TAE buffer at 100 Volt for about 45 min. DNA fragments were visualized using a Kodak Image Station 440 CF.

For preparative electrophoresis, agarose gels were prepared without ethidium bromide. 80 µl of the digestion reactions (2.3.2) were mixed with 20 µl Orange G Loading Buffer and analytical (5 µl) and preparative amounts (95 µl) were separated along with a 1 Kb DNA marker. Marker and the analytical fraction of the digested DNAs were stained with 2.5 µg/ml ethidium bromide for 10 min and visualized under UV light. The position of the DNA fragment of interest was marked and used as reference for excision of the corresponding DNA fragment from the preparative fraction. This allowed omitting deleterious ethidium bromide and UV exposure for the DNA fragment to be subsequently subcloned. The DNA was extracted from the agarose slice using the gel extraction kit QIAquick following the manufacturer's instructions. Gel slices were dissolved in 900 µl buffer QG by incubation for 15 min at 50 °C. Samples were mixed with 300 µl isopropanol and applied to QIAquick spin columns, and then washed sequentially with 500 µl of buffer QG and 750 µl buffer PE. DNA was eluted with 20 µl nuclease-free water.

2.3.4 DNA ligation

The T4 DNA ligase was used to ligate DARPin inserts into the expression vector pMPAG6. Briefly, 0.6 ng of linearized and purified vector DNA was mixed with 30 ng insert DNA at a molar ratio of 1:4. The reaction was performed for 1 h in a total volume of 20 µl using 1 µl T4 DNA ligase and the buffer supplied by the manufacturer (Table 2). For comparison, ligation without insert DNA was performed. After ligation DNA was precipitated by adding 100 µl n-butanol, vortexing and centrifugation for 20 min at 14000 × *g* and

23 ℃. DNA pellets were washed with 500 µl cold 70 % ethanol, centrifuged for 10 min at 14000 × *g* and 4 ℃ and dissolved in 10 µl nuclease-free water.

Table 2. Ligation reaction mixture. The mixture was prepared from all components and the enzyme was added last.

Component	**Amount**
insert	30 ng
vector	0.6 ng
buffer	2 µl
nuclease-free water	q.s.
T4 DNA ligase (20 U/µl)	1 µl
total volume	20 µl

2.3.5 Transformation of *E. coli*

Ligated DNA was transformed into XL1-blue electrocompetent cells using by electroporation. 5 µl of the ligation reaction was gently mixed with 50 µl competent cells and the mixture was transferred into pre-chilled sterile gap cuvette (0.2 cm). A single pulse was applied (25 µF, 2.1 kV, 200 Ω) using a Gene Pulser II apparatus. The cells were immediately resuspended in the pre-warmed LB/Glu medium and incubated at 37 ℃ for 60 min in an orbital shaker at 220 rpm to allow expression of the ampicillin resistance gene. The transformed bacteria were selected by growth on LB/Glu/Amp agar plates.

Ampicillin resistant bacterial cells were screened for the expression of DARPins. Single colonies were picked and inoculated into 150 µl/well expression medium (LB/Glu/Amp) in a 96-well culture plate, covered with a gas permeable adhesive seal and incubated overnight in a moist chamber at 30 ℃ with shaking. 10 µl of the cultures were transferred into new plate with 140 µl/well of LB/Glu/Amp and incubated for 2 h. Subsequently, cells were induced with 50 µl/well of LB/Glu/Amp containing IPTG to reach a final concentration of 0.2 mM and

grown for 4 h. Plate was centrifuged for 10 min at 3000 × *g* and the supernatants were aspirated. Pelleted cells were frozen for 10 min at -80 °C and then lysed with 40 µl B-PER lysis buffer. 10 µl of crude extracts were subsequently analyzed by SDS-PAGE and Imperial Protein Stain (2.4.4).

2.4 Protein chemistry methods

2.4.1 Large scale DARPin expression

DARPins subcloned into pMPAG6 were expressed in *E. coli*. 10 µl of a frozen bacterial stock solution was inoculated into 15 ml of LB/Glu/Amp and incubated overnight in an orbital shaker at 37 °C. The overnight culture was diluted into 200 ml LB/Glc/Amp in a sterile shake flask. Incubation was continued until an OD_{600} of 0.6 was reached. IPTG was added to the final concentration of 0.5 mM and the culture was incubated for another 4 h. Subsequently, cells were collected by centrifugation for 10 min at 5000 × *g* and 4 °C. The supernatant was discarded and the pellet was frozen in liquid nitrogen and stored at -80 °C until further use. At each step of the protein expression cells of 0.1 ml culture aliquots were collected and analyzed by SDS-PAGE.

2.4.2 DARPin purification

DARPin purification was performed in several steps as depicted in Figure 11. DARPins expressed in *E. coli* were purified by metal-ion affinity chromatography followed by dialysis. The purity of the preparations was assessed by SDS-PAGE and Imperial Blue staining. All preparations revealed a purity of 85–95%. Purified DARPins were used for further characterization experiments, such as ELISA, surface plasmon resonance measurements and cellular *in vitro* cell assays. If required DARPins were further purified by preparative ion exchange chromatography and endotoxin was removed. The molecular size of DARPins was analyzed by analytical size exclusion chromatography.

Ni-sepharose affinity chromatography: Frozen bacterial cell pellets (2.4.1) were resuspended in 20 ml TBSN buffer containing 1% (w/v) lysozyme. Cells were ruptured by two passages through a French press (1150 psi, internal cell pressure 18000 psi). The insoluble fraction was removed by centrifugation for 30 min at 13000 × *g* and 4 °C. The supernatant was sterile filtered through a 0.22 µm filter and adjusted to 10% (v/v) glycerol and 20 mM imidazole to reduce unspecific binding. All buffers were sterile filtered and kept on ice and fractions were collected on ice.

Affinity chromatography was performed using an automated protein purification system (Bio-Rad) equipped with UV and conductivity detectors. The supernatant was passed over 2.5 ml Nickel / NTA Sepharose 6 Fast Flow column equilibrated with 40 ml equilibration buffer (TBSN buffer containing 20 mM imidazole and 10% (v/v) glycerol at a flow rate of 1 ml/min. The column was washed with 40 ml equilibration buffer until the base line as detected by UV was reached. DARPins were eluted with 5 ml TBSN containing 250 mM imidazole and 10% (v/v) glycerol. Fractions of 0.5 ml were collected and analyzed by SDS-PAGE. Fractions containing DARPins were pooled, dialyzed overnight against PBS, adjusted to a protein concentration of 0.25 mg/ml based on absorption at 280 nm, sterile filtered and stored at -80 °C.

Ion-exchange chromatography: DARPins are positively charged at pH 7.0, with an isoelectric point between 4.3 and 4.7. For *in vivo* application DARPins were additionally purified by ion-exchange chromatography on a Sartobind Ion Exchange MA Unit Q75 (Sartorius; Germany), which is a strong basic anion exchanger. The resin was equilibrated with 25 mM BisTris buffer pH 6.7. DARPins were diluted in the same buffer and applied to the column. After washing with 10 ml 25 mM BisTris buffer pH 6.7, DARPins were eluted in steps with 2 ml of 25 mM BisTris buffer pH 6.7 containing 0.1 (fraction E0), 0.25 (E1), 0.5 (E2), 0.75 (E3) and 1 M NaCl (E4). Elution was monitored at 280 nm and fractions were collected from each step. Fractions of 0.5 ml were collected and desalted on prepacked PD-10 column using PBS. Purified fractions were analyzed by SDS-PAGE and immunoblotting using anti-RGS-His_4 antibodies.

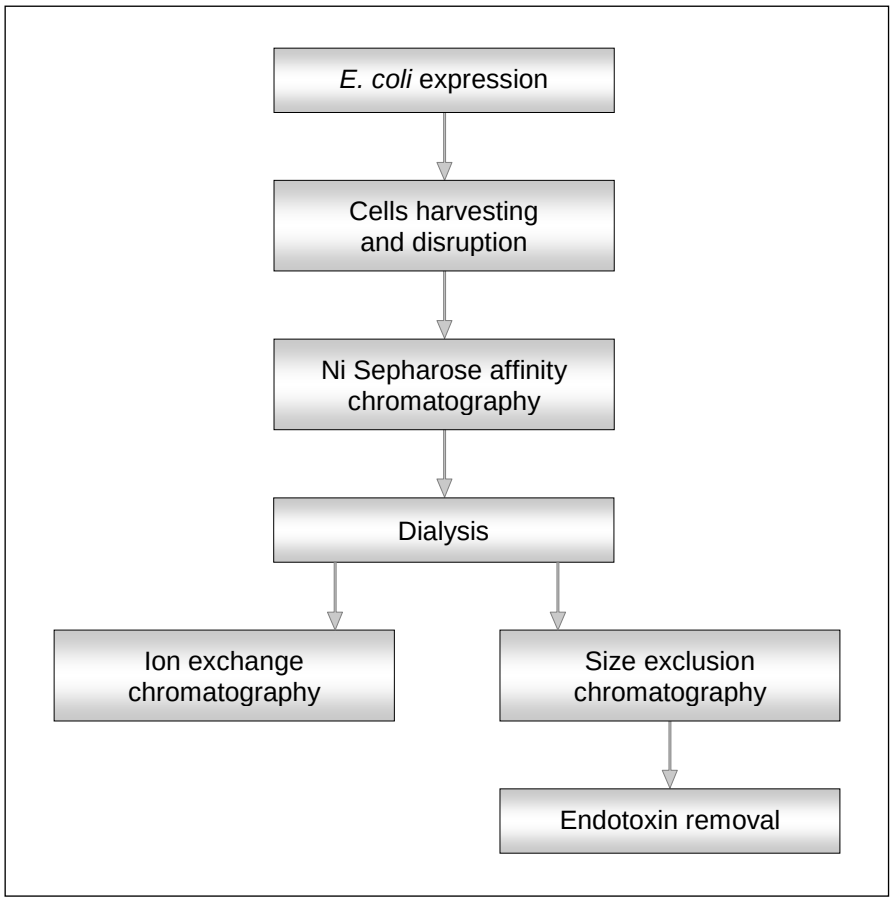

Figure 11. DARPin purification workflow.

Endotoxin removal: Endotoxin was removed using Triton X-114 extraction (Liu et al. 1997). Samples were adjusted with Triton X-114 to a final concentration of 1% (v/v) and incubated under constant rotation for 30 min at 4 °C followed by 10 min at 37 °C. Finally Triton X-114 was separated by centrifugation for 10 min at 20000 × *g* and 25 °C. The upper aqueous phase containing the protein was carefully transferred into a fresh tube. This procedure was repeated a total of four times until the endotoxin level was reduced to 1 EU/mg. No significant lost of the protein was observed.

Endotoxin levels were determined by a chromogenic Limulus Amebocyte Lysate (LAL) test. LAL is an aqueous extract of amoebocytes from the horseshoe crab (Limulus polyphemus), which specifically reacts with endotoxin. 25 µl of sample or standard was mixed with 25 µl LAL and incubated for 10 min at 37 °C. 50 µl of chromogenic substrate was added to each sample, vortexed and further

incubated at 37 °C for 6 min. The reaction was stopped by addition of 50 µl 25% acetic acid. The absorbance was measured at 410 nm using a spectrophotometer. The endotoxin concentration was determined from the standard curve. Finally purified samples were shock-frozen in liquid nitrogen and stored by -80 °C until further analysis.

Size exclusion chromatography: To assess aggregation DARPins were analyzed by size exclusion chromatography using a SMART System equipped with Superdex 200 gel filtration column. Superdex 200 allows separation of proteins in the molecular weight range between 10 and 600 kDa. The column was equilibrated overnight with PBS containing 0.005% Tween 20. 5 µg of affinity-purified DARPins (0.25 mg/ml) were injected and chromatographed at a flow-rate of 60 µl/min. Elution profiles were monitored by absorbance at 280 nm. Cytochrome c (12.4 kDa), carbonic anhydrase (29 kDa), bovine serum albumin (66 kDa), alcohol dehydrogenase (150 kDa) and ß-amylase (200 kDa) were used as molecular mass standards.

2.4.3 Determination of protein concentration

Protein concentrations of DARPin preparations were determined photometrically at 280 nm using a spectrophotometer (NanoDrop). 1 µl of undiluted sample was measured and the concentration was calculated using the extinction coefficient factors in Table 3. The protein concentration of cell lysates was determined by Bradford dye assay (Bradford 1976).

Briefly, 200 µl Bradford's reagent was mixed with 800 µl ddH_2O and 2 µl sample. The absorbance was measured at 495 nm using spectrophotometer. The protein concentration was determined from the BSA standard curve. If required samples were concentrated by centrifugation using Microcon Ultracel YM-3 or Amicon Ultra-4 3K filter devices with molecular weight cut-off of 3 kDa according to the manufacturer's instructions.

Table 3. Molar extinction coefficients were calculated using Vector NTI software based on the amino acid sequence. Extinction coefficients of DARPins vary strongly, due to their different amounts of aromatic residues.

DARPin	molecular weight	molar extinction coefficient	1 A[280] equals × mg/ml
AA5	18286.4	16500	1.11
AB1	21947.26	33570	0.65
AC7	18235.21	17780	1.03
AH5	21485.39	5690	3.78
BD2	21839.13	24750	0.88
BD4	21501.87	10810	1.99
BE1	18307.48	16500	1.11
BG9	18064.1	6400	2.82

2.4.4 SDS-PAGE

SDS-PAGE was performed in precast polyacrylamide gels NuPAGE 4–12% Bis-Tris gels in XCell SureLock Mini-Cell chambers. Samples were adjusted with 1/4 volume (v/v) LDS sample buffer and 1/10 volume (v/v) NuPage reducing agent and denatured for 15 min at 70 ℃. Proteins were separated in 1 × MOPS SDS or 1 × MES SDS running buffer allowing resolution of high molecular weight proteins e.g. EphB4 or low molecular weight proteins e.g. DARPins respectively. Protein molecular weight markers SeeBlue and MagicMark were applied as standards.

Electrophoresis was carried out at a constant current of 200 V in an ice bath until the dye front of the sample buffer reached the bottom of the gel. Polyacrylamide gels were stained with Imperial Protein Stain solution, a coomassie R-250 dye-based reagent according to the manufacturer's instructions. Gels were destained with ddH_2O and thereafter scanned for documentation.

2.4.5 Western blot

Proteins, separated by the SDS-PAGE, were transferred from gel onto PVDF membranes by tank blotting using the XCell II Blot Module according to the manufacturer's instructions. The transfer sandwich was assembled from cathode to anode as follows: sponge, 3 mm filter paper, polyacrylamide gel, membrane, 3 mm filter paper and sponge. Proteins were transferred in transfer solution (190 mM glycine, 25 mM Tris, 0.1% SDS, 20% methanol) for 80 min at 250 mA. Membranes were stained with PonceauS for 10 min, destained with ddH_2O and scanned for documentation.

For immunoblotting unoccupied protein binding sites of the membrane were blocked with blocking buffer (5% (w/v) milk powder in PBST) for 1 h at RT. Membranes were incubated with specific primary antibodies diluted in blocking buffer for 1 h at RT or overnight at 4 °C. Membranes were washed three times for five minutes with PBST and subsequently incubated with the corresponding peroxidase-coupled secondary antibody diluted in blocking buffer for 1 h at RT and washed again as above (Table 4). Membranes were developed with enhanced chemiluminescence (ECL) detection kit SuperSignal WestDura Extended Duration Substrate and exposure to X-ray films. Films were developed in an AGFA™ Curix60 processor.

Table 4 Antibodies used for immunoblotting of DARPins, EphB4 or phosphorylated EphB4 (pEphB4).

Blotted protein	Primary antibody, dilution	Secondary antibody, dilution
DARPin	mouse anti-RGS-His_4, 1:1000	ECL anti-mouse HRP-linked, 1:10000
EphB4	anti-EphB4, 1:500	ECL anti-mouse HRP-linked, 1:10000
pEphB4	anti-phosphotyrosine HRP-linked (clone PY20) , 1:5000	

2.5 Binding analysis

2.5.1 Immobilization of target proteins

Target proteins were adsorbed directly to the surface of MaxiSorp plates (Table 5). 100 µl/well of target proteins in PBS were immobilized for phage display (50 µg/ml) and ELISA experiments (3-5 µg/ml) by incubation overnight at 4 ℃. Coated wells were washed three times with 300 µl PBST (PBS, 0.05% Tween20). Unspecific binding sites were blocked with 300 µl 0.2% BSA in PBST for 1 h at RT on an orbital shaker and wells were finally washed with PBST as above.

Table 5. Proteins immobilized for phage display and ELISA.

Target protein	Residues of EphB receptor	Protein description
Extracellular domains of EphB receptors		
human EphB4 monomeric	Leu 16 – Ala 539	hEphB4 ECD
murine EphB4 with Fc fusion	Leu 16 – Ala 539	mEphB4-Fc ECD
rat EphB1 with Fc	Met 18 – Gln 538	rEphB1-Fc ECD
murine EphB2 with Fc	Val 27 – Lys 548	mEphB2-Fc ECD
murine EphB3 with Fc	Leu 30 – Thr 537	mEphB3-Fc ECD
human EphB6 with Fc	Leu 17 – Ser 579	hEphB6-Fc ECD
murine EphB6 with Fc	Leu 33 – Ser 587	mEphB6-Fc ECD
Human EphB4 with Fc fusion	Leu 16 – Ala 539	hEphB4-Fc ECD
Intracellular domains of EphB receptors		
GST-mEphB4-SAM	Ser 907 – Gln 971	GE4S
GST-mEphB3-SAM	Thr 920 – Gln 984	GE3S
His_6-tagged human EphB1	Ser 564 – 984 Ala	EphB1 ICD
His_6-tagged human EphB2	Val 560 – 1055 Gly	EphB2 ICD
His_6-tagged human EphB3	Lys 596 – Val 998	EphB3 ICD
His_6-tagged human EphB4	Tyr 596 – Tyr 987	EphB4 ICD

2.5.2 Enzyme-linked Immunosorbent Assay (ELISA)

Phage ELISA: The binding of enriched pool of phage particles from each panning cycle was analyzed by phage pool ELISA. 500 µl phage particles precipitated from 5 ml culture and normalized to the equal concentration (as described in 2.2.2 and 2.2.5) were supplemented with 500 µl 0.4% BSA in PBST and incubated for 20 min. For screening purpose, individual clones from the amplified phage pool of the third panning cycle were grown overnight as described above (2.2.4.) 150 µl supernatant was supplemented with 150 µl 0.4% BSA in PBST and incubated for 20 min.

96-well plates were coated with target proteins (0.5 µg/well in PBS) or lysozyme as unrelated control protein, blocked with BSA and washed with PBST. 100 µl of phage particles solution was applied to the wells with immobilized target or control protein (2.5.1) and incubated for 2 h with orbital shaking. Plates were washed three times with 300 µl PBST. Bound phage were detected by incubation with 100 µl anti-M13-phage antibody conjugated to horseradish peroxidase diluted 1:10000 in PBST for 1 h. After repeated washing as above, plates were developed with 100 µl HRP substrate 3-aminophthalhydrazide. Chemiluminescence was measured after 5 min in a luminometer (Wallac Victor Lumicount) and expressed as relative light units (RLU).

DARPin ELISA: 100 µl of affinity-purified DARPins (0.5 µg/well) was applied to coated plates (as described in 2.5.1) and incubated for 1 h with orbital shaking. DARPin solutions were aspirated and the wells were washed with PBST as above. DARPin binding was detected with 100 µl/well mouse anti-RGS-His_4, diluted 1:1000 in PBSTB and incubated for 1 h. Plates were washed as above. Subsequently, 100 µl/well of the secondary peroxidase-conjugated goat anti-mouse IgG + IgM antibody diluted 1:5000 in PBST was added to plates. After 1 h incubation, plates were washed and developed as described above.

ELISA was also performed with DARPins in dimerized format as DARPin **/** IgG complex. Therefore, prior to their application to the coated wells DARPins were incubated with anti-RGS-His_4 antibody at a molar ratio 2:1 (DARPin : antibody) for 30 min. Binding of dimerized DARPins was detected with the secondary

peroxidase-conjugated goat anti-mouse IgG + IgM antibody as described above.

Cell ELISA: Monoclonal phage were analyzed for their binding to EphB4 on viable cells. U-2 OS-hEphB4 and untransfected U-2 OS cells were seeded into 96-well plate at 5×10^4 cells ***/*** well and cultured overnight. Cells were washed once with 300 µl PBS with Ca^{2+} and Mg^{2+} (PBS^{++}), then blocked with 300 µl/well 2% milk powder and 1% BSA in PBS^{++} for 1 h and washed again with PBS^{++}. Subsequently, wells were incubated with 100 µl/well precipitated phage solution from 5 ml overnight culture for 1 h (2.2.2 and 2.2.5). The phage solution was removed and cells were washed three times with 300 µl PBS^{++}. Bound phage were detected as described above for the phage ELISA. A 5-fold signal difference between U-2 OS-hEphB4 and U-2 OS was considered specific.

2.5.3 Flow cytometry analysis

Binding of affinity-purified DARPins to EphB4 on U-2 OS-hEphB4, U-2 OS and MCF7 cells was analyzed by flow cytometry. Cells were trypsinized, washed with PBS^{++} and resuspended in FACS buffer (PBS^{++} containing 0.5% BSA) to a concentration of 5×10^6 cells/ml. Cell trypsinizing does not affect the membrane receptor EphB4, as showed by the positive control. 100 µl cell suspension was incubated with either 100 µl purified phage solution (2.2.5) or 100 µl DARPins at the end concentrations of 0.5, 0.05 and 0.005 µg/ml in 96-well V-bottom plate. Prior to their application, DARPins were incubated with anti-RGS-His_4 antibody at a molar ratio 2:1 (DARPin : antibody) for 30 min at RT.

Cells were then sequentially incubated with the secondary and tertiary antibodies as listed in Table 6. All incubation steps were performed for 1 h at 4 °C with orbital shaking, followed by two washing steps with 150 µl/well FACS buffer. Incubations with fluorescently labeled antibodies were performed in the dark. Binding of ephrin-B2-Fc at the end concentrations of 0.005 µg/ml was used as positive control. A control DARPin and secondary antibodies alone

were used for comparison. Untreated cells were applied to monitor the intrinsic fluorescence. After antibody incubations cells were washed two times and resuspended in 250 µl FACS buffer. 1×10^5 cells were analyzed by flow cytometry using a BD FACS Calibur. The obtained results were evaluated and presented using the CellQuest Pro software.

Table 6. Antibodies used for FACS analyses.

Primary binder:	Secondary antibody (dilution):	Tertiary antibody (dilution):
Phage	anti-M13 monoclonal antibody (1:300)	FITC-conjugated anti-mouse IgG antibody (1:100)
DARPin (0.5, 0.05, 0.005 µg/ml)	mouse anti-RGS-His_4 antibody (complexed with DARPin at a molar ratio 2:1, DARPin : IgG)	R-Phycoerythrin-conjugated $F(ab')_2$ fragment goat anti-mouse IgG antibody (1:200)
ephrin-B2-Fc (0.005 µg/ml)	FITC-conjugated goat anti-human IgG + IgM (H+L) antibody (1:100)	–

2.5.4 Surface plasmon resonance analysis of protein interaction

Surface plasmon resonance (SPR) analysis was performed using BIAcore 2000 instrument. BIAcore system allows a label free method for probing interactions between molecules, an analyte in a solution and a ligand immobilized on the surface of a chip (O'Shannessy 1994).

Protein immobilization: Target proteins were immobilized onto a CM5 chip following the standard amine coupling protocol. The analysis was performed by simultaneous use of all four flow cells with three active and one control surfaces. Experiments to determine the optimal immobilization conditions (buffer pH, ligand concentration) were performed as described in Table 7. The carboxymethyldextran surface of the flow cell was activated with 0.4 M 1-ethyl-3-(3-dimethylaminopropyl)-carbodiimide (EDC) and 0.1 M N-hydroxysuccinimide (NHS) injected at a ratio of 1:1 for 7 min. Proteins were immobilized until the target loading density listed in the

Table 8 was achieved. Human EphB4-Fc ECD and mouse EphB4-Fc ECD diluted to 10 µg/ml in 25 mM MES, pH 6.0 were immobilized to a final density of 1134.8 and 1072.4 resonance units (RU), respectively and human EphB4 ECD monomer (10 µg/ml in 25 mM MES, pH 6.0) to 649.5 RU. The control channel was immobilized with lysozyme protein (10 µg/ml in 25 mM Hepes, pH 7.0) to 406.7 RU. Remaining activated groups were inactivated by injection of 1 M ethanolamine-HCl, pH 8.5 for 7 min.

Analysis of binding kinetics: All measurements were performed in HBS-EP running buffer (10 mM Hepes, 150 mM NaCl, 3 mM EDTA, 0.005% Tween-20) at RT. Affinity-purified DARPins and ephrin-B2-Fc as positive control were injected at a flow rate of 30 µl/min for 2–5 min at concentrations ranging from 4 to 1000 nM in HBS-EP buffer. Their dissociation was analyzed by injection of running buffer at the same flow rate for 10 to 30 min. The signals corresponding to unspecific binding to an uncoated reference channel and the running buffer (blank) were recorded and subtracted from the sensorgrams (double referencing). The kinetic data from three separate experiments were evaluated by global fitting to the 1:1 Langmuir binding, bivalent analyte or steady-state model using the BIA evaluation software 4.1.

Competitive binding analysis: Competitive binding to hEphB4-Fc ECD was performed using the BIAcore command “co-inject” which allows two consecutive injections of analytes without intermediate washings. The analysis was performed in HBS-EP running buffer at a flow rate of 30 µl/min. First 60 µl of analyte 1 (ephrin-B2-Fc or DARPin at 1 µM in running buffer) were injected followed by injection of 60 µl analyte 2 (ephrin-B2-Fc, DARPin or a mixture of both at molar ratio of 1:1) according to Table 10. Pair wise competition of DARPins was analyzed whereby an injection of 60 µl DARPin 1 (1 µM) was followed by the injection of 60 µl of DARPin 1 mixed with another DARPin at molar ratio of 1:1 to achieve final concentrations of 1 µM (Table 10, experiment 4). A control DARPin or running buffer alone was used for comparison to the analyte 2. Binding responses were normalized to the response level of the first analyte. Computerized fitting was conducted using Graphpad Prism 3.0 software.

Table 7. Experimental test conditions to achieve optimal target immobilization to the BIAcore sensor surface. The target proteins (ligands) were diluted to different concentrations in buffers with pH values below their isoelectric point (pI) to ensure positive charge. Pre-concentration of the proteins on the surface was performed by electrostatic interaction.

Target (ligand)	concentration	pI	immobilization buffers tested
human EphB4-Fc	10 µg/ml	6.67	25 mM MES, pH 6.5, 25 mM MES, pH 6.0, 25 mM MES, pH 5.5, 10 mM acetate, pH 5.5, 10 mM acetate, pH 5.0, 10 mM acetate, pH 4.5
human EphB4 monomer	10 µg/ml	6.50	
mouse EphB4-Fc	5, 10, 25, 50 µg/ml	6.71	
lysozyme	10 µg/ml	9.39	25 mM Hepes, pH 8.0, 25 mM Hepes, pH 7.5, 25 mM Hepes, pH 7.0

Table 8. Conditions for immobilization of the targets (ligands) on the CM5 chip. A target density of 1000 RU was aimed for dimerized EphB4 (85 kDa) and densities of 700 RU for monomeric EphB4 (58 kDa) and 200 RU for lysozyme (15 kDa) were calculated to achieve equimolar loading. Additionally, mEphB4-Fc was immobilized for the maximal level of 8000 RU.

Target (ligand)	Concentration	Immobilization buffer	Targeted density	Final density
human EphB4-Fc	10 µg/ml	25 mM MES, pH 6.0	1000 RU	1134.8 RU
human EphB4 monomer	10 µg/ml	25 mM MES, pH 6.0	700 RU	649.5 RU
mouse EphB4-Fc	10 µg/ml	25 mM MES, pH 6.0	1000 RU	1072.4 RU
mouse EphB4-Fc	10 µg/ml	10 mM acetate, pH 5.0	8000 RU	7664.4 RU
lysozyme	10 µg/ml	25 mM Hepes, pH 7.0	200 RU	406.7 RU

Table 9. Experimental set-up and sequence of analyte injection for competition binding analysis.

experiment	analyte 1	analyte 2
1	ephrin-B2-Fc	ephrin-B2-Fc + DARPin
2	ephrin-B2-Fc	DARPin
3	DARPin	ephrin-B2-Fc
4	DARPin 1	DARPin 1 + DARPin 2

2.5.5 Immunoprecipitation

Immunoprecipitation is a technique that enables detection of antigens in cell extracts. Precipitated proteins are detected using SDS-PAGE and Western blot analysis. EphB4 was immunoprecipitated from U-2 OS hEphB4 cell lysate using DARPins binding to the intracellular domain of EphB4 or an anti-c-myc antibody. Cells were grown to 90% confluency in 300 cm^2 flask and washed with PBS (2.6.1). Subsequently, cells were lysed with 8 ml cell lysis buffer per 300 cm^2 flask for 30 min at 4 °C with orbital shaking. Cell lysates were collected in ice-cold microcentrifuge tubes and insoluble material was removed by centrifugation for 15 min at 14000 × *g* and 4 °C in table top centrifuge. Protein concentration in the supernatants was determined (2.4.3) and adjusted to 1 mg/ml using lysis buffer.

For immunoprecipitation, 20 µl protein G Sepharose 4 Fast Flow beads were equilibrated with lysis buffer. Beads were washed two times by centrifugation for 5 min at 500 × *g* and 4 °C and resuspended 1:1 (v/v) in lysis buffer. Subsequently, beads were coupled with either 1 µg anti-c-myc antibody or consecutively with 1 µg anti-RGS-His_4 and then with 5 µg of DARPin for 1 h at 4 °C with gentle end-over-end rotation. In between and at the end beads were washed three times with 0.5 ml lysis buffer. 20 µl antibody coupled beads were then added to 500 µl U-2 OS hEphB4 cell lysate and incubated overnight at 4 °C with gentle end-over-end rotation.

Beads were washed three times with 0.5 ml lysis buffer, collected by centrifugation and finally resuspended in 25 µl lysis buffer containing 7.5 µl LDS sample buffer and 3 µl reducing agent. Bound proteins were eluted by incubation for 15 min at 70 °C. Beads were collected by centrifugation and the supernatant was separated by SDS-PAGE in MOPS SDS running buffer (2.4.4). Immunoprecipitates were analyzed by Western Blot (2.4.5) using an anti-EphB4 antibody (1:500) and peroxidase-coupled secondary anti-mouse IgG (1:10000).

2.6 Cellular assays

2.6.1 Cell lines and culture

The human U-2 OS osteosarcoma and U-2 OS-hEphB4 cell lines were cultured in Dulbecco's modified eagle's medium (DMEM) without phenol red, containing high glucose (4.5 g/l) and supplemented with 5% heat-inactivated fetal bovine serum (FBS) and 2% L-glutamine. Cells were cultivated at 37 ℃ in a humidified incubator at 7.5% CO_2.

MCF7 breast adenocarcinoma cells were cultured in Roswell Park Memorial Institute 1640 (RPMI-1640) medium without phenol red containing 10% FBS, 1% L-glutamine, 0.1 nM estradiol and 0.2 U/ml bovine insulin. The human umbilical vein endothelial cells (HUVECs) were cultured up to three passages as recommended by the supplier in Endothelial Cell Growth Medium-2 supplemented with growth factors and cytokines (SingleQuots kit). MCF7 and HUVECs cells were grown at 37 ℃ in a cell incubato r in a 5% CO_2.

Cells were cultured in antibiotic free media according to standard procedures. For the *in vitro* assays, cells were grown till the 80% confluence, washed with HEPES Buffered Saline Solution, detached with trypsin / EDTA solution and neutralized with Trypsin Neutralizing Solution. Cells were harvested by centrifugation for 5 min at 800 × *g*. The cell number and viability was determined using a CASY cell counter.

2.6.2 Kinase phosphorylation assay

EphB4 receptor tyrosine kinase activity can be determined in a cell-based assay after stimulation with ephrin-B2. EphB4-myc tagged is captured from the cell lysate by immobilized anti-c-myc antibody and the relative amount of phosphorylated EphB4 can be measured using the appropriate antibody. U-2 OS-hEphB4 cells were seeded at the density of 2×10^4 cells / well in 100 µl complete medium in 96-well cell plates and grown overnight to reach about 70% confluency. The cells were washed once with 200 µl PBS^{++} and then treated

with medium containing DARPins at various concentrations for 30 min at RT. Subsequently, cells were stimulated by addition of ephrin-B2-Fc to a final concentrations of 1 µg/ml for 30 min at RT. Cells were washed with PBS and lysed with 120 µl/well lysis buffer for 30 min at 4 ℃ with orbital shaking.

To detect pEphB4 in the cell lysates, 100 µl anti-c-myc antibody (5 µg/ml in PBS) was immobilized on the surface of Lumitrac 96-well plates by overnight incubation at 4 ℃. Plates were washed with 300 µl PBST, blocked with 250 µl 5% Prionex Reagent in PBST for 2 h at RT and washed again three times with PBST. 100 µl of lysates were transferred to these plates followed by 100 µl anti-phosphotyrosine HRP-conjugate diluted 1:5000 in lysis buffer. Plates were incubated overnight at 4 ℃, washed three times wit h PBST and developed with 100 µl HRP substrate 3-aminophthalhydrazide. Chemiluminescence was measured after 5 min at 425 nm in a luminometer (Wallac Victor Lumicount).

2.6.3 Tube formation assay

Tube formation assay evaluates the ability of endothelial cells to form three-dimensional capillary-like tubular structures when cultured on the extracellular matrix. HUVECs cultured as described in 2.6.1 were resuspended to 2.3×10^5 cells/ml and 100 µl/well were seeded into 48-well cell culture plates coated with 30 µl/well matrigel. Cells were incubated for 15 min at 37 ℃ and then 200 µl of EphB4 or control DARPins diluted in culture medium were added to achieve final concentrations of 1, 10, 100 µg/ml. Incubation was continued for 24 h at 37 ℃ and then the medium was removed. Cells were fixed with 250 µl 4% formalin containing 4 g/l glucose for 10 min at RT and subsequently permeabilized for 15 min with 250 µl of Cell Permeabilisation Solution. Cells were washed with 250 µl PBS containing 0.1% BSA and blocked with 250 µl pre-warmed blocking solution (PBS containing 1% BSA) for 30 min at 37 ℃. Cells were stained with anti-human CD31 antibody and a corresponding secondary IgG alkaline phosphatase conjugate using the Tubule Staining Kit, according to the manufacturer’s instructions. Fixed cells were sequentially incubated with 250 µl antibody diluted 1:500 in blocking solution and incubated

for 1 h at 37 °C. After each incubation step cells were washed three times with 250 µl 0.1% BSA in PBS and finally with ddH_2O. Cells were stained with 250 µl/well BCIP / NBT substrate (1 tablet / 20 ml ddH_2O). Tube formation was examined and documented by photography using a phase-contrast microscope equipped with a digital photo camera. Images were analyzed with Particle analysis Software. *In vitro* angiogenesis was quantified by measuring length of all tubes within one well at a 1.25× magnification. The total number of tubes and mean tube length were determined in all wells for each experimental group.

2.6.4 Apoptosis assay

Apoptosis was measured using a Caspase-Glo 3/7 assay according to the manufacturer's instructions. U-2 OS and U-2 OS hEphB4 cells were seeded in 50 µl medium at 5000 cells / well in a 96-well white-walled plate and incubated overnight at 37 °C. On the next day cells were treated with 50 µl/well DARPins diluted in culture medium to achieve final concentrations of 500, 100, 20, 4 µg/ml and incubation was continued for 24 h. 100 µl/well of Caspase-Glo 3/7 substrate was added and plates were incubated for 1 h in the dark at RT. Finally the luminescence was measured in a luminometer (Wallac Victor Lumicount). Luminescence is proportional to the amount of caspase activity present. Staurosporine at final concentrations of 1000, 100, 10 and 1 nM was used as positive control.

2.6.5 Internalization

For internalization experiments U-2 OS, U-2 OS hEphB4 and MCF7 cells 1000 cells / well were seeded in 90 µl of medium into a 96-well black-walled plate and grown overnight at 37 °C to reach about 20% confluency. 10 µl of DARPin / anti-RGS-His_4 / Mab-ZAP complexes previously generated by combining the individual components in PBS and incubation for 15 min at RT were added to achieve a final concentration of 16 ,8 and 4 nM, respectively. Cells were

incubated for 72 h at 37 °C and then number of living cells was determined by detection of their metabolic activity using Alamar Blue assay (Ahmed et al. 1994). Alamar Blue reagent was added to the wells to a final concentration of 10% and cells were incubated for 2 to 5 h at 37 °C. Then fluorescence was measured at 590 nm with an excitation wavelength of 530 nm using a microtiter well plate reader (Wallac Victor2). Values were analyzed after subtraction of the background values generated by the Alamar Blue reagent in culture medium alone. The cytotoxic potency of the internalized complex was calculated as a difference between the number of the cells treated with saporin-free complex (primary **/** secondary antibody) and number of cells treated with the whole complex (primary **/** secondary **/** tertiary antibody). Ephrin-B2 and commercially available anti-EphB4 antibodies were used as positive controls. To assess non-specific Mab-ZAP cell toxicity, single components and complexes with a control or no DARPin were analyzed as listed in Table 10.

Table 10. Saporin (ZAP) complexes tested in the internalization assay.

Sample	Primary binder	Secondary antibody	Tertiary antibody
Test	DARPin	anti-RGS-His_4	Mab-ZAP
Negative control	DARPin	anti-RGS-His_4	Mab-ZAP
Positive control #1	ephrin-B2-Fc	Mouse anti-human Fc	Mab-ZAP
Positive control #2	–	Goat anti-EphB4 (N-19)	Goat-ZAP
Positive control #3	–	Mouse anti-EphB4 (M01)	Mab-ZAP
Positive control #4	–	Rabbit anti-EphB4 (H200)	Rab-ZAP

2.6.6 EphB4 inhibition by cell transfection of ICD-EphB4 DARPins

DARPin directed against intracellular domain of EphB4 were transferred into cells using PULSin, a cationic amphiphile molecule, following the manufacture's instruction. 2×10^4 U-2 OS-hEphB4 cells were seeded in 100 µl/well culture medium into 96-well plates and incubated overnight at 37 °C. On the next day

cells which had reached about 70% confluency, were washed once with 200 µl/well PBS^{++} to remove the serum. Then 180 µl/well fresh medium without serum was added. 3 µg DARPin (3 mg/ml) with PULSin reagent (1.2 µl) at a ratio of 5:2 (w:v) were diluted in 17.8 µl 20 mM Hepes (supplied with the kit) and incubated for 15 min. 20 µl/well of the DARPin **/** PULSin complex was added to cells and incubated for 4 h at 37 °C. The protein transfer solution was removed and cells were washed twice with 200 µl/well PBS^{++} and once with 200 µl/well medium. Subsequently, the cells were treated with 100 µl ephrin-B2-Fc diluted in medium to achieve a final concentration of 1 µg/ml for 30 min at RT. Cells were washed with 200 µl/well PBS and lysed with 120 µl/well lysis buffer for 30 min at 4 °C with orbital shaking. 20 µl aliquot s of cell lysates were separated by SDS-PAGE, blotted on PVDF membranes (2.4.4 and 2.4.5) and and developed with anti-RGS-His_4 antibody (1:2000) and the corresponding peroxidase-linked secondary antibody (1:10000) to detect transfected DARPins. Peroxidase-linked anti-phosphotyrosine antibody (1:5000) was used to detect phosphorylated EphB4.

2.7 Directed *in vivo* angiogenesis assay

Effects of EphB4 DARPins on angiogenesis *in vivo* were analyzed using the Directed In Vivo Angiogenesis Assay Kit, a modified matrigel plug assay which allows quantitative analysis of antiangiogenic efficacy *in vivo*. The matrigel was applied into sterile 0.15 × 1 cm long semiclosed surgical silicone tubes (angioreactors) and solidified before implantation in mouse using following the manufacturer's instructions. Briefly, angioreactors were filled under sterile conditions with 20 µl high-concentration basement membrane extract (matrigel) previously adjusted to 10 µg/ml heparin. Additionally matrigel was supplemented with 1.5 µg/ml FGF-2 and 0.5 µg/ml VEGF (positive control) alone or with DARPins to 200 µg/ml or supplemented with the corresponding amount of PBS (negative control). Tubes were immediately inverted after filling and incubated for 1 h at 37 °C to allow matrigel to solidify. Female Balb/C mice (Strain 028, 6 weeks old) obtained from Charles River, were lightly anesthetized

by intraperitoneally application of 0.1 ml / 10 g body weight of 5% Rompun / 10% Ketavet diluted in 0.9% NaCl. Two angioreactors were implanted subcutaneously into their dorsal flank on both sides of the spine (Figure 12). Mice were kept for 14 days, and then euthanized and the reactors were removed and photographed.

The matrigel was recovered and digested with 150 µl/sample CellSperse buffer (supplied with the kit) supplemented with 1 mg/ml collagenase and dispase. Samples were incubated in a 96-well plate for 1 to 3 h at 37 ℃ to disintegrate the blood vessels into single cells and release their hemoglobin. 150 µl/well Drabkin's reagent was added to the plates and incubated for 15 min at RT in the dark. The hemoglobin concentration was determined by photometric measurement at 595 nm and comparison to a hemoglobin standard curve developed in parallel.

The amounts of endothelial cells in the samples were subsequently determined by labeling with fluorescein isothiocyanate-labeled Griffonia Simplicifolia lectin I as follows. Cells and insoluble fractions were collected by centrifugation for 5 min at 250 × *g* in 96-well V-bottom plate. Pellets were washed with 150 µl/well DIVAA wash buffer and centrifuged again. Pellets were resuspended in 300 µl/well of DMEM medium and incubated at 37 ℃ for 1 h to allow endothelial cells recovery. Cells were washed three times as above and resuspended in 200 µl/well 1× FITC-Lectin Dilution Buffer containing FITC-labeled Lectin diluted in 1:200. Plates were incubated overnight at 4 ℃ in the dark under light agitation. Cells were washed three times as above, finally resuspended in 100 µl/well DIVAA wash buffer and transferred into black-walled 96-well plates. The relative fluorescence was determined at 510 nm in a spectrofluorometer with an excitation wavelength of 485 nm (Wallac Victor2). A minimum of 10 angioreactors per treatment group were measured and the mean value ± SD was calculated for each group.

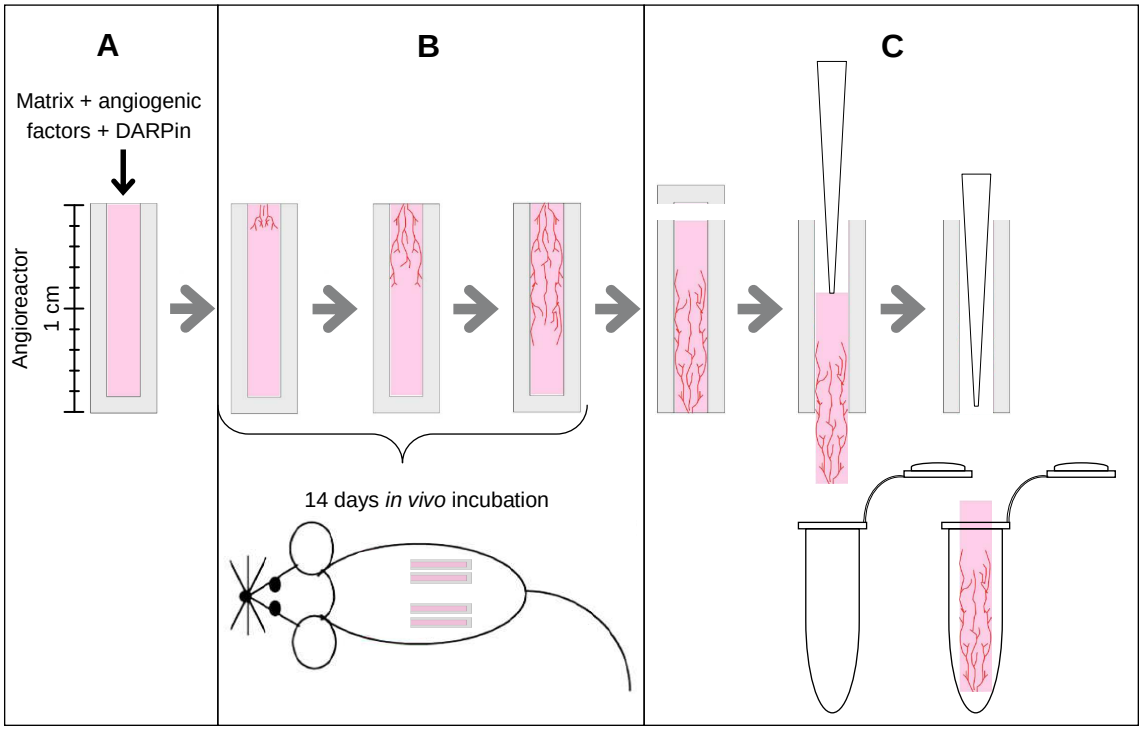

Figure 12. Schematic diagram of the directed *in vivo* angiogenesis assay. A Preparation: Matrigel was premixed with pro-angiogenic factors, DARPin and controls respectively. Samples were filled in semiclosed silicone cylinders, called angioreactors. B Implantation: Angioreactors were implanted subcutaneously in the dorsal flanks of mice. Within 14 days endothelial cells migrate into the angioreactor functional blood vessels containing hemoglobin are formed. C Content analysis: The sealed end was removed and matrigel was recovered into a sterile microtube or a 96-well plate.

2.8 Statistical analysis

All results are reported as mean of three values ± standard deviation (SD). For the *in vivo* angiogenesis study, comparisons to PBS or control DARPin treatment group were performed using one-way analysis of variance (ANOVA). Because statistically significant differences were observed (P-values ≤ 0.05), the groups were compared by Tukey's honest significance test which allows multiple comparisons simultaneously. Statistical analysis was performed using SigmaStat 3.5 (Systat).

3 RESULTS

3.1 EphB4 DARPin isolation and characterization workflow

The main goal of this study was directed to an isolation and characterization of EphB4 specific DARPins. The workflow presented in Figure 13 was designed for this procedure. The first step was to isolate EphB4 binders from a DARPin library by phage display. Secondly unique phage clones were isolated from this population of EphB4 binders by means of a screening procedure followed by sequencing of the DARPin inserts. Third, DARPin inserts were subcloned into a bacterial expression vector and soluble DARPins were produced, purified and subjected to biochemical and functional characterization. For that and as step four the binding characteristics were determined including an analysis of the specificity to EphB4 in comparison to other members of the EphB receptor family. Moreover, the binding kinetics and the ability to compete for the binding with the EphB4 ligand ephrin-B2 were investigated. Finally EphB4 DARPins were functionally characterized *in vitro* using cellular assays and *in vivo*. The focus was to identify DARPin which can block EphB4 signaling, thereby inhibiting angiogenesis which eventually would prevent tumor growth.

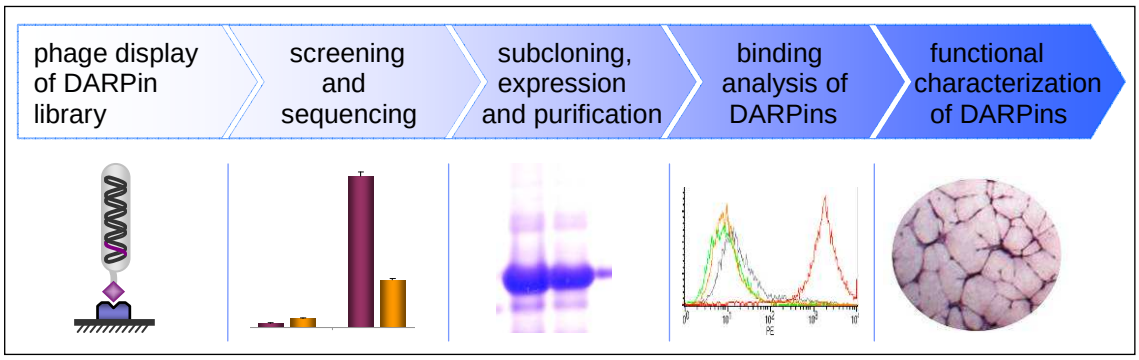

Figure 13. Schematic diagram of the work flow for the isolation and characterization of EphB4 DARPins.

3.2 Selection of DARPins against the extracellular domain of human EphB4

3.2.1 Phage display of DARPin library

Specific binders were selected from combinatorial library using phage display method as described above (chapters 1.3.2, 2.2 and Figure 10). DARPin library chosen for this studies, consists of members designed of two or three randomized ankyrin repeats modules between N-terminal and C-terminal capping, named N2C and N3C, respectively (Steiner et al. 2006). For isolation of EphB4 binders from a DARPin library commercially available recombinant monomeric extracellular domain of human EphB4 (hEphB4 ECD) was used as a target protein. It was assumed that this antigen would allow the selection of a wider spectrum of binders compared to the dimerized form of EphB4 ECD and would include for example also potential receptor dimerization inhibitors.

Three panning cycles were performed as described in Materials and methods (chapter 2.2). The titer of the eluates of bound phage after each section cycle was determined for monitoring the panning efficacy (Table 11). The almost 2 times higher output titer in the 3rd cycle compared to the 2nd cycle of panning, indicates an enrichment of specific phage.

Table 11. Titer of the phage eluates. After each selection cycle bound phage were eluted and the phage titer of the eluates was determined as described in Materials and methods (2.2.3). Titer is given as colony forming units (cfu)/ml. The enrichment factor is calculated from the absolute amount of phage (phage titer × 10 ml culture) compared to the previous cycle and reflects increased / decreased number of specific phage.

Panning cycle	**1**	**2**	**3**
Phage titer (cfu/ml)	1.5E+06	6.0E+05	1.0E+06
Enrichment factor	1	0.4	1.7

3.2.2 Isolation of EphB4 specific phage binders from DARPin library

The phage eluates obtained after each cycle were analyzed by phage ELISA to assess the enrichment of phage binders to EphB4. Figure 14 A presents the binding of the pools of eluted phage of three panning cycles to the immobilized hEphB4 ECD and to lysozyme, an unrelated control protein analyzed for comparison. The third cycle showed significant signal of binding to the target, increased by a factor of 34 compared to the second cycle, which indicates for an enriched population of EphB4 binders. Although parallel some signal increase (5-fold) was observed for the lysozyme binding, the absolute EphB4 signal of the third cycle eluate was 3-fold higher than of the lysozyme, suggesting that EphB4 specific binders were selected. No significant signal increase was observed between cycles 1 and 2.

Hence, the pool from the third selection cycle was taken to isolate individual phage clones. Phage from 184 randomly picked colonies were amplified and investigated for their binding to EphB4 by phage ELISA. As shown in Figure 14 B, several EphB4 specific phage clones were identified. In total 30 specific clones with signals at least 3-fold above background were isolated from the initially 184 picked (~16%). None of the phage clones showed significant binding to the unrelated control protein lysozyme.

The DARPin inserts of the 30 positive phage clones were sequenced. DNA sequence comparison revealed eight unique sequences which differed in their variable region, designated AA5, AB1, AC7, AH5, BD2, BD4, BE1, BG9. This corresponds to ~5% of initially screened 184 clones (Figure 15 A). The frequency of identical sequences varied strongly (Table 12). One dominant sequence (AH5) occurred 17 times, whereas other sequences appeared only one to three times. Four of the inserts contained DARPin constructs with three ankyrin repeat modules between the N-terminal and C-terminal capping sequences (N3C), whereas unexpectedly, the other four sequences contained four repeat modules (N4C). No repeat duplication within the scaffold was observed (Appendix 5.4). The DARPin library used here was designed to contain 2 and 3 repeat units, however it was previously reported that N4C constructs were found to be present at a very low level (Steiner et al. 2008).

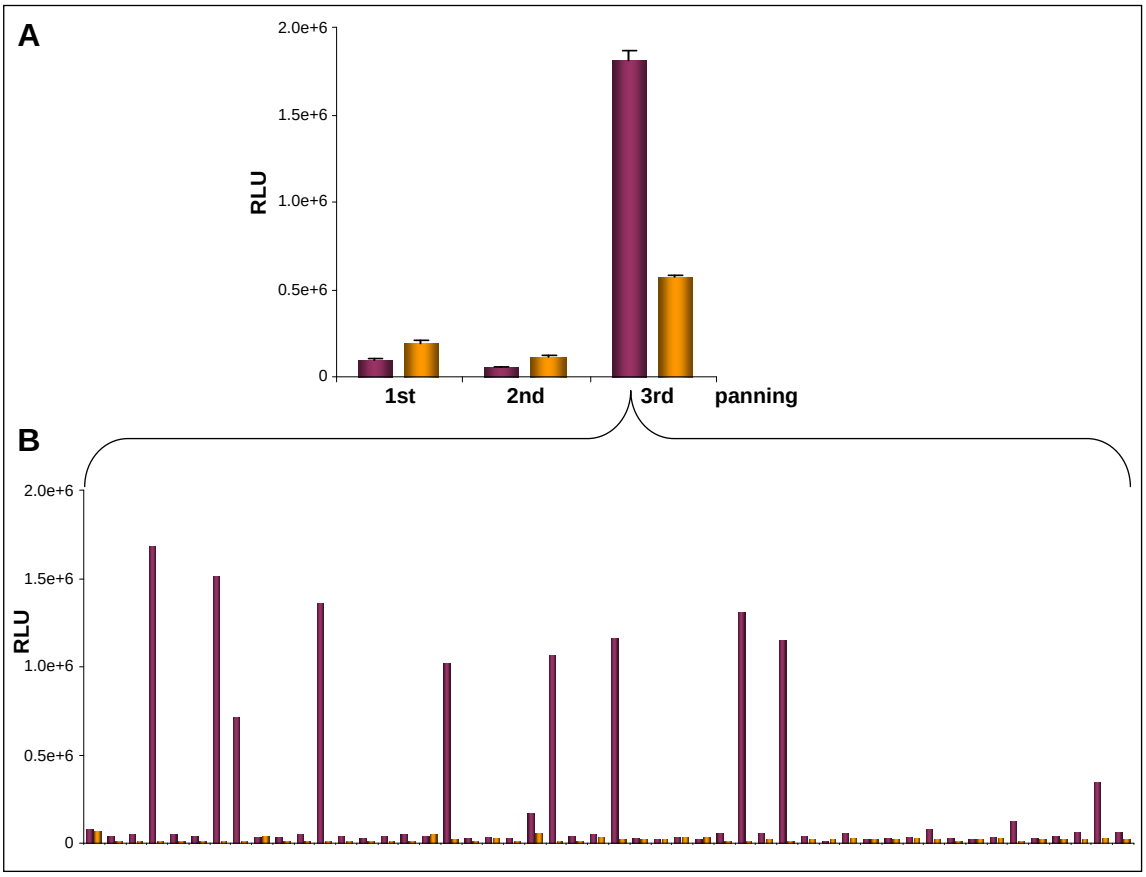

Figure 14. Identification of phage DARPin binding to the monomeric human EphB4 ECD. Equivalent fractions of the phage eluates from the panning cycles 1-3 (A) or monoclonal phage (B) were tested for binding to hEphB4 ECD (red bars) and lysozyme, an unrelated control protein (yellow bars). The bound phage particles were detected with an anti-M13 antibody phage antibody as described in Materials and methods (2.5.2). In (A) values are depicted as means of three measurements ± SD. In (B) 50 of the 184 picked clones for the screening are shown as example.

Table 12. Frequency of identical sequences per clone within 30 analyzed DARPin inserts.

Clone	Frequency	Clone	Frequency
AA5	3	BD2	2
AB1	1	BD4	3
AC7	1	BE1	1
AH5	17	BG9	2

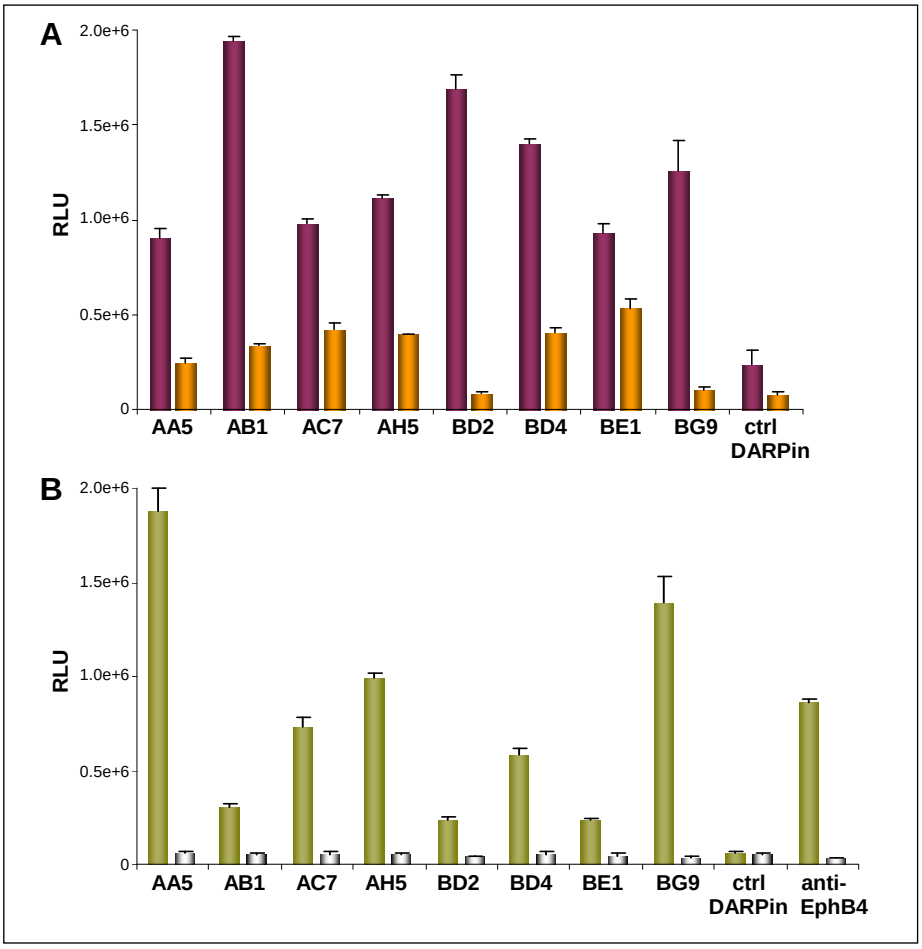

Figure 15. Binding of selected phage DARPin to recombinant EphB4 protein (A) and EphB4 expressing cells (B). (A) Recombinant hEphB4 ECD (red bars) and lysozyme (yellow bars) was coated to the surfaces of 96-well plates. (B) U-2 OS EphB4 cells (green bars) and U-2 OS cells (grey bars) were grown in the 96-well plates. Bound EphB4 phage were detected with anti-M13 phage antibody (2.5.2). Antibody against human EphB4 and phage DARPin against lysozyme were used as controls. Values are depicted as means of three measurements ± SD.

Phage display for isolating EphB4 binders was performed under rather unphysiological conditions using recombinant EphB4 which was directly coated to the plastic surface. Therefore, the isolated phage clones were tested whether they could also bind native EphB4 receptor expressed on the cell surface. DARPin binding to living U-2 OS cells stably transfected with human EphB4 (U-2 OS-hEphB4) grown in 96-well plate was analyzed by a cell ELISA (2.5.2). As shown in Figure 15 B, all eight phage clones selectively bound to

EphB4 expressing but not to untransfected U-2 OS cells, which were used for comparison.

Interestingly, the signal intensities generated by phage AA5 and BG9 were similar in the cell ELISA and the ELISA using coated protein (Figure 15 A), whereas in the other clones showed lower signals in the cell ELISA. The reason for this difference could be that the phage particles displaying DARPins interfere with the binding to certain sites of cellular EphB4. The cell ELISA was verified using flow cytometry analysis and presented similar results (Appendix 5.1, Figure 43). Altogether these results indicate that all eight isolated DARPins even when displayed on the phage surface as fusion with the M13 phage coat protein pIII recognized the native receptor and can be subjected to further functional analysis.

3.2.3 Expression and purification of DARPin

For detailed characterization EphB4 DARPin-pIII fusion proteins were converted into soluble DARPin proteins by subcloning into the bacterial expression vector pMPAG6 to eliminate a conceivable dependence on the phage format. Thus, the phagemid inserts were successfully excised by restriction with enzymes BamHI and HindIII and purified by preparative agarose gel electrophoresis (Figure 16 A). As expected, inserts of the four N3C clones and four N4C clones separated according to their different sizes (~474 bp vs 573 bp; Figure 16 C). The gel purified DNA fragment was transferred into the corresponding restriction sites of pMPAG6 and subjected to the control digestion (Figure 16 B). All eight inserts were successfully subcloned and amp resistant colonies were isolated. DARPins were expressed in *E. coli* after IPTG induction and initially purified by IMAC via their N-terminal His-tag as described in the Materials and methods chapter (2.4.2). An example of the single step IMAC purification of DARPin BG9 is shown in Figure 17 A. DARPin expression was induced by IPTG (Figure 17; compared in lanes C and C+). Crude bacterial lysate was solubilized without detergent in a physiological salt buffer (Figure 17; lane S). DARPin bound to the column at 20 mM imidazole and was eluted with buffer

containing 250 mM imidazole (Figure 17A; lanes FT and E1). IMAC was deliberately performed under saturating conditions to minimize binding of unspecific proteins. This results in residual amounts of DARPin in the flow through and wash fractions (Figure 17 A; lanes FT, W). The majority of the DARPin was eluted in fraction 1 (Figure 17 A; compared in lanes E1 and E2). The chromatogram in Figure 17 B shows that the DARPin elutes as a sharp homogeneous peak indicating for a high degree of purity. All other DARPins were purified in the same way and the IMAC-purified material is shown in Figure 17 C. Corresponding to their repeat pattern (N3C or N4C) and their calculated molecular weights DARPins migrated as major bands at ~17 and 20 kDa. Additional minor proteins were observed, which appear in a regular pattern. This suggests that they are DARPin related and may constitute either mulitmeric forms or degradation products. Routinely purities of 75–90% were achieved after IMAC preparations of all eight DARPin proteins. DARPins were produced at high levels reaching about 20–55 mg/liter (Figure 17 D).

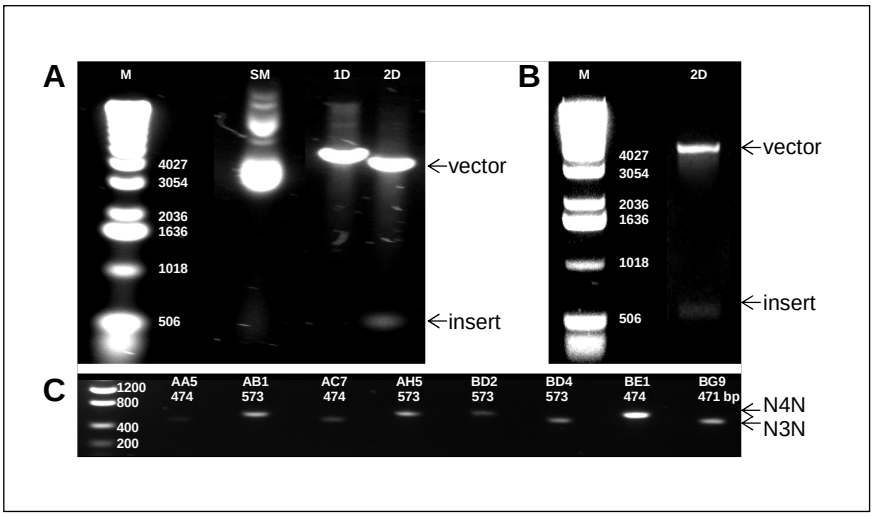

Figure 16. Isolation of DARPin DNA inserts form selected phagemids. (A) DARPin inserts, here exemplified by AC7 were excised by sequential digestion of phagemid DNA (SM) with BamHI (1D) followed by HindIII (2D) and analyzed by agarose gel electrophoresis and EtBr staining. (B) Successful subclonig of DARPin insert was verified by the sequential digestion of pMAG6 with BamHI and HindIII. (C) Gel purified DNA inserts of selected DARPins. The size corresponds to N3C or N4C inserts, 474 and 573 bp respectively. DNA markers (M) are shown in the left lanes with sizes in bp.

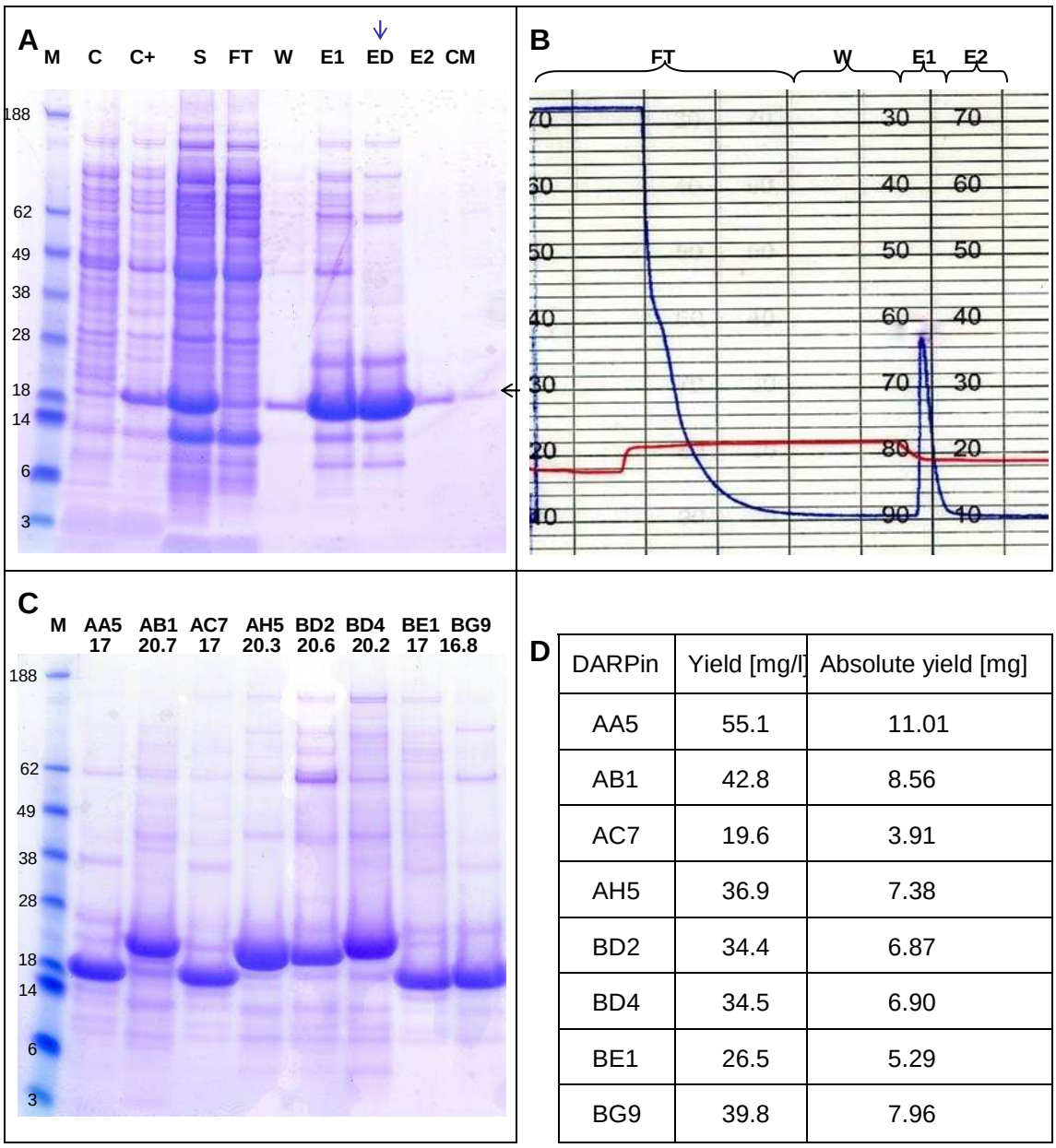

DARPin	Yield [mg/l]	Absolute yield [mg]
AA5	55.1	11.01
AB1	42.8	8.56
AC7	19.6	3.91
AH5	36.9	7.38
BD2	34.4	6.87
BD4	34.5	6.90
BE1	26.5	5.29
BG9	39.8	7.96

Figure 17. Expression and purification of EphB4 DARPins. DARPins were expressed and IMAC-purified as described in Materials and methods (2.4.2). (A) Aliquots of various fractions obtained during expression and IMAC purification were separated by SDS-PAGE and stained with Imperial protein stain. DARPin BG9 is shown as example. (C-,C+, bacterial cell lysate before and after IPTG induction; S, soluble fraction – start material; FT, IMAC flow through; W, wash fraction; E1-2, elution fractions; ED, dialyzed E1; CM, IMAC column material; M, molecular weight marker). Arrows indicate the end material (blue) and the band corresponding to DARPin protein (black). (B) Chromatogram of IMAC purification of BG9 (blue line: A280 nm; red line: conductivity). (C) SDS-PAGE of IMAC purified DARPins (5 µg/lane). Staining was carried out with Imperial Protein Stain. Calculated molecular weights of DARPins are indicated in kDa. (D) Expression yields of DARPins. Representative data out of two independent experiments are shown.

In an attempt to remove contaminating proteins IMAC-purified material was subjected to the anion exchange chromatography (Ahamed et al. 2008). The majority of contaminating proteins could be successfully removed as shown in (Figure 18 A). As indicated by the Western blot in Figure 18 B, many of the proteins considered as contaminants were DARPin derived and were detected by an anti-RGS-His_4 antibody. They resemble either dimerized DARPins or degradation products.

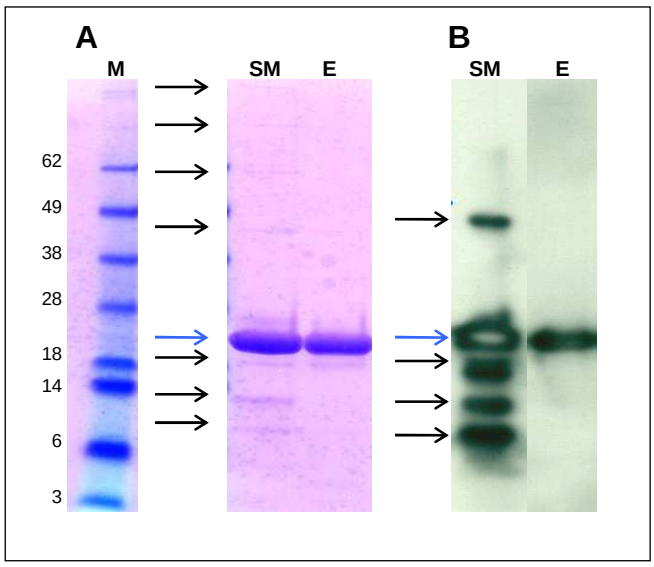

Figure 18. Ion exchange chromatography of IMAC-purified DARPin. IMAC-purified DARPins (here exemplified by AB1) were purified by IEC as described in Materials and methods (2.4.2). Aliquots of fractions in equivalent amounts (SM: start material, E: eluate fraction) were analyzed by (A) SDS-PAGE and (B) Western blot using an anti-RGS-His_4 antibody. DARPin is indicated by blue arrow, contaminants by black arrows (M: molecular weight marker in kDa).

3.2.4 Characterization of DARPins by size exclusion chromatography

For further biochemical characterization IMAC-purified DARPins were subjected to size exclusion chromatography (SEC) to assess their molecular size. Additionally samples which were routinely stored at -80 ℃ were compared to samples stored at 4 ℃ for more than a month to investigate effects of storage conditions on the DARPin. Figure 19 shows the elution profiles of four representative DARPins. Their size was estimated from the elution volume

compared to the standard proteins. BG9 eluted as a sharp single peak at the relative position corresponding to the calculated molecular weight of 17 kDa, independent of whether sample was stored at -80 ℃ or at 4 ℃ (Figure 19 A). This shows that BG9 occurs as stable monomeric protein in solution.

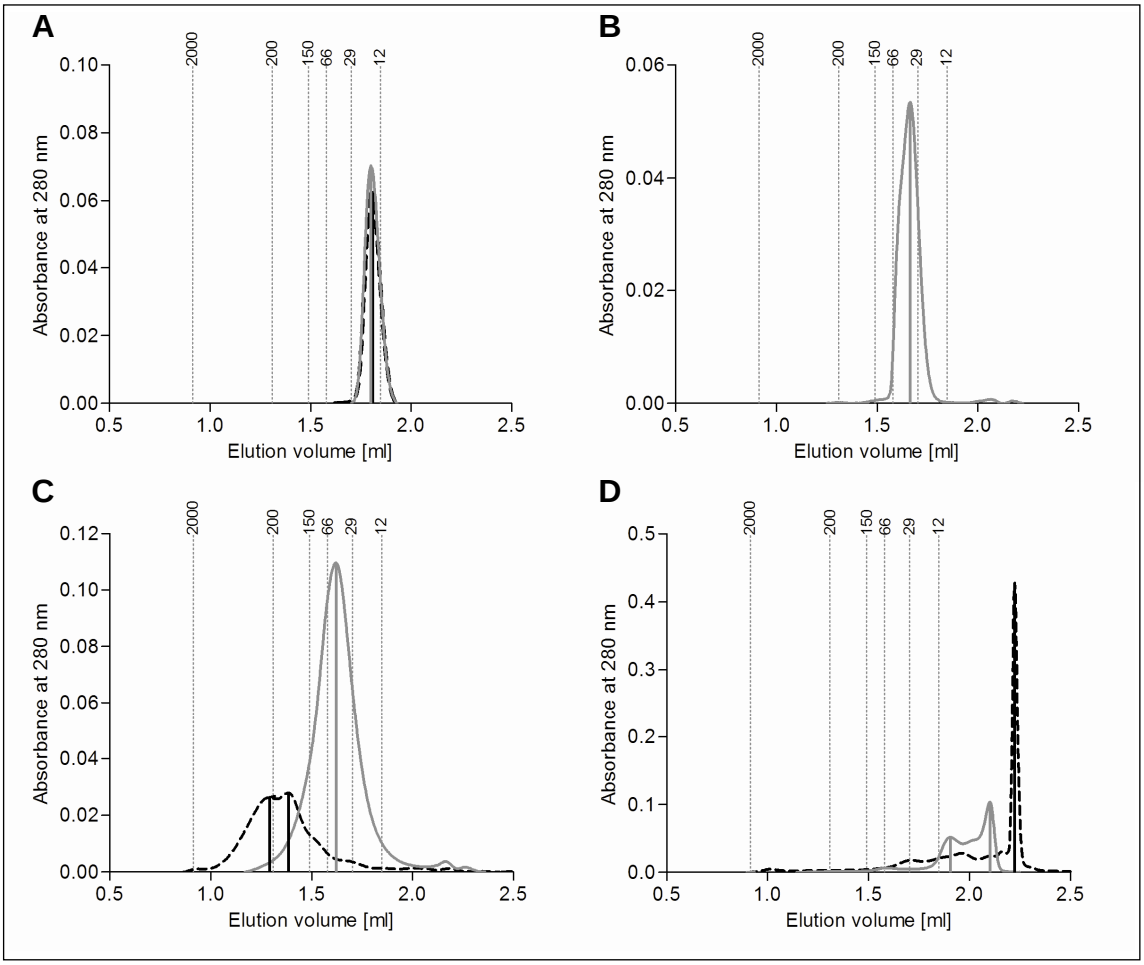

Figure 19. Analytical size exclusion chromatography of IMAC-purified DARPin. The SEC fractionation of DARPins was performed on a Superdex 200 column as described in 2.4.2 (5 µg of sample). The panel shows overlays of elution profiles of selected DARPins: BG9 (A), AH5 (B), AB1 (C) and AC7 (D). Chromatograms given by grey solid lines refer to IMAC purified DARPins stored at -80 ℃, whereas samples stored fo r more than a month at 4 ℃ are plotted in black dashed lines. Dotted lines indicate the elution volume of the standard proteins: blue dextran 2000 kDa, β-amylase 200 kDa, alcohol dehydrogenase 150 kDa, albumin 66 kDa, carbonic anhydrase 29 kDa and cytochrom C 12.4 kDa (chromatograms are presented in Appendix 5.1, Figure 40). Representative data out of two independent experiments are shown.

DARPins AH5 and AB1 stored at -80 ℃ showed single elution peaks at positions corresponding to the calculated molecular weights of their dimers (Figure 19 B-C). AB1 eluted a broader peak compared to AH5 which may be attributed to overloading. Similar to BG9 the elution profile of AH5 stored at 4 ℃ was unchanged (data not shown). In contrast, AB1 tends to oligomerize when stored at 4 ℃ since it eluted at the relative position of ~200 kDa (Figure 19 C). DARPin AC7 stored at -80 ℃ eluted late in several peaks beyond the expected relative position of 17 kDa, indicating that the material is degraded. Enhanced degradation seems to occur upon storage at 4 ℃, as this material eluted even later (Figure 19 D). DARPin AC7 seems to be unstable when stored in PBS at 0.25 mg/ml and -80 ℃ which may be an intrinsic property of this protein. Taken together these results indicate that EphB4 DARPins occur not exclusively as monomer, but can also form dimers and upon storage at 4 ℃ may form higher oligomeric aggregates. Their stabilities can be affected by the storage conditions like temperature and buffer. Improvements may be achievable at a later stage by changing some of these parameters. For this study DARPins were stored in PBS at 0.25 mg/ml at -80 ℃ since most of them were stable under these conditions.

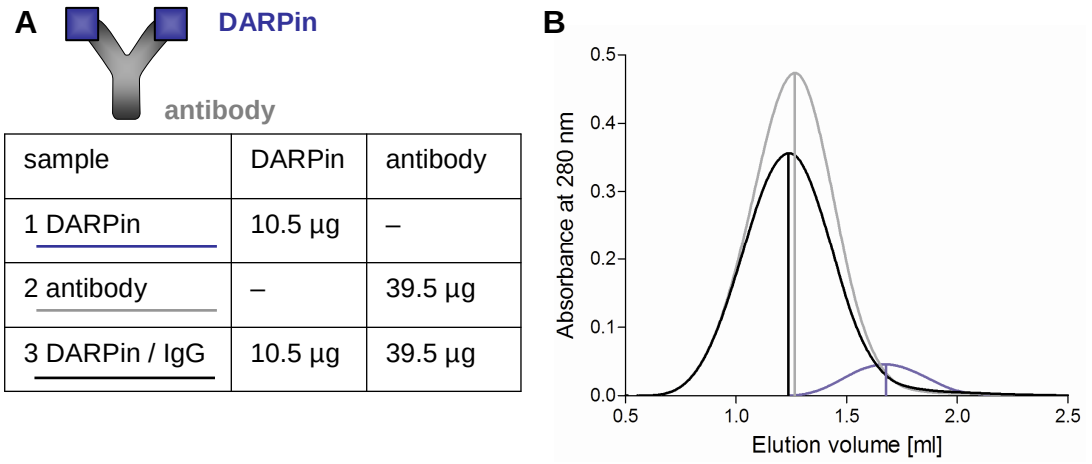

sample	DARPin	antibody
1 DARPin	10.5 µg	–
2 antibody	–	39.5 µg
3 DARPin / IgG	10.5 µg	39.5 µg

Figure 20. Analytical size exclusion chromatography of DARPin AA5 / anti-RGS-His$_4$ IgG antibody complexes. DARPin AA5 (shown as example) was incubated with an anti-RGS-His$_4$ antibody at a molar ratio of 2:1 and the resulting complexes (A) were analyzed by SEC as described (2.4.2). An overlay of the elution profile of the samples is displayed (B).

To analyze the effect of DARPins dimers in particular studies such as binding analysis to the EphB4, DARPins were bound via their N-terminal His-tag to an anti-RGS-His_4 antibody. The resulting complexes formed after incubation of DARPin at a 2-fold molar excess with the antibody were analyzed by SEC (Figure 20). One distinct peak was observed, which eluted slightly faster than the His-tag antibody alone, indicating that the DARPin / IgG complexes were successfully formed with undetectable amounts of unbound DARPin left. Such complexes were applied in the binding analysis to the recombinant protein or cell surface..

3.3 Analysis of the binding characteristics of EphB4 DARPins

3.3.1 DARPin binding to the recombinant hEphB4 ECD

DARPin format modification from phage to soluble protein could influence the biophysical properties of the initial library members. To confirm that the EphB4 selected DARPins did not loose their favorable binding to hEphB4 after conversion from DARPin-pIII fusion proteins their binding ability was re-investigated by ELISA. Figure 21 shows that all DARPins retained their binding and specifically recognized hEphB4 ECD with 2- to 19-fold higher signals compared to the unrelated control protein. The binding signals were also significantly higher than of the control DARPin. Therefore, all DARPins were subjected to further analysis.

DARPins were selected based on binding to the monomeric extracellular domain of EphB4 to possibly obtain binders preferentially binding to the monomer. Such binders could perhaps prevent receptor dimerization and its activation after interaction with its ligand upon cellular interactions *in vivo*. Therefore, DARPin binding to a recombinant Fc-fusion protein of the extracellular domain hEphB4 which generates a dimerized form of the receptor (hEphB4-Fc ECD) was analyzed. As shown in Figure 22, all DARPins recognized also recombinant dimer of hEphB4, which suggests that the binding epitopes are accessible on the monomeric and dimeric receptor molecules.

Notably DARPins demonstrated in fact stronger binding signals to the hEphB4-Fc ECD. DARPins were applied in dimerized format as DARPin / IgG complexes, as such could favor EphB4 dimer over the monomer. Although the distinguished binding levels could be result of differences in immobilization of the proteins. The EphB4 ECDs were coated at the equimolar ratio, however the Fc fragment possibly arranges the EphB4 ECD more available for DARPin binders. Direct immobilization to the surface can partly cover the epitopes of the monomer in higher degree than of the Fc fusion, resulting in stronger binding signal to the dimerized EphB4.

A

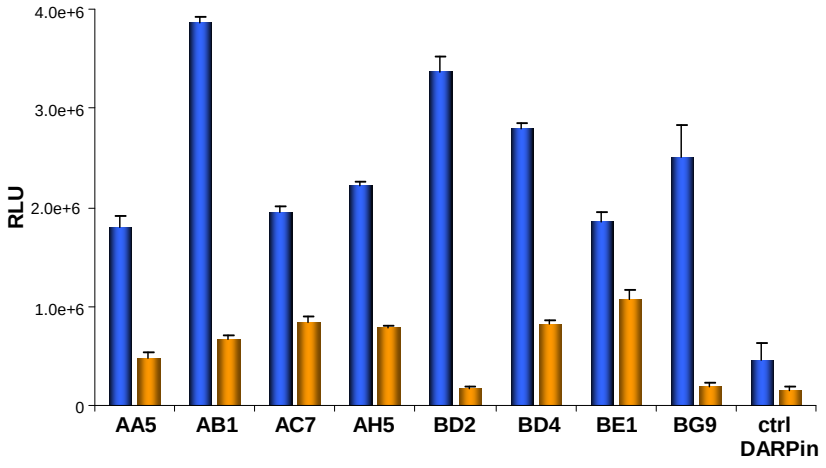

B

DARPin	AA5	AB1	AC7	AH5	BD2	BD4	BE1	BG9	ctrl.
Signal ratio of EphB4 / lysozyme	4	6	2	3	19	3	2	13	3

Figure 21. Binding of IMAC-purified EphB4 DARPins to the recombinant monomeric hEphB4 ECD. (A) Binding of DARPins to monomeric hEphB4 ECD (blue bars) was analyzed by ELISA as described in Materials and methods (2.5.2). Bound DARPins were detected via their N-terminal His-tag using an anti-RGS-His_4 antibody. Lysozyme (yellow bars) was used as an unrelated control protein. Off7, DARPin directed against MBP protein was used as a control DARPin. Values are depicted as means of three measurements ± SD. (B) Binding specificity was calculated as a ratio between binding signals to the EphB4 and to the unrelated control protein.

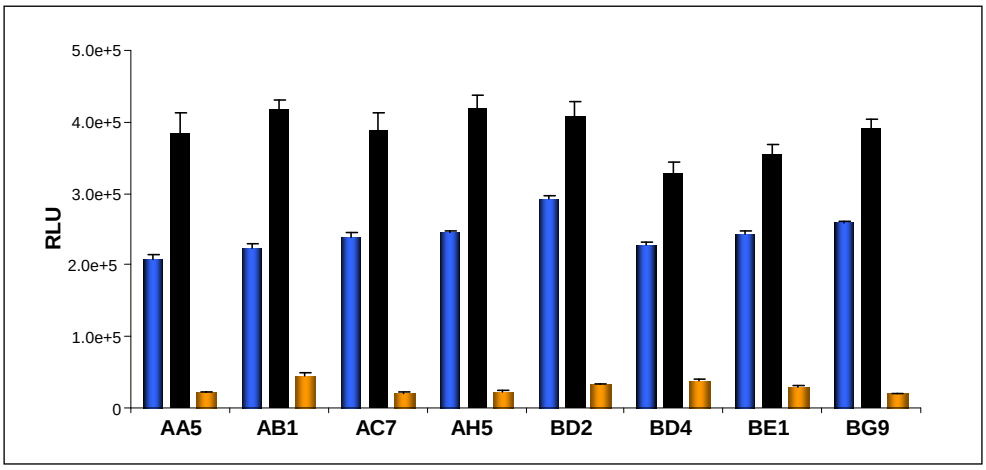

Figure 22. Binding of EphB4-selected DARPins to hEphB4 ECD monomer and dimer. Binding of DARPins to hEphB4 ECD was analyzed by ELISA as described in Materials and methods (2.5.2). Antigens were immobilized at the equimolar concentration: EphB4 monomer (340 ng/well, blue bars), EphB4 dimer (5 µg/ml, black bars) and lysozyme as an unrelated control (500 ng/well, yellow bars). The IMAC purified DARPins were dimerized through anti-RGS-His_4 antibody at the molecular ratio 2:1. Values are depicted as means of three measurements ± SD.

3.3.2 Binding of EphB4 DARPins to other EphB receptors

The aim of this work was to select DARPins, which specifically bind to hEphB4 and not to other EphB receptors. The EphB receptor family consists of five members, which are structurally homologous. To investigate the specificity of the EphB4 selected DARPins all commercially available recombinant proteins of the extracellular domains of EphB receptors were immobilized and DARPin binding was analyzed by ELISA. In cases where the respective human fusion protein was not available the corresponding proteins from rat or mouse were used. Murine EphB4 was included in this assay to assess the cross reactivity of the EphB4 DARPins with their mouse ortholog which would allow their application for functional *in vivo* studies in mice. The results are shown in Figure 23.

6 of 8 DARPins bound specifically to EphB4: AA5, AC7, AH5, BD4, BE1, and BG9. Two DARPins (AB1, BD2) recognized also murine but not human EphB6, but their binding signals were significantly lower compared to EphB4. Three

DARPins (AB1, BD2, BD4) which include those recognizing mEphB6 cross reacted to various degree with murine EphB4. The binding signals of AB1 to human and murine EphB4 were very similar whereas the mEphB4 signals of BD2 and BD4 were significantly lower than those of hEphB4. No binding was observed to EphB 1-3, despite successful immobilization of their fusion proteins (Appendix 5.1). Although rodent EphB1-3 proteins were used it is considered likely that also the human proteins are not recognized since they share homology of over 94% with the human receptors (Table 17). Furthermore, the extracellular domains of EphB receptors possess only sequence identities between 34.6% and 41.5% (Table 16), which may attribute to the isolation of DARPins which bind EphB4 with high specificity.

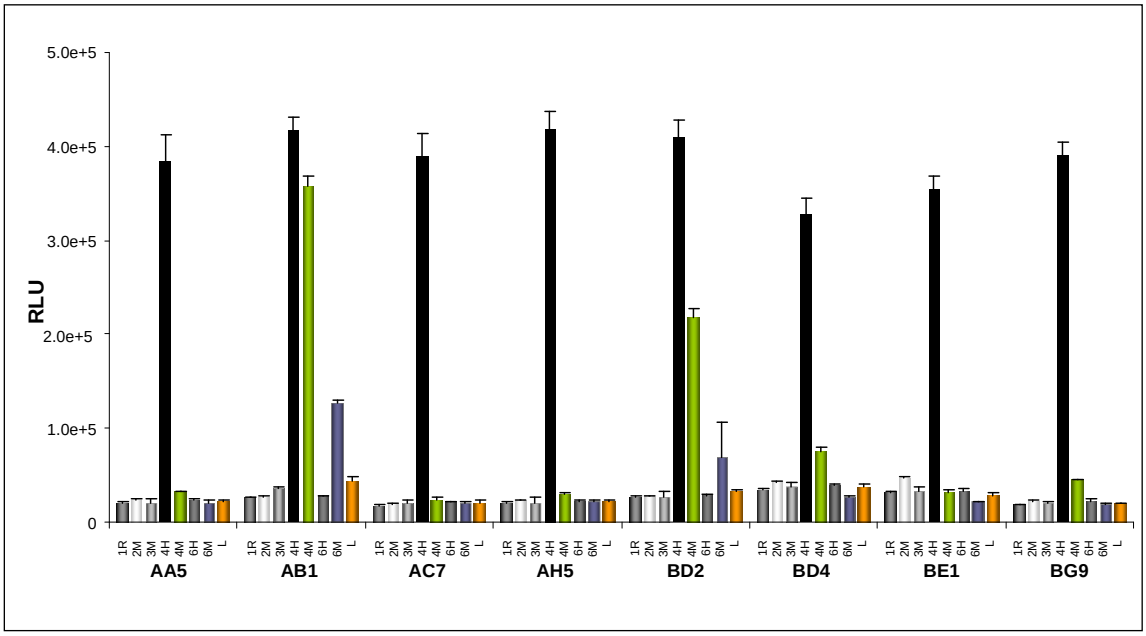

Figure 23. Binding specificity of EphB4 DARPins to mammalian EphB receptors. Recombinant Fc-fusion proteins of rat EphB1 (1R), murine EphB2 (2M), murine EphB3 (3M), human EphB4 (4H), murine EphB4 (4M), human EphB6 (6H) and murine EphB6 (6M) were immobilized and DARPin binding was analyzed by ELISA as described in Materials and methods (2.5.2). Lysozyme (L) was used to determine unspecific binding. The immobilization of Fc-fusion proteins was confirmed using an HRP-labeled anti-Fc antibody (Appendix 5.1, Figure 41). Values are depicted as means of three measurements ± SD.

3.3.3 Analysis of EphB4 DARPins binding to EphB4 expressing cells

So far *in vitro* characterization of the binders had solely been performed with the isolated ectodomain of EphB4. For the *in vitro* and *in vivo* functional analysis it is necessary that the DARPin bind also the target expressed on the cell surface. Therefore, their cell binding was determined by flow cytometry analysis using tumor cell lines which express EphB4 after stable transfection (U-2 OS-hEphB4) compared to the U-2 OS parental cell line with minimal expression level of EphB4. Moreover, breast tumor cell line MCF7, reported to express significant amounts of endogenous EphB4 (Kumar et al. 2006) was included in the analysis. Cells incubated with the DARPin / IgG antibody complexes, were subsequently labeled with a fluorescent dye and thereafter analyzed by flow cytometry analysis.

All DARPins specifically bound to stably transfected U-2 OS-hEphB4 cells as indicated by the strong fluorescent signals observed (Figure 24; left panel, red profiles). The control DARPin (orange profiles) showed no signals above background. Significantly reduced binding to untransfected U-2 OS cells was observed (Figure 24; centre panel, pink profiles), which is consistent with the observation that untransfected U-2 OS cells express low amounts of EphB4 (Appendix 5.1, Figure 42). This demonstrates that DARPin binding to the cell surface was mediated by the specific interaction with EphB4.

All EphB4 DARPins labeled also MCF7 breast tumor cells, but the shift of fluorescence intensity was generally not as strong as displayed by the U-2 OS-hEphB4 cells (Figure 24, right panel, green profiles). This observation is also consistent with the lower EphB4 expression levels in MCF7 cells. Interestingly, DARPins AA5 and BE1 showed only very low fluorescent signals in MCF7 cells suggesting that the cellular context of EphB4 may affect the binding of certain EphB4 DARPins. The poor binding to EphB4 on the cell surface could be also resulted by lower affinities. Taken together, the above results demonstrated that all isolated EphB4 can bind also to the cell surface-expressed receptor and that this binding may be affected by the cellular context or various affinities. Therefore, the kinetic parameters of the interaction should be analyzed next.

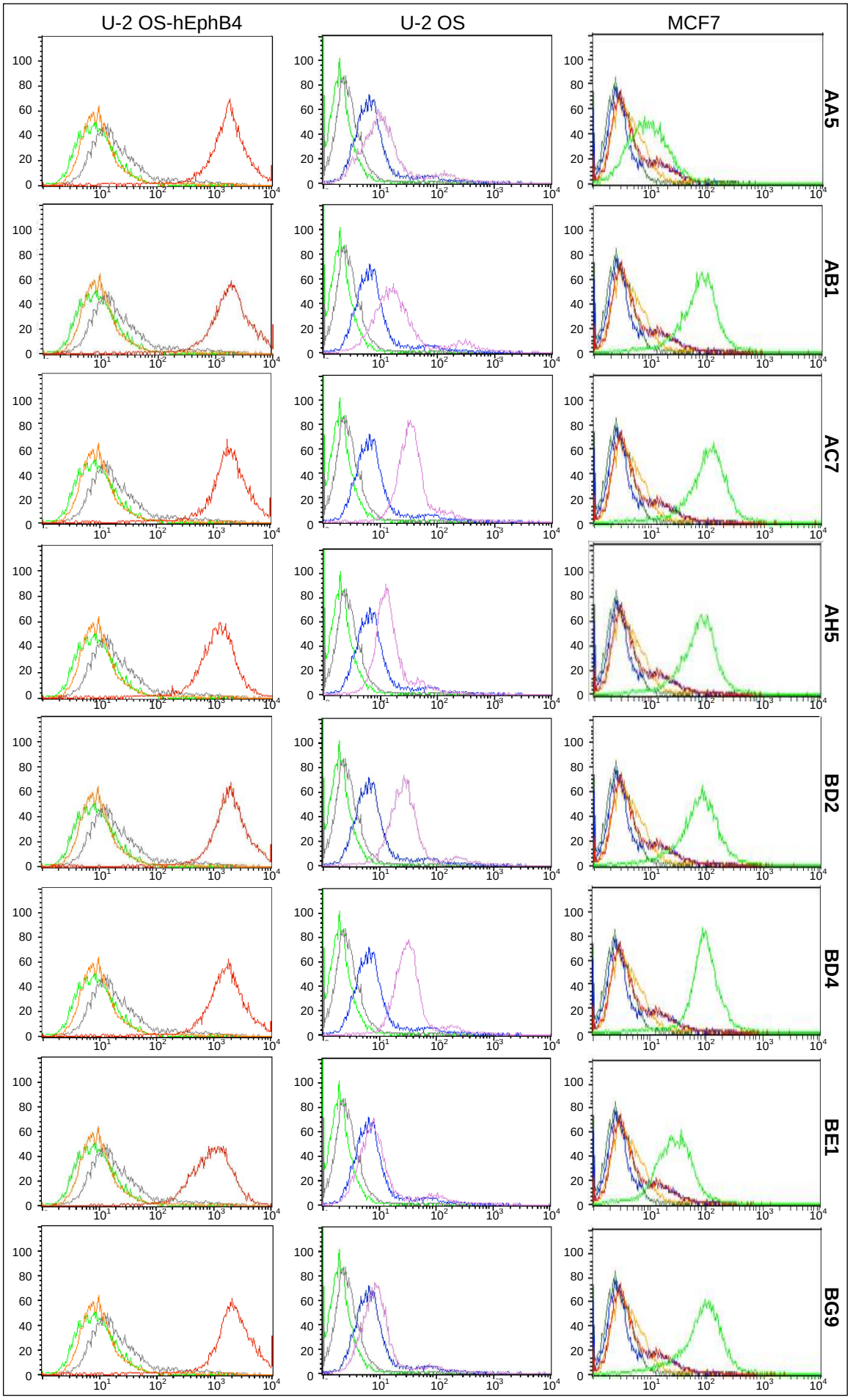
U-2 OS-hEphB4
U-2 OS
MCF7
AA5
AB1
AC7
AH5
BD2
BD4
BE1
BG9

Figure 24. Flow cytometry analysis of EphB4 DARPin binding to EphB4 on U-2 OS and MCF7 cells. DARPin binding to U-2 OS cells stably transfected with hEphB4 (left panel), U-2 OS untransfected cells (centre panel) or MCF7 (right panel) was analyzed by flow cytometry analysis as described in Materials and methods (2.5.3). The IMAC purified DARPins were dimerized through an anti-RGS-His_4 antibody at the molecular ratio 2:1. Bound DARPin / IgG complexes were detected using an R-Phycoerythrin-coupled secondary antibody. Overlays of the FACS signal profiles of EphB4 DARPins and controls (cells without antibodies, cells with control DARPin or only with secondary antibody) are shown as indicated below. The logarithm of the fluorescence intensity (X axis) was plotted versus the cell count (Y axis). Representative data out of three independent experiments are shown.

Colour code:	U-2 OS-hEphB4	U-2 OS	MCF7
Cells only			
Control DARPin			
2nd antibody only			
EphB4 DARPin			

3.3.4 Binding kinetics of EphB4 DARPins to EphB4

Surface Plasmon Resonance (SPR) technology is a label-free method that allows monitoring of interactions between biomolecules in the real time in a cell free system. This method provides quantitative information about the stoichiometry of interacting partners, association and dissociation kinetics (k_{on}, k_{off}) and their binding affinities ($K_D = k_{off} / k_{on}$). During the analysis the protein of interest (analyte) binds to the partner protein (target) immobilized to the carboxymethylated dextran-gold surface resulting in an increasing and measurable response. While the interaction reaches equilibrium, the response remains constant, and decreases upon the dissociation of the analyte, when the sample is replaced by buffer. The entire binding process, measured in resonance units (RU), are plotted as a function of time, thereby generating a sensorgram, which is used to calculate the association and dissociation constants.

SPR was used to investigate the binding kinetics of EphB4 DARPins to either monomeric or Fc-dimerized human EphB4 ECD coated on the BIAcore sensor

chip. At first the EphB4 proteins were immobilized onto a carboxymethylated dextran-coated (CM5) chip's surface. The analysis was performed by simultaneous use of three active flow cells and one control channel. In order to analyze an optimal pH and a protein concentration for the efficient coating pre-concentration of the target on the sensor surface was performed by electrostatic interaction. The target proteins were immobilized using a standard amine-coupling procedure as described in Materials and methods (chapter 2.5.4). The aim was to achieve the optimal coating density of EphB4 ectodomains to perform kinetic analysis. 1000 RU corresponds to an immobilized protein concentration of approximately 1 ng/mm^2. Immobilization finally resulted in 1135 RU and 649 RU for hEphB4 dimer and monomer respectively as shown in the sensorgram (Appendix 5.1, Figure 44). The reference channel was coated with lysozyme at the equimolar level of 407 RU. Due to the marginal response, the mouse EphB4 coated surface (1072 RU) was excluded from the analysis. The immobilization of highest possible amount of the target protein on the chip surface (7664 RU) resulted in unspecific binding of DARPins and hindered kinetic analysis (data not shown).

Prior to the DARPin measurements the set-up was evaluated by analyzing the binding kinetics of ephrin-B2 to hEphB4-Fc and comparing it with published data. Binding was performed using the Fc fusion protein of ephrin-B2 in a concentration range between 4 and 300 nM of ligand. Typically, 50-70 % of the EphB4 molecules immobilized on the chip were able to bind ephrin-B2 upon covalent coupling and at least 40% of them conserved their binding capacity until the end of a single experiment (data not shown). The interaction data were fitted to the Langmuir binding model which assumes a 1:1 interaction. A dissociation constant of 0.8 nM was derived (Table 13), which is consistent with the published value of approximately 0.5 nM (Blits-Huizinga et al. 2004). Ephrin-B2 has two binding interfaces enabling simultaneous binding to two receptor molecules (Himanen and Nikolov 2003a). Since dimerized ephrin-B2-Fc fusion protein was used in this study, the binding data were also analyzed with bivalent analyte model (Figure 25 A). This algorithm assumes a bivalent two-step binding model of analyte (A) with the receptor (R), starting with a 2:1 interaction, followed by a second 2:2 interaction ($2R + A2 \leftrightarrow RA2 + R \leftrightarrow R2A2$).

With this model a statistically significant better fit was obtained, which is reflected by an 8-fold lower χ^2 value (Table 14). Based on this model an apparent dissociation constant of 15 nM for the initial 2:1 interaction was calculated, which is about 18-fold less compared to the K_D derived from the Langmuir model. These results are in agreement with recently published data by Pabbisetty et al. 2007, who observed in their predictions a 30-fold difference in the affinity of ephrin-B2 to the receptor depending on the interaction model used.

Binding of ephrin-B2 to the monomeric EphB4 was examined similarly by the monovalent and bivalent model, resulting in 7-fold lower χ^2 value for the bivalent analyte model. In this case equilibrium dissociation constants of 27 nM and 1.4 nM were observed, depending on the evaluation model (Table 13). The 2-fold increase in the apparent equilibrium dissociation constants, suggests higher affinity to the dimeric EphB4 receptor compared with the monomeric (Figure 25 B). To support the analysis, data were additionally evaluated with the steady-state binding model ($R_{eq} = (R_{max} \times C) / (C+K_D)$)[3] delivering affinity constants similar to the values obtained with the bivalent analyte model (Table 13, Figure 25 C-D). Based on this results, binding kinetics of the EphB4 DARPins were analyzed in a similar manner.

Table 13. Affinity constants of the interaction between ephrin-B2-Fc and the monomeric or dimerized EphB4. K_D values expressed in nM were determined using three binding models of the BIAcore software 4.1. Data depicted represent one of three independent measurements.

Evaluation model:	**EphB4 dimer**	**EphB4 monomer**
1:1 Langmuir	0.8	1.4
Bivalent analyte	14.7	26.9
Steady-state binding	13	25.4

[3] R_{eq} - response at equilibrium, R_{max} - maximal response, C- concentration

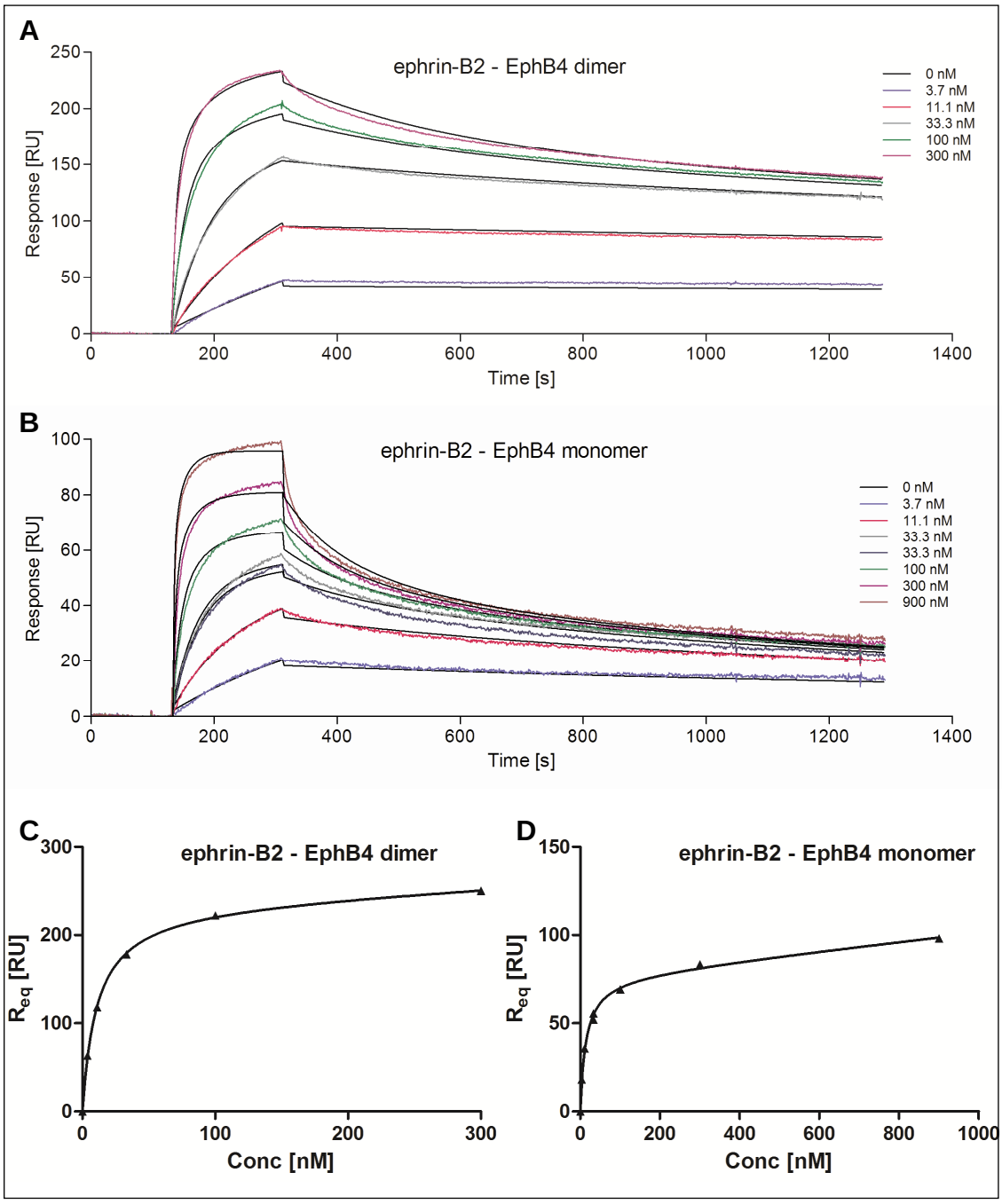

Figure 25. SPR analysis of ephrin-B2 binding to human EphB4 ECD. The interaction of ephrin-B2-Fc was analyzed at the indicated concentrations to the immobilized receptor EphB4 dimer (A) and monomer (B) fitted with the bivalent analyte model. The binding curves of ephrin-B2 are illustrated as double-referenced sensorgrams (shown as colored lines) overlaid with the respective global fits (black lines). The steady-state analysis was performed by fitting of the concentration versus the response at the equilibrium (R_{eq}) for the ephrin-B2-Fc interaction with either EphB4 dimer (C) or monomer (D). Data depicted in (A) and (C) represent one of three independent measurements, similarly as in (B) and (D).

EphB4 DARPins were shown to bind to the monomer and to the Fc-dimerized EphB4 by ELISA (Figure 22). To determine their binding kinetics in more detail SPR analysis was performed. The measured response, determined in RU by the BIAcore detector, depends mainly on the molecular weight of the bound analyte. Based on the binding kinetics of ephrin-B2 and taking the difference in molecular weight into account the maximal DARPin responses were predicted to be five times lower resulting in ~30 RU at a concentration of 33 nM. Primary, it was evaluated whether responses in that range could be detected. As shown in Figure 26, response of about 30 RU was measured for DARPins: AB1, BG9 and AH5. The maximum binding responses of these DARPins were within the expected range, considering the effective number of active EphB4 molecules on the chip surface and the above-mentioned activity decrease associated to repeated regeneration steps. Responses for DARPins AC7, BD2, BD4 and BE1 were lower and in the range of 15 to 5 RU, which suggests that perhaps only a certain fraction of the DARPin preparation is able for binding. Unfortunately, no binding could be measured for AA5 for unknown reasons and therefore, this DARPin was excluded from further analysis.

The binding kinetics of the DARPins to monomeric and dimeric hEphB4 were determined in a concentration range between 3 and 900 nM as presented in Figure 27. Although DARPins are designed to occur as monomers, gel filtration analysis revealed also higher forms, for example AH5 or AB1, which appeared as a dimer (Figure 19 B). Therefore, similarly to ephrin-B2, the SPR measurements of DARPins were fitted using both the 1:1 Langmuir and the bivalent analyte binding models. Analysis of χ^2 values for DARPins interaction with the monomeric EphB4 revealed a comparable statistical relevance of the fits obtained with both models (Table 14). DARPin binding to the EphB4-dimer showed only slightly better fit when evaluated with the bivalent analyte model. However, interaction data for AH5 with EphB4 monomer and dimer fit significantly better to the bivalent model indicated by 3- and 7-fold lower χ^2 respectively. These results suggest that this is the most likely model of interaction and AH5 might exist at least in dimerized form. Otherwise the χ^2 values of AB1 fitting differed only by 1.5–1.8 factor. Based on this information

the bivalent binding model was used to fit AH5, and the 1:1 Langmuir model to evaluate the other DARPin binding data (Figure 27, Table 15).

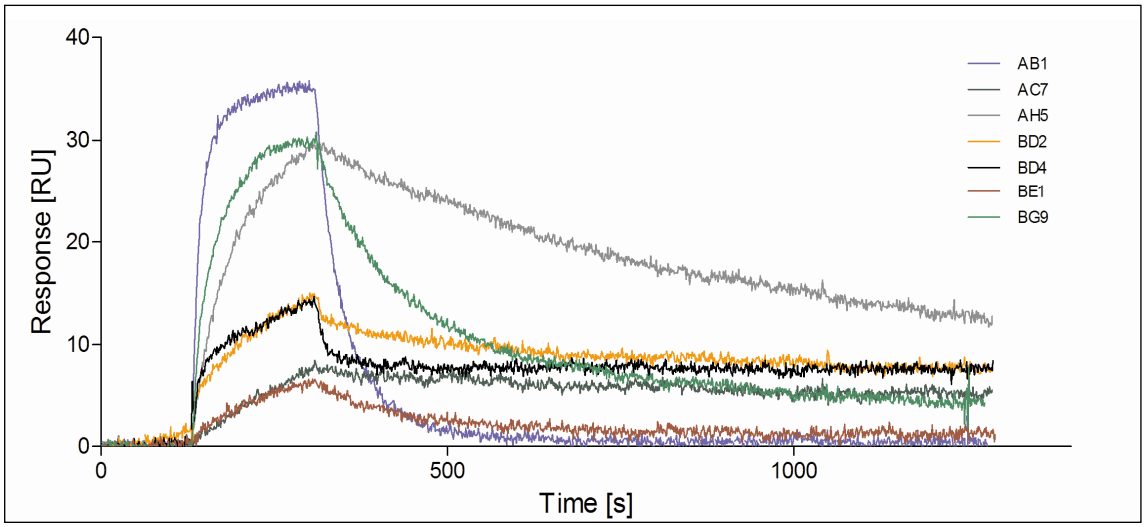

Figure 26. SPR analysis of EphB4 DARPin binding to human EphB4-Fc ECD. The binding kinetic of EphB4 DARPins to hEphB4-Fc ECD was recorded at a DARPin concentration of 33 nM. Data depicted represent one of three independent measurements.

Table 14. Statistical analysis of the SPR measurements of the interaction between EphB4 and ephrin-B2 or DARPins. Data were fitted with 1:1 Langmuir and bivalent analyte models and their quality was determined by χ^2 values. Lower χ^2 values correspond to better closeness to the fit. Data depicted represent one of three independent measurements.

Target format:		**EphB4 dimer**		**EphB4 monomer**	
Model:		**1:1 Langmuir**	**bivalent analyte**	**1:1 Langmuir**	**bivalent analyte**
Analyte	**ephrin-B2**	59.6	7.88	13.5	2.03
	AB1	0.708	0.483	0.638	0.35
	AC7	0.69	0.307	0.288	0.187
	AH5	2.33	0.351	3.45	1.45
	BD2	1.4	0.392	0.554	0.305
	BD4	1.07	0.466	0.335	0.226
	BE1	0.572	0.175	0.196	0.139
	BG9	1.59	0.94	1.56	1.07

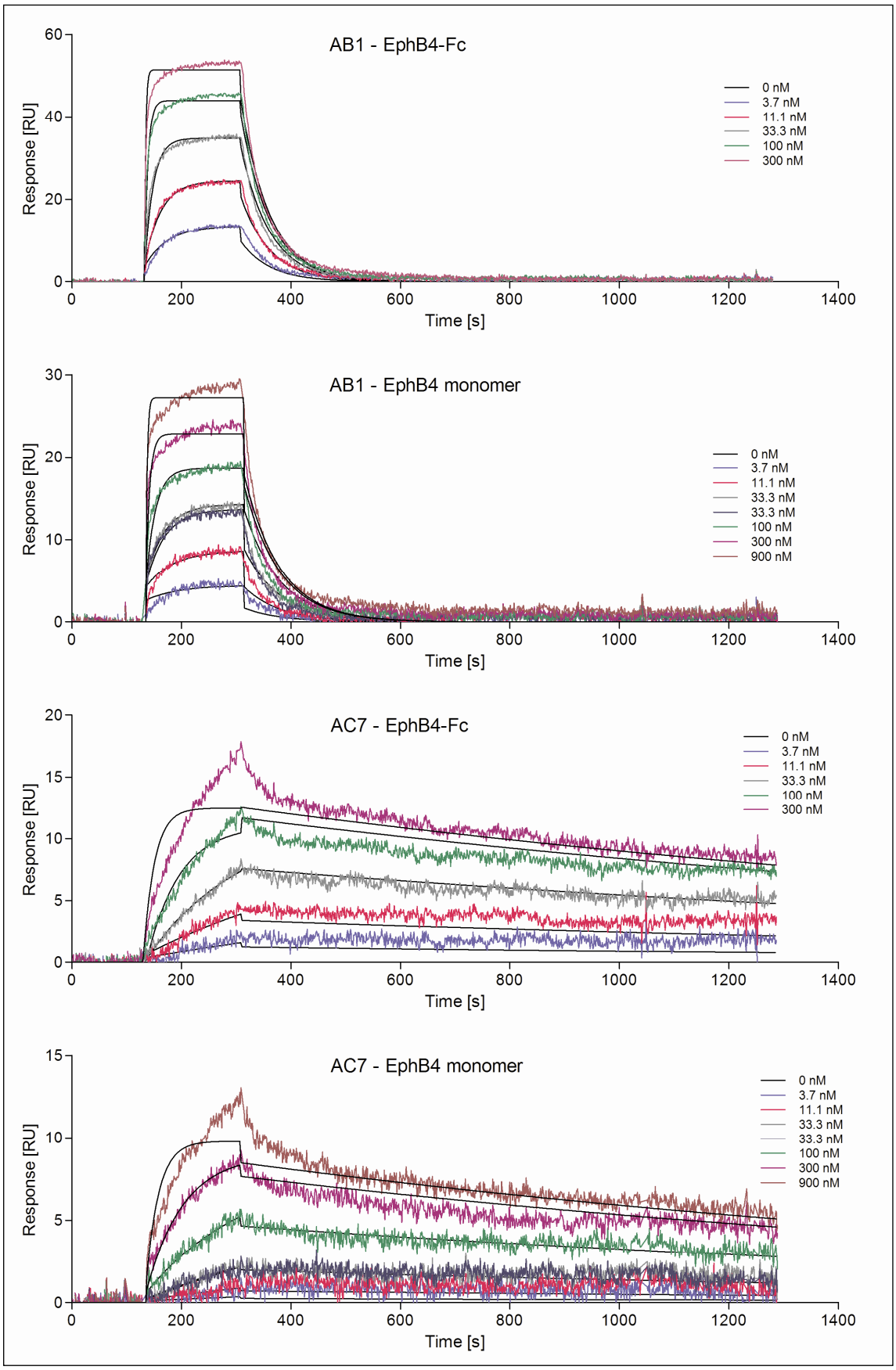
AB1 - EphB4-Fc
Response [RU]
Time [s]
0 nM
3.7 nM
11.1 nM
33.3 nM
100 nM
300 nM
AB1 - EphB4 monomer
Response [RU]
Time [s]
0 nM
3.7 nM
11.1 nM
33.3 nM
33.3 nM
100 nM
300 nM
900 nM
AC7 - EphB4-Fc
Response [RU]
Time [s]
0 nM
3.7 nM
11.1 nM
33.3 nM
100 nM
300 nM
AC7 - EphB4 monomer
Response [RU]
Time [s]
0 nM
3.7 nM
11.1 nM
33.3 nM
33.3 nM
100 nM
300 nM
900 nM

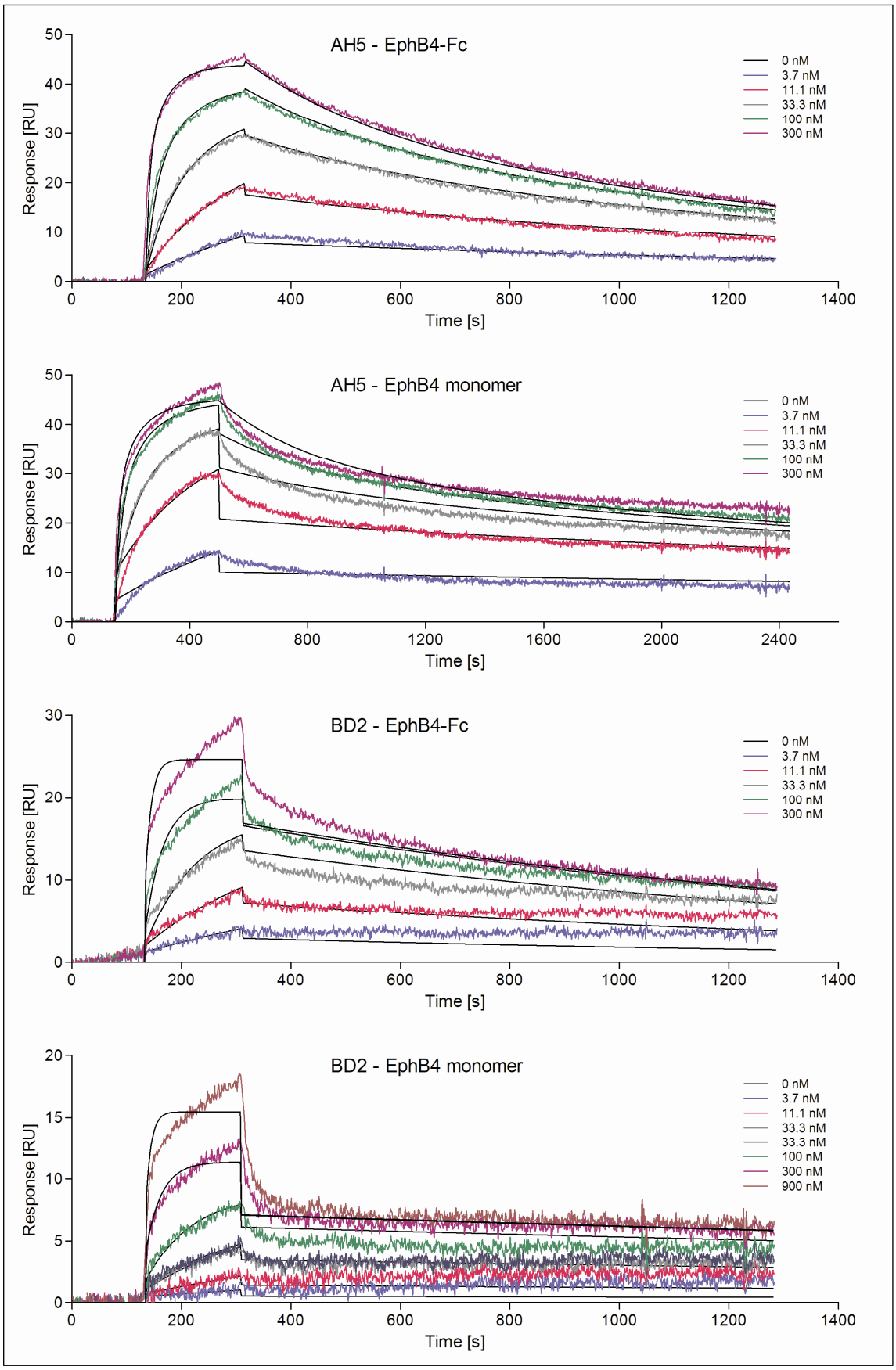
AH5 - EphB4-Fc
Response [RU]
Time [s]
0 nM
3.7 nM
11.1 nM
33.3 nM
100 nM
300 nM
AH5 - EphB4 monomer
Response [RU]
Time [s]
0 nM
3.7 nM
11.1 nM
33.3 nM
100 nM
300 nM
BD2 - EphB4-Fc
Response [RU]
Time [s]
0 nM
3.7 nM
11.1 nM
33.3 nM
100 nM
300 nM
BD2 - EphB4 monomer
Response [RU]
Time [s]
0 nM
3.7 nM
11.1 nM
33.3 nM
33.3 nM
100 nM
300 nM
900 nM

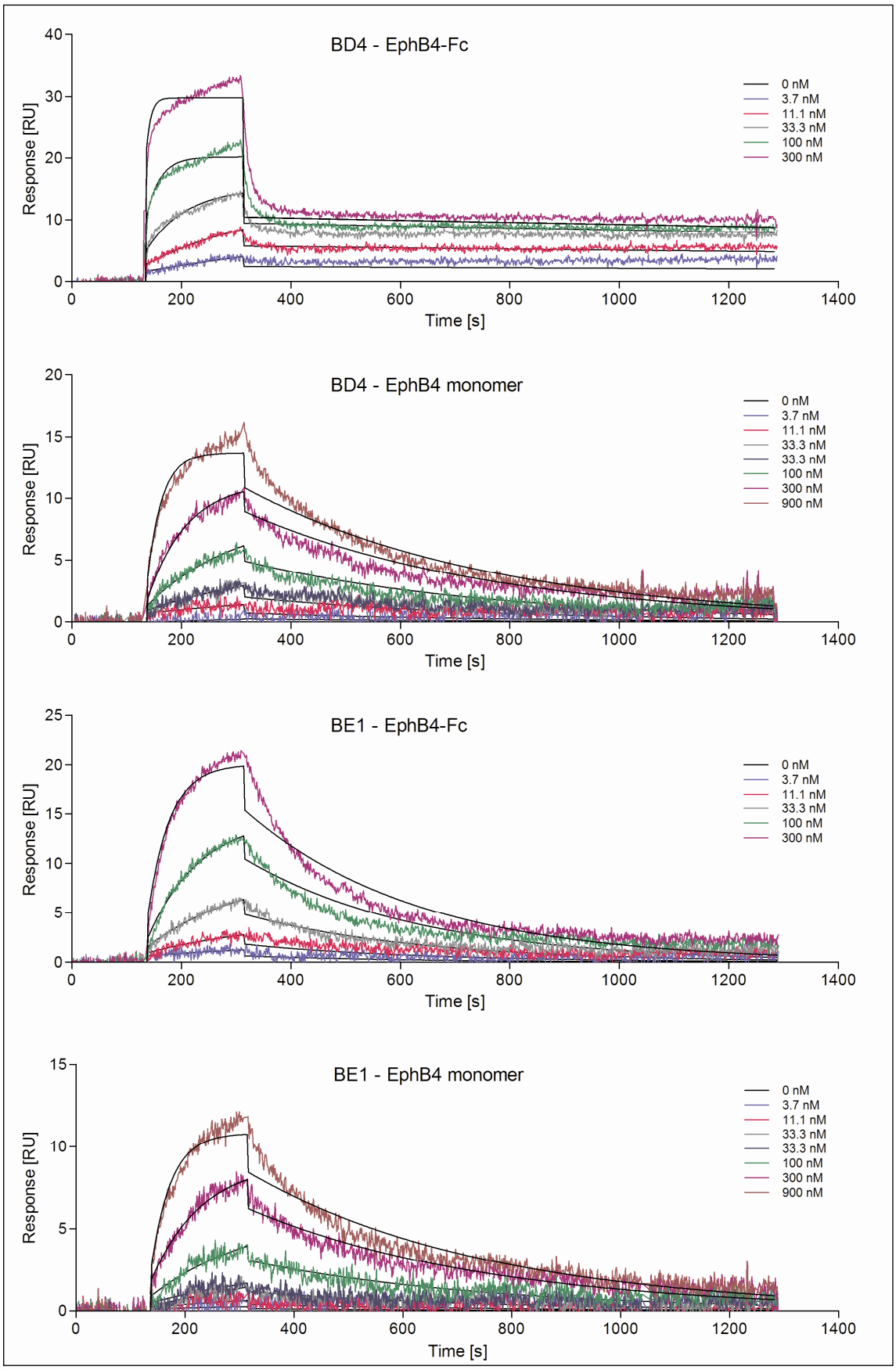
BD4 - EphB4-Fc
Response [RU]
Time [s]
0 nM
3.7 nM
11.1 nM
33.3 nM
100 nM
300 nM
BD4 - EphB4 monomer
Response [RU]
Time [s]
0 nM
3.7 nM
11.1 nM
33.3 nM
33.3 nM
100 nM
300 nM
900 nM
BE1 - EphB4-Fc
Response [RU]
Time [s]
0 nM
3.7 nM
11.1 nM
33.3 nM
100 nM
300 nM
BE1 - EphB4 monomer
Response [RU]
Time [s]
0 nM
3.7 nM
11.1 nM
33.3 nM
33.3 nM
100 nM
300 nM
900 nM

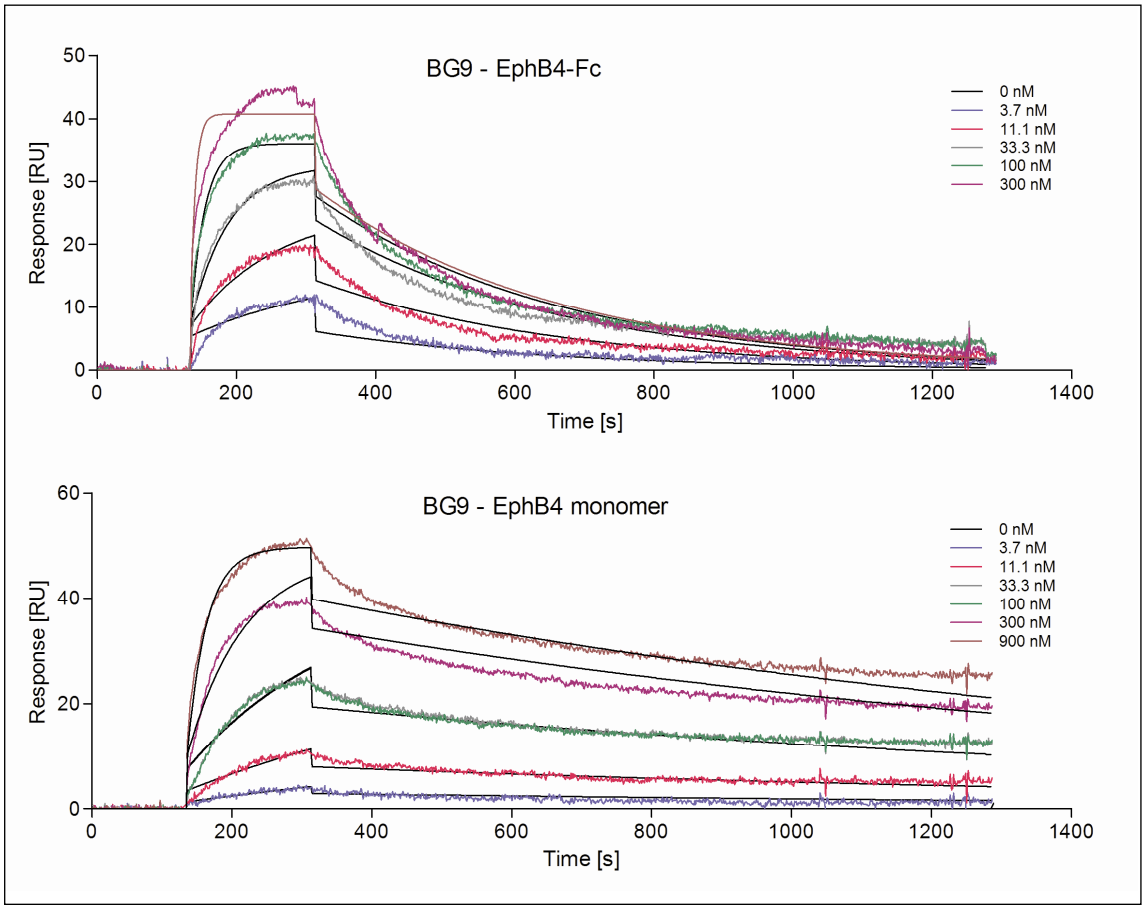

Figure 27. SPR analysis of EphB4 DARPin binding to monomeric and dimeric hEphB4 ECD. The interaction of EphB4 DARPins was analyzed at the indicated concentrations to the immobilized monomer or dimer of hEphB4 as indicated and the measured data were fitted with the monovalent (AB1, AC7, BD2, BD4, BE1, BG9) or bivalent analyte model (AH5). The binding curves are illustrated as double-referenced sensorgrams (colored lines) overlaid with the respective global fits (black lines) evaluated Data depicted represent one of three independent measurements.

EphB4 DARPins bound to hEphB4 ECD (monomeric and dimeric) with high affinities ranging between 0.4 and 81 nM, which are comparable to binding affinities of DARPins recently isolated against the Fc domain of human IgG (Steiner et al. 2008) and to the binding affinity of ephrin-B2. In general EphB4 DARPins bound to monomeric and dimeric EphB4 with similar affinities (Table 15). K_D values differed maximally 4-fold, whereby the affinity was usually weaker to the monomer. One exception was BD4 with the highest dissociation constant of 0.4 nM to the EphB4 dimer, which is about 130-fold better than the K_D for the monomer. DARPins BD2 and BG9 displayed the highest affinities for

both monomeric and dimeric EphB4 with K_D values of about 2 nM and 5.5 nM respectively. The affinity of BE1 was rather low and the parameters for AA5 could not be measured, what is in a good agreement with performed FACS experiments (Figure 24).

Table 15. Kinetic parameters of the interaction between EphB4 DARPins and ephrin-B2-Fc with the monomeric and dimerized EphB4 ECD determined by SPR. The binding modus was analyzed using 1:1 Langmuir binding (a) or bivalent analyte models (b) of the BIAcore software 4.1. Data depicted represent one of three independent analyses. *The alternative evaluation model is presented for the comparison of evaluation models for ephrin-B2, AB1 and AH5.

Analyte	**hEphB4 format**	**k_a (× 10^4 M^{-1} s^{-1})**	**k_d (× 10^{-3} s^{-1})**	**K_D (nM)**	**χ^2**
ephrin-B2 [b]	dimer monomer	12.0 18.8	1.8 5.1	14.7 26.9	7.88 2.03
ephrin-B2 [a] *	dimer monomer	40.4 66.7	0.3 0.9	0.8 1.4	59.6 13.5
AB1 [a]	dimer monomer	138.0 42.5	18.7 15.2	13.5 35.8	0.708 0.638
AB1 [b] *	dimer monomer	48.7 18.8	39.6 20.3	81.3 108.0	0.483 0.35
AC7 [a]	Dimer monomer	16.3 4.8	0.5 0.5	2.9 10.9	0.69 0.288
AH5 [b]	dimer monomer	15.0 8.0	1.9 1.6	12.9 19.7	0.351 1.45
AH5 [a] *	dimer monomer	36.1 29.1	1.0 0.3	2.8 1.1	2.33 3.45
BD2 [a]	dimer monomer	29.8 11.7	0.7 0.2	2.2 1.7	1.4 0.554
BD4 [a]	dimer monomer	40.7 3.9	0.2 2.2	0.4 56.0	1.07 0.335
BE1 [a]	dimer monomer	7.3 2.8	3.2 2.3	43.4 80.8	0.572 0.196
BG9 [a]	dimer monomer	48.8 11.7	2.7 0.7	5.5 5.6	1.59 1.56

Regarding the association and dissociation kinetics of the DARPin / EphB4 interaction, most of the EphB4 DARPins associate to the receptor with rates comparable to ephrin-B2 (Table 15). Mainly the differences in affinity among the DARPins are otherwise dictated by the varying dissociation rates. A prominent exception is AB1, which shows the fastest k_{on} and k_{off} rates of all other DARPins and of ephrin-B2. Moreover, the interaction of BG9 with the EphB4 dimer showed a 4-fold faster k_{on} rate than ephrin-B2. DARPins AC7 and BE1 did not reach the equilibrium and showed relative low k_{on} rates and were therefore classified as slow binders. Summarizing these results showed different kinetic behaviors of EphB4 DARPins, which possibly can influence their mode of action.

3.4 Functional characterization of EphB4 DARPins

3.4.1 Competitive binding analysis of EphB4 DARPins and ephrin-B2

EphB4 receptors are activated by binding of the ligand ephrin-B2 and the blockade this binding for example by EphB4 DARPins could inhibit receptor function. Therefore, it was analyzed whether the isolated DARPins can compete with ephrin-B2 for EphB4 binding using the SPR technique. Competition experiments were performed on the EphB4 ECD coated surface of the BIAcore sensor chip by sequential injection of analytes as indicated in Figure 28 A. The response of the bound analyte during the second injection compared to the control correlates with competitive (Figure 28 B; solid line) or non-competitive binding (Figure 28 B; dashed line).

In the first set of experiments the effects of the DARPins on established ephrin-B2 / EphB4 complexes on the surface of a BIAcore chip were analyzed by co-injection of individual DARPins and ephrin-B2 at equimolar concentrations. The results are shown in Figure 29 A. In the first injection ephrin-B2-Fc was applied until a binding equilibrium with EphB4-Fc ECD was achieved and the measured response reached a plateau. In the second injection ephrin-B2 together with the analytical DARPin was applied. Analysis of the resulting sensorgrams

revealed an increase of the binding signal upon co-injection of DARPins BG9 and BD2 (Figure 29 A; green and orange curves, respectively) compared to the control DARPin (red curve). This demonstrated that these DARPins bound to the receptor in addition to ephrin-B2 presumably at non-overlapping sites. Similar results were obtained for AH5 and BD4 (data not shown). In contrast, injection of AB1 (Figure 29 A; blue curve) did not increase the SPR binding signal above the levels detected for ephrin-B2 alone (Figure 29 A; grey curve). This observation suggests that AB1 could not bind to the receptor in the presence of ephrin-B2, because of competing binding sites. DARPins AC7 and BE1 also did also not increase the response (data not shown). Notably, in the dissociation phase of this experiment, which reflects both dissociation of DARPins and ephrin-B2, the BD2 curve decreased slightly faster than the one of BG9, despite a slower off-rate of BD2 in the absence of ephrin-B2 (Figure 29 A; orange curve). This suggested that the presence of ephrin-B2 changed the binding kinetics of BD2 and accelerated dissociation of the complexes.

In the second set of experiments the effects of the DARPins on the dissociation of ephrin-B2 were analyzed (Figure 29 B). DARPins were injected to the surface of a BIAcore chip carrying EphB4 saturated with ephrin-B2. The DARPin application phase, which reflects the combined effects of DARPin association and ephrin-B2 dissociation, was examined. Application of AB1 led to an enhanced loss of the binding signal compared to the control DARPin (Figure 29 B; blue and red curves), which could be explained by an accelerated dissociation of ephrin-B2. On the contrary, upon loading of BD2 a reduced loss of the binding signal was observed (Figure 29 B; orange curve), which may be due to a retarded dissociation of ephrin-B2. The sensorgram of BG9 (Figure 29 B; green curve) revealed a small peak at the beginning of its application presumably reflecting the additional binding of this DARPin. The signal subsequently declined with a small increment compared to the signal of the control DARPin which reflects the bound BG9, whereas ephrin-B2 continues to dissociate from EphB4. AH5 and BD4 showed similar effects as BG9, whereas AC7 and BE1 loading gave no change of the binding signal (data not shown). As expected, the binding response was unchanged from the steady state signal

attained in the initial loading phase, when ephrin-B2 was applied in the second injection for comparison (Figure 29 B; grey curve).

A

Set of experiment	1st injection	2nd injection
1	ephrin-B2-Fc	ephrin-B2-Fc + DARPin X
2	ephrin-B2-Fc	DARPin
3	DARPin X	ephrin-B2-Fc
4	DARPin AB1	DARPin AB1 + DARPin X

B

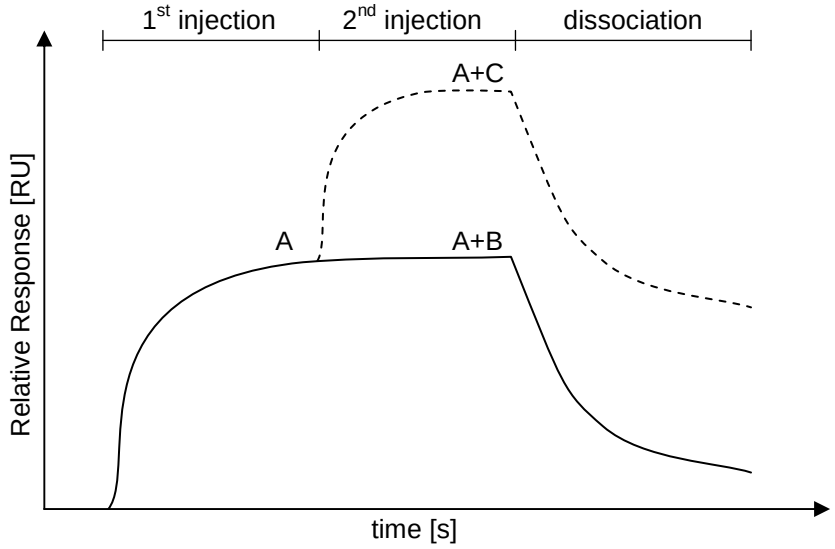

Figure 28. Experimental design of competition binding analysis using SPR technique. (A) The analysis was performed by co-injection of a single analyte sequentially with the second analyte or a mixture of two analytes at equimolar concentrations. The table presents the sequence of analyte injection in the set-up of four experiments. (B) Schematic illustration of a sensorgram of the competition analysis. The 1st injection of analyte A, followed by the 2nd injection of analyte A and B shows no changes in binding response, when B binds competitively with A (solid line). Non competitive analyte C injected as a mixture with A gives an increase in binding response (dashed line).

The impact of DARPins on the association kinetics of ephrin-B2 was analyzed in a reverse set of experiments, whereby DARPins were loaded first until equilibrium was reached followed by the injection of ephrin-B2. The

examination of sensorgrams demonstrated no changes on association of ephrin-B2 (2nd injection) after the injection of the EphB4 DARPin compared to the control DARPin (Figure 29 C; red curve). However, after injection of AB1 (Figure 29 C; blue curve) in contrast to the remaining DARPins, the analysis revealed differences in the curve shape of ephrin-B2 binding suggesting impaired association of ephrin-B2 and delayed reaching of its steady state.

In the fourth set of experiments the effects of DARPins on established complexes between AB1 and EphB4 were analyzed by the co-injection of AB1 with other DARPins at equimolar concentrations. The results presented in Figure 29 D showed that the injection of 1 µM AB1 for 2 min was sufficient to saturate all its binding sites on the sensorchip. In the following second injection AB1 together with other analytical DARPins were applied to analyze the simultaneous binding of AB1 with other DARPin. Very similar to the results with ephrin-B2, DARPins BG9 and BD2 (Figure 29 D; green and orange graphs, respectively) bound to EphB4 in the presence of AB1, as demonstrated by increasing response upon their application. This suggests that these DARPins as well as AH5 and BD4 (data not shown) bind to epitopes different from the AB1 binding site. Co-injection of AC7, BE1 or a control DARPin (Figure 29 D; red graph) did not affect the response. Inspection of the sensorgrams of the dissociation phase revealed that the signal of BD2 declined more rapidly compared to the signal of AB1 alone or with the other DARPins. This analysis suggests that AB1 may affect BD2 binding kinetics similar to ephrin-B2 and accelerate dissociation of both DARPins AB1 and BD2 from EphB4 complexes.

In summary, SPR studies allowed the differentiation between at least two groups of EphB4 DARPins. The first group comprises DARPins AB1, AC7 and BE1 (data of the latter two not shown) which share their binding sites with a region involved in ephrin-B2 binding and thereof AB1 can compete with ligand for binding. Based on these experiments it can be assumed that AC7 and BE1 although bind to an overlapping epitope with ephrin-B2, but cannot compete with the natural ligand for binding presumably because of their low affinity or slow k_{on} rate. The second group contains BD2, BG9, BD4 and AH5 (data of the latter two not shown) which bind to regions different form the ligand binding site.

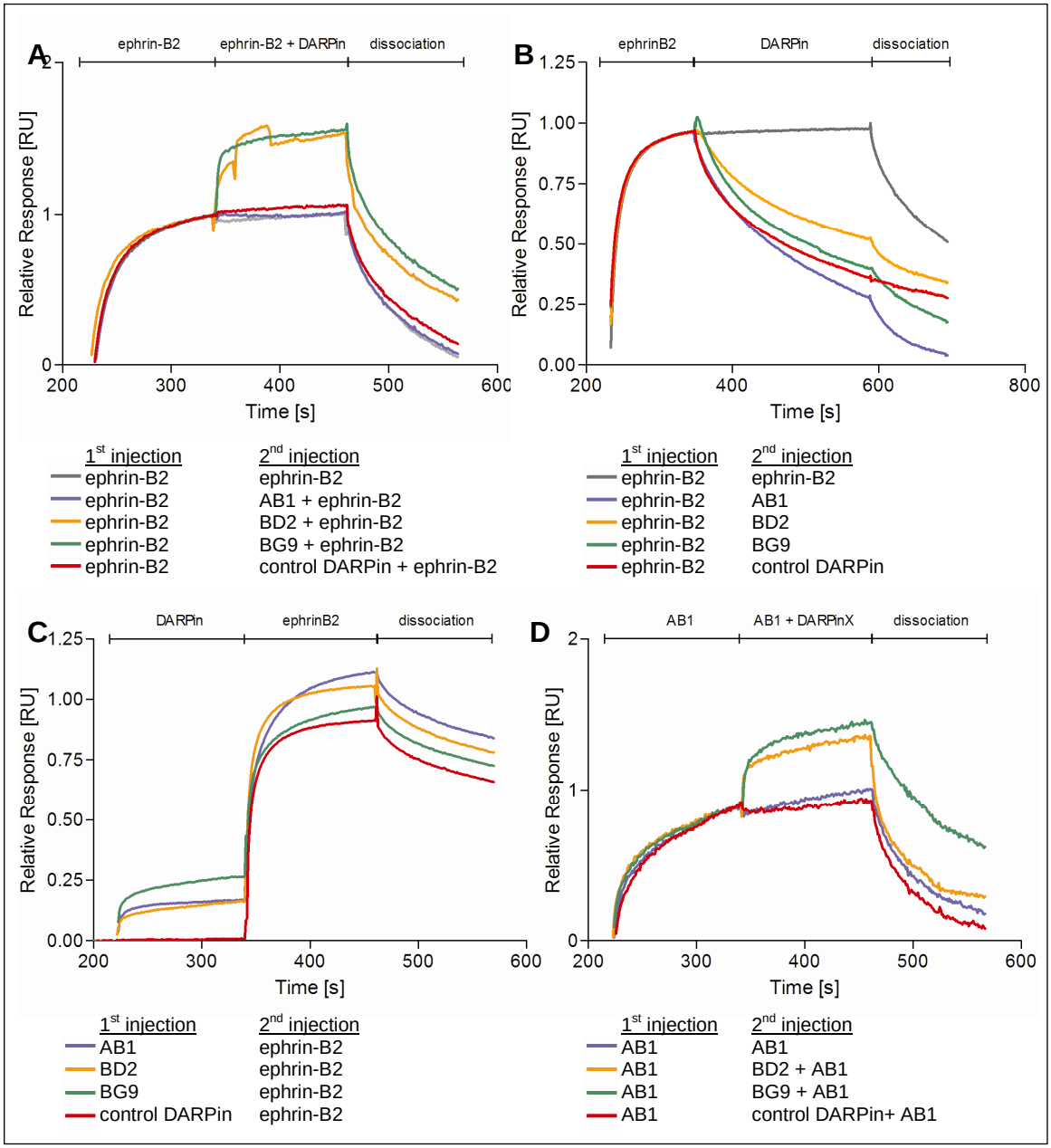

Figure 29. SPR analysis of the competitive binding of ephrin-B2 and DARPins. The sensorgrams present sequential binding of ephrin-B2 (grey), AB1 (blue), BD2 (orange), BG9 (green), control DARPin (red) combined with ephrin-B2 or AB1 performed as described in Materials and methods (2.5.4). Complexes of EphB4-Fc ECD with ephrin-B2 (A and C) or DARPin (B and D) were established by their initial injection for 120 sec until equilibrium was achieved, followed by a second injection of analytes ephrin-B2 + DARPin (A), DARPin (B), ephrin-B2 (C) or AB1 + DARPin X (D) for 120–240 sec. Finally PBS was injected to monitor the dissociation of the bound molecules (dissociation). All analytes were applied in the concentration of 1 µM. Sensorgrams were normalized to the total response of the first injected analyte (A, B and D) or to the immobilization level (C).

3.4.2 Inhibition of ligand induced EphB4 receptor phosphorylation using EphB4 DARPins

Ephrin-B2 activates the EphB4 receptor by binding to its ligand binding domain, which leads to the receptor dimerization and autophosphorylation of tyrosine residues by the receptor's intracellular kinase domain. This activation of EphB4 receptor initiates the intracellular signaling cascade. The effect of EphB4 DARPins on the activity of the receptor was determined in a cell-based assay. U-2 OS-hEphB4 cells were pre-treated with DARPins and then incubated with ephrin-B2 or PBS. EphB4 was subsequently captured from cell lysate using an anti-myc tag antibody and its phosphorylation level was detected with an anti-phosphotyrosine antibody (Figure 30 A). As expected, the ephrin-B2-Fc chimeric protein at the concentration 1 µg/ml rapidly stimulated tyrosine phosphorylation of the EphB4 receptor in the U-2 OS-hEphB4 cells. None of the DARPins induced EphB4 phosphorylation, when cells were treated with DARPins alone up to a concentration of 10 µg/ml (Figure 30 C). Similarly, DARPins dimerized via their His-tag using an anti-RGS-His_4 antibody prior to their application did not activate EphB4 in the absence of ephrin-B2 (Appendix 5.1, Figure 45). This indicates that DARPins in contrast to ephrin-B2 seem unable to dimerize EphB4 receptor molecules leading to their activation. However, when ephrin-B2 was added to cells, pre-incubated with DARPins AB1 or BG9 EphB4 activation was suppressed in a dose-dependent manner (Figure 30 B). The level of tyrosine phosphorylation of EphB4 was reduced up to 80% in AB1 treated cells. Based on the SPR results (Figure 29), this effect could be explained by the binding of AB1 to the common site of ephrin-B2 and thereby preventing the ligand to bind.

Surprisingly, BG9 which did not compete for ligand binding in the SPR studies also revealed an inhibitory effect, which was almost 90% at 10 µg/ml. This suggests a different mode of action for BG9, which may rather prevent receptor monomers from forming dimers upon ligand binding. Interestingly, potentiating of ligand-induced EphB4 phosphorylation was observed, when cells were treated with BD2 (Figure 30 B-C). Although BD2 alone did not activate the receptor, it significantly enhanced the phosphorylation status triggered by the

ligand up to 165%. AH5 presented similar effect as BD2, increasing the activation of the receptor in the presence of ephrin-B2 (data not shown). The remaining EphB4 DARPins demonstrated only marginal inhibitory effects on the receptor activation; therefore, they were excluded from the further analysis.

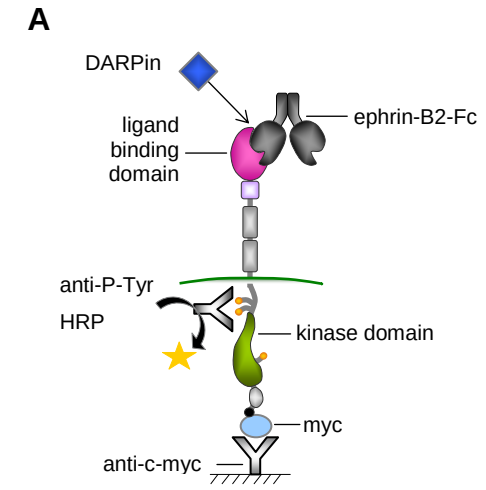

B

Sample		pEphB4 level (%)
no DARPin		100
AB1	1 µg/ml 10 µg/ml	85 19
BD2	1 µg/ml 10 µg/ml	165 117
BG9	1 µg/ml 10 µg/ml	48 12
Control DARPin	1 µg/ml 10 µg/ml	69 77

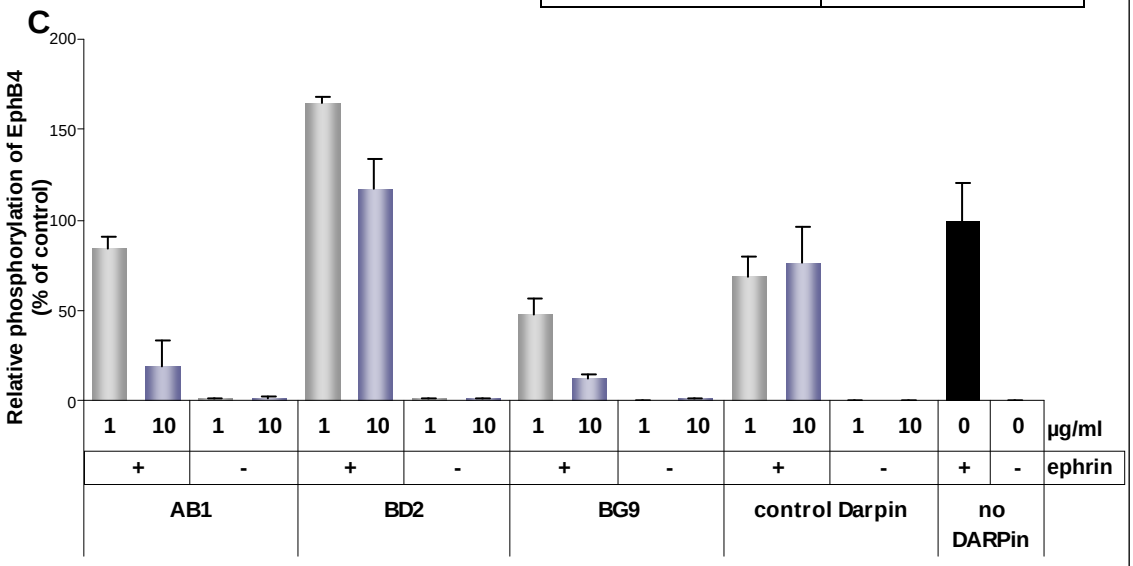

Figure 30. Analysis of the effects of EphB4 DARPins on EphB4 activity in U-2 OS-hEphB4 cells. (A) Schematic diagram of the sandwich ELISA used to detect phosphorylated EphB4. The ELISA was performed as described in Materials and methods (2.6.2). EphB4 was captured via an anti-myc antibody and the phosphorylation was detected using an HRP-conjugated anti-phosphotyrosine antibody (anti-P-Tyr HRP). (B) Relative phosphorylation levels of EphB4 (pEphB4) after DARPin treatment of U-2 OS-EphB4 cells in the presence of ephrin-

B2-Fc. Levels were related to pEphB4 in control cells treated with ephrin-B2-Fc in the absence of DARPin. (C) Dose dependent inhibition of ephrin-B2 induced phosphorylation of EphB4 by DARPins. U-2 OS-hEphB4 cells were incubated with the given concentrations of DARPins and subsequently treated with 1 µg/ml ephrin-B2-Fc (+ ephrin) or PBS (- ephrin). pEphB4 was determined by ELISA and the relative chemiluminescence intensity was calculated from cells treated with ephrin-B2 in the absence of DARPin, which was defined as 100%. The off7 DARPin was used as control. Values are depicted as means of three measurements ± SD.

3.4.3 Effect of EphB4 DARPins on tube formation of endothelial cells *in vitro*

EphB4 and ephrin-B2 are expressed in endothelial cells and are essential for the vascular development (chapter 1.2.4). Tube formation is a primary event of the development of blood vessels. It is a spontaneous process, which starts with cell attachment to the extracellular matrix, cell migration and cell–cell adhesion, followed by formation of capillary-like tubules and elongation of these structures. Inhibition of EphB4 was shown to block capillary tube formation of endothelial cells (Kertesz et al. 2006). Based on these results the effects of EphB4 DARPins on the tube formation of HUVECs, which were reported to express EphB4 receptor and ephrin-B2 ligand (Salvucci et al. 2006) was investigated.

A tube formation assay was performed by culturing HUVECs on matrigel as described in chapter 2.6.3. A regular network of interconnecting tubules was obtained within 24 h as shown qualitatively in Figure 31. The results were quantified by measuring the number of all tubes in each well using particle analyzing software (Figure 32). Cells treated with the control DARPin revealed no significant changes in tube morphology and number in well even at concentrations of 100 µg/ml (Figure 31 C-D) compared to the untreated cells (Figure 31 A-B). In contrast the tube forming activity of HUVECs was impaired in a dose-dependent manner, when cells were treated with DARPins AB1 (Figure 31 C-D) or BG9 (Figure 31 E-H).

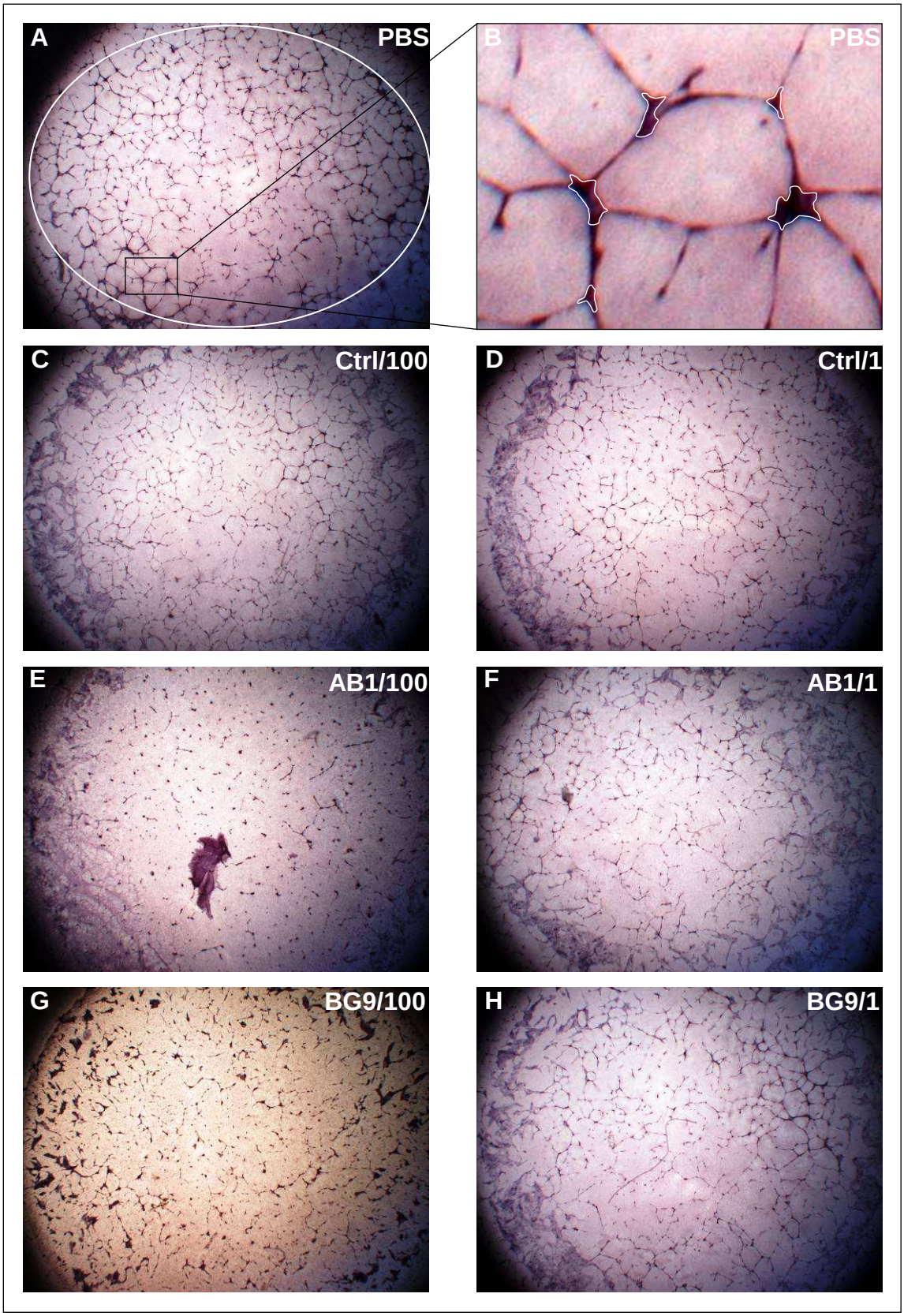

Figure 31. Effect of EphB4 DARPins on tube formation by HUVECs. The tube formation assay was performed as described in Materials and methods (2.6.3). HUVECs plated onto matrigel were treated for 24 h with DARPins AB1 (E-F), BG9 (G-H), control DARPin (C-D) or

PBS (A-B) at the final concentrations of 1 µg/ml (D, F, H) and 100 µg/ml (C, E, G). Tube formation was detected by staining of fixed HUVECs with an endothelial cell-specific anti-CD31 antibody. Photographs of each well were taken with phase-contrast microscopy using a Nikon camera (original magnification 1.25×). For quantification areas of interests were defined in the visual field of each well as indicated in the image A (outlined in white). The image B presents a 10× magnification of the selected field of the image A showing endothelial cells (outlined in white) and tube structures (dark purple). The particle analysis software (Olympus) counts the number of tube structures between the cells. One representative image of duplicate wells is shown.

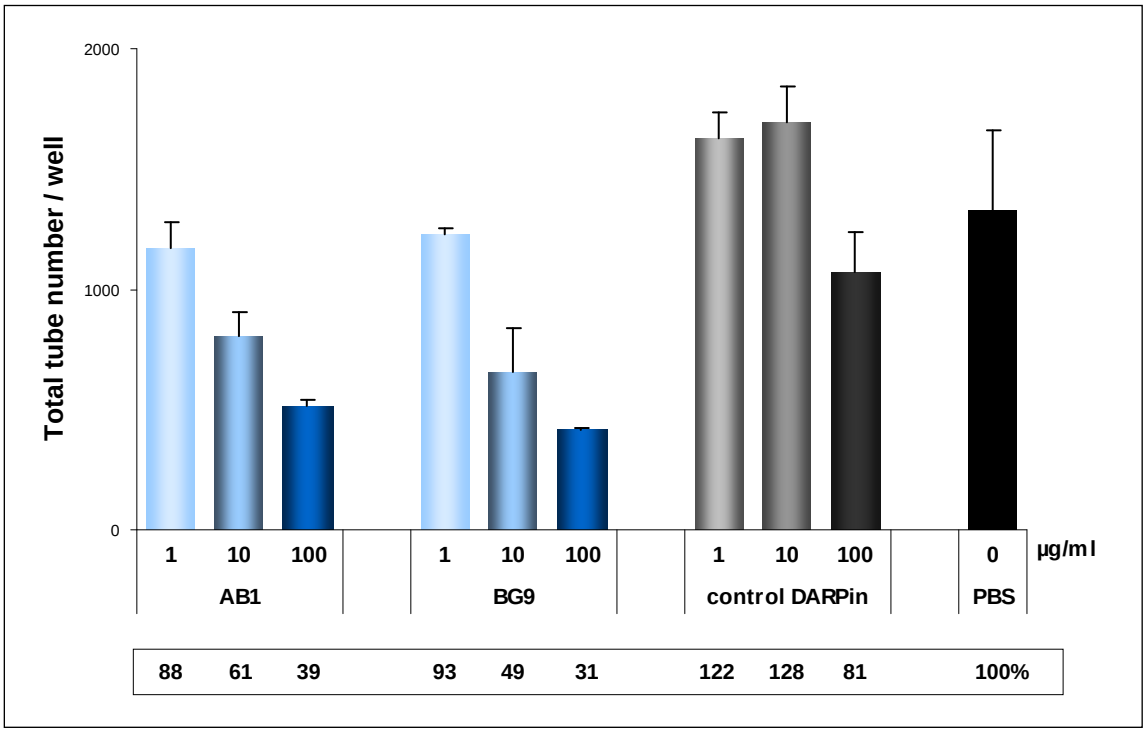

Figure 32. Quantitative analysis of the effect of EphB4 DARPins on HUVEC tube formation. The tube formation assay was performed as described in Materials and methods (2.6.3). HUVECs were treated with DARPins at the given concentrations. Pictures of each well taken with phase-contrast microscopy using a Nikon camera (original magnification ×1.25) were analyzed using particle analysis software (Olympus). Results reflect the total number of tubes per visual field in one well, which was determined as the number of vascular joints, between the endothelial cells. Each column represents the mean of duplicate wells ± SD. The numbers below the chart indicate the relative number of tubes compared to the positive control (PBS) defined as 100%.

Quantitative analysis confirmed that DARPins AB1 and BG9 prevented tube formation in a dose-dependent manner (Figure 32). Inhibition by AB1 was 39% at 10 µg/ml and 61% at 100 µg/ml. The inhibition level of BG9 appeared more pronounced with 51% at 10 µg/ml and 69% at 100 µg/ml, which is consistent with the kinase inhibition results of these DARPins (Figure 30). The tube number was not affected by the control DARPin. These results indicate that DARPins form both classes competing (AB1) and non-competing (BG9) for ligand binding can interfere with the tube formation of endothelial cells *in vitro*. As a next step it was investigated, whether the they could also inhibit angiogenesis in an *in vivo* analysis. In the first line AB1 was chosen for the experiment due to the cross reactivity to the murine EphB4.

3.4.4 Effects of EphB4 DARPins on angiogenesis *in vivo*

For the *in vivo* evaluation of effects on angiogenesis the Directed In Vivo Angiogenesis Assay (DIVAA, Trevigen) was used as described in Materials and methods (2.7). Semiclosed silicone cylinder tubes called angioreactors were filled with extracellular matrix premixed with DARPins in the presence or absence of angiogenic factors. Tubes were implanted subcutaneously into mice and incubated for 2 weeks. Angiogenesis was measured by quantification of the invaded mouse endothelial cells, which migrated from vessels into the matrix and proliferated in response to the angiogenic factors. Cells extracted from matrigel were stained using FITC-labeled Griffonia simplicifolia lectin I, which selectively binds to alpha-D galactosyl and N-acetyl galactosaminyl groups specific for the surface of ECs. Moreover, the evaluation was performed by measuring the amount of hemoglobin in the cylinder. However, the results on the hemoglobin levels need to be interpreted with caution because the blood content is also affected by the size and permeability of vessels.

As presented above, two DARPins (AB1, BG9) showed inhibition of the angiogenesis *in vitro*. The assay was performed with AB1, because of its cross reactivity with murine EphB4 (Figure 23). Unfortunately, BG9 does not cross react with murine EphB4, and could therefore not be applied in this assay. To

avoid inflammatory mediated induction of angiogenesis, by residual amounts of bacterial contaminants the DARPins used here were further purified by anion exchange chromatography and by removing endotoxin to a level of 1 EU/mg. The results of the analysis are presented in Figure 33.

As expected, a significant invasion of blood vessels was observed in cylinders supplemented with VEGF and FGF-2 compared to cylinders where no growth factors were added. Results obtained by quantification of the numbers of invaded ECs were consistent with measured hemoglobin levels (Figure 33 B-C). Interestingly, DARPin AB1 was able to very effectively inhibit the VEGF / FGF-2 induced angiogenesis at the applied concentration of 0.2 mg/ml in this assay. Compared to the positive growth factor control, angiogenesis measured by EC invasion was reduced by 80%, which was statistically highly significant ($p<0.001$). A control DARPin had no effect on the number of invaded ECs and a very similar signal compared to the positive growth factor control was observed. The antiangiogenic effect of AB1 was also statistically significant when compared to the control DARPin ($P < 0.01$). Some angiogenic response was measured in the control sample containing PBS, even though there were no blood filled vessels visible in the cylinders (Figure 33 A). A small number of ECs may have migrated into the angioreactors due to potential proangiogenic activities intrinsic to matrigel, but these were insufficient to form a visible amount of mature vessels. Notably some of this activity seems to be also inhibited by DARPin AB1.

Similar results were obtained, when the degree of vessel formation was evaluated by measuring hemoglobin levels, which is proportional to the number of red blood cells (Figure 33 C). VEGF and FGF-2 presented increased hemoglobin content. In case of the control DARPin even higher hemoglobin levels were observed for reasons which are unknown. In angioreactors without growth factors increased red blood cell infiltration into matrix was observed, which could be a result of immature vessels with an increased permeability. Taken together, it was demonstrated that DARPin AB1 could profoundly suppress angiogenesis *in vivo* and could potentially be used for antiangiogenic tumor therapy.

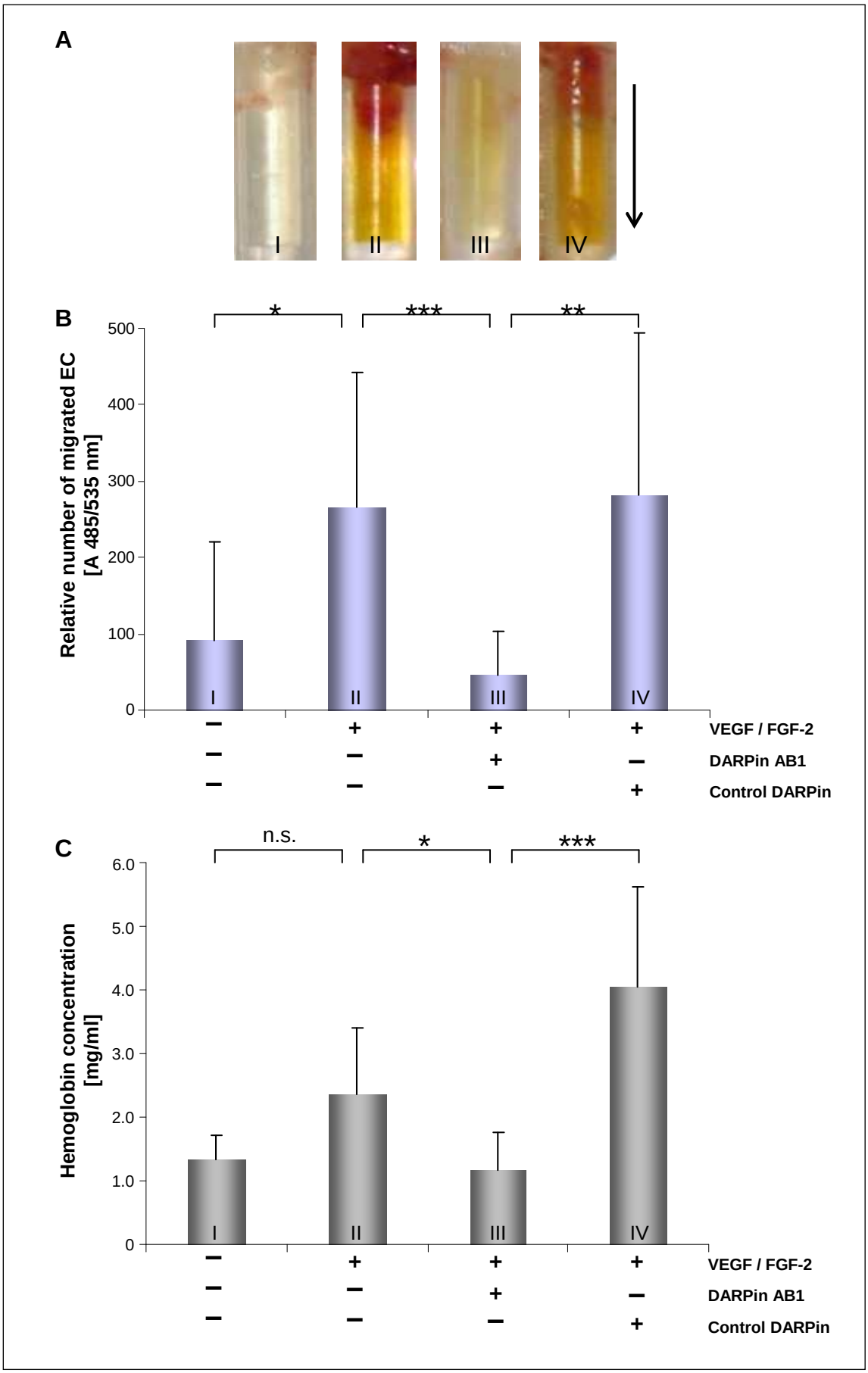
A
I
II
III
IV
B
Relative number of migrated EC
[A 485/535 nm]
500
400
300
200
100
0
*
***
**
I
II
III
IV
VEGF / FGF-2
DARPin AB1
Control DARPin
C
Hemoglobin concentration
[mg/ml]
6.0
5.0
4.0
3.0
2.0
1.0
0
n.s.
*
***
I
II
III
IV
VEGF / FGF-2
DARPin AB1
Control DARPin

Figure 33. Inhibition of VEGF / FGF-2 induced angiogenesis *in vivo* by DARPin AB1. Effects of AB1 on angiogenesis were determined by DIVAA analysis as described in Materials and methods (2.7). Angioreactors filled with 20 µl matrigel premixed with or without the angiogenic factors and test DARPins were implanted subcutaneously in BALB/c mice for 14 days. The angioreactors were recovered, photographed and the content of tubes was analyzed for the hemoglobin level and endothelial cells invasion. (A) Representative images of matrigel cylinders were presented for each treatment group containing PBS (I); VEGF / FGF-2 (II); DARPin AB1 combined with VEGF / FGF-2 (III); control DARPin combined with VEGF / FGF-2 (IV). Arrow indicates direction of in-growing blood vessels from open end. (B) The relative number of ECs migrated into matrigel was determined after their extraction from matrigel and labeling with FITC lectin I. Results are expressed in fluorescence units as the mean values of at least 10 matrigel cylinders per treatment group ± SD. Statistical comparisons were performed using 1-way ANOVA followed by the Tukey test and indicated in the chart: * $P<0.05$, ** $P<0.01$, *** $P<0.001$ using SigmaStat 3.5 (Systat). Moreover, the comparison of the group I vs. III and II vs. IV revealed no significance, whereas the group I vs. IV showed $P<0.05$. The representative experiment is shown from a total of 3 performed. (C) Angiogenesis was quantified by measuring the hemoglobin content spectrophotometrically from the hemoglobin standard curve using Drabkin method. Results are presented in mg/ml of hemoglobin as a mean value of at least 10 matrigel cylinders per group ± SD. The statistical comparisons of the group I vs. III revealed no significance, whereas the group II vs. IV showed $P<0.01$ and the group I vs. IV $P<0.001$.

3.4.5 Effects of EphB4 DARPins on apoptosis in tumor cells *in vitro*

Knockdown of EphB4 using small interfering RNA results in increased apoptosis and cell death in tumor cells (Kumar et al. 2006). To asses whether EphB4 DARPins can induce apoptosis in EphB4 expressing tumor cells, U-2 OS-hEphB4 cells were incubated with increasing amounts of DARPin. Apoptosis induction was determined by measuring activation of caspase-3/7 pathway. As shown in Figure 34, no caspase activation was observed after treatment with AB1 up to concentrations of 100 µg/ml. This result is similar to a control DARPin, which also demonstrated no effect. Staurosporine which was used for comparison induced caspase-3/7 activity at a concentration as low as 1 nM.

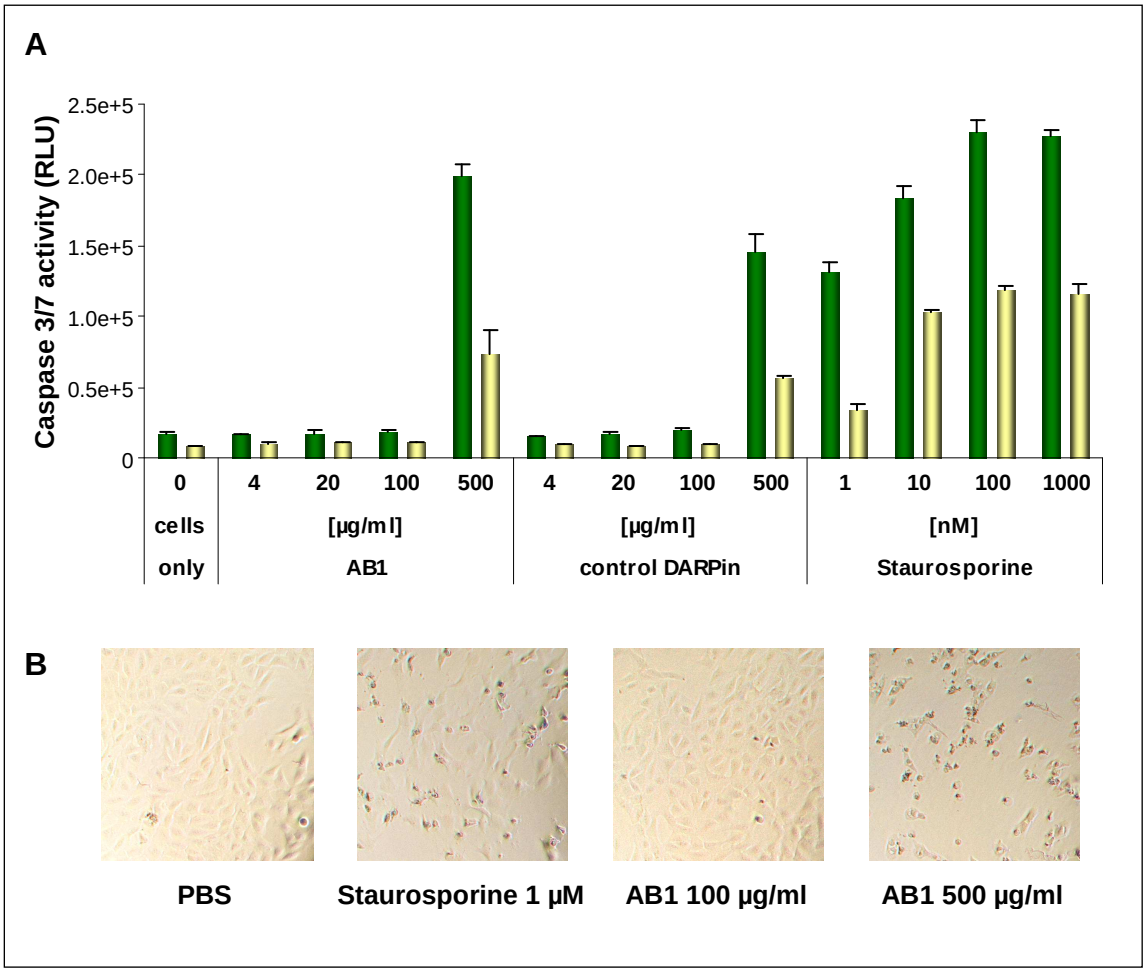

Figure 34. Induction of apoptosis in U-2 OS-hEphB4 cells by DARPin AB1 *in vitro*. (A) Analysis of apoptosis was performed as described in Materials and methods (2.6.4). U-2 OS-hEphB4 (green bars) and U-2 OS cells (yellow bars) treated with AB1, control DARPin and staurosporine at the given concentrations were grown for 24 hours. The induction of caspases 3 and 7 was measured using a luminescence based assay. Luminescence signal given as RLU is proportional to the amount of caspase activity present. Values are depicted as means of three measurements ± SD. (B) Representative phase contrast images of U-2 OS-hEphB4 cell after indicated treatments are shown for one out of two independent experiments (original magnification 10×). Apoptotic cells are indicated by the darker and round cells detaching from the surface.

After treatment with DARPin at a concentration of 500 µg/ml, induction of apoptosis at the level as high as at saturating concentrations of staurosporine was observed. However, application of the control DARPin at the same concentration also strongly induced apoptosis. This indicates that the high dose

effect of AB1 is rather unspecific and may be attributed to bacterial contaminants.

The morphological changes observed at the high concentration of DARPin were similar to the staurosporine treatment (Figure 34 B). The stimulation of caspase 3/7 activity was also observed for the remaining EphB4 DARPins at the highest concentration (data not shown). Very similar effects were seen in U-2 OS cells, which also suggest that the apoptotic effects are not specific for the EphB4 DARPin.

3.4.6 Analysis of DARPin-induced internalization of EphB4

EphB4 / ephrin-B2 complexes are internalized into the receptor expressing cell by endocytosis (Pasquale 2005), which suggests that EphB4 binders may also undergo internalization. To assess whether EphB4 DARPins induce receptor endocytosis and can be used for drug targeting, internalization studies were performed. The assay to determine cell viability after internalization of toxin coupled to the DARPin was designed as shown in Figure 35 A. DARPins served as a primary binder, followed by a secondary anti-RGS-His_4 tag antibody and a saporin-coupled anti-mouse IgG (Mab-ZAP) as a tertiary antibody. Once the complex is internalized, saporin is released and induces apoptosis by irreversible ribosome inactivation and inhibition of protein synthesis. After 72 hours cell viability was measured by Alamar Blue staining. The internalization grade was determined as the cytotoxic potency, calculated from the difference between number of cell treated with the DARPin / anti-RGS-His_4 complex and the DARPin / anti-RGS-His_4 / Mab-ZAP complex (Figure 35 A).

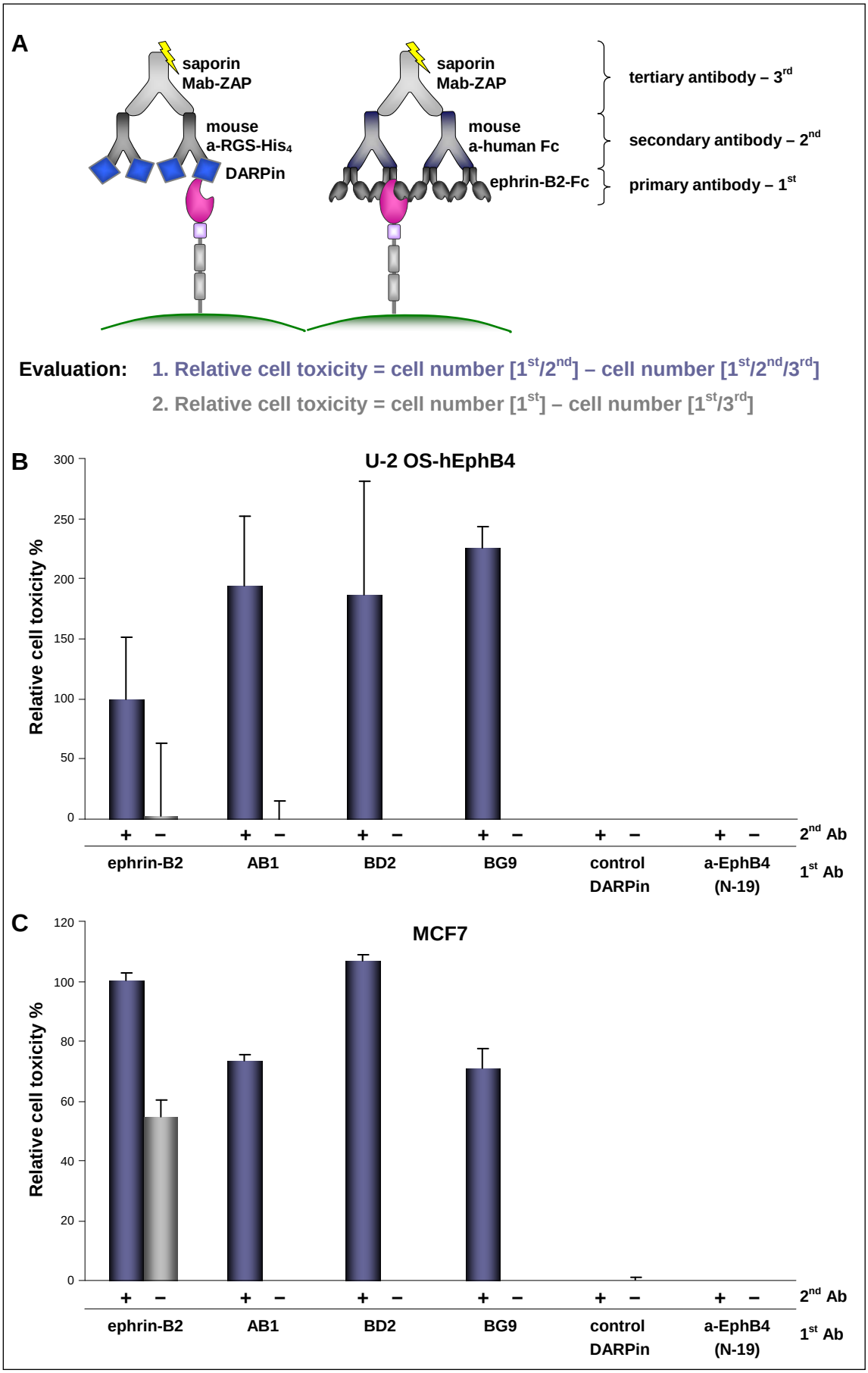
A
saporin
Mab-ZAP
mouse
a-RGS-His4
DARPin
saporin
Mab-ZAP
mouse
a-human Fc
ephrin-B2-Fc
tertiary antibody – 3rd
secondary antibody – 2nd
primary antibody – 1st
Evaluation: 1. Relative cell toxicity = cell number [1st/2nd] – cell number [1st/2nd/3rd]
2. Relative cell toxicity = cell number [1st] – cell number [1st/3rd]
B
U-2 OS-hEphB4
Relative cell toxicity %
300
250
200
150
100
50
0
+ – + – + – + – + – + –
2nd Ab
ephrin-B2
AB1
BD2
BG9
control DARPin
a-EphB4 (N-19)
1st Ab
C
MCF7
Relative cell toxicity %
120
100
80
60
40
20
0
+ – + – + – + – + – + –
2nd Ab
ephrin-B2
AB1
BD2
BG9
control DARPin
a-EphB4 (N-19)
1st Ab

Figure 35. Internalization of EphB4 DARPins by EphB4 expressing cells. (A) Schematic diagram represents the experimental set-up of the internalization assay. Internalization of the toxin labeled Mab-ZAP is mediated by EphB4 binder. Internalization was analyzed in U-2 OS-hEphB4 (B) and MCF7 cell line (C). Cell vitality was determined after 72 h using an Alamar Blue assay as described in Materials and methods (2.6.5). The fluorescence of the metabolized substrate was determined 8 h (B) and 4 h (C) after substrate addition. The cell toxicity was expressed as the potency difference between the complex with and without Mab-ZAP: the first series cell number of [$1^{st}/2^{nd}$] - cell number of [$1^{st}/2^{nd}/3^{rd}$] (blue bars) and the second series omitting the secondary binder [1st] - [$1^{st}/3^{rd}$] (grey bars). Values were normalized to the toxic effect of the ephrin-B2 / Mab-ZAP complex, which was defined as 100%. Data are depicted as means of three measurements ± SD.

U-2 OS–hEphB4 and MCF7 cells, which express endogenous EphB4, were used for this study and the results are shown in Figure 35 B and C. None of the components used in this assay including Mab-ZAP showed an effect when applied individually. Significant cytotoxicity was observed both in U-2 OS-hEphB4 and MCF7 cells, when ephrin-B2, the natural ligand of EphB4 was used together with the respective secondary antibody and Mab-ZAP (Figure 35 B-C). To assess the specificity of the assay controls were included where the respective secondary antibodies were omitted. In this case a minor cytotoxic effect was detected in U-2 OS-hEphB4 cells, whereas enhanced to 50% cytotoxicity occurred in MCF7 cells.

This unexpected result is very likely due to the cross reactivity of Mab-ZAP antibody to the human Fc fragment of the recombinant ephrin-B2-Fc fusion protein used in this assay, but this was not further investigated. The complex where ephrin-B2 was omitted showed no cytotoxic effect (data not shown). In general these results indicate that mediated by ephrin-B2 the saporin-labeled antibody complex was efficiently internalized.

The analysis of AB1, BD2 and BG9 showed cytotoxicity for all three DARPins in both cell lines (Figure 37 B-C). When compared to ephrin-B2 the level of cell apoptosis was two times higher in U-2 OS-EphB4 than in MCF7 cells, although complexes were applied at calculated equimolar concentrations of saporin. A control DARPin showed no cytotoxic effect, similar to controls where the

respective secondary antibody was omitted. Unexpectedly also a commercial goat EphB4 antibody directed against the N-terminus (He et al. 2005) did not induce cell death (Figure 37 B-C). None of the tested commercial anti-EphB4 IgG antibodies (Table 10) were efficiently internalized and demonstrated no measurable toxic effects (data not shown). DARPins and ephrin-B2 were not internalized by the parental U-2 OS cells, which express EphB4 only at a very low level (data not shown). The remaining EphB4 DARPins were also included in the analysis. In general all eight DARPins could induce cytotoxicity although at various degrees in U-2 OS-hEphB4 cells (Appendix 5.1, Figure 46). Six of the DARPins were also internalized into MCF7 cells, what is consistent with the FACS data (Figure 24) and correlates with their EphB4 binding capability.

Taken together, these results indicate that EphB4 DARPins can be internalized and therefore, appear to be suitable for targeting cytotoxic drugs to EphB4 expressing tumor cells. Experiments with DARPins, which are directly labeled with a cytotoxic drug, are required to further support this concept.

4 DISCUSSION

The interplay between EphB4 and its ligand ephrin-B2 promotes tumor growth by stimulating angiogenesis via activation of the intracellular kinase domain (Noren et al. 2004). Targeting this pathway has therefore become of greater interest for therapy purposes in cancer and other diseases. Consequently, a number of approaches are being developed for targeting EphB4 using either small molecule kinase inhibitors or biologics directed against EphB4 to block the signaling of this pathway (Krasnoperov et al. 2010). Therapeutic intervention in advanced solid tumors is currently being evaluated in clinical trials using the EphB4 kinase inhibitor JI-101 (Sharma et al. 2010).

Since EphB4 has promising potential as a drug target, the development of novel binding molecules is of particular interest. A new opportunity for this is provided by antibody like molecules with improved properties like designed ankyrin repeat proteins (Binz et al. 2003), which have been developed as next generation alternatives to conventional antibodies. The aim of this work was therefore to isolate and characterize functional EphB4 DARPins, which bind human EphB4 with high affinity and specificity.

4.1 Isolation of EphB4 binders from a DARPin phage library

The goal of the phage display was to design an optimal procedure, which allows early on during the screening to obtain an enriched population of specific DARPins. A signal recognition particle mediated phage library was used, with proteins displayed on the surface of a filamentous phage fused to the minor coat protein III. The high stability of this technique allows selection of phage binders in the complex environment. Various parameters were considered and tested, like the way of presenting of the antigen. The EphB4 target was used either as a recombinant protein with or without fusion part or exposed on cells. Moreover, ultimate selection methods were practiced during phage isolation

against GST-mEphB4-SAM protein (chapter 5.2), such as panning strategies with pre- and post-adsorption or counter screening procedures.

Procedures with pre- and post-adsorption of the phage library to either related proteins like EphB3-SAM or to GST the fusion partner prior to the display to the actual target allow reducing of non-specific binding upfront (Milovnik et al. 2009). The other option is exposing EphB4-SAM by binding via its GST part to glutathione coated plates or post-absorption of phage particles after the initial selection procedure to for example GST. Nevertheless none of these strategies improved the outcome of the phage selection (data not shown). Finally the most straightforward and successful approaches of coating of the recombinantly expressed and purified target protein directly to microtiter plates were very successful in this work. Targets for the phage display were applied either as a recombinant protein without fusion part (EphB4 ECD) or as a fusion with GST in case of DARPin selection against the SAM domain of EphB4 ICD. SAM domain was selected because it is the least conserved region within the intracellular domains of the EphB receptors (EphB4 ICD DARPins; Appendix 5.2). The homology between EphB4 and EphB3 SAM domains is 63%; in addition the small size of the target protein of around 10 kDa limits the epitopes available for the panning. Despite these challenges, a standard panning protocol followed by an extended screening of individual phage resulted in the identification of two specific EphB4 ICD binders (Figure 48). Similarly, eight DARPins were obtained, which recognize EphB4 ECD.

The focus of this thesis was the isolation of DARPins, which bind with high affinity and specificity to the extracellular domain of EphB4. The commercially available recombinant monomeric extracellular domain of EphB4 was chosen for the selection procedure instead of the dimerized Fc fusion protein. It was speculated that this antigen allows isolation of a larger variety of binders including ones binding to sites exposed only on the monomer, which could later prevent receptor dimerization. A more pragmatic reason for target selection was to avoid the isolation of binders to the Fc portion requiring added counter selection procedures. The phage library was panned on the target protein which was directly immobilized to the surface of a microtiter plate. Significant

enrichment of binders was obtained already after three selection cycles (Figure 14). The successful enrichment is reflected by the fact that although only 184 clones from the third cycle phage eluate were screened 16% positive EphB4 binders containing eight unique binders were isolated. The rapid enrichment of specific binders is characteristic for the DARPin library (Steiner et al. 2008). Interestingly, half of the positive binders turned out to have the same sequence (AH5). The reasons for the enrichment of this particular clone are not known, but it can be possibly a binder of an easily accessible epitope. Further work was focused on the initially isolated eight EphB4 binders, but a more thorough screening of the phage eluate of cycle 3 may result in the identification of additional distinct EphB4 binders. In this case methods should be included to counter select for the already identified clones by cell ELISA analysis or affinity determination using SPR analysis.

All isolated binders were successfully converted from their phage fusion protein format into soluble DARPins (Steiner et al. 2008), which fully retained their binding activity and specificity for EphB4 (Figure 21). DARPin proteins have been reported to have several favorable physicochemical properties (Binz et al. 2003). For example they are designed to occur as monomer and are highly soluble and stable (Kohl et al. 2003). They can be expressed at high levels in bacteria and easily purified by IMAC via their N-terminal His-tag. The expression yields of all EphB4 DARPins were in a high range of 20–55 mg/liter of shake flask culture (Figure 17) which correlate with the reported levels of 100 mg/liter culture (Steiner et al. 2008). They were well soluble in simple physiological buffers like PBS and similarly 75–90% purity was obtained after a single IMAC purification step from a total bacterial lysate without any optimizations steps.

The monomer content of the DARPins and their stability at various storage conditions were analyzed by size exclusion chromatography. All DARPins were routinely stored in PBS without any additive for cryoconservation at a concentration of 0.25 mg/ml at -80 °C. Some sample s were stored at 4 °C for several weeks, where conventional antibodies are usually unstable. DARPin BG9 occurred as monomer, as judged from their elution profiles (Figure 19) and

was stable without showing signs of aggregation or degradation upon extended storage times at 4 ℃. DARPins AH5 and AB1 stored at -80 ℃ appeared predominantly as dimers. At 4 ℃ DARPin AB1 formed aggregates. The elution profiles of AC7 stored at -80 ℃ and 4 ℃ showed si gns of increasing degradation, indicating that this protein is very unstable. However, no enhanced degradation compared to the other DARPins was observed after initial IMAC purification (Figure 17). Similarly, multimerisation or degradation were described also for other DARPins like APH kinase inhibitors (Amstutz et al. 2005), suggesting that this may be attributed to residues in the variable regions. Since most of the DARPins were stable under the routine storage conditions, no attempts were made in this studies to optimize for example the storage buffer or modify individual DARPins by changing their amino acid sequence for more stabilization. Such experiments will be required if a DARPins is further developed for clinical application.

4.2 Selected DARPins bind EphB4 with high specificity

EphB4 belongs the largest family of receptor tyrosine kinases. To date, fourteen members of this Eph family were identified in mammals divided into two subfamilies EphA (EphA1-8, EphA10) and EphB (EphB1-4, EphB6) (Himanen and Nikolov 2003b). Eph receptors play an essential role in embryonic development (Holder and Klein 1999) and regulate functions of the adult brain (Yamaguchi and Pasquale 2004). Since the other family members are expressed in normal organs and inhibiting their functions would be disadvantageous, the specificity of selected DARPins to EphB4 is of particular interest.

EphB4 DARPin binding specificity was clearly shown in an ELISA analysis using commercially available recombinant extracellular domains of all five EphB receptors (Figure 23). All EphB4 DARPins bound only to EphB4 except for DARPins AB1 and BD2, which showed low binding level to murine EphB6 but not to human EphB6. This is reasonable since the ECD of EphB receptors are only weakly conserved with an amino acid sequence identities between 34.6

and 41.5% (Table 16). AB1 and BD2 bound also to murine EphB4. Surprisingly only these two DARPins showed cross reactivity, although EphB4 shares a 85% homology with its human ortholog (Table 17). None of the isolated DARPins bound to EphB1, 2 and 3 receptors. The human orthologs from rat (EphB1) or mouse (EphB2 and 3) were tested, because the corresponding human proteins were not available. Nevertheless it is most likely that the selected DARPins also do not bind to the human proteins, because of very high amino acid sequence homology between them (94 to 99%). These observations suggest that AB1 and BD2 bind to the region of EphB4 which is conserved between mouse and human EphB4 and mouse EphB6, but not among EphB1-3. On the contrary the remaining DARPins bind most probably to the regions of EphB4 which are not conserved among the analyzed receptors.

EphB4 receptors are overexpressed in a variety of human tumors (reviewed in Heroult et al. 2006 and chapter 1.2.5). Specific and high affinity binding to the antigen on tumor cells surface is obligatory in case of a tumor targeting approach. EphB4 DARPins were selected using the recombinantly expressed and purified extracellular domain fragment of EphB4. The target protein was immobilized directly on the solid plastic surface and may only partially reflect its native conformation within the full receptor. All isolated DARPins bound to U-2 OS-hEphB4 cells, which were used as positive control based on their stable transfection with human EphB4 in the FACS analysis (Figure 24). This showed that they can recognize the full receptor localized in the cellular plasma membrane. EphB4 DARPins also weakly labeled untransfected U-2 OS cells, which correlates with their low EphB4 expression level (Figure 42). EphB4 DARPins labeled also MCF7 breast cancer cells reported to express endogenous EphB4 (Kumar et al. 2006). The signal was higher than in untransfected U-2 OS cells but lower than in U-2 OS-hEphB4 cells, suggesting that MCF7 cells express intermediate levels of EphB4. In addition, it demonstrates the DARPins capability to recognize endogenously expressed EphB4 and indicates their specificity for EphB4 binding. Interestingly, DARPins AA5 and BE1 bound only weakly the MCF7 cells, suggesting their lower affinities, therefore the kinetic analysis was performed using SPR technique.

Table 16. Amino acid sequence homology of the hEphB4 extracellular domain with other human and mammalian EphB receptors. Amino acid sequences of ECDs (aa 16 to 539) of human EphB1-3, 6, rat EphB1, mouse EphB2, 3, 6 were aligned and their homology to hEphB4 was calculated using VECTOR NTI software.

Eph receptor	**Homology to human EphB4**	
species	**murine / rat**	**human**
EphB1	39.4%	41.1%
EphB2	39.3%	40.3%
EphB3	41.5%	41.3%
EphB6	34.8%	34.6%

Table 17. Amino acid sequence homology of mouse and rat with human extracellular domains of EphB receptors. Amino acid sequences of ECDs (aa 16 to 539) of mouse and rat EphB receptors were aligned with their corresponding human proteins and their homology was calculated using VECTOR NTI software.

Eph receptor	**Homology**
rat to hEphB1	99.3%
mouse to hEphB2	96.6%
mouse to hEphB3	94%
mouse to hEphB4	85.5%
mouse to hEphB6	88.3%

4.3 DARPins bind EphB4 with nanomolar affinities as determined by SPR

SPR analysis was used to determine the binding affinity and the association / dissociation kinetics of EphB4 DARPins with EphB4. Moreover, the binding analysis in combination with ephrin-B2 or with each other was performed to gain preliminary insight with respect to their relative binding sites. The assay used for these studies was validated by a close recapitulation of the K_D values for the ephrin-B2 / EphB4 interaction reported in the literature (Blits-Huizinga et al. 2004; Pabbisetty et al. 2007). The isolated DARPins potently

bound EphB4 with affinities in the range of 0.4 to 80 nM (Table 15). These affinities are in the typical range of affinities of DARPins, which have been isolated against the Fc domain of human IgG after primary screenings (Zahnd et al. 2006). If required it should be possible to further optimize EphB4 DARPins by affinity maturation to achieve picomolar affinities (Zahnd et al. 2007). BE1 showed the lowest affinities with 40–80 nM and AA5 could not be detected, although their ELISA binding signals were comparable to the other DARPins in this assay (Figure 21). The difference could be attributed to the 15-fold higher target density on the ELISA plate compared to the chip surface, leading to re-binding effects of the low affinity binders in the ELISA. In addition, with BIAcore interactions are measured at real time, whereas long incubation times during ELISA assays may compensate for low affinity interactions.

In general, the affinities of EphB4 DARPins were very similar to the affinity of ephrin-B2 for binding to either the dimeric or the monomeric EphB4. Only slightly lower K_D value where calculated for the interaction with EphB4-Fc, which is in agreement with the ELISA data (Figure 22). The affinity differences among the DARPins are in most cases related to the varying dissociation rates. Regarding the kinetics of the interaction “slow” and “fast” binders were identified. A faster association rate could be of advantage for those DARPins, which inhibit EphB4 by competing for ligand binding. DARPins AC7 and BE1 associated to EphB4 with rates lower than ephrin-B2 and were classified as slow binders (Table 15). AB1 revealed exceptional kinetics with k_{on} and k_{off} rates faster than ephrin-B2 and all other DARPins. BG9 showed a 5-fold higher k_{on} rate than ephrin-B2 for the interaction with EphB4-Fc. Taken together these results show that the binding characteristics of EphB4 DARPins to EphB4 are similar to ephrin-B2 and that AB1 may have the best chances for competing with ephrin-B2 based on its fast k_{on} rate.

4.4 DARPins interact with EphB4 in monovalent or bivalent binding model

The binding of ephrin-B2-Fc to the monomeric and dimeric EphB4 were evaluated in relation to the interaction model. The bivalent binding model

assuming the initial 2:1 and subsequent 2:2 interaction was statistically more significant for the ephrin-B2 / EphB4 interaction as indicated by the lower χ^2 values detected in the BIAcore experiments (Table 15). This result is consistent with the binding model deduced from the co-crystal structure of the ephrin-B2 ligand and the ligand binding domain of the EphB2 receptor (Himanen et al. 2001). Each Eph receptor and ephrin ligand has two independent binding sites, which increase the affinity of their interaction and lead to a 2:2 complex.

DARPins were initially designed as monomers, but dimers and in higher order forms, have been reported (Amstutz et al. 2005). The gel filtration studies indicated that some DARPins (e.g. BG9) occur as monomers, whereas others (e.g. AH5) behave as dimers. SPR sensorgrams for DARPin binding were therefore fitted using the 1:1 Langmuir and the bivalent binding models of the BIAeval software. In this work, no significant differences in the quality of fit and the statistical robustness were observed when the bivalent model was used for the evaluation of the interaction of most of the DARPin with the monomeric EphB4. Only slightly higher statistical relevance of the fits was obtained for DARPins binding to dimeric EphB4-Fc using the bivalent analyte binding. For example AB1 showed only 1.5-fold higher χ^2 for the bivalent model (Table 15), although in the gel filtration AB1 occurred as a dimer. This result could be interpreted that DARPins as AB1 indeed exist and bind in multimeric forms or that it is the consequence of fitting to a model with a higher degree of free parameters and less stringency. One exception was binding of AH5 to both the monomer and the dimer of EphB4, which could be clearly better fitted to the bivalent model with 3- and 7-fold higher χ^2. This might be explained by the fact that AH5 was observed as dimer during size exclusion chromatography and possibly could bind to the target forming a 2:2 complex. It should be mentioned here that some of the analyzed DARPins (AC7, BD4) displayed unusual sensorgrams when injected at saturating concentrations in BIAcore, suggesting that protein aggregation has occurred at these high concentrations (Figure 27). This might be also the reason why the measured binding response of these DARPins was lower than the predicted response (Figure 26). Still, DARPins showed specific binding to the target, regardless of the eventual multimerization state.

Oligomerization of DARPins is a consequence of the individual sequence (Amstutz et al. 2005). It was speculated that amino acid sequences in the variable regions, which are responsible for the interaction with the target are also involved in formation of dimers or higher order structures. The observations derived from the SPR studies, together with previous results from gel filtration analyses suggested three binding models (Figure 36). The monomeric form of the DARPins (e.g. BG9) showed by the gel filtration and confirmed by BIAcore led to assume an 1:1 binding model (Figure 36 A). DARPin with dimer profile (e.g. AH5) bind to the target forming a 2:1 and subsequent 2:2 complexes (Figure 36 B-C). DARPins with dimerization tendency presented by gel filtration (e.g. AB1) could possibly in the presence of antigen loose their dimer format and induce a defined 1:1 EphB4 DARPin protein complex (Figure 36 A) as showed by SPR analysis. Further studies will be required to confirm this hypothesis.

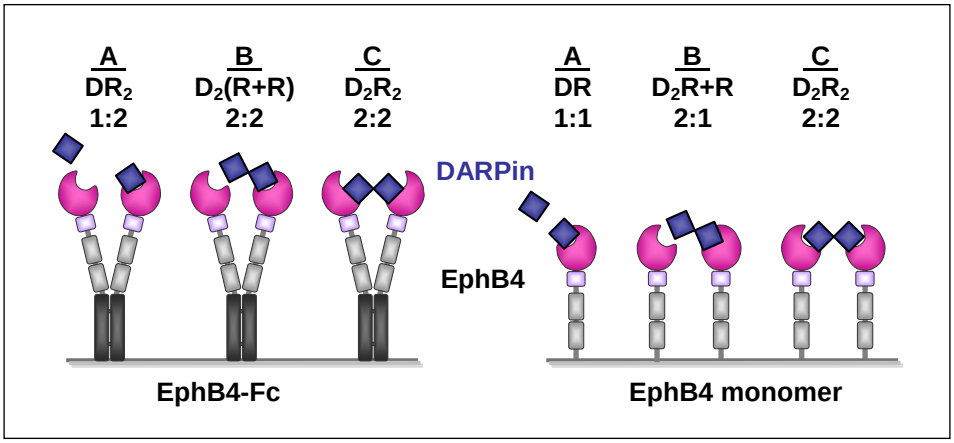

Figure 36. The interaction models of DARPins (D) to the immobilized EphB4 receptor (R).

4.5 EphB4 DARPin binds competitively to EphB4

SPR analysis was additionally applied to identify the binding epitopes of the EphB4 DARPins relative to ephrin-B2 and thereby gain preliminary insight into their potential mode of action. At least two classes of DARPins could be identified, which differ in their ability to bind to EphB4 in the presence of ephrin-

B2. AB1 could not bind to EphB4 when co-administered with ephrin-B2, which suggested that they bind to overlapping epitopes (Figure 29 A). Moreover, AB1 enhanced the dissociation of ephrin-B2 from pre-established complexes with the receptor and an EphB4 surface saturated with AB1 retarded association of ephrin-B2, which further supports their competitive binding (Figure 29 B-C). Similar results were obtained for DARPins AC7 and BE1, which did not bind to bind to EphB4 in the presence of ephrin-B2. However, none of them influenced the kinetic of ephrin-B2 possibly due to their slow association rate and lower affinity than AB1.

The second class of DARPins, which encompasses AH5, BD2, BD4 and BG9, did bind to EphB4 in the presence of either ephrin-B2 or AB1, demonstrated by an increased EphB4 binding signal (Figure 29 A, D). This indicates that they bind to sites which are different from the cognate ephrin-B2 binding site. A similar classification in competitive- and non-competitive binders was described for DARPins targeting the ubiquitin-binding / oligomerization domain of NEMO (Wyler et al. 2007). DARPin BD2 appeared to retard the dissociation of ephrin-B2, which is exceptional to the other DARPins (Figure 29 B). Ephrin-B2 induces conformational changes of the receptor (Himanen et al. 2001), it can be assumed that this conformation is favored by BD2.

4.6 EphB4 DARPins bind to different sites of EphB4

Previous results on binding to EphB receptors (Figure 23) and the competitive binding studies (Figure 29) allowed the prediction of EphB4 interaction regions for the isolated DARPins. Amino acid sequence homology and crystal structure data of the extracellular domain of EphB4 receptor may provide hints for the binding sites of DARPins. The crystal structure of an EphB2-LBD / ephrin-B2 complex identified two binding interfaces between the receptor and the ligand (Himanen et al. 2001). A high-affinity binding interface mediates dimerization of Eph and ephrin molecules (Figure 38; amino acids highlighted in red). A distinct smaller interface with lower-affinity is responsible for tetramer assembly (Figure 38; amino acids highlighted in yellow). The three-dimensional structures of the

LBDs of EphB4 and EphB2 receptors are similar and allowed the assignment of the EphB4 / ephrin-B2 interaction residues (Chrencik et al. 2006b). Guided by the results that AB1 binds competitively with ephrin-B2 and cross reacts with murine EphB4 and EphB6 but not with other EphB receptors candidate sites can be indicated. Two amino acids were identified within the ligand interaction site, which are common for mouse and human EphB4 and mouse EphB6, but distinct from other tested EphB sequences (Figure 38; outlined in blue). Based on this analysis it is likely that AB1 binds to the high affinity interface of EphB4, recognizing a non-linear epitope.

The specificity of a protein – protein interaction is determined by their three-dimensional structure. In case of the ephrin-B2 / EphB2 interaction it was found that the G-H loop of the ephrin-B2 is inserted into a hydrophobic channel of the EphB2 LBD (Himanen et al. 2001). Interestingly, a peptide TNYL-RAW identified by phage display screening for EphB4 binders could inhibit ephrin-B2 binding by occupying the hydrophobic cleft required for the G-H loop interaction of ephrin-B2 (Chrencik et al. 2006b). However, it is considered unlikely that AB1 binds in a similar manner, because the randomized surface responsible for DARPin binding was reported to be rather flat surface (Binz et al. 2004). Therefore, it is speculated that AB1 may rather bind to an exposed flat area.

DARPins AC7 and BE1 were classified as ephrin-B2 and also AB1 competitive binders, suggesting binding to the high affinity interface of EphB4. However, their specificity to human EphB4 indicates binding to the site non-conserved between the EphB receptors (Figure 38, outlined in black). It was assumed that AC7 and BE1 bind to an overlapping, but not exactly the same epitope of AB1.

Besides ephrin-B2 competitive DARPins, non-competitive binders (AH5, BD2, BD4 and BG9) were isolated, which could bind to other domains of EphB4 ECD such as the cysteine-rich domain or one of the two fibronectin domains FN1 and FN2 (Himanen and Nikolov 2003a). DARPins could possibly bind to one of these regions in a similar fashion as the recently described monoclonal antibodies, whose binding sites were mapped to the FN domains of EphB4 (Krasnoperov et al. 2010). These antibodies were also shown to inhibit EphB4 signaling. In contrast to the LBD, no crystal structures are available from the

other domains of Eph receptors, which could help to identify the epitopes of the non-competitive DARPins.

Amino acid sequence alignments and cross reactivity data where also used to narrow the epitopes. BD2 bound to the human and murine EphB4 but not to other EphB receptors (Figure 23), which suggests interaction to the homologous regions (Figure 38; outlined in orange). The low binding signal of BD2 to mouse EphB4 was comsidered as unrelevant for this analysis, AH5, BD4 and BG9 specifically bound to human EphB4 and neither to murine EphB4 nor to other EphB ECDs. Their epitopes may be located in the non-homologous areas (Figure 38; outlined in green). Based on this analysis it is considered unlikely that the binding sites of BD2 and BG9 overlap, but to this end it has not been directly tested for example by SPR competition experiments. Summarizing the experiments allowed to identify at least four groups of DARPins binding to distinct regions of EphB4 receptor (Figure 37). Further studies are necessary to exactly map the epitopes of EphB4 DARPins for example by peptide mapping.

	ephrin-B2 competitive binding	Binding to sites		Groups of DARPins:
		conserved within:	different from EphB:	
DARPins binding to the extracellular domain of EphB4	ephrin-B2 competitive	**4H, 4M, 6M**	1R, 2M, 3M, 6H	AB1
		4H	1R, 2M, 3M, 4M, 6H, 6M	AC7, BE1
	ephrin-B2 non-competitive	**4H, 4M**	1R, 2M, 3M, 6H, 6M	BD2
		4H	1R, 2M, 3M, 4M, 6H, 6M	AH5, BD4, BG9

Figure 37. Classification of EphB4 DARPins based on the prediction of binding epitope. DARPins were divided into ephrin-B2 competitive and non-competitive binders. Further classification was based on binding specificity to human EphB4 (4H) and EphB6 (6H), murine EphB2 (2M), EphB3 (3M) and EphB4 (4M) and rat EphB1 (1R). Chart represents the structure of the EphB4 ECD, which contains a LBD (pink), a cysteine-rich region (purple) and two fibronectin type III repeats (grey) and EphB4 DARPins (rhombs) an their predicted binding sites.

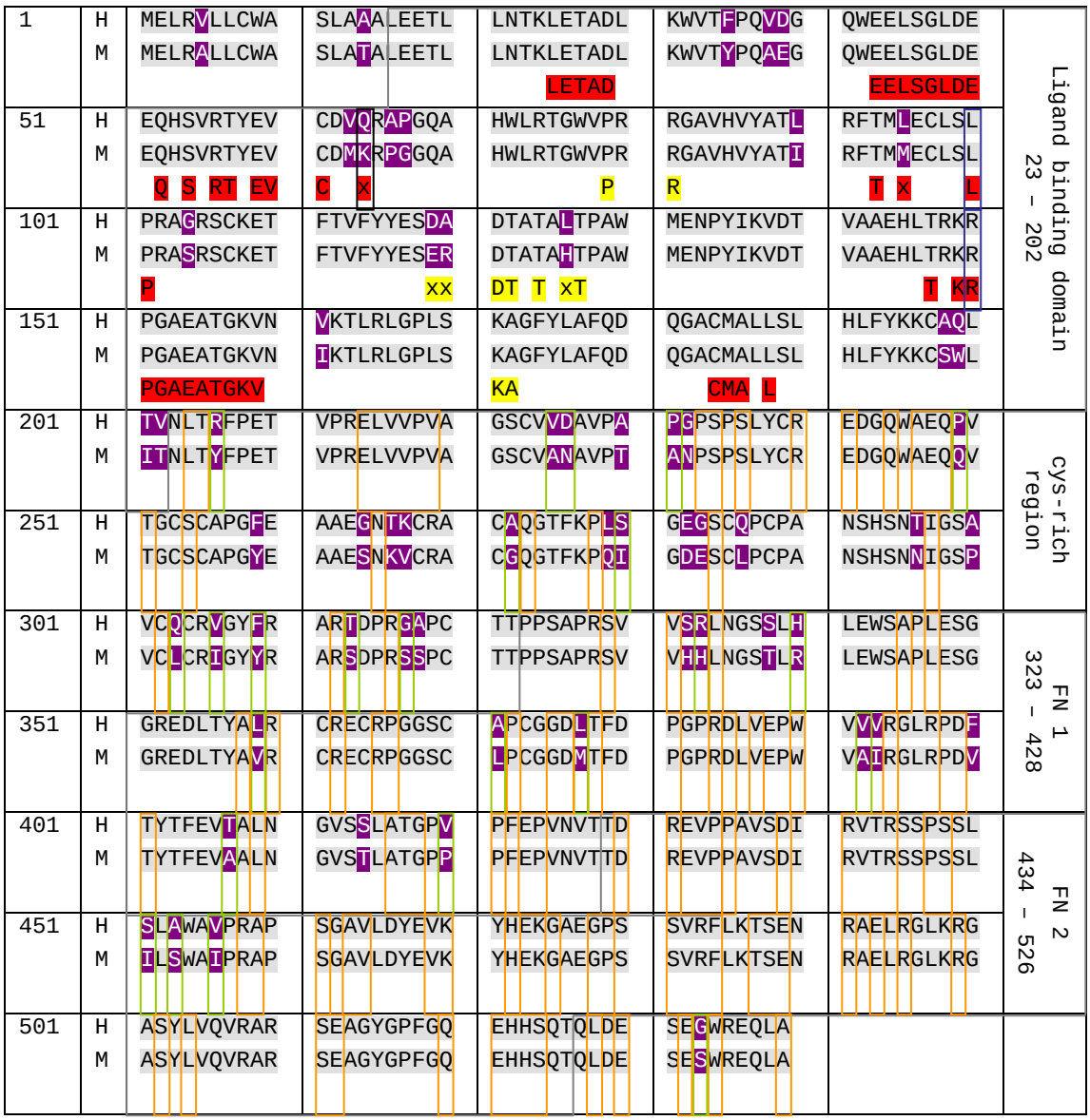

Figure 38. Amino acids sequence alignment and domain structure of the extracellular domains of human and mouse EphB4. The amino acid sequences of human (H) and murine (M) EphB4 ECD were aligned using Vector NTI software. Numbers correspond to the first residue of the protein sequence in line. The ligand binding domain (LBD), a cysteine-rich region and the two fibronectin domains (FN) are indicated. Identical amino acids are highlighted in grey and similar amino acids in purple. Below the sequence alignment amino acids involved in the high (highlighted in red) and low (highlighted in yellow) affinity binding are shown. Amino acids conserved between LBD of hEphB4, mEphB4 and mEphB6 but not other EphB are most probable interaction residues for AB1 (outlined in blue). Amino acids conserved only between human and mouse EphB4 could be bound by BD2 (outlined in orange), whereas amino acid residues individual for hEphB4 are possible interaction site for AH5, BD4, BG9 (outlined in green) or AC7 and BE1 (outlined in black).

4.7 EphB4 DARPins prevent ligand-induced EphB4 phosphorylation

Disruption of EphB4 – ephrin-B2 signaling by soluble EphB4 ECD was shown to inhibit angiogenesis and tumor growth (Martiny-Baron et al. 2004). Therefore, it was of great interest to assess whether EphB4 DARPins can affect the receptor activity and could also exert antiangiogenic effects. DARPins were functionally characterized in several cell-based assays *in vitro*. In a receptor activation analysis it was shown that no EphB4 autophosphorylation was observed, when EphB4 expressing U-2 OS tumor cells were incubated with DARPins alone in the absence of ephrin-B2. Notably, this was also not the case for DARPins like AH5 which appear to occur as dimer (Figure 19 B) and it also did not occur, when cells where incubated with DARPins, which where dimerized with an anti-His antibody (Figure 45). This indicates that DARPins alone have no agonistic effect on EphB4.

Different effects were observed, when DARPins were analyzed in the presence of ephrin-B2. Preincubation of U-2 OS-hEphB4 cells with DARPins dose-dependently inhibited the ephrin-B2 induced autophosphorylation of EphB4 (Figure 30). For AB1 this could be simply explained by its competition for ephrin-B2 binding to the receptor. However, BG9 did not bind to the same site as AB1 and ephrin-B2, and thus, its mechanism of inhibition must be different. The above results suggested a new mode of action for BG9 as depicted in a cartoon in Figure 39. BG9 might either inhibit receptor dimerization by inducing conformational changes or by binding to a site, which is essential for receptor activation for example a site involved in receptor dimerization. It could act similar to panitumumab, an anti-EGF receptor antibody, which impairs EGFR signaling by preventing receptor dimerization after ligand binding (Astsaturov et al 2006). Another hypothesis assumes that BG9 stimulates receptor endocytosis and lysosomal degradation as recently described for anti-EphB4 antibody (Krasnoperov et al. 2010). Further investigations are required in order to identify its binding site in EphB4 and to elucidate its precise mechanism of action.

Surprisingly DARPin BD2 enhanced the ligand induced EphB4 receptor signaling (Figure 30). Since BD2 alone did not activate the receptor, the

enhancement must be mediated by an indirect effect. The kinetic analyses (Figure 29 B) indicated that BD2 can retard the dissociation of ephrin-B2. Potentially this could lead to a proangiogenic effect of BD2, which could be useful for the therapy of certain vascular diseases with insufficient angiogenesis such as arteriosclerosis, myocardial infarction or wound repair.

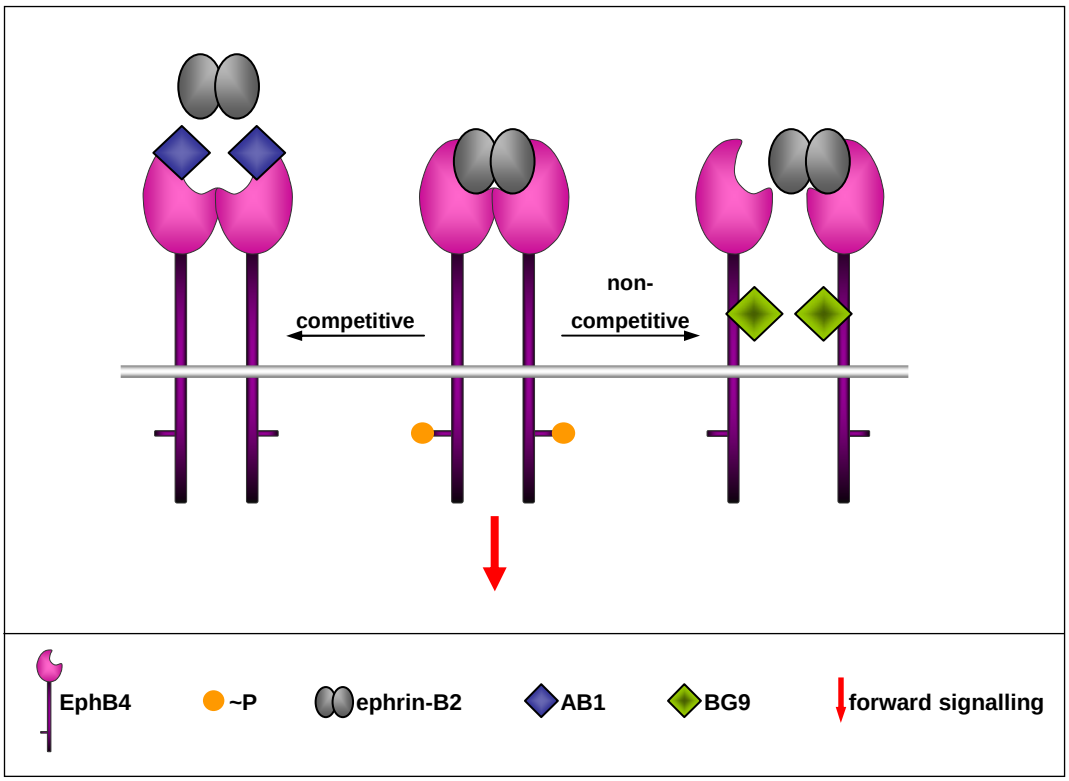

Figure 39. Schematic representation of EphB4 signaling inhibition by DARPins AB1 and BG9. In the physiological context (diagram center) ephrin-B2 binds to the LBD of EphB4 inducing receptor dimerization, autophosphorylation of intracellular tyrosine residues (P) and forward signaling in EphB4-expressing cells. AB1 (left) binds to the cognate binding site of ephrin-B2, thereby preventing its interaction with EphB4 and inhibiting receptor activation. On the other hand BG9 (right) seems to associate with ephrin-B2 at an allosteric site and is equally able to inhibit ligand-induced EphB4 phosphorylation.

4.8 EphB4 DARPin AB1 exert antiangiogenic effects *in vitro* and *in vivo*

Angiogenesis involves the recruitment and attachment of endothelial cells at the site of vascularization followed by their proliferation and organization into

capillary-like tubular structures (Conway et al. 2001). EphB4 receptor is expressed on ECs and plays a significant role in this process (Salvucci et al. 2006). To address the involvement of EphB4 in the proangiogenic activity of endothelial cells, DARPins which showed inhibitory effects on the EphB4 activation were further analyzed in a tube formation assay using HUVECs. AB1 and BG9 exhibited antiangiogenic effects, as demonstrated by a specific and dose dependent reduction of the number of tubes (Figure 32). BG9 appeared to be more potent in this assay than AB1. This was consistently seen also in the EphB4 activation assay (Figure 30).

The study was consequently aimed at the investigation of the antiangiogenic effect of AB1 and BG9 *in vivo.* Unfortunately, BG9 could not be analyzed in the mouse model because - unlike AB1 - it did not cross react with the murine EphB4 (Figure 23). DARPins were reported to have high stability for over 4 weeks at 37 °C (Zahnd et al. 2010). In the gel filtration analysis AB1 showed oligomerization tendency upon storage at 4 °C (Figure 19). Therefore, in the experiments relatively high AB1 concentrations (up to 200 µg/ml) were used to compensate for possible inactivation of the DARPin due to formation of multimers at mouse body temperature. The angiogenesis was assessed by measuring the invasion of endothelial cells and formation of vascular structures as a response to the growth factors VEGF and FGF-2 (Carmeliet 2000). Using this model, a significant inhibition of the VEGF / FGF-2 induced angiogenesis was measured at the level of 80% compared to the control (Figure 33). This result is in line with previous findings, which showed suppression of tube formation *in vitro* and inhibition of the angiogenic effects of growth factors (VEGF and FGF-2) *in vivo* by the soluble domain of EphB4 (Kertesz et al. 2006). Further studies will be required to demonstrate whether EphB4 DARPins are able to prevent tumor growth in an *in vivo* xenograft assay.

4.9 DARPins induce EphB4 internalization in tumor cells

It was previously described that EphB4 is overexpressed in several solid human tumors (Berclaz et al. 2003; Xia et al. 2005b; Kumar et al. 2006; Xia et al. 2006;

Kumar et al. 2007). Furthermore, targeted knockdown of EphB4 expression in several EphB4 positive tumor cell lines by small interference RNA activated apoptosis and led to cell death (Xia et al. 2005b; Kumar et al. 2006; Kumar et al. 2007). Similarly, treatment of EphB4-positive cells: PC3M prostate cancer, Hey ovarian cancer or SCC15 head and neck cancer cell lines with an anti-EphB4 antibody induced tumor cell apoptosis and growth inhibition (Krasnoperov et al. 2010).

When tested in U-2 OS-hEphB4 cells in this study EphB4 DARPins did not specifically affect proliferation or induce apoptosis. To eventually take advantage of DARPins as an agent for the delivery of toxic drugs into tumor cells, this requires their specific internalization into cells expressing EphB4 receptor. Stimulation of EphB4 expressing cells with ephrin-B2-Fc leads to the internalization of the ligand / receptor complex (Heroult et al. 2010). Antibody-triggered endocytosis of EphB4 was reported for the anti-EphB4 IgG, which binds to the FN III domain 1, but not for the IgG binding to the FN III 2 (Krasnoperov et al. 2010).

In this work, all EphB4 DARPins were efficiently internalized as a complex with a saporin-labeled antibody by receptor-mediated endocytosis into U-2 OS-hEphB4 (Figure 35). Moreover, internalization was observed into MCF7 cells, also expressing EphB4, for DARPins which showed binding to this cell line (Figure 24). Notably, both AB1 and BG9 are internalized even though based on the SPR competition experiments (Figure 29) they are expected to bind to different regions of EphB4. DARPins were previously shown to successfully deliver siRNA into the cells (Winkler et al. 2009). Taken together these results support the possibility to use DARPins as drug conjugates for the antitumor therapy.

4.10 EphB4 DARPins present different characteristics

Summarizing eight EphB4 DARPins were isolated and analyzed with regard to their binding specificity and functional impact on the EphB4 receptor (Table 18).

Table 18. Summary of the EphB4 DARPin data. Data were grouped according to their activities in the various assays. Green: good; orange: intermediate; yellow: low; white: no effects or not determined (n.d).

Selected clone			**AA5**	**AB1**	**AC7**	**AH5**	**BD2**	**BD4**	**BE1**	**BG9**
Modular structure			N3C	N4C	N3C	N4C	N4C	N4C	N3C	N3C
Molar weight (kDa)			18.3	21.9	18.2	21.5	21.8	21.5	18.3	18.1
DARPin-pIII	Binding to hEphB4		+++	++	++	+++	+++	+++	+++	+++
	Binding to U-2 OS-EphB4 (ELISA)		++++	+	++	+++	+	++	+	++++
	Binding to U-2 OS-EphB4 (FACS)		+++	++	++	+++	++	+	+	++
DARPin binding to hEphB4/background			20	6	4	5	19	3	4	13
DARPin binding to hEphB4-Fc			+	+	+	+	+	+	+	+
Selectivity to hEphB4			+	–	+	+	–	+	+	+
Cross reactivity to mEphB4			-	+++	–	–	++	+	–	–
Binding to mEphB6			-	++	–	–	+	–	–	–
Binding to U-2 OS-EphB4			+++	+++	+++	++	+++	+++	++	+++
Binding to MCF7			-	++	++	++	++	++	+	++
Kinetic in BIAcore	EphB4 dimer	K_D (nM)	n.d.	13.5	2.9	12.9	2.2	0.4	43.4	5.5
		k_a (x10^4 M^{-1} s^{-1})	n.d.	138	16.3	15.0	29.8	40.7	7.3	48.8
		kd (x10–3 s–1)	n.d.	18.7	0.5	1.9	0.7	0.2	3.2	2.7
	EphB4 mono.	K_D (nM)	n.d.	35.8	10.9	19.7	1.7	56.0	80.8	5.6
		k_a (x10^4 M^{-1} s^{-1})	n.d.	42.5	4.8	8.0	11.7	3.9	2.8	11.7
		kd (x10–3 s–1)	n.d.	15.2	0.5	1.6	0.2	2.2	2.3	0.7
Monovalent (1), bivalent (2) binding model			n.d.	1	1	2	1	1	1	1
Competition with ephrin-B2			n.d.	+++	+	–	–	–	+	–
Kinase inhibition			n.d.	++	+	–	–	+	+	+++
Internalization U-2 OS-EphB4			+++	+++	n.d.	++	+++	+++	++	+++
Internalization MCF7			+	++	++	++	+++	++	–	++
Inhibition of tube formation			n.d.	+	n.d.	n.d.	n.d.	n.d.	n.d.	+
Inhibition of angiogenesis *in vivo*			n.d.	+	n.d.	n.d.	n.d.	n.d.	n.d.	n.d.

With the help of these studies a candidate for *in vivo* experiment was selected. The crucial criteria were inhibitory effect on the receptor activity and cross reactivity to the mouse EphB4. Selected DARPins bound human EphB4 recombinant protein with high specificity and two DARPins presented cross reactivity to the mouse receptor. Using surface plasmon resonance analysis DARPins with high affinity and favorable association and dissociation rates were identified. Competition studies allowed distinguishing between DARPins which compete with ephrin-B2 for the binding to a common site (AB1) and those targeting different epitopes of the receptor (BG9). Another highly affine binder BD2 interestingly influenced the dissociation of ephrin-B2.

These findings helped to predict that AB1, BD2 or BG9 can have biological effects on the function of EphB4, and therefore were analyzed in the cell based assays. Notably, competitive DARPin AB1 and non-competitive BG9 could inhibit ligand induced receptor autophosphorylation and angiogenesis *in vitro*. Furthermore, it was shown that DARPin AB1, which recognizes also murine EphB4, could prevent angiogenesis *in vivo*.

4.11 Conclusions and potential applications of DARPins

In summary, the present study revealed for the first time DARPins, a novel class of binding molecules specific for the human EphB4 receptor. Eight unique DARPins were isolated which bound to the extracellular domain of hEphB4 with high affinity. Two unique DARPins specifically bound the to intracellular SAM domain of EphB4. ECD DARPins inhibited EphB4 receptor signaling by ephrin-B2-competitive and -non-competitive binding and prevented angiogenesis *in vitro* and *in vivo*. Besides their function blocking activity, EphB4 DARPins were shown to be internalized into EphB4 expressing tumor cells. Additional studies are required to further characterize these DARPins in more detail and for example investigate whether they could prevent tumor growth *in vivo*.

In general they provide the foundation for a wide spectrum of potential applications. Primary EphB4 DARPins exploit function blocking activities as

therapeutic for tumor therapy via an antiangiogenic mechanisms. In case of their good tolerance, DARPins could be administered in combination with other therapies. For application of DARPins certain parameters like protein stability, pharmacokinetic and immunogenic behavior have to be investigated and perhaps optimized. Due to their small size of ~20kDa it can be expected that they are rapidly cleared from circulation, in the range of minutes. Modifications like PEGylation and Hesylation could extend their half lives up to 19 hours as shown for HER2 DARPins (Zahnd et al. 2010). On the other hand their small size could favor better tumor penetration over IgGs and in conjunction with their high affinity lead to improved tumor accumulation. Tumors which are highly vascularized like renal cell carcinoma could be a target indication. Other angiogenesis-dependent diseases like age-related macular degeneration or diabetic retinopathy could also benefit from EphB4 DARPin. For this indication direct application of DARPin into the eye would allow to avoid the pharmacokinetic issues speculated for the systemic administration.

Secondary, it will be interesting to see during further characterizations, whether BD2 has proangiogenic effect *in vivo*, and if so, it might become useful for the therapy of cardiovascular diseases with insufficient angiogenesis (arteriosclerosis, myocardial infarction) or wound repair. The activation of EphB4 is already in focus for ischemic cardiovascular diseases or vascular injuries (Foubert et al. 2007).

The third potential application of EphB4 DARPin is usage as delivery agents for cytotoxic drugs. Initial studies with saporin-IgG complex have shown that EphB4 DARPins are internalized by EphB4 expressing cells, but it remains to be seen whether the DARPin directly conjugated with drug can exert the same effect. Tumors with overexpression of EphB4, like melanoma, prostate, breast or ovarian carcinoma could be target indications.

Fourth, DARPins with their high stability and pharmacokinetic in the range of minutes meet the requirements to be applied as a diagnostic tool by combining them with suitable detection systems. $^{99m}Tc(CO)_3$-labeled HER2 DARPin was effectively used for tumor visualization (Zahnd et al. 2010). Additionally, an EphB4-specific ^{64}Cu-labeled TNYL-RAW peptide was recently demonstrated as

an successful radiotracer for the detection of EphB4 in CT26 and PC3M tumor xenografts (Xiong et al. 2010). The peptide undergoes fast metabolic degradation, and the molecular integrity of the radiopharmaceutical is essential. Therefore, EphB4 DARPins having more suitable biophysical properties could be used for patients' identification, monitoring of the response to EphB4-directed therapy and to improve patient outcomes.

Finally these EphB4 DARPins are valuable as a research tool to further unravel the mechanisms of EphB4 function and signaling. They could be simply used for co-immunoprecipitation experiments to isolate EphB4 receptor complexes with associated molecules and thereby uncover components involved in its signaling. The analysis of these molecules may possibly help to identify downstream pathways and new important candidates for cancer and other disease therapies.

To conclude, these studies show for the first time a novel class of DARPin binders directed against human tyrosine kinase receptor EphB4. They inhibit the receptor signaling either ephrin-B2-competitively- or non-competitively and prevent angiogenesis *in vitro* and *in vivo*. Altogether these results encourage further optimization studies in order to develop EphB4 DARPins for clinical applications.

5 APPENDIX

5.1 Supplementary results

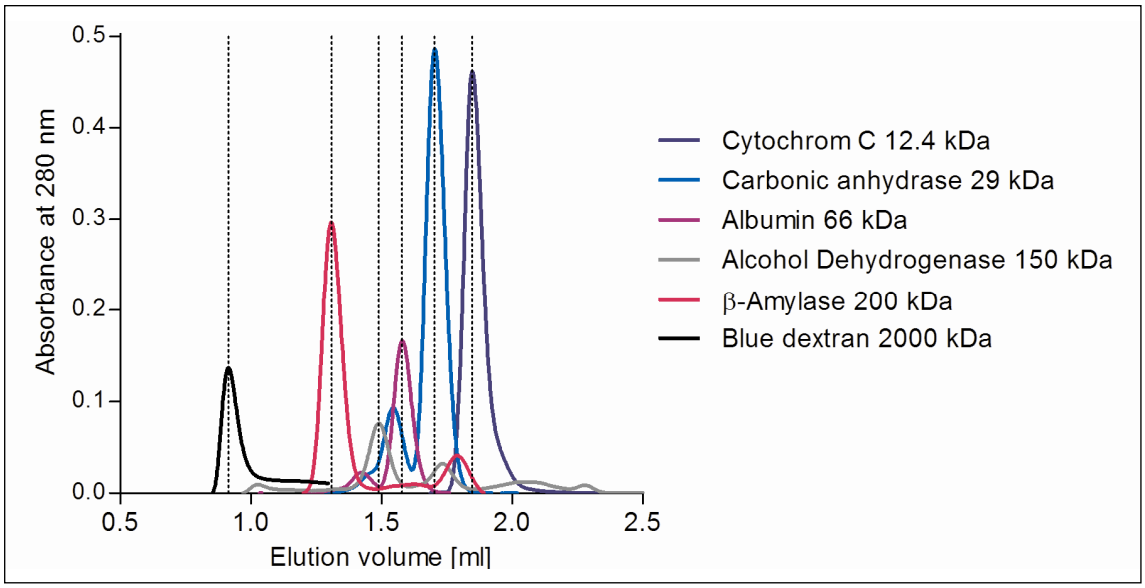

Figure 40. The elution profiles of marker proteins were assessed via size exclusion chromatography to determine the molecular weight of analyzed DARPin. The analysis was performed on a Superdex 200 column (SMART-System, Pharmacia), which ensures the optimal separation of proteins in the molecular weight range between 10000 and 600000. The gel filtration was monitored by the absorbance at 280 nm. 5 µg of sample was loaded and run at a flow rate of 60 µl/min in PBST. Panel shows overlays of blue dextran 2000 kDa (black), β-amylase 200 kDa (pink), alcohol dehydrogenase 150 kDa (grey), albumin 66 kDa (purple), carbonic anhydrase 29 kDa (blue) and cytochrom C 12.4 kDa (dark blue) (chapter 3.2.4). Representative data out of two independent experiments are shown.

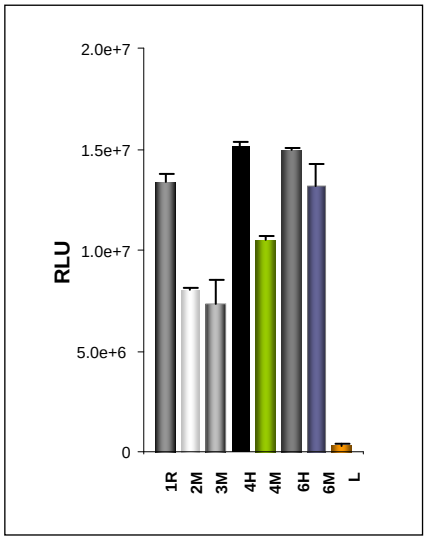

Figure 41. The immobilization control of mammalian EphB receptors. Recombinant Fc-fusion proteins of rat EphB1 (1R), murine EphB2 (2M), murine EphB3 (3M), human EphB4 (4H), murine Eph B4 (4M), human EphB6 (6H) and murine EphB6 (6M) were coated for ELISA analysis of DARPin binding as described in Materials and methods (2.5.2). Lysozyme (L) was used to determine unspecific binding. The immobilization of Fc-fusion proteins was confirmed using an HRP-labeled anti-Fc antibody. Values are depicted as means of three measurements ± SD.

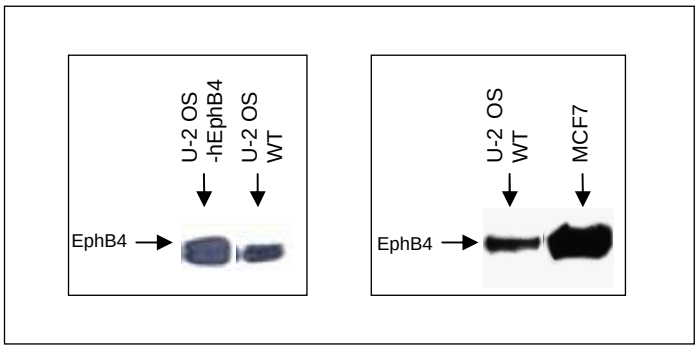

Figure 42. Western blot analysis of EphB4 expression in tumor cell lines. Total cell lysates of U-2 OS cells stably transfected with hEphB4, U-2 OS parental cells (U-2 OS WT) and MCF7 cells were subjected to SDS-PAGE and the Western blotting as described in Materials and methods (2.4.4 and 2.4.5). Membranes were developed using anti-EphB4 antibody. Loading was controlled using Ponceau S staining.

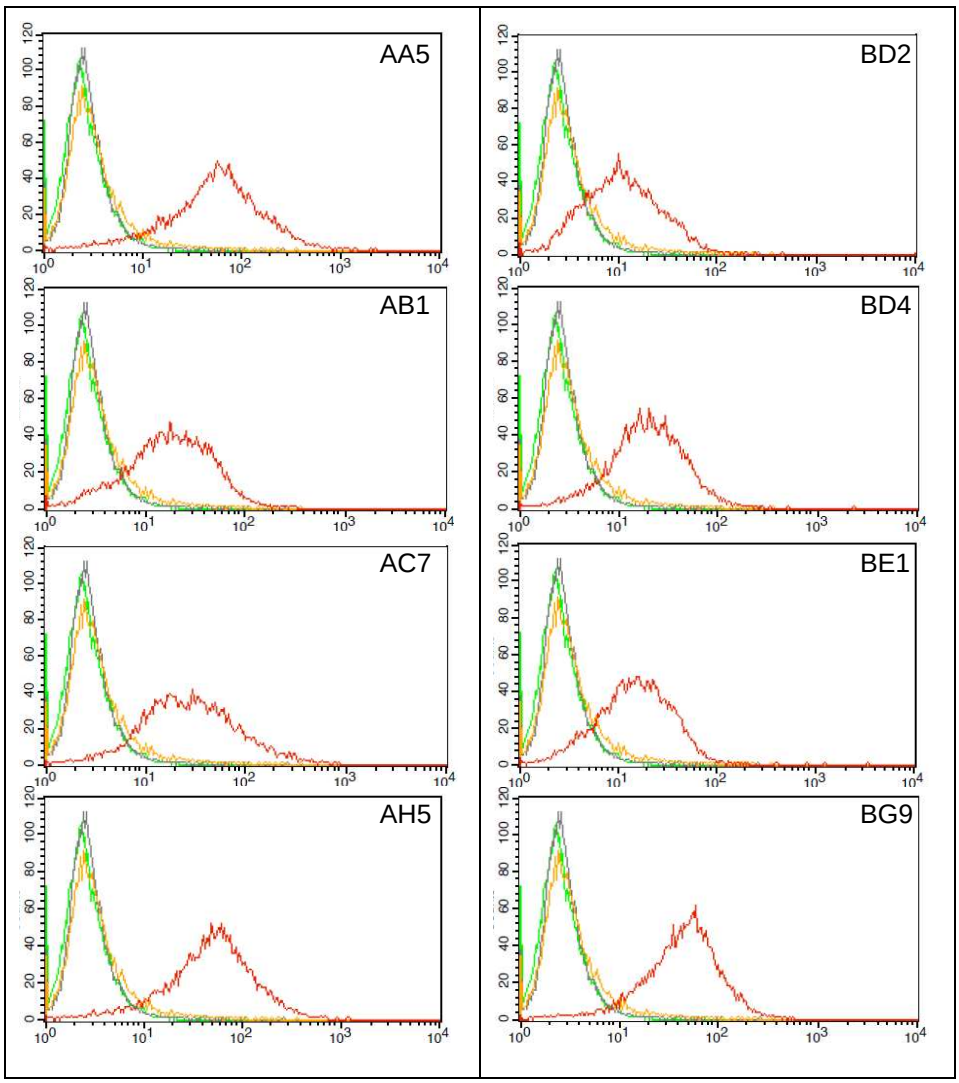

Figure 43. Flow cytometry analysis of EphB4 DARPin-pIII fusion proteins binding to on U-2 OS-hEphB4 cells. DARPin binding to U-2 OS cells stably transfected with hEphB4 was analyzed by FACS as described in Materials and methods (2.5.3). Bound phage were detected using an M13 specific mouse antibody and a secondary FITC-coupled antibody. Overlays of the FACS signal profiles of EphB4 DARPins (red profile) and control phage (orange profile) are shown. For blank controls primary antibody was omitted (grey profile) and the background fluorescent of unlabeled cells was measured (green profile). The logarithm of the fluorescence intensity (X axis) was plotted versus the cell count (Y axis). Representative data out of three independent experiments are shown.

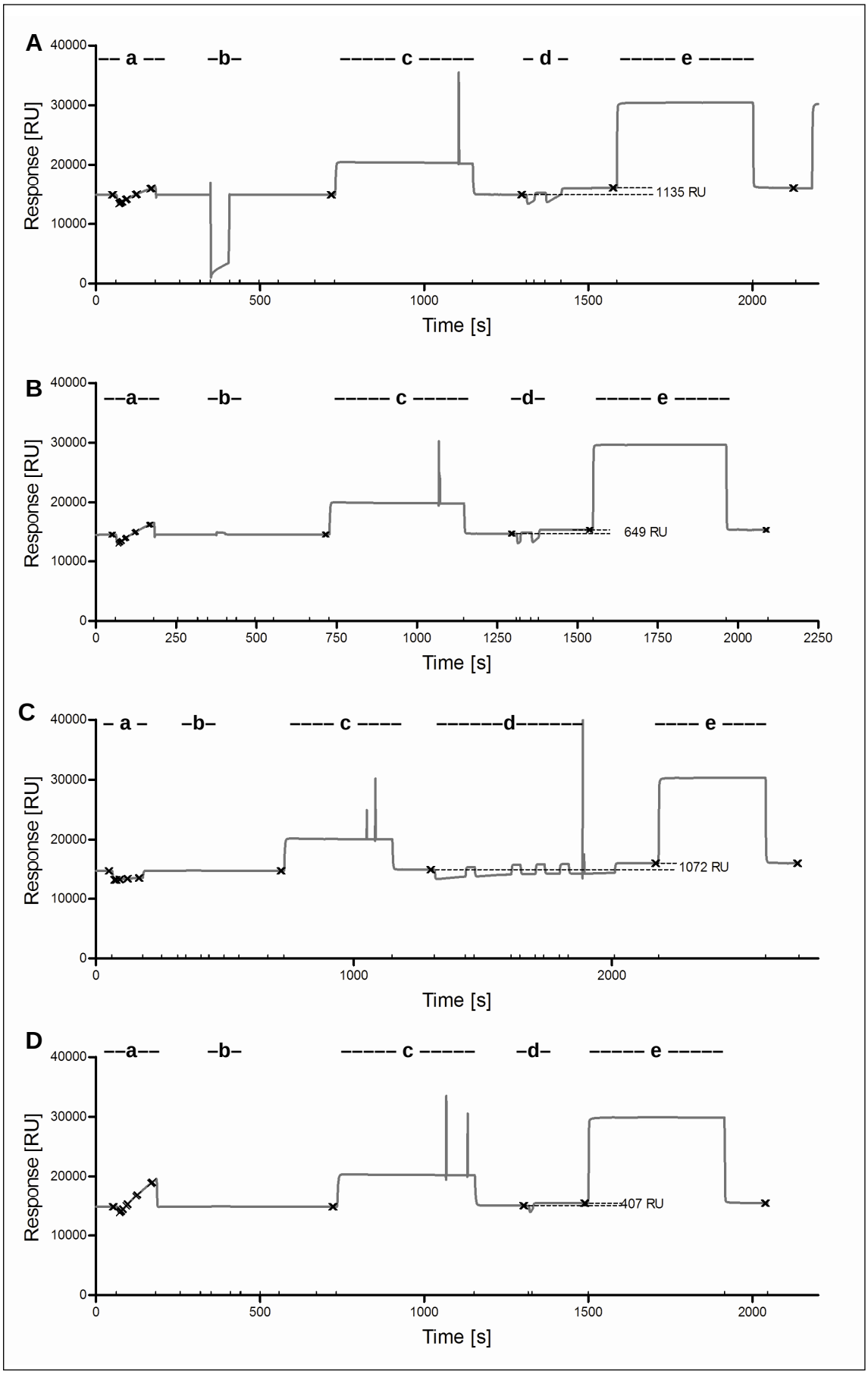
A
a
b
c
d
e
1135 RU
Response [RU]
Time [s]
B
649 RU
C
1072 RU
D
407 RU

Figure 44. Diagrams monitoring the immobilization of target proteins to the BIAcore sensor surface. Initially the target binding rate was determined (a), then the chip was washed to remove the target (b) and the surface was subsequently activated with a mixture of EDC / NHS (c). The target protein was injected and covalently coupled till reaching the target response level (d) and the remaining active groups were deactivated with ethanolamine (e). (A) Human EphB4-Fc – final density 1135 RU (aimed 1000 RU); (B) human EphB4 monomer – 649 RU (700 RU); (C) mouse EphB4-Fc – 1072 RU (1000 RU); (D) lysozyme – 407 RU (200 RU).

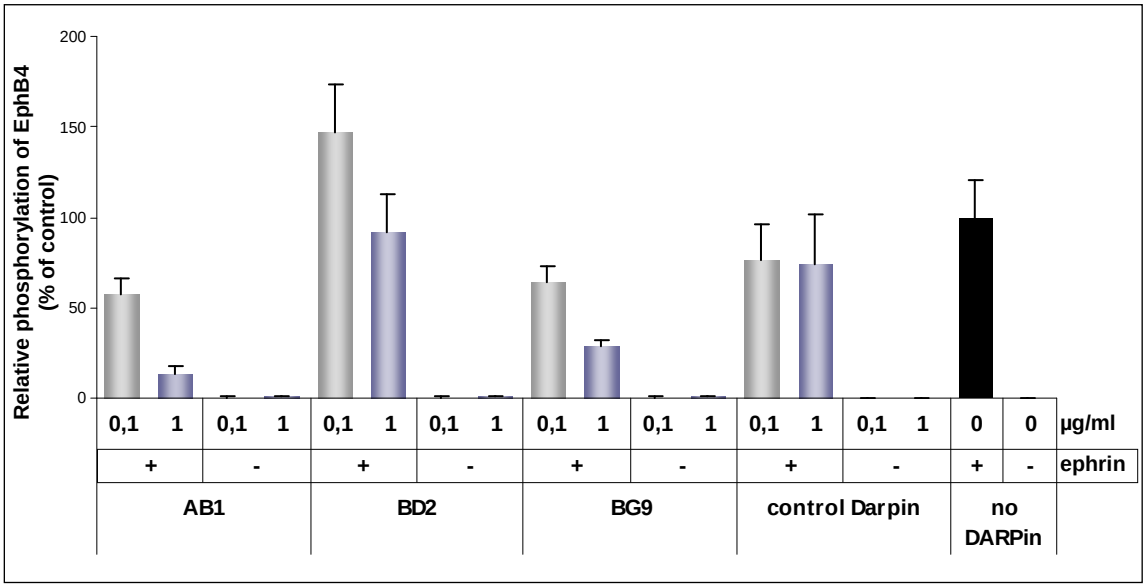

Figure 45. Dose dependent inhibition of ephrin-B2 induced phosphorylation of EphB4 by dimerized DARPins. U-2 OS-hEphB4 cells were incubated with the given concentrations of DARPins / IgG complex and subsequently treated with 1 µg/ml ephrin-B2-Fc (+ ephrin) or PBS (- ephrin). pEphB4 was determined by ELISA and the relative chemiluminescence intensity was calculated from cells treated with ephrin-B2 in the absence of DARPin, which was defined as 100%. The off7 DARPin was used as control. Values are depicted as means of three measurements ± SD.

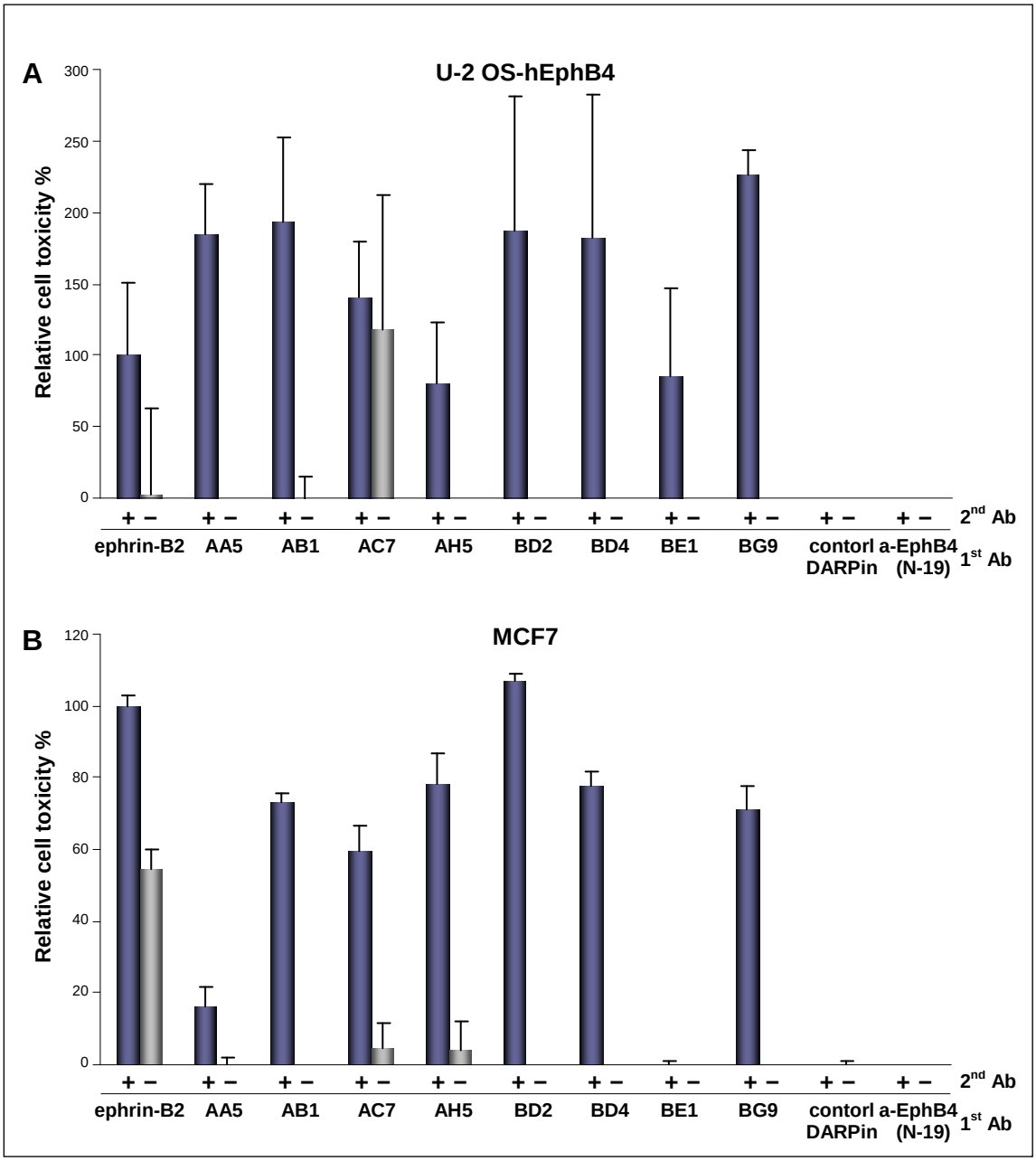

Figure 46. Internalization of EphB4 DARPins by EphB4 expressing cells. Internalization was analyzed in U-2 OS-hEphB4 (A) and MCF7 cell line (B). Cell vitality was determined after 72 h using an Alamar Blue assay as described in Materials and methods (2.6.5). The fluorescence of the metabolized substrate was determined 8 h (A) and 4 h (B) after substrate addition. The cell toxicity was expressed as the potency differences between the complex with and without Mab-ZAP: the first series cell number of [$1^{st}/2^{nd}$] - [$1^{st}/2^{nd}/3^{rd}$] (blue bars) and the second series omitting the secondary binder [1st] - [$1^{st}/3^{rd}$] (grey bars). Values were normalized to the toxic effect of the ephrin-B2 / Map-ZAP complex, which was defined as 100%. Data are depicted as means of three measurements ± SD.

5.2 EphB4 ICD DARPins

5.2.1 Isolation and characterization of DARPins against the intracellular domain of EphB4

The isolation of EphB4 selective binders from the phage library was very successful using the monomeric extracellular domain of EphB4. Therefore, the next approach was, to isolate specific binders against the intracellular domain of EphB4 for the use of a specific functional analysis of intracellular EphB4 signaling. The initial goal was to select binders which specifically recognize EphB4 and not the other members of the EphB receptor family. Amino acid sequence comparisons suggested using the sterile alpha motif (SAM) domain that is the least conserved region within the intracellular domain (Table 19). The highest sequence homology among the SAM domains is between EphB4 and EphB3 which share 63.3% identical amino acids. A recombinant protein of mouse EphB4-SAM fused to glutathione S-transferase (GST) was available and since mouse and human SAM domains share 99% homology (Table 19), this was used for the phage display (GST-mEphB4-SAM, GE4S). In addition a similar GST fusion protein with mouse EphB3-SAM (GST-mEphB3-SAM, GE3S) was used for counter selection.

Table 19. Amino acid sequence homology of hEphB4-SAM with SAM domains of other Eph receptors. Amino acid sequence alignments of ICDs of EphB receptors (aa876 – aa973) were performed and the homology was calculated using VECTOR NTI software.

Eph receptor	Homology to human EphB4-SAM
mouse EphB4	99%
human EphB3	63.3%
human EphB2	60.6%
human EphB1	57.1%
human EphB6	35.4%

5.2.2 Isolation of EphB4 ICD specific phage DARPin binders

The combinatorial DARPin library was panned against the recombinant GST-mEphB4-SAM protein directly absorbed to the plastic surface of a 96-well plate after several earlier strategies which were unsuccessful. These strategies attempted to improve the selection by preabsorption of the phage library to GST and GE3S or using various procedures including binding the GST fusion protein to a glutathione coupled plate. Four panning cycles were performed; the 2nd and 3rd cycles were repeated because of the low titer of the phage eluates (Table 20). 882 individual phage clones were randomly picked from the phage eluates of cycles 3A, 3B and 4A and analyzed by phage ELISA for binding to GE4S, GE3S and GST as described in Materials and methods (2.2 and 2.5.2).

Table 20 Titers of phage eluates after each selection cycle. Titers of the eluted phage after each selection cycle were determined as described in Materials and methods (2.2.3) by counting the number of ampicillin-resistant colonies, given as colony forming units (cfu) per ml.

Cycle	**1**	**2A**	**3A**	**4A**	**2B**	**3B**
Titer (cfu/ml)	1.2E+07	5.7E+06	9.0E+05	1.1E+08	n.d.	6.8E+06

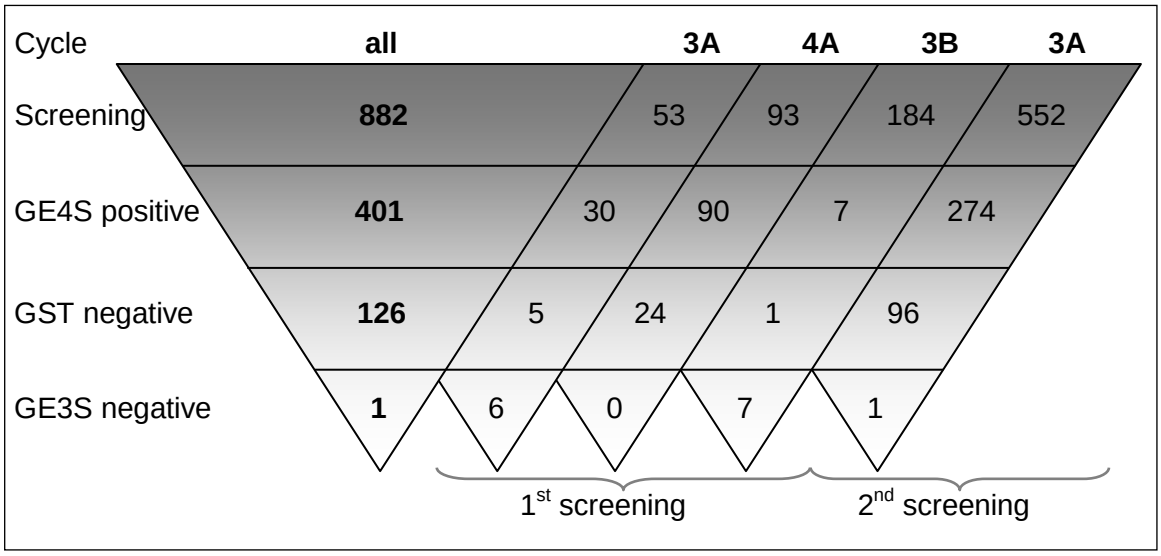

Figure 47. Schematic diagram of the screening for EphB4 ICD phage binders. The number of individual phage clones is summarized for two screening analyses.

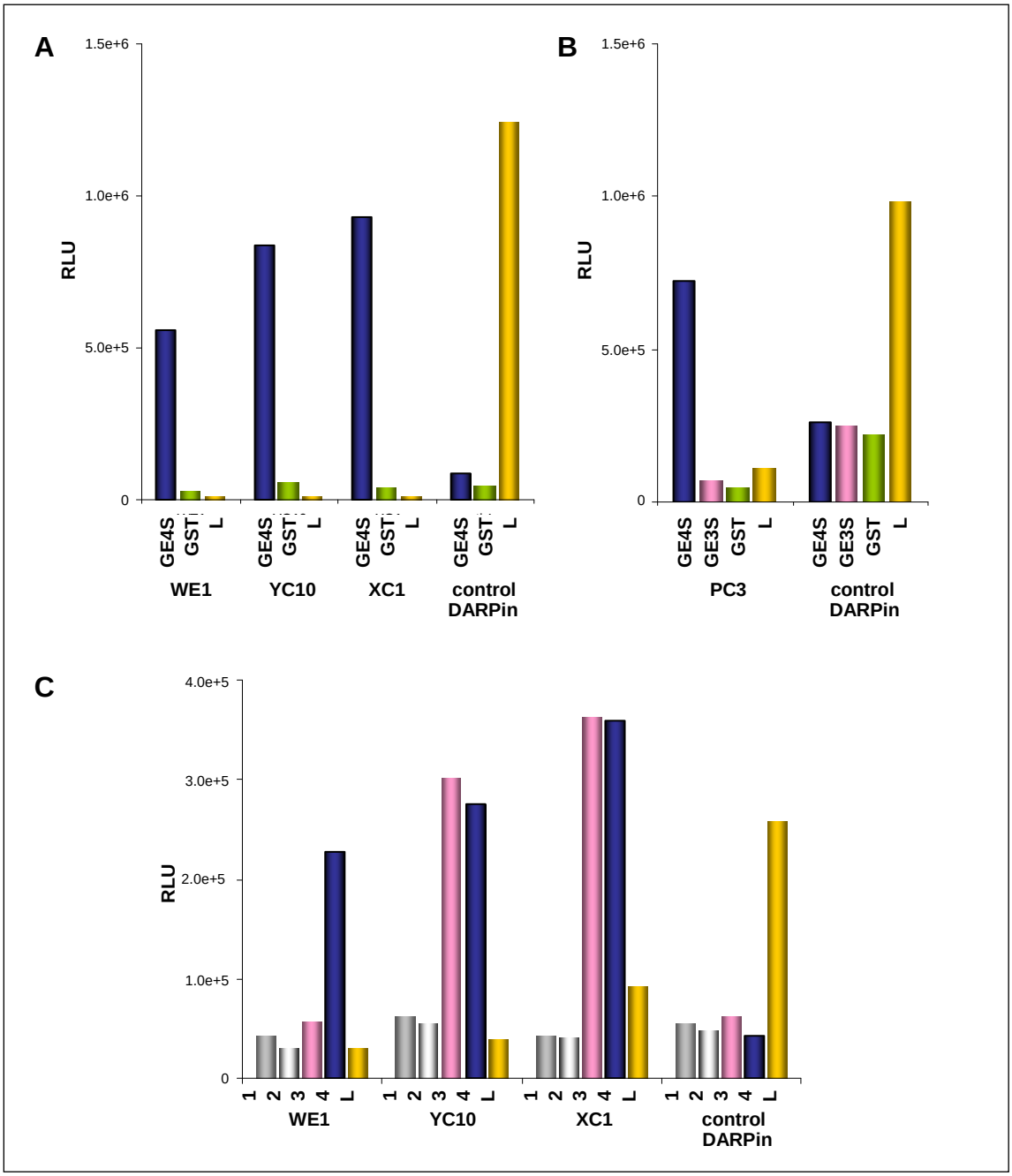

Figure 48. Analysis of EphB4 selective binding of isolated GE4S phage binders by ELISA. Phage clones of the eluates from cycles 3 and 4 were randomly picked and analyzed by ELISA as described in Materials and methods (2.5.2) for binding to GST-mEphB4-SAM (GE4S), GST-mEphB3-SAM (GE3S), GST and lysozyme (L) as an unrelated control protein (A, B). Selected clones were further analyzed for binding to the intracellular domains of human receptors EphB1 (1), EphB2 (2), EphB3 (3), EphB4 (4) and lysozyme (C). Representative binders of the first (A, C) and second (B) screening are displayed. Bound phage particles were detected by an anti-M13 / HRP monoclonal antibody. Lysozyme specific DARPin was used as a control.

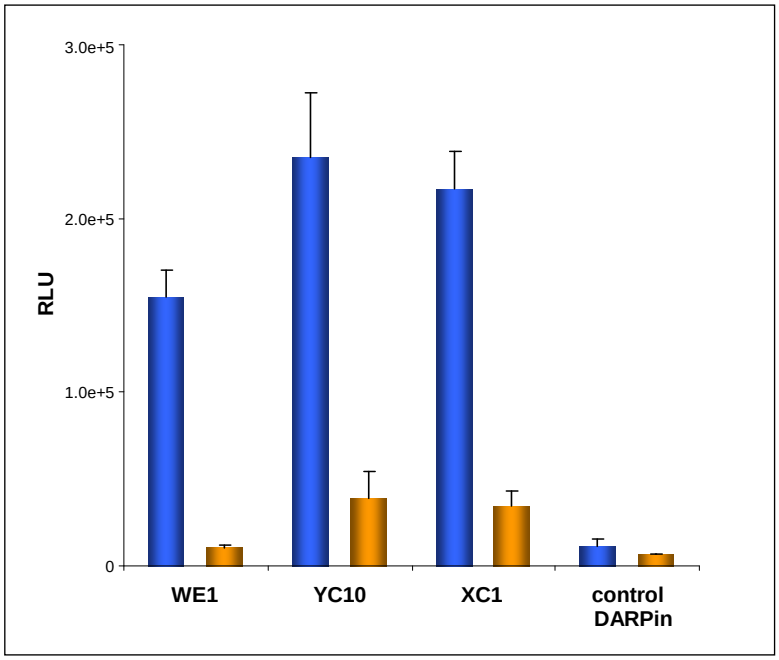

Figure 49. Binding of IMAC-purified DARPins to recombinant GE4S. Binding of EphB4 ICD DARPins to GST-mEphB4-SAM (blue bars) and lysozyme (yellow bars) an unrelated control protein was determined by ELISA as described in Materials and methods (2.5.2). Bound DARPins were detected via their N-terminal His-tag. Values are depicted as means of three measurements ± SD.

401 GE4S-positive binders were identified in two screening analyses and further tested for binding to GST (Figure 47). 126 phage clones did not bind to GST indicating that they bind to the fused SAM domain of EphB4 (Figure 48 A and data not shown). To assess their EphB4 specificity 30 GE4S binders identified in the first screening were tested for their binding to the intracellular domains of human EphB1, EphB2, EphB3 and EphB4. 7 phage clones specifically recognized only EphB4, whereas the residual 23 bound also to EphB3 (Figure 48 C and data not shown). None of the selected binders bound to EphB1 or EphB2. Sequencing of the DARPin inserts of the 7 EphB4 specific clones revealed one unique sequence of the clone termed as WE1. To increase the number EphB4 binders 552 more phage of the phage eluate of cycle 3A were screened and one additional unique binder termed PC3 was identified (Figure 47 and Figure 48 B). Two binders (YC10, XC1) which

recognize both EphB4 and EphB3 were randomly selected and also used for further analysis.

DARPin inserts of selected phage clones were subcloned into a bacterial expression vector as described in Materials and methods (2.3). DARPins were expressed and purified in a single step by immobilized metal ion affinity chromatography. WE1, YC10 and XC1 retained their binding ability to the recombinant GST-mEphB4-SAM after conversion from pIII fusion as shown by ELISA (Figure 49). Binding signals of the EphB4 ICD DARPins to the target protein were 6- to 14-fold higher than to the unrelated control protein indicating their specificity.

5.2.3 Functional characterization of EphB4 ICD DARPins

To assess whether EphB4 ICD DARPins are able to bind to the EphB4 receptor under native conditions immunoprecipitation experiments were performs using cell lysates from U-2 OS-hEphB4 cells. EphB4 / DARPin complexes were captured by an anti-RGS-His_4 antibody and protein G Sepharose beads. For comparison the myc-tagged EphB4 was immunoprecipitated using an anti-myc antibody and protein A Sepharose beads. Immunoprecipitated EphB4 was detected on Western blots with EphB4-specific antibodies.

DARPins WE1, XC1 and YC10 precipitated EphB4 from the cell lysate (Figure 50 and data not shown). Western blot analysis showed a protein bands, which corresponds to the anti-myc precipitated EphB4 and was detected by EphB4 specific antibodies. No signals were detected with a control DARPin. It should be noted that a weaker signal was observed for DARPin WE1, which may indicate a weaker binding. This correlates with its lower binding level signal in the ELISA assay (Figure 49). These results show that EphB4 ICD DARPins recognize the native human EphB4 receptor and can be used for the isolation of EphB4 associated proteins by co-immunoprecipitation or for intracellular functional analysis.

Anti-c-myc tag antibody	+	+						
anti-RGS-His_4 tag antibody			+	+	+	+	+	
DARPin XC1			+	+				
control DARPin					+	+		
U-2 OS EphB4 lysate	+		+		+		+	+
Lysis buffer		+		+		+		
EphB4 (~120 kDa) →								

Figure 50. Immunoprecipitation of EphB4 by DARPin XC1. Cell lysates from U-2 OS-hEphB4 cells and EphB4 immunprecipitation was performed as described in Materials and methods (2.5.5) using 500 µl of cell lysate at 1 mg/ml. XC1 and control DARPins were captured with an anti-His tag antibody and protein G beads. Anti-c-myc antibody was bound to protein A Sepharose beads. IP material was analyzed by Western blotting using EphB4-specific antibody (Zymed, 1:500) and a corresponding secondary anti-mouse HRP-linked antibody (1:10000). Loading of equal amounts of IP material was controlled by PonceauS protein staining. The apparent molecular weight of the EphB4 was as expected around 120 kDa. Representative data out of two independent experiments are shown.

U-2 OS EphB4 lysate			+	+	+	+	+	+	+	
ephrin-B2 stimulation		+		+				+	+	
PULSin	+				+		+		+	
DARPin						+	+	+	+	+
DARPin YC10										
control DARPin										

Figure 51. DARPin transfection into U-2 OS-EphB4 cells. U-2 OS EphB4 cells were transfected with IMAC-purified endotoxin-free DARPins using a cationic amphiphile molecule (Protein Delivery Reagent PULSin) and subsequently treated with ephrin-B2 or buffer as described in Materials and methods (2.6.6). 20 µl of cell lysates were analyzed by Western Blotting using an anti-phosphotyrosine specific antibody. Loading of equal amounts of the material was controlled by PonceauS protein staining. Protein bands, which corresponds to the EphB4 (120 kDa) were detected. The effect was compared to the cells treated only with transfection reagent (outlined in red) or with the control DARPin.

In a first attempt to analyze, whether EphB4 ICD DARPins can affect intracellular signaling of EphB4 receptor DARPins were transferred into living U-2 OS-hEphB4 cells using a Protein Delivery Reagent (PULSin). Subsequently EphB4 phosphorylation after cellular stimulation with ephrin-B2 was determined. Total cell lysates were analyzed by Western Blotting using an anti-phosphotyrosine specific antibody. As expected, increased EphB4 phosphorylation was observed in cells treated with ephrin-B2 (Figure 51). Very interestingly, EphB4 phosphorylation was significantly reduced in cells transfected with EphB4 ICD DARPin YC10 but not in cells transfected with a control DARPin. This suggests that DARPins which bind to the SAM domain of EphB4 can prevent receptor phosphorylation. Further experiments are necessary to understand the precise mode-of-action of this process. Nevertheless these DARPins may allow investigation of the consequences of highly specific inhibition of EphB receptor not only by DARPin transfection but potentially also after stable transfection under the control of a regulable promoter.

5.3 Vector maps

5.3.1 Vector pMPAG3

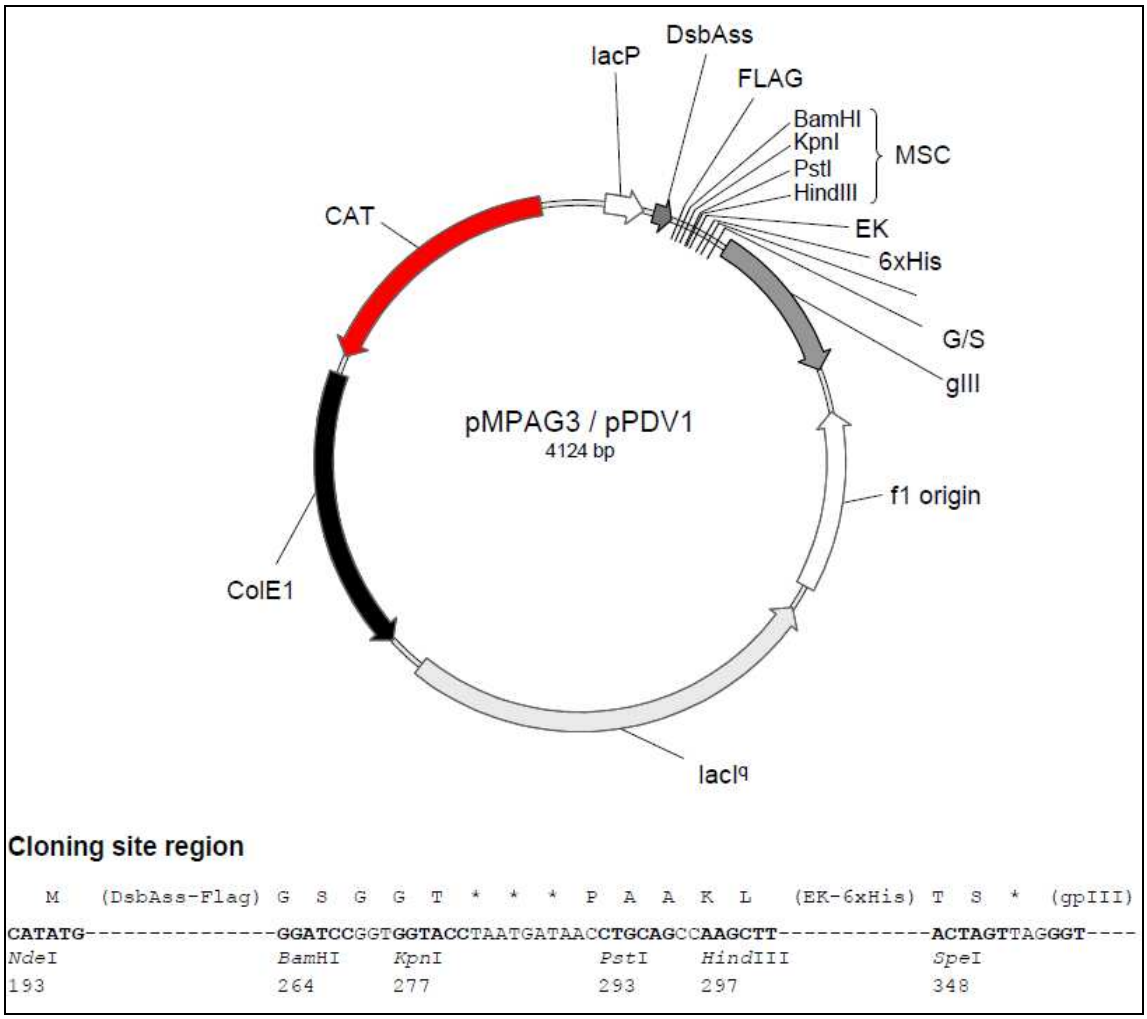

Figure 52. Phagemid vector pMPAG3 for monovalent filamentous phage display. DARPin sequences are cloned into the restriction sites BamHI and HindIII. The sequence is inserted in the multiple cloning site (MCS) between the DsbAss-Flag, which ensures SPR phage display and filamentous phage gene III (gIII), coding for the minor coat protein III (gpIII). Fusion to gIII allows display on the surface of filamentous phage particles after expression (DARPin-pIII). DARPins are expressed under control of a lac promoter / operator element. Vector carries a plasmid origin (ColE1) and a f1 origin of replication which permits production of virions using VCSM13 helper phage. The gene for chloramphenicol acetyl transferase (Cat) is an antibiotic resistance marker, which provides resistance to Cam and allows propagation as a plasmid in *E. coli*. The oligonucleotide odst03 (5'-CATAATCAAAATCACCGGAACCAG-3'), corresponding to position 390 to 367 of the complement strand of pMPAG3 reading upstream the p3 fusion gene can be used for sequencing inserts present in the MCS.

5.3.2 Vector pMPAG6

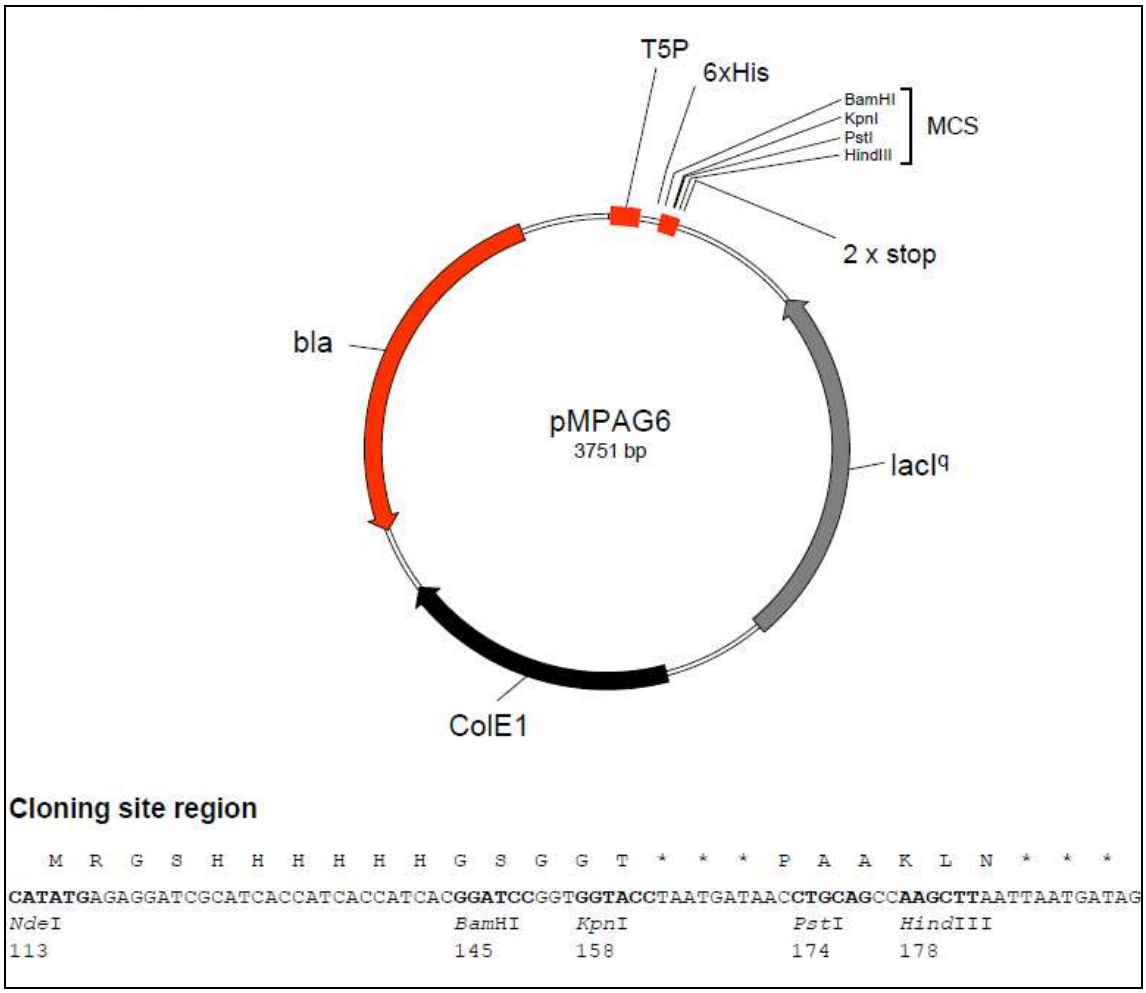

Figure 53. Phagemid vector pMPAG3 for cytoplasmic protein expression in *E. coli*. Sequence of DARPin from pMPAG3 vector can be subcloned by transfer of the BamHI / HindIII encoding fragment into the multiple cloning site (MCS) of pMPAG6, which is compatible to the MCS of pMPAG3 vector. Vector pMPAG6 has a plasmid origin (ColE1) and an ampicillin resistance marker, provided by β-lactamase, to allow propagation as a plasmid in *E. coli*. The expression of the DARPin protein is under the control of a phage T5 promoter / lac operator element. The phage T5 promoter is recognized by the endogenous RNA polymerase of *E. coli*. High-level expression is induced by Isopropyl-β-D-thiogalactopyranosid (IPTG) added to the expression culture, whereas addition of glucose to the growth media helps to further repress the promoter in its uninduced state by catabolite repression. Vector introduces His_6-tag coding sequence 5' to MCS, for protein recognition and IMAC purification. Two consecutive stop codons after the MCS ensure efficient translation termination in one reading frame. The oligonucleotide T7_term (5'-TGCTAGTTATTGCTCAGCGG-3'; position 277 to 258 of the complement strand; reading reverse) can be used to sequence inserts present in the MCS.

5.4 Structure of EphB4 DARPin

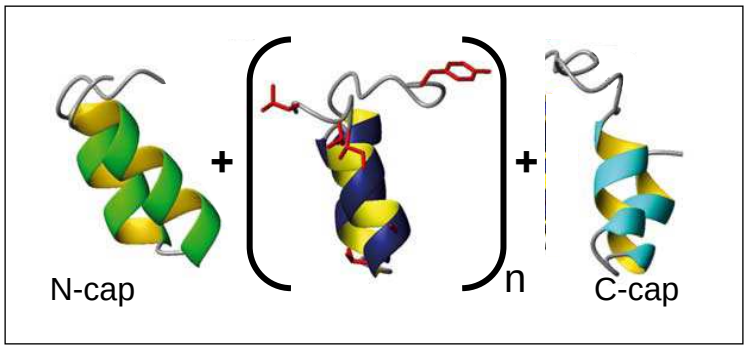

Figure 54. Modular architecture of DARPin containing n number of 33-amino acids long repeats between N- and C-terminal capping.

Structure of N3C DARPin (AA5, AC7, BE1, BG9, WE1, XC1, YC10)		
N-terminal cap	1 aa	MRGSHHHHHHGSDLGKKLLEAARAGQDDEVRILMANGADVNAX
AR module 1 2 3	44 aa 77 aa 110 aa	DXXGXTPLHLAAXXGHLEIVEVLLKZGADVNAX DXXGXTPLHLAAXXGHLEIVEVLLKZGADVNAX DXXGXTPLHLAAXXGHLEIVEVLLKZGADVNAX
C-terminal cap	143 aa	QDKFGKTAFDISIDNGNEDLAEILQKLN - 170 aa
Structure of N4C DARPin (AB1, AH5, BD2 and BD4)		
N-terminal cap	1 aa	MRGSHHHHHHGSDLGKKLLEAARAGQDDEVRILMANGADVNAX
AR module 1 2 3 4	44 aa 77 aa 110 aa 143 aa	DXXGXTPLHLAAXXGHLEIVEVLLKZGADVNAX DXXGXTPLHLAAXXGHLEIVEVLLKZGADVNAX DXXGXTPLHLAAXXGHLEIVEVLLKZGADVNAX DXXGXTPLHLAAXXGHLEIVEVLLKZGADVNAX
C-terminal cap	176 aa	QDKFGKTAFDISIDNGNEDLAEILQKLN - 203 aa

Figure 55. Sequence of DARPin scaffold. Selected by phage display designed AR proteins present modular architecture with 3 or 4 repeats between N and C terminal caps (N3C and N4C respectively). No repeat duplication within the scaffold was observed.

LIST OF FIGURES

Figure 1. Vasculogenesis and angiogenesis process. 14

Figure 2. Microscopic imaging of normal and tumor vasculature. 16

Figure 3. The domain structure of the Eph receptor and its ligand. 20

Figure 4. Formation of Eph / ephrin complex and activation of the bidirectional signaling. 21

Figure 5. Crystal structure of LBD of EphB2 / ephrin-B2 complex. 22

Figure 6. Internalization of the Eph / ephrin complex together with the surrounding plasma occurs via endocytosis. 25

Figure 7. Potential anti-EphB4 strategies. 29

Figure 8. Modular architecture of DARPin. 32

Figure 9. Crystal structure of DARPin off7 in complex with maltose binding protein. 36

Figure 10. Schematic diagram of a DARPin phage display selection cycle. 52

Figure 11. DARPin purification workflow. 61

Figure 12. Schematic diagram of the directed *in vivo* angiogenesis assay. 78

Figure 13. Schematic diagram of the work flow for the isolation and characterization of EphB4 DARPins. 79

Figure 14. Identification of phage DARPin binding to the monomeric human EphB4 ECD. 82

Figure 15. Binding of selected phage DARPin to recombinant EphB4 protein (A) and EphB4 expressing cells (B). 83

Figure 16. Isolation of DARPin DNA inserts form selected phagemids. 85

Figure 17. Expression and purification of EphB4 DARPins. 86

Figure 18. Ion exchange chromatography of IMAC-purified DARPin. 87

Figure 19. Analytical size exclusion chromatography of IMAC-purified DARPin. 88

Figure 20. Analytical size exclusion chromatography of DARPin AA5 / anti-RGS-His_4 IgG antibody complexes. 89

Figure 21. Binding of IMAC-purified EphB4 DARPins to the recombinant monomeric hEphB4 ECD. 91

Figure 22. Binding of EphB4-selected DARPins to hEphB4 ECD monomer and dimer. 92

Figure 23. Binding specificity of EphB4 DARPins to mammalian EphB receptors. 93

Figure 24. Flow cytometry analysis of EphB4 DARPin binding to EphB4 on U-2 OS and MCF7

cells. 96

Figure 25. SPR analysis of ephrin-B2 binding to human EphB4 ECD. 99

Figure 26. SPR analysis of EphB4 DARPin binding to human EphB4-Fc ECD. 101

Figure 27. SPR analysis of EphB4 DARPin binding to monomeric and dimeric hEphB4 ECD. 105

Figure 28. Experimental design of competition binding analysis using SPR technique. 109

Figure 29. SPR analysis of the competitive binding of ephrin-B2 and DARPins. 111

Figure 30. Analysis of the effects of EphB4 DARPins on EphB4 activity in U-2 OS-hEphB4 cells. 113

Figure 31. Effect of EphB4 DARPins on tube formation by HUVECs. 115

Figure 32. Quantitative analysis of the effect of EphB4 DARPins on HUVEC tube formation. 116

Figure 33. Inhibition of VEGF / FGF-2 induced angiogenesis *in vivo* by DARPin AB1. 116

Figure 34. Induction of apoptosis in U-2 OS-hEphB4 cells by DARPin AB1 *in vitro*. 116

Figure 35. Internalization of EphB4 DARPins by EphB4 expressing cells. 116

Figure 36. The interaction models of DARPins (D) to the immobilized EphB4 receptor (R). .. 116

Figure 37. Classification of EphB4 DARPins based on the prediction of binding epitope. 116

Figure 38. Amino acids sequence alignment and domain structure of the extracellular domains of human and mouse EphB4. 116

Figure 39. Schematic representation of EphB4 signaling inhibition by DARPins AB1 and BG9. 116

Figure 40. The elution profiles of marker proteins were assessed via size exclusion chromatography to determine the molecular weight of analyzed DARPin. 116

Figure 41. The immobilization control of mammalian EphB receptors. 116

Figure 42. Western blot analysis of EphB4 expression in tumor cell lines. 116

Figure 43. Flow cytometry analysis of EphB4 DARPin-pIII fusion proteins binding to on U-2 OS-hEphB4 cells. 116

Figure 44. Diagrams monitoring the immobilization of target proteins to the BIAcore sensor surface. 116

Figure 45. Dose dependent inhibition of ephrin-B2 induced phosphorylation of EphB4 by dimerized DARPins. 116

Figure 46. Internalization of EphB4 DARPins by EphB4 expressing cells. 116

Figure 47. Schematic diagram of the screening for EphB4 ICD phage binders. 116

Figure 48. Analysis of EphB4 selective binding of isolated GE4S phage binders by ELISA. 116

Figure 49. Binding of IMAC-purified DARPins to recombinant GE4S. 116

Figure 50. Immunoprecipitation of EphB4 by DARPin XC1. 116

Figure 51. DARPin transfection into U-2 OS-EphB4 cells. 116

Figure 52. Phagemid vector pMPAG3 for monovalent filamentous phage display. 116

Figure 53. Phagemid vector pMPAG3 for cytoplasmic protein expression in *E. coli*. 116

Figure 54. Modular architecture of DARPin containing n number of 33-amino acids long repeats between N- and C-terminal capping. 116

Figure 55. Sequence of DARPin scaffold. 116

LIST OF TABLES

Table 1. Digestion reaction mixture. 56

Table 2. Ligation reaction mixture. 58

Table 3. Molar extinction coefficients were calculated using Vector NTI software based on the amino acid sequence. 63

Table 4 Antibodies used for immunoblotting of DARPins, EphB4 or phosphorylated EphB4 (pEphB4). 64

Table 5. Proteins immobilized for phage display and ELISA. 65

Table 6. Antibodies used for FACS analyses. 68

Table 7. Experimental test conditions to achieve optimal target immobilization to the BIAcore sensor surface. 70

Table 8. Conditions for immobilization of the targets (ligands) on the CM5 chip. 70

Table 9. Experimental set-up and sequence of analyte injection for competition binding analysis. 70

Table 10. Saporin (ZAP) complexes tested in the internalization assay. 75

Table 11. Titer of the phage eluates. 80

Table 12. Frequency of identical sequences per clone within 30 analyzed DARPin inserts. .. 82

Table 13. Affinity constants of the interaction between ephrin-B2-Fc and the monomeric or dimerized EphB4. 98

Table 14. Statistical analysis of the SPR measurements of the interaction between EphB4 and ephrin-B2 or DARPins. 101

Table 15. Kinetic parameters of the interaction between EphB4 DARPins and ephrin-B2-Fc with the monomeric and dimerized EphB4 ECD determined by SPR. 106

Table 16. Amino acid sequence homology of the hEphB4 extracellular domain with other human and mammalian EphB receptors. 116

Table 17. Amino acid sequence homology of mouse and rat with human extracellular domains of EphB receptors. 116

Table 18. Summary of the EphB4 DARPin data. 116

Table 19. Amino acid sequence homology of hEphB4-SAM with SAM domains of other Eph receptors. 116

Table 20 Titers of phage eluates after each selection cycle. 116

REFERENCES

Adams RH, Wilkinson GA, Weiss C, Diella F, Gale NW et al. (1999) Roles of ephrinB ligands and EphB receptors in cardiovascular development: demarcation of arterial/venous domains, vascular morphogenesis, and sprouting angiogenesis. Genes Dev 13(3): 295-306.

Ahamed T, Chilamkurthi S, Nfor BK, Verhaert PD, van Dedem GW et al. (2008) Selection of pH-related parameters in ion-exchange chromatography using pH-gradient operations. J Chromatogr A 1194(1): 22-29.

Ahmed SA, Gogal RM, Jr., Walsh JE (1994) A new rapid and simple non-radioactive assay to monitor and determine the proliferation of lymphocytes: an alternative to [3H]thymidine incorporation assay. J Immunol Methods 170(2): 211-224.

Amstutz P, Koch H, Binz HK, Deuber SA, Pluckthun A (2006) Rapid selection of specific MAP kinase-binders from designed ankyrin repeat protein libraries. Protein Eng Des Sel 19(5): 219-229.

Amstutz P, Binz HK, Parizek P, Stumpp MT, Kohl A et al. (2005) Intracellular kinase inhibitors selected from combinatorial libraries of designed ankyrin repeat proteins. J Biol Chem 280(26): 24715-24722.

Bardelle C, Cross D, Davenport S, Kettle JG, Ko EJ et al. (2008) Inhibitors of the tyrosine kinase EphB4. Part 1: Structure-based design and optimization of a series of 2,4-bis-anilinopyrimidines. Bioorg Med Chem Lett 18(9): 2776-2780.

Berclaz G, Karamitopoulou E, Mazzucchelli L, Rohrbach V, Dreher E et al. (2003) Activation of the receptor protein tyrosine kinase EphB4 in endometrial hyperplasia and endometrial carcinoma. Ann Oncol 14(2): 220-226.

Bergers G, Benjamin LE (2003) Tumorigenesis and the angiogenic switch. Nat Rev Cancer 3(6): 401-410.

Bikfalvi A, Klein S, Pintucci G, Rifkin DB (1997) Biological roles of fibroblast growth factor-2. Endocr Rev 18(1): 26-45.

Binz HK, Stumpp MT, Forrer P, Amstutz P, Pluckthun A (2003) Designing repeat proteins: well-expressed, soluble and stable proteins from combinatorial libraries of consensus ankyrin repeat proteins. J Mol Biol 332(2): 489-503.

Binz HK, Amstutz P, Kohl A, Stumpp MT, Briand C et al. (2004) High-affinity binders selected from designed ankyrin repeat protein libraries. Nat Biotechnol 22(5): 575-582.

Blits-Huizinga CT, Nelersa CM, Malhotra A, Liebl DJ (2004) Ephrins and their receptors: binding versus biology. IUBMB Life 56(5): 257-265.

Bork P (1993) Hundreds of ankyrin-like repeats in functionally diverse proteins: mobile modules that cross phyla horizontally? Proteins 17(4): 363-374.

Boyd AW, Lackmann M (2001) Signals from Eph and ephrin proteins: a developmental tool kit. Sci STKE 2001(112): re20.

Bradford MM (1976) A rapid and sensitive method for the quantitation of microgram

quantities of protein utilizing the principle of protein-dye binding. Anal Biochem 72: 248-254.

Bruckner K, Klein R (1998) Signaling by Eph receptors and their ephrin ligands. Curr Opin Neurobiol 8(3): 375-382.

Bruckner K, Pablo Labrador J, Scheiffele P, Herb A, Seeburg PH et al. (1999) EphrinB ligands recruit GRIP family PDZ adaptor proteins into raft membrane microdomains. Neuron 22(3): 511-524.

Cadena DL, Gill GN (1992) Receptor tyrosine kinases. Faseb J 6(6): 2332-2337.

Carmeliet P (2000) Mechanisms of angiogenesis and arteriogenesis. Nat Med 6(4): 389-395.

Carmeliet P (2005) Angiogenesis in life, disease and medicine. Nature 438(7070): 932-936.

Chrencik JE, Brooun A, Kraus ML, Recht MI, Kolatkar AR et al. (2006a) Structural and biophysical characterization of the EphB4*ephrinB2 protein-protein interaction and receptor specificity. J Biol Chem 281(38): 28185-28192.

Chrencik JE, Brooun A, Recht MI, Kraus ML, Koolpe M et al. (2006b) Structure and thermodynamic characterization of the EphB4/Ephrin-B2 antagonist peptide complex reveals the determinants for receptor specificity. Structure 14(2): 321-330.

Committee EN (1997) Unified nomenclature for Eph family receptors and their ligands, the ephrins. Eph Nomenclature Committee. Cell 90(3): 403-404.

Conway EM, Collen D, Carmeliet P (2001) Molecular mechanisms of blood vessel growth. Cardiovasc Res 49(3): 507-521.

Egea J, Klein R (2007) Bidirectional Eph-ephrin signaling during axon guidance. Trends Cell Biol 17(5): 230-238.

Escudier B, Eisen T, Stadler WM, Szczylik C, Oudard S et al. (2007) Sorafenib in advanced clear-cell renal-cell carcinoma. N Engl J Med 356(2): 125-134.

Ferrara N, Kerbel RS (2005) Angiogenesis as a therapeutic target. Nature 438(7070): 967-974.

Ferrara N, Gerber HP, LeCouter J (2003) The biology of VEGF and its receptors. Nat Med 9(6): 669-676.

Ferrara N, Hillan KJ, Gerber HP, Novotny W (2004) Discovery and development of bevacizumab, an anti-VEGF antibody for treating cancer. Nat Rev Drug Discov 3(5): 391-400.

Folkman J (1971) Tumor angiogenesis: therapeutic implications. N Engl J Med 285(21): 1182-1186.

Folkman J (1972) Anti-angiogenesis: new concept for therapy of solid tumors. Ann Surg 175(3): 409-416.

Forrer P, Stumpp MT, Binz HK, Pluckthun A (2003) A novel strategy to design binding molecules harnessing the modular nature of repeat proteins. FEBS Lett 539(1-3): 2-6.

Foubert P, Silvestre JS, Souttou B, Barateau V, Martin C et al. (2007) PSGL-1-mediated activation of EphB4 increases the proangiogenic potential of endothelial progenitor cells. J Clin Invest 117(6): 1527-1537.

Fuller T, Korff T, Kilian A, Dandekar G, Augustin HG (2003) Forward EphB4 signaling in endothelial cells controls cellular repulsion and segregation from ephrinB2 positive cells. J Cell Sci 116(Pt 12): 2461-2470.

Gale NW, Holland SJ, Valenzuela DM, Flenniken A, Pan L et al. (1996) Eph receptors and ligands comprise two major specificity subclasses and are reciprocally compartmentalized during embryogenesis. Neuron 17(1): 9-19.

Gendreau SB, Ventura R, Keast P, Laird AD, Yakes FM et al. (2007) Inhibition of the T790M gatekeeper mutant of the epidermal growth factor receptor by EXEL-7647. Clin Cancer Res 13(12): 3713-3723.

Gerety SS, Wang HU, Chen ZF, Anderson DJ (1999) Symmetrical mutant phenotypes of the receptor EphB4 and its specific transmembrane ligand ephrin-B2 in cardiovascular development. Mol Cell 4(3): 403-414.

Hamada K, Oike Y, Ito Y, Maekawa H, Miyata K et al. (2003) Distinct roles of ephrin-B2 forward and EphB4 reverse signaling in endothelial cells. Arterioscler Thromb Vasc Biol 23(2): 190-197.

Hashizume H, Baluk P, Morikawa S, McLean JW, Thurston G et al. (2000) Openings between defective endothelial cells explain tumor vessel leakiness. Am J Pathol 156(4): 1363-1380.

Hattori M, Osterfield M, Flanagan JG (2000) Regulated cleavage of a contact-mediated axon repellent. Science 289(5483): 1360-1365.

He S, Ding Y, Zhou J, Krasnoperov V, Zozulya S et al. (2005) Soluble EphB4 regulates choroidal endothelial cell function and inhibits laser-induced choroidal neovascularization. Invest Ophthalmol Vis Sci 46(12): 4772-4779.

Henkemeyer M, Orioli D, Henderson JT, Saxton TM, Roder J et al. (1996) Nuk controls pathfinding of commissural axons in the mammalian central nervous system. Cell 86(1): 35-46.

Heroult M, Schaffner F, Augustin HG (2006) Eph receptor and ephrin ligand-mediated interactions during angiogenesis and tumor progression. Exp Cell Res 312(5): 642-650.

Heroult M, Schaffner F, Pfaff D, Prahst C, Kirmse R et al. (2010) EphB4 promotes site-specific metastatic tumor cell dissemination by interacting with endothelial cell-expressed ephrinb2. Mol Cancer Res 8(10): 1297-1309.

Himanen JP, Nikolov DB (2003a) Eph signaling: a structural view. Trends Neurosci 26(1): 46-51.

Himanen JP, Nikolov DB (2003b) Eph receptors and ephrins. Int J Biochem Cell Biol 35(2): 130-134.

Himanen JP, Henkemeyer M, Nikolov DB (1998) Crystal structure of the ligand-binding domain of the receptor tyrosine kinase EphB2. Nature 396(6710): 486-491.

Himanen JP, Rajashankar KR, Lackmann M, Cowan CA, Henkemeyer M et al. (2001)

Crystal structure of an Eph receptor-ephrin complex. Nature 414(6866): 933-938.

Himanen JP, Chumley MJ, Lackmann M, Li C, Barton WA et al. (2004) Repelling class discrimination: ephrin-A5 binds to and activates EphB2 receptor signaling. Nat Neurosci 7(5): 501-509.

Hirai H, Maru Y, Hagiwara K, Nishida J, Takaku F (1987) A novel putative tyrosine kinase receptor encoded by the eph gene. Science 238(4834): 1717-1720.

Holder N, Klein R (1999) Eph receptors and ephrins: effectors of morphogenesis. Development 126(10): 2033-2044.

Holen HL, Shadidi M, Narvhus K, Kjosnes O, Tierens A et al. (2008) Signaling through ephrin-A ligand leads to activation of Src-family kinases, Akt phosphorylation, and inhibition of antigen receptor-induced apoptosis. J Leukoc Biol 84(4): 1183-1191.

Huang X, Yamada Y, Kidoya H, Naito H, Nagahama Y et al. (2007) EphB4 overexpression in B16 melanoma cells affects arterial-venous patterning in tumor angiogenesis. Cancer Res 67(20): 9800-9808.

Jussila L, Alitalo K (2002) Vascular growth factors and lymphangiogenesis. Physiol Rev 82(3): 673-700.

Kalluri R (2003) Basement membranes: structure, assembly and role in tumour angiogenesis. Nat Rev Cancer 3(6): 422-433.

Kerbel RS (1997) A cancer therapy resistant to resistance. Nature 390(6658): 335-336.

Kertesz N, Krasnoperov V, Reddy R, Leshanski L, Kumar SR et al. (2006) The soluble extracellular domain of EphB4 (sEphB4) antagonizes EphB4-EphrinB2 interaction, modulates angiogenesis, and inhibits tumor growth. Blood 107(6): 2330-2338.

Kohl A, Binz HK, Forrer P, Stumpp MT, Pluckthun A et al. (2003) Designed to be stable: crystal structure of a consensus ankyrin repeat protein. Proc Natl Acad Sci U S A 100(4): 1700-1705.

Krasnoperov V, Kumar SR, Ley E, Li X, Scehnet J et al. (2010) Novel EphB4 Monoclonal Antibodies Modulate Angiogenesis and Inhibit Tumor Growth. Am J Pathol.

Kumar SR, Singh J, Xia G, Krasnoperov V, Hassanieh L et al. (2006) Receptor tyrosine kinase EphB4 is a survival factor in breast cancer. Am J Pathol 169(1): 279-293.

Kumar SR, Masood R, Spannuth WA, Singh J, Scehnet J et al. (2007) The receptor tyrosine kinase EphB4 is overexpressed in ovarian cancer, provides survival signals and predicts poor outcome. Br J Cancer 96(7): 1083-1091.

Labrador JP, Brambilla R, Klein R (1997) The N-terminal globular domain of Eph receptors is sufficient for ligand binding and receptor signaling. Embo J 16(13): 3889-3897.

Li J, Mahajan A, Tsai MD (2006) Ankyrin repeat: a unique motif mediating protein-protein interactions. Biochemistry 45(51): 15168-15178.

Liu S, Tobias R, McClure S, Styba G, Shi Q et al. (1997) Removal of endotoxin from recombinant protein preparations. Clin Biochem 30(6): 455-463.

Llovet JM, Ricci S, Mazzaferro V, Hilgard P, Gane E et al. (2008) Sorafenib in advanced hepatocellular carcinoma. N Engl J Med 359(4): 378-390.

Martiny-Baron G, Korff T, Schaffner F, Esser N, Eggstein S et al. (2004) Inhibition of tumor growth and angiogenesis by soluble EphB4. Neoplasia 6(3): 248-257.

McDonald DM, Choyke PL (2003) Imaging of angiogenesis: from microscope to clinic. Nat Med 9(6): 713-725.

Miao H, Burnett E, Kinch M, Simon E, Wang B (2000) Activation of EphA2 kinase suppresses integrin function and causes focal-adhesion-kinase dephosphorylation. Nat Cell Biol 2(2): 62-69.

Miao H, Wei BR, Peehl DM, Li Q, Alexandrou T et al. (2001) Activation of EphA receptor tyrosine kinase inhibits the Ras/MAPK pathway. Nat Cell Biol 3(5): 527-530.

Milovnik P, Ferrari D, Sarkar CA, Pluckthun A (2009) Selection and characterization of DARPins specific for the neurotensin receptor 1. Protein Eng Des Sel 22(6): 357-366.

Morikawa S, Baluk P, Kaidoh T, Haskell A, Jain RK et al. (2002) Abnormalities in pericytes on blood vessels and endothelial sprouts in tumors. Am J Pathol 160(3): 985-1000.

Mosavi LK, Cammett TJ, Desrosiers DC, Peng ZY (2004) The ankyrin repeat as molecular architecture for protein recognition. Protein Sci 13(6): 1435-1448.

Motzer RJ, Michaelson MD, Redman BG, Hudes GR, Wilding G et al. (2006) Activity of SU11248, a multitargeted inhibitor of vascular endothelial growth factor receptor and platelet-derived growth factor receptor, in patients with metastatic renal cell carcinoma. J Clin Oncol 24(1): 16-24.

Noren NK, Lu M, Freeman AL, Koolpe M, Pasquale EB (2004) Interplay between EphB4 on tumor cells and vascular ephrin-B2 regulates tumor growth. Proc Natl Acad Sci U S A 101(15): 5583-5588.

Noren NK, Yang NY, Silldorff M, Mutyala R, Pasquale EB (2009) Ephrin-independent regulation of cell substrate adhesion by the EphB4 receptor. Biochem J 422(3): 433-442.

Nyberg P, Xie L, Kalluri R (2005) Endogenous inhibitors of angiogenesis. Cancer Res 65(10): 3967-3979.

O'Shannessy DJ (1994) Determination of kinetic rate and equilibrium binding constants for macromolecular interactions: a critique of the surface plasmon resonance literature. Curr Opin Biotechnol 5(1): 65-71.

Pabbisetty KB, Yue X, Li C, Himanen JP, Zhou R et al. (2007) Kinetic analysis of the binding of monomeric and dimeric ephrins to Eph receptors: correlation to function in a growth cone collapse assay. Protein Sci 16(3): 355-361.

Pascall JC, Brown KD (2004) Intramembrane cleavage of ephrinB3 by the human rhomboid family protease, RHBDL2. Biochem Biophys Res Commun 317(1): 244-252.

Paschke M (2006) Phage display systems and their applications. Appl Microbiol Biotechnol 70(1): 2-11.

Pasquale EB (2005) Eph receptor signalling casts a wide net on cell behaviour. Nat Rev Mol Cell Biol 6(6): 462-475.

Plank MJ, Sleeman BD (2003) Tumour-induced Angiogenesis: A Review -- Review Article. Journal of Theoretical Medicine 5(3): 137 - 153.

Robinson DR, Wu YM, Lin SF (2000) The protein tyrosine kinase family of the human genome. Oncogene 19(49): 5548-5557.

Salvucci O, de la Luz Sierra M, Martina JA, McCormick PJ, Tosato G (2006) EphB2 and EphB4 receptors forward signaling promotes SDF-1-induced endothelial cell chemotaxis and branching remodeling. Blood 108(9): 2914-2922.

Schweizer A, Roschitzki-Voser H, Amstutz P, Briand C, Gulotti-Georgieva M et al. (2007) Inhibition of caspase-2 by a designed ankyrin repeat protein: specificity, structure, and inhibition mechanism. Structure 15(5): 625-636.

Sergeeva A, Kolonin MG, Molldrem JJ, Pasqualini R, Arap W (2006) Display technologies: application for the discovery of drug and gene delivery agents. Adv Drug Deliv Rev 58(15): 1622-1654.

Sharma S, Mullangi R, Wade M, Gurav S, Sajja S et al. PK/PD models using a selective EphB4 inhibitor, JI-101 alone and in combination with other targeted agents and chemotherapy: Results of preclinical and ex vivo studies; 2010 Nov 17; Berlin, Germany. 22nd EORTC-NCI-AACR symposium on “Molecular targets and Cancer Therapeutics”. pp. 196.

Skerra A (2007) Alternative non-antibody scaffolds for molecular recognition. Curr Opin Biotechnol 18(4): 295-304.

Smith FM, Vearing C, Lackmann M, Treutlein H, Himanen J et al. (2004) Dissecting the EphA3/Ephrin-A5 interactions using a novel functional mutagenesis screen. J Biol Chem 279(10): 9522-9531.

Stein E, Lane AA, Cerretti DP, Schoecklmann HO, Schroff AD et al. (1998) Eph receptors discriminate specific ligand oligomers to determine alternative signaling complexes, attachment, and assembly responses. Genes Dev 12(5): 667-678.

Steiner D, Forrer P, Pluckthun A (2008) Efficient selection of DARPins with sub-nanomolar affinities using SRP phage display. J Mol Biol 382(5): 1211-1227.

Steiner D, Forrer P, Stumpp MT, Pluckthun A (2006) Signal sequences directing cotranslational translocation expand the range of proteins amenable to phage display. Nat Biotechnol 24(7): 823-831.

Steinle JJ, Meininger CJ, Forough R, Wu G, Wu MH et al. (2002) Eph B4 receptor signaling mediates endothelial cell migration and proliferation via the phosphatidylinositol 3-kinase pathway. J Biol Chem 277(46): 43830-43835.

Thanos CD, Goodwill KE, Bowie JU (1999) Oligomeric structure of the human EphB2 receptor SAM domain. Science 283(5403): 833-836.

Toth J, Cutforth T, Gelinas AD, Bethoney KA, Bard J et al. (2001) Crystal structure of an ephrin ectodomain. Dev Cell 1(1): 83-92.

van der Geer P, Hunter T, Lindberg RA (1994) Receptor protein-tyrosine kinases and

their signal transduction pathways. Annu Rev Cell Biol 10: 251-337.

Wang HU, Chen ZF, Anderson DJ (1998) Molecular distinction and angiogenic interaction between embryonic arteries and veins revealed by ephrin-B2 and its receptor Eph-B4. Cell 93(5): 741-753.

Wetzel SK, Settanni G, Kenig M, Binz HK, Pluckthun A (2008) Folding and unfolding mechanism of highly stable full-consensus ankyrin repeat proteins. J Mol Biol 376(1): 241-257.

Winkler J, Martin-Killias P, Pluckthun A, Zangemeister-Wittke U (2009) EpCAM-targeted delivery of nanocomplexed siRNA to tumor cells with designed ankyrin repeat proteins. Mol Cancer Ther 8(9): 2674-2683.

Wyler E, Kaminska M, Coic YM, Baleux F, Veron M et al. (2007) Inhibition of NF-kappaB activation with designed ankyrin-repeat proteins targeting the ubiquitin-binding/oligomerization domain of NEMO. Protein Sci 16(9): 2013-2022.

Xia G, Kumar SR, Masood R, Koss M, Templeman C et al. (2005a) Up-regulation of EphB4 in mesothelioma and its biological significance. Clin Cancer Res 11(12): 4305-4315.

Xia G, Kumar SR, Stein JP, Singh J, Krasnoperov V et al. (2006) EphB4 receptor tyrosine kinase is expressed in bladder cancer and provides signals for cell survival. Oncogene 25(5): 769-780.

Xia G, Kumar SR, Masood R, Zhu S, Reddy R et al. (2005b) EphB4 expression and biological significance in prostate cancer. Cancer Res 65(11): 4623-4632.

Xiong C, Huang M, Zhang R, Song S, Lu W et al. (2010) In Vivo Small-Animal PET/CT of EphB4 Receptors Using 64Cu-Labeled Peptide. J Nucl Med 52(2): 241-248.

Yamaguchi Y, Pasquale EB (2004) Eph receptors in the adult brain. Curr Opin Neurobiol 14(3): 288-296.

Yancopoulos GD, Davis S, Gale NW, Rudge JS, Wiegand SJ et al. (2000) Vascular-specific growth factors and blood vessel formation. Nature 407(6801): 242-248.

Yarden Y, Ullrich A (1988) Growth factor receptor tyrosine kinases. Annu Rev Biochem 57: 443-478.

Zahnd C, Pecorari F, Straumann N, Wyler E, Pluckthun A (2006) Selection and characterization of Her2 binding-designed ankyrin repeat proteins. J Biol Chem 281(46): 35167-35175.

Zahnd C, Wyler E, Schwenk JM, Steiner D, Lawrence MC et al. (2007) A designed ankyrin repeat protein evolved to picomolar affinity to Her2. J Mol Biol 369(4): 1015-1028.

Zahnd C, Kawe M, Stumpp MT, de Pasquale C, Tamaskovic R et al. (2010) Efficient tumor targeting with high-affinity designed ankyrin repeat proteins: effects of affinity and molecular size. Cancer Res 70(4): 1595-1605.

ACKNOWLEDGEMENTS

I wish to express my sincere gratitude to all those persons without whom this dissertation would never come to this point.

I would like to thank Dr. Dieter Zopf for giving me the opportunity to pursue my PhD thesis and for his valuable guidance and discussions during my work.

I am very grateful to my supervisor Prof. Sanna-Maria Käkönen for her advice and reading of my thesis.

Furthermore I would also like to thank my reviewer Professor Rupert Mutzel for his time to read this manuscript.

Great thanks go to Amaury Fernandez for his significant contribution to this project.

I deeply appreciate all the support of my colleagues Heike, Katrin D, Stefan, Marina, Yong-Jiang, Jessi, Kate, Katrin W., Karola, Claudia M, Kathrin, Franziska…Thank you for your continous help, advice, comments on my work and finally also the friendship.

My beloved family and dear friends, thank you for your understanding, support and love. My biggest THANK goes to Houssam, my parents and Tomasz. Bez was nie byłabym tu gdzie jestem!

Dziękuję!

EHRENWÖRTLICHE ERKLÄRUNG

Hiermit versichere ich, dass ich die vorliegende Arbeit selbstständig durchgeführt und verfasst habe. Dabei wurden keine anderen als die angegebenen Quellen und Hilfsmittel verwendet.

Berlin, 15.02.2011

Weronika Trun